

Neutrophil and Macrophage Response to *Streptococcus iniae* Infection in Zebrafish Larvae

By

Elizabeth A. Harvie

A dissertation submitted in partial fulfillment of

the requirements for the degree of

Doctor of Philosophy

(Microbiology)

at the

UNIVERSITY OF WISCONSIN-MADISON

2015

Date of final oral examination: 5/8/2015

The dissertation is approved by the following members of the Final Oral Committee:

Anna Huttenlocher, Professor, Pediatrics; Medical Microbiology and Immunology

Heidi Goodrich-Blair, Professor, Bacteriology

Mary Halloran, Professor, Zoology

Margaret McFall-Ngai, Professor, Medical Microbiology and Immunology

John-Demian Sauer, Assistant Professor, Medical Microbiology and Immunology

TABLE OF CONTENTS

Abstract	ii
Acknowledgements	iii
Chapter 1	Introduction	1
Chapter 2	Innate immune response to <i>Streptococcus iniae</i> infection in zebrafish larvae	78
Chapter 3	Regulation of macrophage inflammation in a larval zebrafish model of <i>Streptococcus iniae</i> infection	131
Chapter 4	Conclusions and Future Directions	172
Appendix I	Non-invasive imaging of the innate immune response in a zebrafish larval model of <i>Streptococcus iniae</i> infection	183
Appendix II	Heat shock modulates neutrophil motility in zebrafish	219
Appendix III	Distinct signaling mechanisms mediate neutrophil attraction to bacterial infection and tissue injury	252

Abstract

Neutrophils and macrophages are an important first line of defense against invading pathogens. While best known for their antimicrobial activities, these phagocytic cells also are important modulators of the immune response. Understanding how neutrophils and macrophages interact with one another to coordinate the host response to infection is of major importance and is the topic of this dissertation. Here, I use the transparent zebrafish larva to investigate the host innate immune response to localized infection with the fish and human pathogen, *Streptococcus iniae*. In Chapter 2, I show that both neutrophils and macrophages are rapidly recruited to the site of infection and can phagocytose *S. iniae*. Depletion of either cell type results in increased susceptibility to infection. As part of the inflammatory response, I show in Chapter 3 that macrophages aggregate in the tail of infected larvae. The development of these aggregate structures is mediated, at least in part, by neutrophils and leukotriene B4 (LTB4) production since larvae with impaired neutrophil function or larvae lacking Lta4h, the enzyme responsible for LTB4 production, do not develop macrophage aggregates and also have increased susceptibility to infection. Neutrophil-specific expression of Lta4h is sufficient to induce macrophage aggregation and rescues the survival defect in Lta4h-deficient larvae. Taken together, I have shown that the phagocyte response to *S. iniae* infection is crucial to host defense, and in addition to their antimicrobial activities, neutrophils can modulate macrophage behavior to *S. iniae* infection through Lta4h signaling.

Acknowledgements

It is hard to believe that I have finally reached the end of my PhD, and what an exciting journey it has been! I could not have made it this far without the love, support and encouragement of my family, friends and mentors. A huge thanks to all of you for helping me find my way! First, I would like to thank Dr. Donald A. Bryant, Dr. Carl Sillman and Dr. Philip Mohr at Penn State University for encouraging my scientific curiosity both in lab and in the classroom – without your support, I never would have made the leap to grad school!

I would like to express my gratitude to my advisor, Dr. Anna Huttenlocher, for her mentorship throughout this entire process. The freedom you have provided to try out new ideas and collaborations has helped me grow as a scientist by learning how to think both independently and creatively. Thank you for all of your support.

To my thesis committee: Dr. Heidi Goodrich-Blair, Dr. Margaret McFall-Ngai, Dr. Mary Halloran, Dr. JD Sauer and Dr. Bruce Klein - you have all been instrumental in providing new perspectives, sharing new ideas and giving constructive criticism. Additionally, I have thoroughly enjoyed some of our scientific collaborations.

To the Huttlab family, both past and present members, I am not sure how I would have made it through this without you! Words cannot express how grateful I am to have such amazingly talented, helpful, supportive and FUN labmates. Thanks for all of the great times both in lab and outside – our terrace trips, trivia nights, potlucks, camping trip, etc., have provided a great distraction from long hours in lab. David and Julie (and their army of undergrads!), there is no way the lab would be able to run without you, so thank you for all of

the hard work you do! To my office buddies, Lindsay, Katie and Penny – I will miss all of our conversations; you all have been such great friends and a fantastic support system. I would also like to extend my thanks to Peter Cavnar for your guidance when I first joined the lab and your continued support and encouragement. I feel honored to have met all of you; I know you will all continue to do great things, and I cannot wait to hear about it!

To my Madison friends and in particular Beth D., Emilia, Kedren, Kristy, Kristen, Caryn, Coral and Patricia, thanks for forcing me to get out of the lab and have some fun every once in awhile; may we have many more adventures to come! And last, but certainly not least, thank you to my parents, Ed and Sue Harvie, and my sister, Erica. Your faith in me has never wavered, and for that I am most grateful. I guess now that I am wrapping up my PhD, it is time to finally get a real job!

Chapter 1

Introduction

Part of this Chapter is modified from the following published review article:

Harvie, E. A., and Huttenlocher, A. (2015) “Neutrophils in host defense: new insights from zebrafish.” *Journal of Leukocyte Biology*.

The innate immune response to infection

The innate immune response is a critical first line of defense against invading microorganisms. Host cells with pattern recognition receptors (PRRs) are able to sense the presence of microorganisms by recognizing conserved structures known as microbe-associated molecular patterns (MAMPs). Four different classes of PRRs have been identified: transmembrane Toll-like receptors (TLRs) and C-type lectin receptors (CLRs) as well as cytoplasmic Retinoic acid-inducible gene receptors (RIG-I-like) and NOD-like receptors (NLRs) (1). Activation of PRRs results in upregulation in transcription of genes involved in the pro-inflammatory response. As part of this response, leukocytes, including neutrophils and macrophages, are rapidly recruited to contain the infection. Neutrophils and macrophages are the main phagocytes of the innate immune response and are the focus of this dissertation work.

Macrophages are a component of both human and zebrafish innate immune systems. Tissue-resident macrophages patrol host tissues using their PRRs to sense the presence of microorganisms. Once activated, macrophages utilize a variety of antimicrobial effector functions. Following phagocytosis, digestive enzymes such as proteases, nucleases, and lysozyme degrade the microbe in acidified phagosomes. Production of antimicrobial peptides and reactive nitrogen or oxygen species can kill or damage ingested microbes. Both autophagy (2) and pyroptosis (3) are also mechanisms by which macrophages target intracellular bacteria for destruction. In addition to their antimicrobial functions, activated

macrophages produce chemokines and cytokines to recruit other host leukocytes to the site of infection.

Neutrophils are the most abundant type of circulating leukocyte in both humans and zebrafish and are typically the first responders recruited to sites of tissue injury or infection (4, 5). To traffic to a site of infection, neutrophils mobilize from hematopoietic tissue and travel through the vasculature. Once at the site of infection, these highly motile cells play a critical role in initial defense through phagocytosis of microbes, secretion of granule proteins and other antimicrobials, production of reactive oxygen species, and release of neutrophil extracellular traps (NETs) (6, 7). Neutrophils also mediate the pro-inflammatory response to infection by releasing cytokines that recruit and activate other immune cells. The crucial importance of neutrophils in host defense against infection is demonstrated by enhanced susceptibility of neutropenic patients to a wide range of bacterial and fungal infections (5).

The use of zebrafish larvae to study the innate immune response to infection

The progression of infectious disease is determined by dynamic and complex interactions between host defense systems and pathogen virulence factors. While detailed *in vitro* analyses have provided critical insight into this delicate interaction, its complexity is more easily studied *in vivo*, especially when both host and pathogen are amenable to genetic analysis. There has been increasing use of the larval zebrafish (*Danio rerio*) to study infectious disease because its optical accessibility and potential for genetic manipulations allow visualization of the immune response to infection inside a living, intact vertebrate host.

Genetic tools in zebrafish allow for the generation of transgenic lines with fluorescently labeled cell populations including neutrophils (8, 9) and macrophages (10). The vertebrate innate immune system is highly conserved in zebrafish and includes: complement (11), Toll-like receptors (12, 13), macrophages (14) and neutrophils (4, 15). The adaptive immune system is not functionally mature until 4-6 weeks post fertilization (16-18), and thus, the study of host-pathogen interactions in the embryonic and larval stages of development allows for an understanding of the specific contribution of innate immunity to host defense. Importantly, transient manipulation of gene expression is readily available in the larval zebrafish including injection of synthetic mRNA for overexpression and injection of antisense morpholino oligonucleotides for gene suppression. Recently, the generation of null mutants has become easier and faster with the application of gene editing tools including CRISPR/Cas (19) and TALENs (20).

Zebrafish macrophage and neutrophil development

Myelopoiesis in zebrafish is genetically controlled by the transcription factor Pu.1/Spi1 (21). Pu.1-expressing myeloid precursors are first detected about 12 hours post fertilization (hpf) (22). Neutrophils and macrophages originate in the developing larval zebrafish from both the primitive and definitive waves of hematopoiesis. During the primitive wave, myeloid precursors arise in the rostral blood island (RBI; also known as the anterior lateral plate mesoderm) and migrate over the yolk sac, where they differentiate into primitive macrophages by 22 hpf (14). These primitive macrophages either invade the head

mesenchyme where they differentiate into microglial cells (23) or they enter the blood where their roles include removing apoptotic bodies or phagocytosing invading microbes (14). A subset of these primitive macrophages then differentiate further into neutrophils by 33 hpf (15). Definitive or multilineage hematopoiesis begins as early as 24 hpf when a transient population of pluripotent erythromyeloid progenitor cells differentiates within the posterior blood island (PBI), an area that later expands to become the caudal hematopoietic tissue (CHT) (24, 25). These cells are soon replaced by another group of hematopoietic stem cells that migrates from the aorta-gonad-mesonephros (AGM) through the blood to start colonizing the CHT by 48 hpf (26), where they also give rise to neutrophils and tissue-resident macrophages (25). Neutrophil distribution in the developing larva includes a population of neutrophils in the CHT as well as a population of randomly migrating neutrophils in the head mesenchyme (**Fig. 1A**; supplemental Video 1). By 4 dpf, the kidney marrow begins to mature and will become the site of definitive hematopoiesis in adult fish (27).

Zebrafish macrophages and neutrophils are fully functional in the early developmental stages, capable of phagocytosis by 28-30 hpf (14, 15) and of generating a respiratory burst by 72 hpf (28). Zebrafish neutrophils are also capable of NETosis (29), the release of decondensed chromatin, histones and granule proteins into the extracellular space to physically trap and kill microbes by exposing them to high local concentrations of antimicrobial molecules (30, 31). Direct visualization of neutrophils in response to wounding has led to new insight into neutrophil behavior at sites of tissue damage. Indeed, a study of the neutrophil response to wounds in zebrafish provided the first direct demonstration that

resolution of neutrophil infiltration at wounds can occur by neutrophil reverse migration and not apoptosis (8). Reverse transmigration of neutrophils from a site of inflammation has also been reported with primary human neutrophils *in vitro* (32) and more recently in a mouse model of ischemia-reperfusion injury (33). This highlights the advantage of using zebrafish as a model for visualizing leukocyte behavior *in vivo*, and supports the idea that zebrafish represent an important model system that complements studies using mouse and human immune cells.

Tools for imaging neutrophils and macrophages in zebrafish

Neutrophils can be imaged in whole fixed zebrafish using Sudan Black, which stains the rod-shaped cytoplasmic granules irreversibly (15), or immunostaining. Differentiated neutrophils and macrophages both express the pan-leukocyte marker L-plastin (*lcp1*) (34), and immunolabeling of L-plastin has been used to visualize leukocytes in fixed larvae (35). For live *in vivo* imaging, the generation of transgenic lines that label zebrafish neutrophils and macrophages has provided an important tool to image phagocyte behavior. Transgenic lines with fluorescently labeled leukocytes have been made possible, in part, by the Tol2 system, which allows for the efficient integration of exogenous DNA into the genome (36). Photoconvertible proteins such as Dendra2 (37, 38) or Kaede (39, 40) allow for the tracking of individual host cells over the course of infection. Fluorescent transgenic lines using the *pu.1/spi1* promoter have been used to drive expression in all myeloid cell precursors (41, 42). Reporter lines specific for macrophages or neutrophils have also been generated in zebrafish.

Myeloperoxidase and lysozyme C are both components of mammalian neutrophil granules (43), and the myeloid peroxidase (*mpx*) (8, 9) and lysozyme C (*lyz*) (34, 44) promoters are generally neutrophil-specific in zebrafish. Although it has been shown that *lyz* marks both neutrophils and macrophages at 32 hpf (45), *lyz* primarily labels neutrophils by 48 hpf (34, 46). An additional transgenic line with expression in only a subset of neutrophils was generated using an enhancer trap screen (34). Labeled neutrophils in this line are able to respond to both wounds and bacterial infection and make up ~50% of the neutrophil population. This suggests that different subsets of neutrophils serve distinct functions in zebrafish innate immunity. Until recently, a macrophage-specific reporter line did not exist which greatly hindered the study of this cell type. Although the *fli1a* promoter drives expression mainly in endothelial cells, there is also expression in a subset of macrophage-like cells (48, 49). The *fms* (CSF1R) promoter is macrophage-specific in mice (50, 51), and in zebrafish, *fms* is not expressed in neutrophils (34) but is expressed in a population of migratory inflammatory macrophages (52). Although *fms* is also expressed in zebrafish in neural crest cells like xanthophores, these cells are immobile and thus, can be separated from the mobile macrophage (52). The macrophage expressed gene 1 (*mpeg1*) is also expressed specifically in macrophages in mice and humans (53), and reporter lines using the *mpeg1* promoter label macrophages, but not xanthophores in zebrafish (10, 54). With the generation of a macrophage-specific reporter line (10, 54), double transgenic fish allow for the observation of neutrophil-macrophage interactions during inflammation and infection in intact hosts (10).

The use of fluorescently labeled microbes and phagocyte transgenic lines allows for the spatial and temporal imaging of host-pathogen interactions in a living animal (**Fig. 1C** and **1D**; supplemental Videos 2 and 3). As in mammalian models, both localized and systemic infections can be modeled in the larval zebrafish, depending on the initial site of infection. A number of different anatomical sites in the larval zebrafish have been used to investigate the host response to systemic infection (**Fig. 1B**), but the most commonly used injection sites are the caudal vein (CV) and duct of Cuvier (DC). Localized infection in the hindbrain ventricle (HBV) (58), the otic vesicle (OV) (15), dorsal tail muscle (DM) (59, 60), and pericardial cavity (PC) (61) allows imaging of phagocyte recruitment. Visual analysis of phagocyte function *in vivo* is enhanced by using fluorescent reporter probes. During phagocytosis, pHrodo dye can be used to label microbes and will fluoresce when exposed to acidic environments, like the leukocyte phagosome (62). There are also probes for live imaging of the production of reactive oxygen (ROS) (63, 64) and reactive nitrogen species (RNS) (65, 66).

Depletion of neutrophils or macrophages can provide important information about phagocyte function during infection (52). Neutrophils or macrophages can be depleted using zebrafish lines that express the bacterial nitroreductase under control of neutrophil- or macrophage-specific promoters. The *Escherichia coli* nitroreductase converts the drug metronidazole to a cytotoxic product, inducing cell death in expressing cells to achieve tissue-specific ablation (67, 68). Importantly, it has been shown that specific ablation of neutrophils or macrophages using this technique has no effect on the other population (69).

Antisense morpholino oligonucleotides can also be used to deplete specific phagocyte populations. Morpholinos are nucleic acid analogs that act to block splicing or initiation of translation of the target mRNA. Limitations of morpholino technology include lack of tissue specificity and transient effects, typically wearing off after 3 dpf. Morpholinos targeting *pu.1* deplete both neutrophils and macrophages and are often used to examine the effect of myeloid cell loss on host defense. A morpholino targeting *irf8* specifically depletes macrophages, but not neutrophils. However, a caveat of this approach is that depletion of *irf8* results in an expansion of the neutrophil population (70). Recently, an *irf8* null mutant has been generated in which *mpeg*-positive cells are not present until after 4 dpf; in fish older than 4 dpf, immature *mpeg*-positive cells are produced, although in lower numbers than the number of mature macrophages in similarly-aged wild type fish (71). A morpholino target that allows specific depletion of neutrophils has not been reported. Several groups have used a morpholino targeting *granulocyte colony stimulating factor receptor (Gcsfr)/colony stimulating factor 3 receptor (Csf3r)* to reduce neutrophil numbers (65, 72), but *gcsfr/csf3r* is also expressed in a subset of monocytes and macrophages (73), and expression of macrophage-specific *mpeg1* is dependent on *gcsfr/csf3r* signaling (10). Thus, although a Gcsfr/Csf3 morpholino largely reduces the neutrophil population, it also affects a subset of macrophages (74, 75).

Eicosanoids in the innate immune response to infection

In order for a host to successfully contain an infection, there has to be a balance of pro-inflammatory and anti-inflammatory mediators. Pro-inflammatory mediators help limit pathogen growth, but if not kept in check by anti-inflammatory, pro-resolving mediators, they can cause uncontrolled inflammation and tissue damage. On the other hand, if anti-inflammatory, pro-resolving activity is too excessive or occurs too early in infection, this can result in pathogen growth, making the host increasingly susceptible to infection. Eicosanoids, such as leukotrienes and lipoxins, are lipid mediators derived from the oxidation of arachidonic acid and are involved in homeostatic biological functions as well as both the pro-inflammatory and anti-inflammatory sides of inflammation (76).

Leukotrienes

Leukotrienes are pro-inflammatory eicosanoids produced by leukocytes, mainly neutrophils and macrophages, following interaction of cell surface receptors with MAMPs or opsonin molecules (77, 78). Activation of cell surface receptors triggers the release of arachidonic acid from membrane phospholipids by cytosolic phospholipase A2 (cPLA2). Oxygenation of arachidonic acid by 5-lipoxygenase (5-LO) and its helper protein, 5-LO activating protein (FLAP) results in the production of leukotriene A4 (LTA4). LTA4 can be further metabolized by leukotriene A4 hydrolase (LTA4H) into the well-known pro-inflammatory molecule, leukotriene B4 (LTB4).

Binding of LTB₄ to its downstream G-protein coupled receptors, BLT1/BLT2, results in a variety of pro-inflammatory downstream effector functions. LTB₄ is a potent chemoattractant of leukocytes and is responsible for increased leukocyte accumulation at the site of infection due to increased recruitment of circulating leukocytes (79, 80), increased adhesion to the endothelium by upregulation of integrins (81) and decreased apoptosis (46, 82). LTB₄ also activates recruited and resident leukocytes to ingest and kill microbes through enhanced phagocytosis of parasites (83) and bacteria (47, 55, 56), lysosomal enzyme release (57), granule protein release (84) and activation of the NADPH oxidase complex (85, 86) as well as increased production of antimicrobials (87, 88) and nitric oxide (89). In addition, leukotrienes stimulate the production of other pro-inflammatory cytokines from leukocytes such as TNF α (90), IL-8 (91), MCP-1 (92) and IL-6 (93) to further amplify leukotriene production and pro-inflammatory responses.

The first *in vivo* study to suggest a potential antimicrobial role for leukotrienes showed that administration of exogenous LTB₄ enhances clearance of *Salmonella enterica* infection (47). More recently, with the generation of leukotriene-deficient mice generated by disruption of the 5-LO gene (94, 95), a greater understanding of the role leukotrienes play in host defense against infection has been elucidated. A role for endogenous leukotrienes was demonstrated in a study by Bailie et al. who reported that 5-LO^{-/-} mice are increasingly susceptible to pulmonary infection with *Klebsiella pneumoniae* and exogenous LTB₄ is sufficient to rescue the enhanced susceptibility (55). Subsequent studies using leukotriene-

deficient mice have also shown enhanced susceptibility to infection with bacteria (96, 97), fungi (98), and parasites (99).

Excessive leukotriene production can be more detrimental than beneficial to the host. Since chronic, non-resolving inflammation can result in a number of diseases such as asthma (100), cystic fibrosis (101), inflammatory bowel disease (102), psoriasis (103) and rheumatoid arthritis (104, 105), resolution of inflammation is an important mechanism to prevent these complications of excessive or prolonged inflammation.

Lipoxins

Lipoxins are anti-inflammatory, pro-resolving lipid mediators structurally related to leukotrienes. Lipoxins are generated from LTA₄ by 12-lipoxygenase (12-LO) or 15-lipoxygenase (15-LO). Lipoxin production results in inhibition of neutrophil functions, stimulation of monocyte locomotion (106) and phagocytosis of apoptotic leukocytes by monocytes (107). Lipoxins also regulate the pro-inflammatory response by stimulating suppressors of cytokine signaling (SOCS) (108). Although resolution of inflammation is important in preventing excessive tissue damage, these anti-inflammatory, pro-resolving mediators can also increase the susceptibility of the host to chronic infections by preventing the pro-inflammatory responses necessary for microbial clearance. *Toxoplasma gondii* (109), *Mycobacterium marinum* (110), and *Mycobacterium tuberculosis* (111) are several examples of microbes that induce host production of lipoxins, presumably to avoid eradication by the pro-inflammatory response and establish a chronic, persistent infection. In fact, both *T. gondii*

(112) and *Pseudomonas aeruginosa* (113) encode secreted enzymes with 15-LO activity which are hypothesized to use arachidonic acid from their mammalian hosts to produce lipoxins to dampen the pro-inflammatory response and allow establishment of infection.

Interestingly, although a study by Peres et al. (97) found that 5-LO deficient mice were increasingly susceptible to infection with *M. tuberculosis*, another study by Bafica et al. (111) found that 5-LO^{-/-} mice were protected against infection with low dose of *M. tuberculosis*. Work done in the zebrafish model of *Mycobacterium* infection has helped shed some light on the roles of leukotrienes and lipoxins in the host immune response.

Using zebrafish to study the role of leukotrienes and lipoxins in infection

Leukotriene A4 hydrolase (Lta4h) was found to influence host susceptibility to *M. marinum* infection during a zebrafish mutagenesis screen (110). This enzyme is required for production of pro-inflammatory LTB₄ and sits at a key crossroads regulating the balance between pro-inflammatory LTB₄ production and anti-inflammatory lipoxin production. Both Lta4h deficiency and excess resulted in increased host susceptibility to mycobacterial infection. Deficiency in Lta4h results in an increase in production of anti-inflammatory lipoxins, which, in turn, reduces pro-inflammatory TNF levels. This results in enhanced intracellular bacterial burden causing necrosis of granuloma macrophages and extracellular release of bacteria (110, 114). Excess Lta4h results in an initial ability of the host to control bacterial proliferation, but the increased TNF levels induced by the highly pro-inflammatory environment also results in macrophage necrosis and an expanding extracellular bacterial

population (114). Thus, susceptibility to *M. marinum* results from either excessive or inadequate information.

This work done in zebrafish was used to demonstrate that specific therapies chosen based on host genotype could be used to correct the hyper- or hypo-inflamed statuses of *Mycobacterium*-infected hosts. Anti-inflammatories such as aspirin or corticosteroids reduced the pro-inflammatory status of Lta4h-high fish and rescued the hypersusceptibility to disease by triggering production of lipoxins, but this same therapy was detrimental when applied to the Lta4h-deficient fish. On the other hand, therapy aimed at reducing lipoxin levels rescued the hypersusceptibility in the Lta4h-deficient fish but was detrimental to the Lta4h-high fish (114). Thus, the inflammatory status, as mediated by the Lta4h genotype, determined host response to targeted therapies. Similarly, it was found that LTA4H promoter polymorphisms in TB meningitis patients influenced individual patient response to treatment (114) demonstrating the productivity of this larval zebrafish model in providing direct translational applications for human disease treatments.

Models of Primary Immunodeficiency in Zebrafish

Defects in phagocyte function in humans lead to severe, recurrent bacterial and fungal infections. Primary immunodeficiency disorders include neutrophil mobilization and adhesion defects, altered actin-based motility of phagocytes, and impaired microbial killing. The following is a summary of how zebrafish have been used to model human immune deficiencies that affect neutrophil and macrophage function.

Warts, Hypogammaglobulinemia, Infections and Myelokathexis (WHIM) Syndrome

WHIM syndrome is a primary immunodeficiency characterized by warts, hypogammaglobulinemia, infections and myelokathexis, a type of severe, chronic neutropenia with apoptosis of mature myeloid cells in the bone marrow (115, 116). Stromal cell-derived factor 1 (SDF1) is expressed in bone marrow stromal cells and binds the receptor CXCR4 (117), which is expressed on mature neutrophils in the bone marrow (118). In WHIM syndrome, gain of function mutations associated with truncation of CXCR4 prevent CXCR4 internalization and result in the active retention of neutrophils in the bone marrow (118). In a mouse model of WHIM syndrome, expression of the CXCR4 WHIM mutations in hematopoietic stem cells impairs neutrophil release from the bone marrow and increases neutrophil apoptosis (119), causing neutropenia and recapitulating the human disease. A zebrafish model of WHIM syndrome is also associated with reduced circulating neutrophils and recapitulates the neutropenia, although there was no reported effect on neutrophil apoptosis (120). Endogenous expression of Sdf1a mRNA is concentrated in areas of neutrophil production in zebrafish embryos, both in the head and the CHT. Expression of the human WHIM mutations (121) in zebrafish neutrophils impairs Cxcr4b internalization and leads to retention of neutrophils in the CHT. Thus, WHIM neutrophils are not recruited to sites of wounding or infection, resulting in increased susceptibility to infection. Morpholino-mediated depletion of Sdf1a rescues neutrophil retention in the bone marrow (120) indicating that, like in humans and mice, Sdf1a in zebrafish mediates the neutrophil retention signal. Thus, the zebrafish model of WHIM syndrome complements human and mouse WHIM

models and provides the advantage of being amenable to direct visualization of the effects of altered chemokine signaling on neutrophil trafficking *in vivo*.

Leukocyte Adhesion Deficiency (LAD)

Leukocyte Adhesion Deficiency (LAD) represents a group of human disorders characterized by an increase in circulating neutrophils (neutrophilia) and recurrent infections (122). There are different types of LAD, depending on the underlying genetic defect (reviewed in (123)). LAD IV (124) is a recently reported type of LAD identified in two patients with a dominant inhibitory mutation in the hematopoietic tissue-specific Rho GTPase, Rac2 (125 -128). Rac2, the GTP-binding protein in neutrophils (129), plays important roles in neutrophil activation by regulating the actin cytoskeleton, cell migration and NADPH oxidase activity (130). Rac2^{-/-} mice display neutrophilia and impaired emigration out of the vasculature to sites of infection, resulting in increased susceptibility to infections like *Aspergillus fumigatus* (131). The phenotype of Rac2-deficient mice is similar to the phenotype of human patients with a dominant inhibitory mutation in Rac2 (Rac2D57N). Neutrophils from these patients have impaired chemotaxis (126, 128), azurophilic granule secretion (125) and defects in superoxide generation (126, 127, 132). A zebrafish model of LAD IV (LAD fish) also recapitulates the neutrophilia and increased susceptibility to infection (133) seen in mammalian disease. Zebrafish neutrophils expressing the dominant inhibitory Rac2D57N mutation show defects in cell polarization and migration (61, 125, 133). The zebrafish model provides new insight into the mechanisms that contribute

to neutrophilia. LAD fish exhibit both an increase in neutrophil mobilization from hematopoietic tissue and a defect in egress from the vasculature to sites of tissue damage, resulting in neutrophilia. Interestingly, neutrophil retention in the CHT in WHIM fish is attenuated by the expression of Rac2D57N in neutrophils (133), suggesting a critical role for Rac2-Cxcr4 signaling in retaining neutrophils in hematopoietic tissue. Thus, the zebrafish model of LAD recapitulates the human disease and provides new insight into the signaling mechanisms that mediate neutrophil retention in hematopoietic tissue.

Wiskott Aldrich Syndrome (WAS) and X-linked Neutropenia

Leukocyte trafficking to infection requires the ability of leukocytes to sense directional cues and modify their actin cytoskeleton to form an F-actin-rich leading edge. The Wiskott-Aldrich Syndrome protein (WASp) is a key regulator of actin dynamics (134) that binds the actin-nucleating protein Arp2/3, resulting in actin polymerization at branch points along actin filaments (135). Mutations in WASp result in a primary immunodeficiency known as Wiskott Aldrich Syndrome, which is characterized by recurrent infections, autoimmunity and bleeding disorders (136). Zebrafish have two WASp orthologs in hematopoietic cells, zWASp1 and zWASp2, which are 52% and 41% similar to human WASp, respectively (137). Morpholino-mediated depletion of zWASp1 results in impaired directed migration of both neutrophils and macrophages to a tail wound due to defects in pseudopod selection and directed migration (137). To validate the morpholino studies, a zWASp1 mutant was generated (137) by TILLING (138). As in zWASp1 morphants, the

zWASp1 null mutant has a normal number of neutrophils and macrophages, but these leukocytes exhibit impaired recruitment to a tailfin wound (139) with defects in pseudopod selection similar to *in vitro* studies (140, 141). The WASp null mutant also has increased susceptibility to bacterial infection with *Staphylococcus aureus*, recapitulating the infection phenotype of WAS patients (139). Constitutively activating mutations in the GTPase binding domain of WASp results in X-linked Neutropenia (142) and have also been modeled in zebrafish larvae (139) to provide an *in vivo* model for human X-linked Neutropenia.

Chronic Granulomatous Disease (CGD)

Chronic Granulomatous Disease (CGD) is an immunodeficiency characterized by inflammatory granulomatous lesions and enhanced susceptibility to bacterial and fungal infections. CGD is associated with mutations in the phagocyte NADPH oxidase complex (PHOX) that impair the ability of leukocytes to produce an oxidative burst (143, 144). Components of the PHOX complex include the membrane-bound components p22^{phox} and gp91^{phox}, cytosolic components p47^{phox} and p67^{phox}, the regulatory units p40^{phox} and the small GTPase Rac1 or Rac2 (144). Upon phagocyte activation, the cytosolic and membrane-bound components form the intact PHOX complex leading to the generation of superoxide, which is converted to hydrogen peroxide by superoxide dismutase (144). Hydrogen peroxide, in the presence of myeloperoxidase, can be converted further to other antimicrobial reactive oxygen species such as hypochlorous acid (43). These reactive oxygen species activate neutrophil granule proteins and contribute to microbial killing (145). Although there is currently no

transgenic model of CGD in zebrafish, the use of morpholinos targeting different components of the PHOX complex have successfully been used to model CGD (44, 146). These studies demonstrate that phagocyte-mediated killing of *Candida albicans* (146) and *Mycobacterium marinum* (44) are dependent on their ability to generate an oxidative burst.

IRF8 deficiency

Interferon regulatory factor-8 (IRF8), also known as the interferon consensus sequence-binding protein (ICSBP), is expressed predominantly in lymphocytes, macrophages and dendritic cells in mammals and regulates the transcription of interferon genes during the immune response (147). In mice and humans, IRF8 is important for myeloid development, and deficiency results in a reduction of macrophage/monocyte numbers but an expansion of neutrophil numbers (148 -150). IRF8 deficiency is also associated with acute and chronic myeloid leukemia and increased susceptibility to infection in both mice and humans (148 - 152).

The expression pattern of IRF8 is highly conserved among vertebrates. Morpholino-mediated depletion of *Irf8* in zebrafish embryos reveals that *Irf8* acts downstream of Pu.1 in primitive myelopoiesis to promote differentiation of macrophages while suppressing neutrophil formation, and thus, is a critical determinant in macrophage versus neutrophil fate (70). Additionally, *Irf8* morphants have enhanced invasive disease and susceptibility to *A. fumigatus* infection (153). Similar to morphants, *irf8* null mutants lack macrophages during early development and also have an expanded population of neutrophils (71). Once adult

phase definitive hematopoiesis begins, however, immature macrophages begin reappearing, though in much smaller numbers than in age-matched heterozygous siblings (71). Although *irf8* mutants are viable through 3 months post fertilization, their survival rate is reduced compared to heterozygous and wild-type siblings probably due to an increased susceptibility to infection, similar to findings in IRF8 deficient mice and humans (148, 150). In addition, macrophage- (*mpeg*) or neutrophil (*lyz*) –specific expression of *irf8* in *irf8* mutants demonstrated that both immature myeloid and neutrophil populations are capable of developing into mature macrophages when expressing *Irf8*, supporting an *in vitro* study in which forced expression of *irf8* in immortal mouse IRF8-null cell lines promoted macrophage differentiation while suppressing neutrophil development (71, 154). The development of this *Irf8* mutant will allow for the study of the specific contribution of macrophages to infectious disease.

Insights into phagocyte-pathogen interactions in zebrafish

Zebrafish have been used to model both bacterial and fungal disease. For a comprehensive list of zebrafish infection models see **Table 1**. This dissertation focuses on how neutrophils and macrophages contribute to host defense against infection with *Streptococcus iniae*.

S. iniae is a natural fish pathogen and causes systemic disease characterized by meningitis and sepsis in both fish and humans. With a worldwide distribution, *S. iniae* can infect over 25 species of fresh and saltwater fish (155), causing both skin infections as well as

invasive systemic disease. *S. iniae* disease results in 30-50% mortality in affected fish ponds, resulting in \$100 million in annual losses for the aquaculture industry (155- 157). In humans, *S. iniae* is an opportunistic pathogen, infecting mainly the elderly and immunocompromised. Invasive human disease caused by *S. iniae* is characterized by cellulitis of the upper extremities or more invasive disease such as sepsis and meningitis (158), and thus, has similar pathologies to those caused by infection with Group A or Group B streptococci, respectively. Given its similarity to human pathogens and its impact on the aquaculture industry, *S. iniae* is an important pathogen to study.

To evade host defenses and establish disease, *S. iniae* utilizes a number of virulence factors including: an M-like protein that contributes to adhesion and invasion as well as resistance to phagocytic clearance (5, 44, 159), a C5a peptidase (160), Streptolysin S which damages host cell membranes (161, 162), phosphoglucomutase which has important roles in polysaccharide capsule production cell wall morphology (163), a peptidoglycan deacetylase (164), exopolysaccharide (165) and a polysaccharide capsule (54, 166). Capsule is important for *S. iniae* virulence in an adult zebrafish model of infection (166 -168) and a mutagenesis screen for mutants with attenuated virulence identified several mutants with insertions in genes required for capsule biosynthesis, including in the *cpsA* gene of the capsule locus (167, 168). The identified capsule mutants were increasingly susceptible to phagocytosis in whole blood (167) and were internalized more efficiently by a fish macrophage cell line compared to wild-type *S. iniae* (166). The *cpsA* mutant was shown to be deficient in polysaccharide capsule production (168) further supporting an important role for capsule in *S. iniae* disease.

Localized *S. iniae* infection induces recruitment of leukocytes to infection sites in mice and adult zebrafish and infection spreads systemically resulting in rapid host mortality (169, 170). The time between the initial infection and host death is too short a time to involve adaptive immunity, suggesting that the innate immune system is the most critical contributor to host defense against this pathogen. In order to gain a more in-depth understanding into how host neutrophils and macrophages respond to *S. iniae* infection *in vivo*, it is necessary to use a host that is more amenable to non-invasive live imaging, such as the larval zebrafish.

The first larval zebrafish model of *S. iniae* infection is presented here in **Chapter 2**. This model allows live, real-time analysis of the neutrophil and macrophage response to localized otic vesicle infection with wild type *S. iniae* as well as the capsule-deficient *cpsA* mutant. Localized infection allows for the characterization of leukocyte recruitment and phagocytosis of bacteria. In addition, the amenability of the larval zebrafish to genetic manipulations enables the investigation of the individual contributions of neutrophils and macrophages to infection. **Chapter 3** provides a closer look at neutrophil-macrophage crosstalk during infection and how neutrophils influence macrophage behavior through the release of eicosanoids. Overall, this dissertation provides an in-depth look into host-pathogen interactions as well as how host leukocytes interact with each other to coordinate the host response to infection, made possible through the use of the optically transparent larval zebrafish.

References

1. **Takeuchi O, Akira S.** Pattern Recognition Receptors and Inflammation. *Cell* **140**:805–820.
2. **Randow F, Youle RJ.** 2014. Self and nonself: how autophagy targets mitochondria and bacteria. *Cell Host & Microbe* **15**:403–411.
3. **Miao EA, Leaf IA, Treuting PM, Mao DP, Dors M, Sarkar A, Warren SE, Wewers MD, Aderem A.** 2010. Caspase-1-induced pyroptosis is an innate immune effector mechanism against intracellular bacteria. *Nature Immunology* **11**:1136–1142.
4. **Lieschke GJ.** 2001. Morphologic and functional characterization of granulocytes and macrophages in embryonic and adult zebrafish. *Blood* **98**:3087–3096.
5. **Amulic B, Cazalet C, Hayes GL, Metzler KD, Zychlinsky A.** 2012. Neutrophil Function: From Mechanisms to Disease. *Annu. Rev. Immunol.* **30**:459–489.
6. **Borregaard N.** 2010. Neutrophils, from Marrow to Microbes. *Immunity* **33**:657–670.
7. **Nathan C.** 2006. Neutrophils and immunity: challenges and opportunities. *Nature Reviews Immunology* **6**:173–182.
8. **Mathias JR, Perrin BJ, Liu TX, Kanki J, Look AT, Huttenlocher A.** 2006. Resolution of inflammation by retrograde chemotaxis of neutrophils in transgenic zebrafish. *Journal of Leukocyte Biology* **80**:1281–1288.

9. **Renshaw SA, Loynes CA, Trushell DMI, Elworthy S, Ingham PW, Whyte MKB.** 2006. A transgenic zebrafish model of neutrophilic inflammation. *Blood* **108**:3976–3978.
10. **Ellett F, Pase L, Hayman JW, Andrianopoulos A, Lieschke GJ.** 2011. mpeg1 promoter transgenes direct macrophage-lineage expression in zebrafish. *Blood* **117**:e49–56.
11. **Seeger A, Mayer WE, Klein J.** 1996. A Complement Factor B-Like cDNA clone from the Zebrafish (*Brachydanio rerio*). *Mol. Immunol.*
12. **Jault C, Pichon L, Chluba J.** 2004. Toll-like receptor gene family and TIR-domain adapters in *Danio rerio*. *Mol. Immunol.* **40**:759–771.
13. **Meijer AH, Gabby Krens SF, Medina Rodriguez IA, He S, Bitter W, Ewa Snaar-Jagalska B, Spaink HP.** 2004. Expression analysis of the Toll-like receptor and TIR domain adaptor families of zebrafish. *Mol. Immunol.* **40**:773–783.
14. **Herbomel P, Thisse B, Thisse C.** 1999. Ontogeny and behaviour of early macrophages in the zebrafish embryo. *Development* **126**:3735–3745.
15. **Le Guyader D, Redd MJ, Colucci-Guyon E, Murayama E, Kissa K, Briolat V, Mordelet E, Zapata A, Shinomiya H, Herbomel P.** 2008. Origins and unconventional behavior of neutrophils in developing zebrafish. *Blood* **111**:132–141.
16. **Lam SH, Chua HL, Gong Z, Lam TJ, Sin YM.** 2004. Development and maturation of the immune system in zebrafish, *Danio rerio*: a gene expression profiling, in situ hybridization and immunological study. *Developmental & Comparative Immunology*

- 28:9–28.
17. **Danilova N, Steiner LA.** 2002. B cells develop in the zebrafish pancreas. *PNAS* **99**:13711–13716.
 18. **Willett CE, Cortes A, Zuasti A, Zapata A.** 1999. Early Hematopoiesis and Developing Lymphoid Organs in the Zebrafish. *Dev. Dyn.* **214**:323–336.
 19. **Hwang WY, Fu Y, Reyon D, Maeder ML, Tsai SQ, Sander JD, Peterson RT, Yeh J-RJ, Joung JK.** 2013. Brief communications. *Nat Biotechnol* **31**:227–229.
 20. **Hwang WY, Peterson RT, Yeh J-RJ.** 2014. Methods for targeted mutagenesis in zebrafish using TALENs. *Methods* **69**:76–84.
 21. **Rhodes J, Hagen A, Hsu K, Deng M, Liu TX, Look AT, Kanki JP.** 2005. Interplay of pu.1 and gata1 determines myelo-erythroid progenitor cell fate in zebrafish. *Developmental Cell* **8**:97–108.
 22. **Lieschke GJ, Oates AC, Paw BH, Thompson MA, Hall NE, Ward AC, Ho RK, Zon LI, Layton JE.** 2002. Zebrafish SPI-1 (PU.1) marks a site of myeloid development independent of primitive erythropoiesis: implications for axial patterning. *Developmental Biology* **246**:274–295.
 23. **Herbomel P, Thisse B, Thisse C.** 2001. Zebrafish early macrophages colonize cephalic mesenchyme and developing brain, retina, and epidermis through a M-CSF receptor-dependent invasive process. *Developmental Biology* **238**:274–288.
 24. **Bertrand JY, Kim AD, Violette EP, Stachura DL, Cisson JL, Traver D.** 2007. Definitive hematopoiesis initiates through a committed erythromyeloid progenitor in

- the zebrafish embryo. *Development* **134**:4147–4156.
25. **Murayama E, Kissa K, Zapata A, Mordelet E, Briolat V, Lin H-F, Handin RI, Herbomel P.** 2006. Tracing Hematopoietic Precursor Migration to Successive Hematopoietic Organs during Zebrafish Development. *Immunity* **25**:963–975.
 26. **Jin H, Sood R, Xu J, Zhen F, English MA, Liu PP, Wen Z.** 2009. Definitive hematopoietic stem/progenitor cells manifest distinct differentiation output in the zebrafish VDA and PBI. *Development* **136**:647–654.
 27. **Bennett CM, Kanki JP, Rhodes J, Liu TX, Paw BH, Kieran MW, Langenau DM, Delahaye-Brown A, Zon LI, Fleming MD, Look AT.** 2001. Myelopoiesis in the zebrafish, *Danio rerio*. *Blood* **98**:643–651.
 28. **Hermann AC, Millard PJ, Blake SL, Kim CH.** 2004. Development of a respiratory burst assay using zebrafish kidneys and embryos. *Journal of Immunological Methods* **292**:119–129.
 29. **Palić D, Ostojić J, Andreasen CB, Roth JA.** 2007. Fish cast NETs: Neutrophil extracellular traps are released from fish neutrophils. *Developmental & Comparative Immunology* **31**:805–816.
 30. **Brinkmann V, Reichard U, Goosmann C, Fauler B, Uhlemann Y, Weiss DS, Weinrauch Y, Zychlinsky A.** 2004. Neutrophil Extracellular Traps Kill Bacteria. *Science* **303**:1532–1535.
 31. **Fuchs TA, Abed U, Goosmann C, Hurwitz R, Schulze I, Wahn V, Weinrauch Y, Brinkmann V, Zychlinsky A.** 2007. Novel cell death program leads to neutrophil

- extracellular traps. *The Journal of Cell Biology* **176**:231–241.
32. **Buckley CD, Ross EA, McGettrick HM, Osborne CE, Haworth O, Schmutz C, Stone PCW, Salmon M, Matharu NM, Vohra RK, Nash GB, Rainger GE.** 2006. Identification of a phenotypically and functionally distinct population of long-lived neutrophils in a model of reverse endothelial migration. *Journal of Leukocyte Biology* **79**:303–311.
33. **Woodfin A, Voisin M-B, Beyrau M, Colom B, Caille D, Diapouli F-M, Nash GB, Chavakis T, Albelda SM, Rainger GE, Meda P, Imhof BA, Nourshargh S.** 2011. The junctional adhesion molecule JAM-C regulates polarized transendothelial migration of neutrophils in vivo. *Nature Immunology* 1–10.
34. **Meijer AH, van der Sar AM, Cunha C, Lamers GEM, Laplante MA, Kikuta H, Bitter W, Becker TS, Spaik HP.** 2008. Identification and real-time imaging of a myc-expressing neutrophil population involved in inflammation and mycobacterial granuloma formation in zebrafish. *Developmental & Comparative Immunology* **32**:36–49.
35. **Mathias JR, Dodd ME, Walters KB, Yoo SK, Ranheim EA, Huttenlocher A.** 2009. Characterization of zebrafish larval inflammatory macrophages. *Developmental & Comparative Immunology* **33**:1212–1217.
36. **Urasaki A, Morvan G, Kawakami K.** 2006. Functional Dissection of the Tol2 Transposable Element Identified the Minimal cis-Sequence and a Highly Repetitive Sequence in the Subterminal Region Essential for Transposition. *Genetics* **174**:639–

- 649.
37. **Yoo SK, Huttenlocher A.** 2011. Spatiotemporal photolabeling of neutrophil trafficking during inflammation in live zebrafish. *Journal of Leukocyte Biology* **89**:661–667.
 38. **Gurskaya NG, Verkhusha VV, Shcheglov AS, Staroverov DB, Chepurnykh TV, Fradkov AF, Lukyanov S, Lukyanov KA.** 2006. Engineering of a monomeric green-to-red photoactivatable fluorescent protein induced by blue light. *Nat Biotechnol* **24**:461–465.
 39. **Hatta K, Tsujii H, Omura T.** 2006. Cell tracking using a photoconvertible fluorescent protein. *Nat Protoc* **1**:960–967.
 40. **Ando R, Hama H, Yamamoto-Hino M, Mizuno H, Miyawaki A.** 2002. An optical marker based on the UV-induced green- to-red photoconversion of a fluorescent protein. *PNAS* **99**:12651–12656.
 41. **Ward AC, McPhee DO, Condrón MM, Varma S, Cody SH, Onnebo SMN, Paw BH, Zon LI, Lieschke GJ.** 2003. The zebrafish *spi1* promoter drives myeloid-specific expression in stable transgenic fish. *Blood* **102**:3238–3240.
 42. **Hsu K.** 2004. The *pu.1* promoter drives myeloid gene expression in zebrafish. *Blood* **104**:1291–1297.
 43. **Klebanoff SJ.** 2005. Myeloperoxidase: friend and foe. *Journal of Leukocyte Biology* **77**:598–625.
 44. **Yang C-T, Cambier CJ, Davis JM, Hall CJ, Crosier PS, Ramakrishnan L.** 2012.

- Neutrophils exert protection in the early tuberculous granuloma by oxidative killing of mycobacteria phagocytosed from infected macrophages. *Cell Host & Microbe* **12**:301–312.
45. **Hall C, Flores M, Storm T, Crosier K, Crosier P.** 2007. The zebrafish lysozyme C promoter drives myeloid-specific expression in transgenic fish. *BMC Dev Biol* **7**:42.
46. **Lee E, Robertson T, Smith J, Kilfeather S.** 2000. Leukotriene Receptor Antagonists and Synthesis Inhibitors Reverse Survival in Eosinophils of Asthmatic Individuals. *Am. J. Respir. Crit. Care Med.* **161**:1881–1886.
47. **Demitsu T, Katayama H, Saito-Taki T, Yaoita H, Nakano M.** 1989. Phagocytosis and bactericidal action of mouse peritoneal macrophages treated with leukotriene B₄. *Int. J. Immunopharmacol.* **11**:801–808.
48. **Redd MJ, Kelly G, Dunn G, Way M, Martin P.** 2006. Imaging macrophage chemotaxis in vivo: Studies of microtubule function in zebrafish wound inflammation. *Cell Motil. Cytoskeleton* **63**:415–422.
49. **Lawson ND, Weinstein BM.** 2002. In vivo imaging of embryonic vascular development using transgenic zebrafish. *Developmental Biology* **248**:307–318.
50. **Burnett SH, Kershen EJ, Zhang J, Zeng L, Straley SC, Kaplan AM, Cohen DA.** 2004. Conditional macrophage ablation in transgenic mice expressing a Fas-based suicide gene. *Journal of Leukocyte Biology* **75**:612–623.
51. **Sasmono RT, Oceandy D, Pollard JW, Tong W, Pavli P, Wainwright BJ, Ostrowski MC, Himes SR, Hume DA.** 2003. A macrophage colony-stimulating

- factor receptor-green fluorescent protein transgene is expressed throughout the mononuclear phagocyte system of the mouse. *Blood* **101**:1155–1163.
52. **Gray C, Loynes CA, Whyte MKB, Crossman DC, Renshaw SA, Chico TJA.** 2011. Simultaneous intravital imaging of macrophage and neutrophil behaviour during inflammation using a novel transgenic zebrafish. *Thromb Haemost* **105**:811–819.
53. **Spilsbury K, O'Mara MA, Wu WM, Rowe PB, Symonds G, Takayama Y.** 1995. Isolation of a novel macrophage-specific gene by differential cDNA analysis. *Blood* **85**:1620–1629.
54. **Harvie EA, Green JM, Neely MN, Huttenlocher A.** 2013. Innate Immune Response to *Streptococcus iniae* Infection in Zebrafish Larvae. *Infection and Immunity* **81**:110–121.
55. **Bailia MB, Standiford TJ, Laichalk LL, Coffey MJ, Strieter R, Peters-Golden M.** 1996. Leukotriene-Deficient Mice Manifest Enhanced Lethality from *Klebsiella* Pneumonia in Association with Decreased Alveolar Macrophage Phagocytic and Bactericidal Activities. *Journal of Immunology* (Baltimore, Md. : 1950).
56. **Mancuso P, Standiford TJ, Marshall T, Peters-Golden M.** 1998. 5-Lipoxygenase reaction products modulate alveolar macrophage phagocytosis of *Klebsiella pneumoniae*. *Infection and Immunity* **66**:5140–5146.
57. **Serhan CN, Radin A, Smolen JE, Korchak H, Samuelsson B, Weissmann G.** 1982. Leukotriene B4 is a complete secretagogue in human neutrophils: A kinetic

- analysis. *Biochem. Biophys. Res. Commun.*
58. **Davis JM, Clay H, Lewis JL, Ghori N, Herbomel P, Ramakrishnan L.** 2002. Real-time visualization of mycobacterium-macrophage interactions leading to initiation of granuloma formation in zebrafish embryos. *Immunity* **17**:693–702.
59. **Lin A, Loughman JA, Zinselmeyer BH, Miller MJ, Caparon MG.** 2009. Streptolysin S Inhibits Neutrophil Recruitment during the Early Stages of *Streptococcus pyogenes* Infection. *Infection and Immunity* **77**:5190–5201.
60. **Colucci-Guyon E, Tinevez JY, Renshaw SA, Herbomel P.** 2011. Strategies of professional phagocytes in vivo: unlike macrophages, neutrophils engulf only surface-associated microbes. *Journal of Cell Science* **124**:3053–3059.
61. **Wiles TJ, Bower JM, Redd MJ, Mulvey MA.** 2009. Use of Zebrafish to Probe the Divergent Virulence Potentials and Toxin Requirements of Extraintestinal Pathogenic *Escherichia coli*. *PLoS Pathog* **5**:e1000697.
62. **Hall C, Flores MV, Chien A, Davidson A, Crosier K, Crosier P.** 2009. Transgenic zebrafish reporter lines reveal conserved Toll-like receptor signaling potential in embryonic myeloid leukocytes and adult immune cell lineages. *Journal of Leukocyte Biology* **85**:751–765.
63. **Hall CJ, Boyle RH, Astin JW, Flores MV, Oehlers SH, Sanderson LE, Ellett F, Lieschke GJ, Crosier KE, Crosier PS.** 2013. Immunoresponsive gene 1 augments bactericidal activity of macrophage-lineage cells by regulating β -oxidation-dependent mitochondrial ROS production. *Cell Metab.* **18**:265–278.

64. **Hall CJ, Boyle RH, Sun X, Wicker SM, Misa JP, Krissansen GW, Print CG, Crosier KE, Crosier PS.** 2014. Epidermal cells help coordinate leukocyte migration during inflammation through fatty acid-fuelled matrix metalloproteinase production. *Nat Commun* **5**:3880.
65. **Hall CJ, Flores MV, Oehlers SH, Sanderson LE, Lam EY, Crosier KE, Crosier PS.** 2012. Infection-Responsive Expansion of the Hematopoietic Stem and Progenitor Cell Compartment in Zebrafish Is Dependent upon Inducible Nitric Oxide. *Cell Stem Cell* **10**:198–209.
66. **Elks PM, Brizee S, van der Vaart M, Walmsley SR, van Eeden FJ, Renshaw SA, Meijer AH.** 2013. Hypoxia Inducible Factor Signaling Modulates Susceptibility to Mycobacterial Infection via a Nitric Oxide Dependent Mechanism. *PLoS Pathog* **9**:e1003789.
67. **Curado S, Anderson RM, Jungblut B, Mumm J, Schroeter E, Stainier DYR.** 2007. Conditional targeted cell ablation in zebrafish: A new tool for regeneration studies. *Dev. Dyn.* **236**:1025–1035.
68. **Curado S, Stainier DYR, Anderson RM.** 2008. Nitroreductase-mediated cell/tissue ablation in zebrafish: a spatially and temporally controlled ablation method with applications in developmental and regeneration studies. *Nat Protoc* **3**:948–954.
69. **Prajsnar TK, Hamilton R, Garcia-Lara J, McVicker G, Williams A, Boots M, Foster SJ, Renshaw SA.** 2012. A privileged intraphagocyte niche is responsible for disseminated infection of *Staphylococcus aureus* in a zebrafish model. *Cell*

- Microbiol **14**:1600–1619.
70. **Li L, Jin H, Xu J, Shi Y, Wen Z.** 2011. Irf8 regulates macrophage versus neutrophil fate during zebrafish primitive myelopoiesis. *Blood* **117**:1359–1369.
71. **Shiau CE, Kaufman Z, Meireles AM, Talbot WS.** 2015. Differential requirement for irf8 in formation of embryonic and adult macrophages in zebrafish. *PLoS ONE* **10**:e0117513.
72. **Palha N, Guivel-Benhassine F, Briolat V, Lutfalla G, Sourisseau M, Ellett F, Wang C-H, Lieschke GJ, Herbomel P, Schwartz O, Levraud J-P.** 2013. Real-Time Whole-Body Visualization of Chikungunya Virus Infection and Host Interferon Response in Zebrafish. *PLoS Pathog* **9**:e1003619.
73. **Stachura DL, Svoboda O, Campbell CA, Espin-Palazon R, Lau RP, Zon LI, Bartunek P, Traver D.** 2013. The zebrafish granulocyte colony-stimulating factors (Gcsfs): 2 paralogous cytokines and their roles in hematopoietic development and maintenance. *Blood* **122**:3918–3928.
74. **Liongue C, Hall CJ, O'Connell BA, Crosier P, Ward AC.** 2009. Zebrafish granulocyte colony-stimulating factor receptor signaling promotes myelopoiesis and myeloid cell migration. *Blood* **113**:2535–2546.
75. **Feng Y, Renshaw S, Martin P.** 2012. Live imaging of tumor initiation in zebrafish larvae reveals a trophic role for leukocyte-derived PGE₂. *Curr. Biol.* **22**:1253–1259.
76. **Funk CD.** 2001. Prostaglandins and leukotrienes: advances in eicosanoid biology. *Science* **294**:1871–1875.

77. **Peters-Golden M, Canetti C, Mancuso P, Coffey MJ.** 2005. Leukotrienes: Underappreciated Mediators of Innate Immune Responses. *Journal of Immunology* (Baltimore, Md. : 1950) **174**:589–594.
78. **Flamand N, Mancuso P, Serezani CHC, Brock TG.** 2007. Leukotrienes: Mediators that have been typecast as villains. *Cell. Mol. Life Sci.* **64**:2657–2670.
79. **Ford-Hutchinson AW, Bray MA, Doig MV, Shipley ME, Smith MJH.** 1980. Leukotriene B, a potent chemokinetic and aggregating substance released from polymorphonuclear leukocytes. *Nature.*
80. **Matsukawa A, Hogaboam CM, Lukacs NW, Lincoln PM, Strieter RM, Kunkel SL.** 1999. Endogenous Monocyte Chemoattractant Protein-1 (MCP-1) Protects Mice in a Model of Acute Septic Peritonitis: Cross-Talk Between MCP-1 and Leukotriene B₄. *Journal of Immunology* (Baltimore, Md. : 1950) **163**:6148–6154.
81. **Zimmerman BJ, Holt JW, Paulson JC, Anderson DC, Miyasaka M, Tamatani T, Todd RF, Rusche JR, Granger DN.** 1994. Molecular determinants of lipid mediator-induced leukocyte adherence and emigration in rat mesenteric venules. *American Journal of Physiology* **266**:H847–H853.
82. **Hebert M-J, Takano T, Hothofer H, Brady HR.** 1996. Sequential Morphologic Events During Apoptosis of Human Neutrophils. *Journal of Immunology* (Baltimore, Md. : 1950) **157**:3105–3115.
83. **Wirth JJ, Kierszenbaum F.** 1985. Stimulatory effects of leukotriene B₄ on macrophage association with and intracellular destruction of *Trypanosoma cruzi*. *The*

Journal of Immunology.

84. **Borgeat P, Naccache PH.** 1990. Biosynthesis and biological activity of leukotriene B4. *Clin. Biochem.* **23**:459–468.
85. **Dewald B, Baggiolini M.** 1985. Activation of NADPH Oxidase in Human Neutrophils. Synergism Between fMLP and the Neutrophil Products PAF and LTB4. *Biochem. Biophys. Res. Commun.*
86. **Serezani CHC, Aronoff DM, Jancar S, Peters-Golden M.** 2005. Leukotriene B4 mediates p47phox phosphorylation and membrane translocation in polyunsaturated fatty acid-stimulated neutrophils. *Journal of Leukocyte Biology* **78**:976–984.
87. **Flamand L, Borgeat P, Lalonde R, Gosselin J.** 2004. Release of Anti-HIV Mediators after Administration of Leukotriene B4 to Humans. *The Journal of Infectious Diseases* **189**:2001–2009.
88. **Wan M, Sabirsh A, Wetterholm A, Agerberth B, Haeggstrom JZ.** 2007. Leukotriene B4 triggers release of the cathelicidin LL-37 from human neutrophils: novel lipid-peptide interactions in innate immune responses. *The FASEB Journal* **21**:2897–2905.
89. **Talvani A, Machado FS, Santana GC, Klein A, Barcelos L, Silva JS, Teixeira MM.** 2002. Leukotriene B4 Induces Nitric Oxide Synthesis in Trypanosoma cruzi-Infected Murine Macrophages and Mediates Resistance to Infection. *Infection and Immunity* **70**:4247–4253.
90. **Goldman G, Welbourn R, Kobzik L, Valeri CR, Shepro D, Hechtman HB.** 1993.

Lavage with leukotriene B4 induces lung generation of tumor necrosis factor-alpha that in turn mediates neutrophil diapedesis. *Surgery* **113**:297–303.

91. **Kuhns DB, Nelson EL, Alvord WG, Gallin JI.** 2001. Fibrinogen induces IL-8 synthesis in human neutrophils stimulated with formyl-methionyl-leucyl-phenylalanine or leukotriene B(4). *Journal of Immunology (Baltimore, Md. : 1950)* **167**:2869–2878.
92. **Huang L, Zhao A, Wong F, Ayala JM, Struthers M, Ujjainwalla F, Wright SD, Springer MS, Evans J, Cui J.** 2004. Leukotriene B4 strongly increases monocyte chemoattractant protein-1 in human monocytes. *Arterioscler. Thromb. Vasc. Biol.* **24**:1783–1788.
93. **Brach MA, de Vos S, Arnold C, Gruss HJ, Mertelsmann R, Herrmann F.** 1992. Leukotriene B4 transcriptionally activates interleukin-6 expression involving NK-chi B and NF-IL6. *Eur. J. Immunol.* **22**:2705–2711.
94. **Chen X-S, Sheller JR, Johnson EN, Funk CD.** 1994. Role of leukotrienes revealed by targeted disruption of the 5-lipoxygenase gene. *Nature.*
95. **Goulet JL, Snouwaert JN, Latour AM, Coffman TN, Koller BH.** 1994. Altered inflammatory responses in leukotriene-deficient mice. *PNAS* **91**:12852–12856.
96. **Mancuso P, Lewis C, Serezani CH, Goel D, Peters-Golden M.** 2010. Intrapulmonary Administration of Leukotriene B4 Enhances Pulmonary Host Defense against Pneumococcal Pneumonia. *Infection and Immunity* **78**:2264–2271.
97. **Peres CM, de Paula L, Medeiros AI, Sorgi CA, Soares EG, Carlos D, Peters-**

- Golden M, Silva CL, Faccioli LH.** 2007. Inhibition of leukotriene biosynthesis abrogates the host control of *Mycobacterium tuberculosis*. *Microbes Infect.* **9**:483–489.
98. **Medeiros AI, Sá-Nunes A, Turato WM, Secatto A, Frantz FG, Sorgi CA, Serezani CH, Deepe GS, Faccioli LH.** 2008. Leukotrienes are potent adjuvant during fungal infection: effects on memory T cells. *The Journal of Immunology* **181**:8544–8551.
99. **Serezani CH, Perrela JH, Russo M, Peters-Golden M, Jancar S.** 2006. Leukotrienes Are Essential for the Control of *Leishmania amazonensis* Infection and Contribute to Strain Variation in Susceptibility. *Journal of Immunology* (Baltimore, Md. : 1950) **177**:3201–3208.
100. **Dahlen S-E, Hedqvist P, Hammarstrom S, Samuelsson B.** 1980. Leukotrienes are potent constrictors of human bronchi. *Nature.*
101. **Cromwell O, Walport MJ, Morris HR, Taylor GW, Hodson ME, Batten J, Kay AB.** 1981. Identification of leukotrienes D and B in sputum from cystic fibrosis patients. *Lancet* **2**:164–165.
102. **Cole AT, Pilkington BJ, McLaughlan J, Smith C, Balsitis M, Hawkey CJ.** 1996. Mucosal factors inducing neutrophil movement in ulcerative colitis: the role of interleukin 8 and leukotriene B4. *Gut* **39**:248–254.
103. **Ruzicka T, Simmet T, Peskar BA, Ring J.** 1986. Skin levels of arachidonic acid-derived inflammatory mediators and histamine in atopic dermatitis and psoriasis. *The*

- Journal of Investigative Dermatology.
104. **Griffiths RJ, Pettipher ER, Koch K, Farrell CA, Breslow R, Conklyn MJ, Smith MA, Hackman BC, Wimberly DJ, Milici AJ, Scampoli DN, Cheng JB, Pillar JS, Pazoles CJ, Doherty NS, Melvin LS, Reiter LA, Biggars MS, Falkner FC, Mitchell DY, Liston TE, Showell HJ.** 1995. Leukotriene B4 plays a critical role in the progression of collagen-induced arthritis. *PNAS* **92**:517–521.
 105. **Klickstein LB, Shapleigh C, Goetzl EJ.** 1980. Lipoxygenation of arachidonic acid as a source of polymorphonuclear leukocyte chemotactic factors in synovial fluid and tissue in rheumatoid arthritis and spondyloarthritis. *The Journal of Clinical Investigation.*
 106. **Levy BD, Clish CB, Schmidt B, Gronert K, Serhan CN.** 2001. Lipid mediator class switching during acute inflammation: signals in resolution. *Nature Immunology* **2**:612–619.
 107. **Godson C, Mitchell S, Harvey K, Petasis NA, Hogg N, Brady HR.** 2000. Cutting edge: lipoxins rapidly stimulate nonphlogistic phagocytosis of apoptotic neutrophils by monocyte-derived macrophages. *Journal of Immunology (Baltimore, Md. : 1950)* **164**:1663–1667.
 108. **Machado FS, Johndrow JE, Esper L, Dias A, Bafica A, Serhan CN, Aliberti J.** 2006. Anti-inflammatory actions of lipoxin A4 and aspirin-triggered lipoxin are SOCS-2 dependent. *Nat Med* **12**:330–334.
 109. **Aliberti J, Serhan C, Sher A.** 2002. Parasite-induced lipoxin A4 is an endogenous

- regulator of IL-12 production and immunopathology in *Toxoplasma gondii* infection. *J. Exp. Med.* **196**:1253–1262.
110. **Tobin DM, Vary JC Jr, Ray JP, Walsh GS, Dunstan SJ, Bang ND, Hagge DA, Khadge S, King M-C, Hawn TR, Moens CB, Ramakrishnan L.** 2010. The *Ita4h* Locus Modulates Susceptibility to Mycobacterial Infection in Zebrafish and Humans. *Cell* **140**:717–730.
111. **Bafica A, Scanga CA, Serhan CN, Machado F, White S, Sher A, Aliberti J.** 2005. Host control of *Mycobacterium tuberculosis* is regulated by 5-lipoxygenase-dependent lipoxin production. *The Journal of Clinical Investigation.*
112. **Bannenberg GL, Aliberti J, Hong S, Sher A, Serhan CN.** 2004. Exogenous Pathogen and Plant 15-Lipoxygenase Initiate Endogenous Lipoxin A4 Biosynthesis. *J. Exp. Med.*
113. **Vance RE, Hong S, Gronert K, Serhan CN, Mekalanos JJ.** 2004. The opportunistic pathogen *Pseudomonas aeruginosa* carries a secretable arachidonate 15-lipoxygenase. *PNAS.*
114. **Tobin DM, Roca FJ, Oh SF, McFarland R, Vickery TW, Ray JP, Ko DC, Zou Y, Bang ND, Chau TTH, Vary JC, Hawn TR, Dunstan SJ, Farrar JJ, Thwaites GE, King M-C, Serhan CN, Ramakrishnan L.** 2012. Host Genotype-Specific Therapies Can Optimize the Inflammatory Response to Mycobacterial Infections. *Cell* **148**:434–446.
115. **Wetzler M, Talpaz M, Kleinerman ES, King A, Huh YO, Gutterman JU,**

- Kurzrock R.** 1990. A New Familial Immunodeficiency Disorder Characterized by Severe Neutropenia, a Defective Marrow Release Mechanism, and Hypogammaglobulinemia. *The American Journal of Medicine* **89**:663–672.
116. **Gorlin RJ, Gelb B, Diaz GA, Lofsness KG, Pittelkow MR, Fenyk JR Jr.** 2000. WHIM Syndrome, An Autosomal Dominant Disorder: Clinical, Hematological, and Molecular Studies. *American Journal of Medical Genetics* **91**:368–376.
117. **Oberlin E, Amara A, Bachelier F, Bessia C, Virelizier JL, Arenzana-Seisdedos F, Schwartz O, Heard JM, Clark-Lewis I, Legler DF, Loetscher M, Baggiolini M, Moser B.** 1996. The CXC chemokine SDF-1 is the ligand for LESTR/fusin and prevents infection by T-cell-line-adapted HIV-1. *Nature* **382**:833–835.
118. **Furze RC, Rankin SM.** 2008. Neutrophil mobilization and clearance in the bone marrow. *Immunology* **125**:281–288.
119. **Kawai T, Choi U, Cardwell L, DeRavin SS, Naumann N, Whiting-Theobald NL, Linton GF, Moon J, Murphy PM, Malech HL.** 2007. WHIM syndrome myelokathexis reproduced in the NOD/SCID mouse xenotransplant model engrafted with healthy human stem cells transduced with C-terminus-truncated CXCR4. *Blood* **109**:78–84.
120. **Walters KB, Green JM, Surfus JC, Yoo SK, Huttenlocher A.** 2010. Live imaging of neutrophil motility in a zebrafish model of WHIM syndrome. *Blood* **116**:2803–2811.
121. **Hernandez PA, Gorlin RJ, Lukens JN, Taniuchi S, Bohinjec J, Francois F,**

- Klotman ME, Diaz GA.** 2003. Mutations in the chemokine receptor gene CXCR4 are associated with WHIM syndrome, a combined immunodeficiency disease. *Nature Genetics* **34**:70–74.
122. **Etzioni A, Alon R.** 2004. Leukocyte adhesion deficiency III: a group of integrin activation defects in hematopoietic lineage cells. *Current Opinion in Allergy and Clinical Immunology* **4**:485–490.
123. **Etzioni A.** 2009. Defects in the Leukocyte Adhesion Cascade. *Clinic Rev Allerg Immunol* **38**:54–60.
124. **Pai S-Y, Kim C, Williams DA.** 2010. Rac GTPases in human diseases. *Dis. Markers* **29**:177–187.
125. **Ambruso DR, Knall C, Abell AN, Panepinto J, Kurkchubasche A, Thurman G, Gonzalez-Aller C, Hiester A, deBoer M, Harveck RJ, Oyer R, Johnson GL, Roos D.** 2000. Human neutrophil immunodeficiency syndrome is associated with an inhibitory Rac2 mutation. *PNAS* **97**:4654–4659.
126. **Williams DA, Tao W, Yang F, Kim C, Gu Y, Mansfield P, Levine JE, Petryniak B, Darrow CW, Harris C, Jia B, Zheng Y, Ambruso DR, Lowe JB, Atkinson SJ, Dinuer MC, Boxer L.** 2000. Dominant negative mutation of the hematopoietic-specific Rho GTPase, Rac2, is associated with a human phagocyte immunodeficiency. *Blood* **96**:1646–1654.
127. **Accetta D, Syverson G, Bonacci B, Reddy S, Bengston C, Surfus J, Harbeck R, Huttenlocher A, Grossman W, Routes J, Verbsky J.** 2011. Human phagocyte

- defect caused by a Rac2 mutation detected by means of neonatal screening for T-cell lymphopenia. *Journal of Allergy and Clinical Immunology* **127**:535–538.
128. **Berthier E, Surfus J, Verbsky J, Huttenlocher A, Beebe D.** 2010. An arrayed high-content chemotaxis assay for patient diagnosis. *Integr. Biol.* **2**:630.
129. **Heyworth PG, Bohl BP, Bokoch GM, Curnutte JT.** 1994. Rac translocates independently of the neutrophil NADPH oxidase components p47phox and p67phox. Evidence for its interaction with flavocytochrome b558. *The Journal of Biological Chemistry* **269**:30749–30752.
130. **Kaibuchi K, Kuroda S, Amano M.** 1999. Regulation of the cytoskeleton and cell adhesion by the Rho family GTPases in mammalian cells. *Annu. Rev. Biochem.* **68**:459–486.
131. **Roberts AW, Kim C, Zhen L, Lowe JB, Kapur R, Petryniak B, Spaetti A, Pollock JD, Borneo JB, Bradford GB, Atkinson SJ, Dinauer MC, Williams DA.** 1999. Deficiency of the Hematopoietic Cell-Specific Rho Family GTPase Rac2 Is Characterized by Abnormalities in Neutrophil Function and Host Defense. *Immunity* **10**:183–196.
132. **Prajsnar TK, Renshaw SA, Ogryzko NV, Foster SJ, Serror P, Mesnage S.** 2013. Zebrafish as a Novel Vertebrate Model To Dissect Enterococcal Pathogenesis. *Infection and Immunity* **81**:4271–4279.
133. **Deng Q, Yoo SK, Cavnar PJ, Green JM, Huttenlocher A.** 2011. Dual Roles for Rac2 in Neutrophil Motility and Active Retention in Zebrafish Hematopoietic

- Tissue. *Developmental Cell* **21**:735–745.
134. **Derry JMJ, Ochs HD, Francke U.** 1994. Isolation of a Novel Gene Mutated in Wiskott-Aldrich Syndrome. *Cell* **78**:635–644.
135. **Takenawa T, Suetsugu S.** 2007. The WASP–WAVE protein network: connecting the membrane to the cytoskeleton. *Nat Rev Mol Cell Biol* **8**:37–48.
136. **Hans DO, Thrasher AJ.** 2006. The Wiskott-Aldrich syndrome. *Journal of Allergy and Clinical Immunology* **117**:725–738.
137. **Cvejic A, Hall C, Bak-Maier M, Flores MV, Crosier P, Redd MJ, Martin P.** 2008. Analysis of WASp function during the wound inflammatory response - live-imaging studies in zebrafish larvae. *Journal of Cell Science* **121**:3196–3206.
138. **Wienholds E, van Eeden F, Kusters M, Mudde J, Plasterk RHA, Cuppen E.** 2003. Efficient target-selected mutagenesis in zebrafish. *Genome Res.* **13**:2700–2707.
139. **Jones RA, Feng Y, Worth AJ, Thrasher AJ, Burns SO, Martin P.** 2013. Modelling of human Wiskott-Aldrich syndrome protein mutants in zebrafish larvae using in vivo live imaging. *Journal of Cell Science* **126**:4077–4084.
140. **Ishihara D, Dovas A, Park H, Isaac BM, Cox D.** 2012. The Chemotactic Defect in Wiskott-Aldrich Syndrome Macrophages Is Due to the Reduced Persistence of Directional Protrusions. *PLoS ONE* **7**:e30033.
141. **Zicha D, Allen WE, Brickell PM, Kinnon C, Dunn GA, Jones GE, Thrasher AJ.** 1998. Chemotaxis of macrophages is abolished in the Wiskott-Aldrich syndrome.

- British Journal of Haematology **101**:659–665.
142. **Devriendt K, Kim AS, Mathijs G, Frints SGM, Schwartz M, Van den Oord JJ, Verhoef GEG, Boogaerts MA, Fryns J-P, You D, Rosen MK, Vandenberghe P.** 2001. Constitutively activating mutation in WASP causes X- linked severe congenital neutropenia. *Nature Genetics* **27**:313–317.
143. **Segal BH, Leto TL, Gallin JI, Malech HL, Holland SM.** 2000. Genetic, biochemical, and clinical features of chronic granulomatous disease. *Medicine (Baltimore)* **79**:170–200.
144. **Holland SM.** 2009. Chronic Granulomatous Disease. *Clinic Rev Allerg Immunol* **38**:3–10.
145. **Reeves EP, Lu H, Jacobs HL, Messina CGM, Bolsover S, Gabella G, Potma EO, Warley A, Roes J, Segal AW.** 2002. Killing activity of neutrophils is mediated through activation of proteases by K⁺ flux. *Nature* **416**:291–297.
146. **Brothers KM, Newman ZR, Wheeler RT.** 2011. Live Imaging of Disseminated Candidiasis in Zebrafish Reveals Role of Phagocyte Oxidase in Limiting Filamentous Growth. *Eukaryotic Cell* **10**:932–944.
147. **Paun A, Pitha PM.** 2008. The IRF Family, Revisited. *Biochimie* **89**:744–753.
148. **Hambleton S, Salem S, Bustamante J, Bigley V, Boisson-Dupuis S, Azevedo J, Fortin A, Haniffa M, Ceron-Gutierrez L, Bacon CM, Menon G, Trouillet C, McDonald D, Carey P, Ginhoux F, Alsina L, Zumwalt TJ, Kong X-F, Kumararatne D, Butler K, Hubeau M, Feinberg J, Al-Muhsen S, Cant A, Abel**

- L, Chaussabel D, Doffinger R, Talesnik E, Grumach A, Duarte A, Abarca K, Moraes-Vasconcelos D, Burk D, Berghuis A, Geissmann F, Collin M, Casanova J-L, Gros P.** 2011. IRF8 Mutations and Human Dendritic-Cell Immunodeficiency. *N. Engl. J. Med.* **365**:127–138.
149. **Holtzschke T, Lohler J, Kanno Y, Ferh T, Giese N, Rosenbauer F, Lou J, Knobloch K-P, Gabriele L, Waring JF, Bachmann MF, Zinkernagel RM, Morse HC III, Ozato K, Horak I.** 1996. Immunodeficiency and Chronic Myelogenous Leukemia-like Syndrome in Mice with a Targeted Mutation of the ICSBP Gene. *Cell* **87**:307–317.
150. **Turcotte K.** 2005. A mutation in the *Icsbp1* gene causes susceptibility to infection and a chronic myeloid leukemia-like syndrome in BXH-2 mice. *Journal of Experimental Medicine* **201**:881–890.
151. **Pogosova-Agadjanyan EL, Kopecky KJ, Ostronoff F, Appelbaum FR, Godwin J, Lee H, List AF, May JJ, Oehler VG, Petersdorf S, Pogosov GL, Radich JP, Willman CL, Meshinchi S, Stirewalt DL.** 2013. The Prognostic Significance of IRF8 Transcripts in Adult Patients with Acute Myeloid Leukemia. *PLoS ONE* **8**:e70812.
152. **Schmidt M, Nagel S, Proba J, Thiede C, Ritter M, Waring JF, Rosenbauer F, Huhn D, Wittig B, Horak I, Neubauer A.** 1998. Lack of Interferon Consensus Sequence Binding Protein (ICSBP) Transcripts in Human Myeloid Leukemia. *Blood* **91**:22–29.

153. **Knox BP, Deng Q, Rood M, Eickhoff JC, Keller NP, Huttenlocher A.** 2014. Distinct Innate Immune Phagocyte Responses to *Aspergillus fumigatus* Conidia and Hyphae in Zebrafish Larvae. *Eukaryotic Cell* **13**:1266–1277.
154. **Tamura T, Nagamura-Inoue T, Shmeltzer Z, Kuwata T, Ozato K.** 2000. ICSBP Directs Bipotential Myeloid Progenitor Cells to Differentiate into Mature Macrophages. *Immunity* **13**:155–165.
155. **Agnew W, Barnes AC.** 2007. *Streptococcus iniae*: An aquatic pathogen of global veterinary significance and a challenging candidate for reliable vaccination. *Veterinary Microbiology* **122**:1–15.
156. **Eldar A, Bejerano Y, Bercovier H.** 1995. Experimental streptococcal meningo-encephalitis in cultured fish. *Veterinary Microbiology* **43**:33–40.
157. **Shoemaker CA, Klesius PH, Evans JJ.** 2001. Prevalence of *Streptococcus iniae* in tilapia, hybrid striped bass, and channel catfish on commercial fish farms in the United States. *Am. J. Vet. Res.* **62**:174–177.
158. **Weinstein MR, Litt M, Kertesz DA, Wyper P, Rose D, Coulter M, McGeer A, Facklam R, Ostach C, Willey BM, Borczyk A, Low DE.** 1997. Invasive Infections Due to a Fish Pathogen, *Streptococcus iniae*. *New England Journal of Medicine* **337**:589–594.
159. **Baiano JC, Tumbol RA, Umapathy A, Barnes AC.** 2008. Identification and molecular characterisation of a fibrinogen binding protein from *Streptococcus iniae*. *BMC Microbiology* **8**:67.
160. **Locke JB, Aziz RK, Vicknair MR, Nizet V, Buchanan JT.** 2008. *Streptococcus*

- iniae M-Like Protein Contributes to Virulence in Fish and Is a Target for Live Attenuated Vaccine Development. PLoS ONE **3**:e2824.
161. **Fuller J, Camus A, Duncan C, Nizet V, Bast D, Thune R, Low DE, de Azavedo JCS.** 2002. Identification of a Streptolysin S-Associated Gene Cluster and Its Role in the Pathogenesis of. Infection and Immunity **70**:5730–5739.
162. **Locke JB, Colvin KM, Varki N, Vicknair MR, Nizet V, Buchanan JT.** 2007. Streptococcus iniae beta-hemolysin streptolysin S is a virulence factor in fish infection. Dis. Aquat. Org. **76**:17–26.
163. **Buchanan JT, Stannard JA, Lauth X, Ostland VE, Powell HC, Westerman ME, Nizet V.** 2005. Streptococcus iniae phosphoglucomutase is a virulence factor and a target for vaccine development. Infection and Immunity **73**:6935–6944.
164. **Milani CJE, Aziz RK, Locke JB, Dahesh S, Nizet V, Buchanan JT.** 2010. The novel polysaccharide deacetylase homologue Pdi contributes to virulence of the aquatic pathogen Streptococcus iniae. Microbiology **156**:543–554.
165. **Eyngor M, Lublin A, Shapira R, Hurvitz A, Zlotkin A, Tekoah Y, Eldar A.** 2010. A pivotal role for the Streptococcus iniae extracellular polysaccharide in triggering proinflammatory cytokines transcription and inducing death in rainbow trout. FEMS Microbiology Letters **305**:109–120.
166. **Locke JB, Colvin KM, Datta AK, Patel SK, Naidu NN, Neely MN, Nizet V, Buchanan JT.** 2007. Streptococcus iniae Capsule Impairs Phagocytic Clearance and Contributes to Virulence in Fish. Journal of Bacteriology **189**:1279–1287.

167. **Miller JD, Neely MN.** 2005. Large-scale screen highlights the importance of capsule for virulence in the zoonotic pathogen *Streptococcus iniae*. *Infection and Immunity* **73**:921–934.
168. **Lowe BA, Miller JD, Neely MN.** 2007. Analysis of the Polysaccharide Capsule of the Systemic Pathogen *Streptococcus iniae* and Its Implications in Virulence. *Infection and Immunity* **75**:1255–1264.
169. **Neely MN, Pfeifer JD, Caparon MG.** 2002. *Streptococcus-Zebrafish* Model of Bacterial Pathogenesis. *Infection and Immunity* **70**:3904–3914.
170. **Miller JD, Neely MN.** 2004. Zebrafish as a model host for streptococcal pathogenesis. *Acta Tropica* **91**:53–68.
171. **Lü A-J, Hu X-C, Wang Y, Zhu A-H, Shen L-L, Tian J, Feng Z-Z, Feng Z-J.** 2014. Skin immune response in the zebrafish, *Danio rerio*(Hamilton), to *Aeromonas hydrophila*infection: a transcriptional profiling approach. *Journal of Fish diseases* n/a–n/a.
172. **Li J, Ni XD, Liu YJ, Lu CP.** 2011. Detection of three virulence genes *alt*, *ahp* and *aerA* in *Aeromonas hydrophila* and their relationship with actual virulence to zebrafish. *J Appl Microbiol* **110**:823–830.
173. **Cantas L, Midtlyng PJ, Sorum H.** 2012. Impact of antibiotic treatments on the expression of the R plasmid *tra* genes and on the host innate immune activity during pRAS1 bearing *Aeromonas hydrophila* infection in zebrafish (*Danio rerio*). *BMC Microbiology* **12**:37–37.

174. **Rawls JF, Samuel BS, Gordon JI.** 2004. Gnotobiotic zebrafish reveal evolutionarily conserved responses to the gut microbiota. *PNAS* **101**:4596–4601.
175. **Rawls JF, Mahowald MA, Ley RE, Gordon JI.** 2006. Reciprocal Gut Microbiota Transplants from Zebrafish and Mice to Germ-free Recipients Reveal Host Habitat Selection. *Cell* **127**:423–433.
176. **Lin B, Chen S, Cao Z, Lin Y, Mo D, Zhang H, Gu J, Dong M, Liu Z, Xu A.** 2007. Acute phase response in zebrafish upon *Aeromonas salmonicida* and *Staphylococcus aureus* infection: Striking similarities and obvious differences with mammals. *Mol. Immunol.* **44**:295–301.
177. **Bates JM, Mittge E, Kuhlman J, Baden KN, Cheesman SE, Guillemin K.** 2006. Distinct signals from the microbiota promote different aspects of zebrafish gut differentiation. *Developmental Biology* **297**:374–386.
178. **Chu W, Zhou S, Zhu W, Zhuang X.** 2014. Quorum quenching bacteria *Bacillus* sp. QSI-1 protect zebrafish (*Danio rerio*) from *Aeromonas hydrophila* infection. *Sci. Rep.* **4**.
179. **Grisolia CK, Oliveira-Filho EC, Ramos FR, Lopes MC, Muniz DHF, Monnerat RG.** 2009. Acute toxicity and cytotoxicity of *Bacillus thuringiensis* and *Bacillus sphaericus* strains on fish and mouse bone marrow. *Ecotoxicology (London, England)* **18**:22–26.
180. **Li X, Wang S, Qi J, Echtenkamp SF, Chatterjee R, Wang M, Boons G-J, Dziarski R, Gupta D.** 2007. Zebrafish Peptidoglycan Recognition Proteins are

- Bactericidal Amidases Essential for Defense against Bacterial Infections. *Immunity* **27**:518–529.
181. **Lima A, Cha BJ, Amin J, Smith LK, Anderson B.** 2014. Zebrafish Embryo Model of *Bartonella henselae* Infection. *Zebrafish* **11**:434–446.
182. **Deng Y, Boon C, Eberl L, Zhang LH.** 2009. Differential Modulation of *Burkholderia cenocepacia* Virulence and Energy Metabolism by the Quorum-Sensing Signal BDSF and Its Synthase. *Journal of Bacteriology* **191**:7270–7278.
183. **Vergunst AC, Meijer AH, Renshaw SA, O'Callaghan D.** 2010. *Burkholderia cenocepacia* Creates an Intramacrophage Replication Niche in Zebrafish Embryos, Followed by Bacterial Dissemination and Establishment of Systemic Infection. *Infection and Immunity* **78**:1495–1508.
184. **Agnoli K, Schwager S, Uehlinger S, Vergunst A, Viteri DF, Nguyen DT, Sokol PA, Carlier A, Eberl L.** 2011. Exposing the third chromosome of *Burkholderia cenocepacia* complex strains as a virulence plasmid. *Molecular Microbiology* **83**:362–378.
185. **Lü A, Hu X, Wang Y, Shen X, Zhu A, Shen L, Ming Q, Feng Z.** 2013. Comparative Analysis of the Acute Response of Zebrafish *Danio rerio* Skin to Two Different Bacterial Infections. *Journal of Aquatic Animal Health* **25**:243–251.
186. **Petrie-Hanson L, Romano CL, Mackey RB, Khosravi P, Hohn CM, Boyle CR.** 2007. Evaluation of Zebrafish *Danio rerio* as a Model for Enteric Septicemia of Catfish (ESC). *Journal of Aquatic Animal Health* **19**:151–158.

187. **Xiao J, chen T, Wang Q, Zhang Y.** 2012. Comparative analysis of the roles of catalases KatB and KatG in the physiological fitness and pathogenesis of fish pathogen *Edwardsiella tarda*. *Letters in Applied Microbiology* **54**:425–432.
188. **Wang X, Wang Q, Xiao J, Liu Q, Wu H, Xu L, Zhang Y.** 2009. *Edwardsiella tarda* T6SS component *evpP* is regulated by *esrB* and iron, and plays essential roles in the invasion of fish. *Fish & Shellfish Immunology* **27**:469–477.
189. **Pressley ME, Phelan PE III, Eckhard Witten P, Mellon MT, Kim CH.** 2005. Pathogenesis and inflammatory response to *Edwardsiella tarda* infection in the zebrafish. *Developmental & Comparative Immunology* **29**:501–513.
190. **Liu X, Chang X, Wu H, Xiao J, Gao Y, Zhang Y.** 2014. Role of intestinal inflammation in predisposition of *Edwardsiella tarda* infection in zebrafish (*Danio rerio*). *Fish & Shellfish Immunology* **41**:271–278.
191. **Dong X, Fan X, Wang B, Shi X, Zhang XH.** 2013. Invasion of *Edwardsiella tarda* is essential for its haemolytic activity, biofilm formation and virulence towards fish. *J Appl Microbiol* **115**:12–19.
192. **Yang D, Liu Q, Ni C, Li S, Wu H, Wang Q, Xiao J, Zhang Y.** 2013. Gene expression profiling in live attenuated *Edwardsiella tarda* vaccine immunized and challenged zebrafish: Insights into the basic mechanisms of protection seen in immunized fish. *Developmental & Comparative Immunology* **40**:132–141.
193. **van Soest JJ, Stockhammer OW, Ordas A, Bloemberg GV, Spaik HP, Meijer AH.** 2011. Comparison of static immersion and intravenous injection systems for

- exposure of zebrafish embryos to the natural pathogen *Edwardsiella tarda*. *BMC Immunology* **12**:58.
194. **van der Vaart M, van Soest JJ, Spaink HP, Meijer AH.** 2013. Functional analysis of a zebrafish *myd88* mutant identifies key transcriptional components of the innate immune system. *Disease Models & Mechanisms* **6**:841–854.
195. **Phennicie RT, Sullivan MJ, Singer JT, Yoder JA, Kim CH.** 2010. Specific Resistance to *Pseudomonas aeruginosa* Infection in Zebrafish Is Mediated by the Cystic Fibrosis Transmembrane Conductance Regulator. *Infection and Immunity* **78**:4542–4550.
196. **van der Sar AM, Musters RJP, van Eeden FJM, Appelmelk BJ, Vandenbroucke-Grauls CMJE, Bitter W.** 2003. Zebrafish embryos as a model host for the real time analysis of *Salmonella typhimurium* infections. *Cell Microbiol* **5**:601–611.
197. **Lavigne J-P, Vergunst AC, Goret L, Sotto A, Combescure C, Blanco J, O’Callaghan D, Nicolas-Chanoine M-H.** 2012. Virulence Potential and Genomic Mapping of the Worldwide Clone *Escherichia coli* ST131. *PLoS ONE* **7**:e34294.
198. **Wiles TJ, Norton JP, Smith SN, Lewis AJ, Mobley HLT, Casjens SR, Mulvey MA.** 2013. A Phylogenetically Rare Gene Promotes the Niche-specific Fitness of an *E. coli* Pathogen during Bacteremia. *PLoS Pathog* **9**:e1003175.
199. **Sarris M, Masson J-B, Maurin D, Van der Aa LM, Boudinot P, Lortat-Jacob H, Herbomel P.** 2012. Inflammatory Chemokines Direct and Restrict Leukocyte

- Migration within Live Tissues as Glycan-Bound Gradients. *Current Biology* **22**:2375–2382.
200. **Nguyen-Chi M, Phan QT, Gonzalez C, Dubremetz J-F, Levraud J-P, Lutfalla G.** 2014. Transient infection of the zebrafish notochord with *E. coli* induces chronic inflammation. *Disease Models & Mechanisms* **7**:871–882.
201. **Rawls JF, Mahowald MA, Goodman AL, Trent CM, Gordon JI.** 2007. In vivo imaging and genetic analysis link bacterial motility and symbiosis in the zebrafish gut. *PNAS* **104**:7622–7627.
202. **Moyer TR, Hunnicutt DW.** 2007. Susceptibility of zebra fish *Danio rerio* to infection by *Flavobacterium columnare* and *F. johnsoniae*. *Dis. Aquat. Org.* **76**:39–44.
203. **Chang MX, Nie P.** 2008. RNAi suppression of zebrafish peptidoglycan recognition protein 6 (zfPGRP6) mediated differentially expressed genes involved in Toll-like receptor signaling pathway and caused increased susceptibility to *Flavobacterium columnare*. *Veterinary Immunology and Immunopathology* **124**:295–301.
204. **Vojtech LN, Sanders GE, Conway C, Ostland V, Hansen JD.** 2009. Host Immune Response and Acute Disease in a Zebrafish Model of *Francisella* Pathogenesis. *Infection and Immunity* **77**:914–925.
205. **Brudal E, Ulanova LS, O Lampe E, Rishovd AL, Griffiths G, Winther-Larsen HC.** 2014. Establishment of Three *Francisella* Infections in Zebrafish Embryos at Different Temperatures. *Infection and Immunity* **82**:2180–2194.

206. **Aguado-Urda M, Rodríguez-Bertos A, las Heras de AI, Blanco MM, Acosta F, Cid R, Fernández-Garayzábal JF, Gibello A.** 2014. Experimental *Lactococcus garvieae* infection in zebrafish and first evidence of its ability to invade non-phagocytic cells. *Veterinary Microbiology* **171**:248–254.
207. **Davis JM, Haake DA, Ramakrishnan L.** 2009. *Leptospira interrogans* Stably Infects Zebrafish Embryos, Altering Phagocyte Behavior and Homing to Specific Tissues. *PLoS Negl Trop Dis* **3**:e463.
208. **Bates CS, Toukoki C, Neely MN, Eichenbaum Z.** 2005. Characterization of MtsR, a New Metal Regulator in Group A *Streptococcus*, Involved in Iron Acquisition and Virulence. *Infection and Immunity* **73**:5743–5753.
209. **Menudier A, Rougier FP, Bosgiraud C.** 1996. Comparative virulence between different strains of *Listeria* in zebrafish (*Brachydanio rerio*) and mice. *Pathol. Biol.* **44**:783–789.
210. **Levraud J-P, Disson O, Kissa K, Bonne I, Cossart P, Herbomel P, Lecuit M.** 2009. Real-time observation of *Listeria monocytogenes*-phagocyte interactions in living zebrafish larvae. *Infection and Immunity* **77**:3651–3660.
211. **Rojo I, de Ilárduya OM, Estonba A, Pardo MA.** 2007. Innate immune gene expression in individual zebrafish after *Listonella anguillarum* inoculation. *Fish & Shellfish Immunology* **23**:1285–1293.
212. **Oehlers SHB, Flores MV, Hall CJ, O'Toole R, Swift S, Crosier KE, Crosier PS.** 2010. Expression of zebrafish cxcl8 (interleukin-8) and its receptors during

- development and in response to immune stimulation. *Developmental & Comparative Immunology* **34**:352–359.
213. **Bernut A, Herrmann JL, Kissa K, Dubremetz JF, Gaillard JL, Lutfalla G, Kremer L.** 2014. *Mycobacterium abscessus* cording prevents phagocytosis and promotes abscess formation. *PNAS* **111**:E943–E952.
214. **Runft DL, Mitchell KC, Abuaita BH, Allen JP, Bajer S, Ginsburg K, Neely MN, Withey JH.** 2014. Zebrafish as a natural host model for *Vibrio cholerae* colonization and transmission. *Applied and Environmental Microbiology* **80**:1710–1717.
215. **Harriff MJ, Bermudez LE, Kent ML.** 2007. Experimental exposure of zebrafish, *Danio rerio*, to *Mycobacterium marinum* and *Mycobacterium peregrinum* reveals the gastrointestinal tract as the primary route of infection: a potential model for environmental mycobacterial infection. *Journal of Fish diseases*.
216. **van der Sar AM, Spaink HP, Zakrzewska A, Bitter W, Meijer AH.** 2009. Specificity of the zebrafish host transcriptome response to acute and chronic mycobacterial infection and the role of innate and adaptive immune components. *Mol. Immunol.* **46**:2317–2332.
217. **van Leeuwen L, van der Kuip M, Youssef SA, de Bruin A, Bitter W, van Furth AM, van der Sar AM.** 2014. Modeling tuberculous meningitis in zebrafish using *Mycobacterium marinum*. *Disease Models & Mechanisms*.
218. **Clay H, Volkman HE, Ramakrishnan L.** 2008. Tumor Necrosis Factor Signaling Mediates Resistance to *Mycobacteria* by Inhibiting Bacterial Growth and

- Macrophage Death. *Immunity* **29**:283–294.
219. **Carvalho R, de Sonnevile J, Stockhammer OW, Savage NDL, Veneman WJ, Ottenhoff THM, Dirks RP, Meijer AH, Spaik HP.** 2011. A high-throughput screen for tuberculosis progression. *PLoS ONE* **6**:e16779.
220. **Stoop EJM, Mishra AK, Driessen NN, van Stempvoort G, Bouchier P, Verboom T, van Leeuwen LM, Sparrius M, Raadsen SA, van Zon M, van der Wel NN, Besra GS, Geurtsen J, Bitter W, Appelmelk BJ, van der Sar AM.** 2013. Mannan core branching of lipo(arabino)mannan is required for mycobacterial virulence in the context of innate immunity. *Cell Microbiol* **15**:2093–2108.
221. **Volkman HE, Clay H, Beery D, Chang JCW, Sherman DR, Ramakrishnan L.** 2004. Tuberculous granuloma formation is enhanced by a mycobacterium virulence determinant. *PLoS Biol.* **2**:e367.
222. **Nandi B, Behar SM.** 2011. Regulation of neutrophils by interferon- γ limits lung inflammation during tuberculosis infection. *Journal of Experimental Medicine* **208**:2251–2262.
223. **Davis JM, Ramakrishnan L.** 2009. The Role of the Granuloma in Expansion and Dissemination of Early Tuberculous Infection. *Cell* **136**:37–49.
224. **Kanther M, Tomkovich S, Xiaolun S, Grosser MR, Koo J, Flynn EJ, Jobin C, Rawls JF.** 2014. Commensal microbiota stimulate systemic neutrophil migration through induction of serum amyloid A. *Cell Microbiol* **16**:1053–1067.
225. **Cosma CL, Klein K, Kim R, Beery D, Ramakrishnan L.** 2006. Mycobacterium

- marinum Erp Is a Virulence Determinant Required for Cell Wall Integrity and Intracellular Survival. *Infection and Immunity* **74**:3125–3133.
226. **Galindo-Villegas J, Garcia-Moreno D, de Oliveira S, Meseguer J, Mulero V.** 2012. Regulation of immunity and disease resistance by commensal microbes and chromatin modifications during zebrafish development. *PNAS* **109**:E2605–E2614.
227. **Veneman WJ, Marín-Juez R, de Sonneville J, Ordas A, Jong-Raadsen S, Meijer AH, Spaink HP.** 2014. Establishment and Optimization of a High Throughput Setup to Study *Staphylococcus epidermidis* and *Mycobacterium marinum* Infection as a Model for Drug Discovery. *J Vis Exp*.
228. **Hosseini R, Lamers GE, Hodzic Z, Meijer AH, Schaaf MJ, Spaink HP.** 2014. Correlative light and electron microscopy imaging of autophagy in a zebrafish infection model. *autophagy* **10**:1844–1857.
229. **Meijer AH, Verbeek FJ, Salas-Vidal E, Corredor-Adámez M, Bussman J, van der Sar AM, Otto GW, Geisler R, Spaink HP.** 2005. Transcriptome profiling of adult zebrafish at the late stage of chronic tuberculosis due to *Mycobacterium marinum* infection. *Mol. Immunol.* **42**:1185–1203.
230. **Roca FJ, Ramakrishnan L.** 2013. TNF dually mediates resistance and susceptibility to mycobacteria via mitochondrial reactive oxygen species. *Cell* **153**:521–534.
231. **Chao CC, Hsu PC, Jen CF, Chen IH, Wang CH, Chan HC, Tsai PW, Tung KC, Wang CH, Lan CY, Chuang YJ.** 2010. Zebrafish as a Model Host for *Candida albicans* Infection. *Infection and Immunity* **78**:2512–2521.

232. **Volkman HE, Pozos TC, Zheng J, Davis JM, Rawls JF, Ramakrishnan L.** 2010. Tuberculous Granuloma Induction via Interaction of a Bacterial Secreted Protein with Host Epithelium. *Science* **327**:466–469.
233. **Brannon MK, Davis JM, Mathias JR, Hall CJ, Emerson JC, Crosier PS, Huttenlocher A, Ramakrishnan L, Moskowitz SM.** 2009. *Pseudomonas aeruginosa* Type III secretion system interacts with phagocytes to modulate systemic infection of zebrafish embryos. *Cell Microbiol* **11**:755–768.
234. **Llamas MA, van der Sar A, Chu BCH, Sparrius M, Vogel HJ, Bitter W.** 2009. A Novel extracytoplasmic function (ECF) sigma factor regulates virulence in *Pseudomonas aeruginosa*. *PLoS Pathog* **5**:e1000572.
235. **Clatworthy AE, Lee JSW, Leibman M, Kostun Z, Davidson AJ, Hung DT.** 2009. *Pseudomonas aeruginosa* Infection of Zebrafish Involves both Host and Pathogen Determinants. *Infection and Immunity* **77**:1293–1303.
236. **Chand NS, Lee JSW, Clatworthy AE, Golas AJ, Smith RS, Hung DT.** 2011. The Sensor Kinase KinB Regulates Virulence in Acute *Pseudomonas aeruginosa* Infection. *Journal of Bacteriology* **193**:2989–2999.
237. **Deng Q, Harvie EA, Huttenlocher A.** 2012. Distinct signaling mechanisms mediate neutrophil attraction to bacterial infection and tissue injury. *Cell Microbiol.*
238. **Deng Q, Sarris M, Bennin DA, Green JM, Herbomel P, Huttenlocher A.** 2013. Localized bacterial infection induces systemic activation of neutrophils through Cxcr2 signaling in zebrafish. *Journal of Leukocyte Biology* **93**:761–769.

239. **Kanwal Z, Zakrzewska A, Hertog den J, Spaink HP, Schaaf MJM, Meijer AH.** 2013. Deficiency in Hematopoietic Phosphatase Ptpn6/Shp1 Hyperactivates the Innate Immune System and Impairs Control of Bacterial Infections in Zebrafish Embryos. *The Journal of Immunology* **190**:1631–1645.
240. **Ordas A, Hegedus Z, Henkel CV, Stockhammer OW, Butler D, Jansen HJ, Racz P, Mink M, Spaink HP, Meijer AH.** 2011. Deep sequencing of the innate immune transcriptomic response of zebrafish embryos to Salmonella infection. *Fish & Shellfish Immunology* **31**:716–724.
241. **Benard EL, van der Sar AM, Ellett F, Lieschke GJ, Spaink HP, Meijer AH.** 2012. Infection of zebrafish embryos with intracellular bacterial pathogens. *J Vis Exp.*
242. **Oehlers SH, Flores MV, Hall CJ, Swift S, Crosier KE, Crosier PS.** 2011. The inflammatory bowel disease (IBD) susceptibility genes NOD1 and NOD2 have conserved anti-bacterial roles in zebrafish. *Disease Models & Mechanisms* **4**:832–841.
243. **Flores MV, Crawford KC, Pullin LM, Hall CJ, Crosier KE, Crosier PS.** 2010. Dual oxidase in the intestinal epithelium of zebrafish larvae has anti-bacterial properties. *Biochem. Biophys. Res. Commun.* **400**:164–168.
244. **Mostowy S, Boucontet L, Mazon Moya MJ, Sirianni A, Boudinot P, Hollinshead M, Cossart P, Herbomel P, Levraud J-P, Colucci-Guyon E.** 2013. The zebrafish as a new model for the in vivo study of *Shigella flexneri* interaction with phagocytes

- and bacterial autophagy. *PLoS Pathog* **9**:e1003588.
245. **Li Y-J, Hu B.** 2012. Establishment of Multi-Site Infection Model in Zebrafish Larvae for Studying *Staphylococcus aureus* Infectious Disease. *Journal of Genetics and Genomics* **39**:521–534.
246. **Prajsnar TK, Cunliffe VT, Foster SJ, Renshaw SA.** 2008. A novel vertebrate model of *Staphylococcus aureus* infection reveals phagocyte-dependent resistance of zebrafish to non-host specialized pathogens. *Cell Microbiol* **10**:2312–2325.
247. **Bao Y, Li Y, Jiang Q, Zhao L, Xue T, Hu B, Sun B.** 2013. Methylthioadenosine/S-adenosylhomocysteine nucleosidase (Pfs) of *Staphylococcus aureus* is essential for the virulence independent of LuxS/AI-2 system. *International Journal of Medical Microbiology* **303**:190–200.
248. **Huedo P, Yero D, Martinez-Servat S, Estibariz I, Planell R, Martinez P, Ruyra A, Roher N, Roca I, Vila J, Daura X, Gibert I.** 2014. Two Different *rpf* Clusters Distributed among a Population of *Stenotrophomonas maltophilia* Clinical Strains Display Differential Diffusible Signal Factor Production and Virulence Regulation. *Journal of Bacteriology* **196**:2431–2442.
249. **Ferrer-Navarro M, Planell R, Yero D, Mongiardini E, Torrent G, Huedo P, Martínez P, Roher N, Mackenzie S, Gibert I, Daura X.** 2013. Abundance of the Quorum-Sensing Factor Ax21 in Four Strains of *Stenotrophomonas maltophilia* Correlates with Mortality Rate in a New Zebrafish Model of Infection. *PLoS ONE* **8**:e67207.

250. **Hanson BR, Runft DL, Streeter C, Kumar A, Carion TW, Neely MN.** 2012. Functional analysis of the CpsA protein of *Streptococcus agalactiae*. *Journal of Bacteriology* **194**:1668–1678.
251. **Wang Z, Guo C, Xu Y, Liu G, Lu C, Liu Y.** 2014. Two Novel Functions of Hyaluronidase from *Streptococcus agalactiae* Are Enhanced Intracellular Survival and Inhibition of Proinflammatory Cytokine Expression. *Infection and Immunity* **82**:2615–2625.
252. **Patterson H, Saralahti A, Parikka M, Dramsi S, Trieu-Cuot P, Poyart C, Rounioja S, Rämetsä M.** 2012. Adult zebrafish model of bacterial meningitis in *Streptococcus agalactiae* infection. *Developmental & Comparative Immunology* **38**:447–455.
253. **Borst LB, Patterson SK, Lanka S, Suyemoto MM, Maddox CW.** 2011. Zebrafish (*Danio rerio*) as a Screen for Attenuation of Lancefield Group C Streptococci and a Model for Streptococcal Pathogenesis. *Veterinary Pathology* **50**:457–467.
254. **Saralahti A, Piippo H, Parikka M, Henriques-Normark B, Rämetsä M, Rounioja S.** 2014. Adult zebrafish model for pneumococcal pathogenesis. *Developmental & Comparative Immunology* **42**:345–353.
255. **Rounioja S, Saralahti A, Rantala L, Parikka M, Henriques-Normark B, Silvennoinen O, Rämetsä M.** 2012. Defense of zebrafish embryos against *Streptococcus pneumoniae* infection is dependent on the phagocytic activity of leukocytes. *Developmental & Comparative Immunology* **36**:342–348.

256. **Montanez GE, Neely MN, Eichenbaum Z.** 2005. The streptococcal iron uptake (Siu) transporter is required for iron uptake and virulence in a zebrafish infection model. *Microbiology* **151**:3749–3757.
257. **Phelps HA, Runft DL, Neely MN.** 2005. *Adult Zebrafish Model of Streptococcal Infection*. John Wiley & Sons, Inc., Hoboken, NJ, USA.
258. **Fisher M, Huang YS, Li X, McIver KS, Toukoki C, Eichenbaum Z.** 2008. Shr Is a Broad-Spectrum Surface Receptor That Contributes to Adherence and Virulence in Group A Streptococcus. *Infection and Immunity* **76**:5006–5015.
259. **Li Y, Zheng J-X, Zhang H, Fan H-J, Lu C-P.** 2014. Effect of Tran on virulence through regulating metabolism and stress tolerance of *Streptococcus suis* serotype 2. *Microbiological Research* **169**:666–674.
260. **Wu Z, Zhang W, Lu Y, Lu C.** 2010. Transcriptome profiling of zebrafish infected with *Streptococcus suis*. *Microb. Pathog.* **48**:178–187.
261. **He H, Wang Q, Sheng L, Liu Q, Zhang Y.** 2010. Functional Characterization of *Vibrio alginolyticus* Twin-Arginine Translocation System: Its Roles in Biofilm Formation, Extracellular Protease Activity, and Virulence Towards Fish. *Curr Microbiol* **62**:1193–1199.
262. **O’Toole R, Hofsten Von J, Rosqvist R, Olsson P-E, Wolf-Watz H.** 2004. Visualisation of zebrafish infection by GFP-labelled *Vibrio anguillarum*. *Microb. Pathog.* **37**:41–46.
263. **Pan C-Y, Wu J-L, Hui C-F, Lin C-H, Chen J-Y.** 2011. Insights into the

- antibacterial and immunomodulatory functions of the antimicrobial peptide, epinecidin-1, against *Vibrio vulnificus* infection in zebrafish. *Fish & Shellfish Immunology* **31**:1019–1025.
264. **Sieger D, Stein C, Neifer D, van der Sar AM, Leptin M.** 2009. The role of gamma interferon in innate immunity in the zebrafish embryo. *Disease Models & Mechanisms* **2**:571–581.
265. **Bates JM, Akerlund J, Mittge E, Guillemin K.** 2007. Intestinal Alkaline Phosphatase Detoxifies Lipopolysaccharide and Prevents Inflammation in Zebrafish in Response to the Gut Microbiota. *Cell Host & Microbe* **2**:371–382.
266. **Toh MC, Goodyear M, Daigneault M, Allen-Vercoe E, Van Raay TJ.** 2013. Colonizing the Embryonic Zebrafish Gut with Anaerobic Bacteria Derived from the Human Gastrointestinal Tract. *Zebrafish* **10**:194–198.
267. **Kuo Z-Y, Chuang Y-J, Chao C-C, Liu F-C, Lan C-Y, Chen B-S.** 2013. Identification of Infection- and Defense-Related Genes via a Dynamic Host-Pathogen Interaction Network Using a *Candida Albicans*-Zebrafish Infection Model. *J Innate Immun* **5**:137–152.
268. **Brothers KM, Gratacap RL, Barker SE, Newman ZR, Norum A, Wheeler RT.** 2013. NADPH oxidase-driven phagocyte recruitment controls *Candida albicans* filamentous growth and prevents mortality. *PLoS Pathog* **9**:e1003634.
269. **Gratacap RL, Rawls JF, Wheeler RT.** 2013. Mucosal candidiasis elicits NF- κ B activation, proinflammatory gene expression and localized neutrophilia in zebrafish.

Disease Models & Mechanisms **6**:1260–1270.

Figure Legends

Figure 1-1: Live *in vivo* imaging of neutrophil response to infection. (A) Neutrophil (green) distribution at 3 dpf in a *Tg(mpx:dendra2)* larva. Neutrophils in the caudal hematopoietic tissue as well as randomly migrating neutrophils in the head are shown in supplemental material Video 1. The box indicates the region around the otic vesicle imaged in panels (C) and (D). Scale bar, 500 μm (B) Commonly used sites of infection in embryonic and larval zebrafish. CHT = caudal hematopoietic tissue, CV = caudal vein, DC = duct of Cuvier, HBV = hind brain ventricle, DM = dorsal muscle, OV = otic vesicle, PC = pericardial cavity, Y = yolk sac (C) Live imaging of a 3 dpf *Tg(mpx:dendra2)* larva infected with *P. aeruginosa* (Pa) strain PAK (pMKB1::mCherry) in the otic vesicle (white dotted line). Four frames were extracted from a 3 hour movie (see supplemental Video 2) and show neutrophil (green) recruitment and phagocytosis of Pa (magenta). Scale bar, 40 μm . (D) Live imaging of a 3 dpf *Tg(mpx:dendra2)* larva infected with CellTracker Red-labeled *S. iniae* (Si) strain 9117 in the otic vesicle (white dotted line). Four frames were extracted from a 4 hour movie (see supplemental Video 3) and show neutrophil (green) recruitment and phagocytosis of Si (magenta). Scale bar, 40 μm .

Figure 1-1:

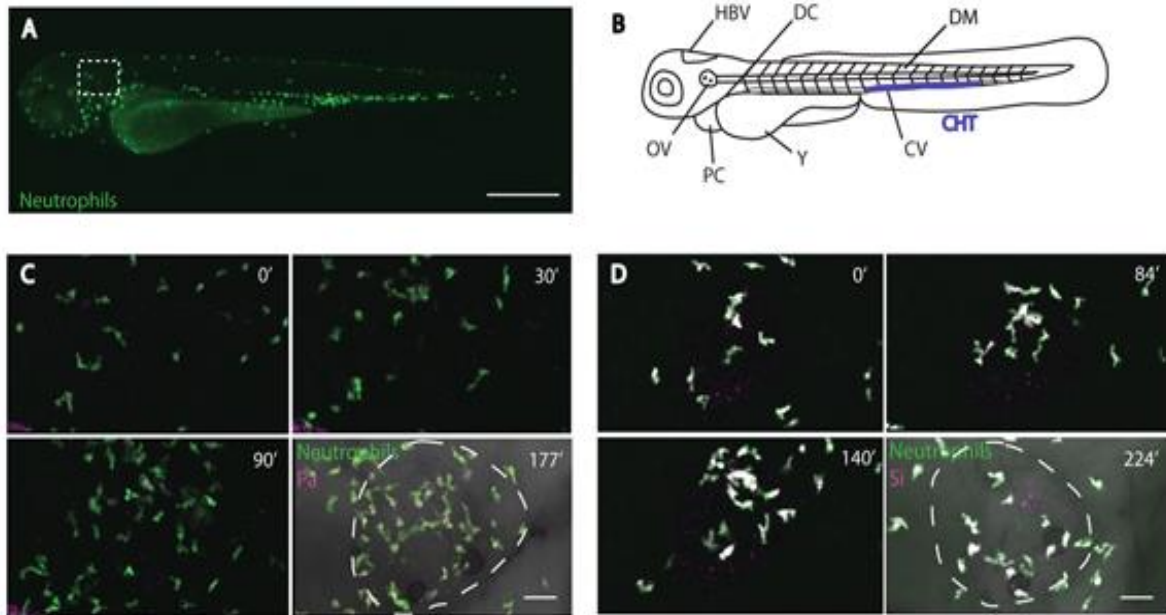


Table 1-1: The Role of Neutrophils and Macrophages in Zebrafish Models of Infection

Bacterium	Age of Zebrafish	Route of Infection	Role of Neutrophils and Macrophages
<i>Aeromonas hydrophila</i>	adult	Immersion (171); IP (172, 173)	N/A
	larva	Immersion (174, 175)	N/A
<i>Aeromonas salmonicida</i>	adult	Immersion after wounding ^a (176)	N/A
<i>Aeromonas veronii</i>	larva	Immersion (177)	N/A
<i>Bacillus</i> sp.	adult	Mixed with feed (178)	N/A
<i>Bacillus sphaericus</i>	adult	Immersion (179)	N/A
<i>Bacillus subtilis</i>	embryo	CV (14); DC (180)	Recruitment and phagocytosis (60)
	larva	DM (60)	
<i>Bacillus thuringiensis</i>	adult	Immersion (179)	N/A
<i>Bartonella henselae</i>	embryo	CV, DC, Yolk (181)	Recruitment and phagocytosis (181)
<i>Burkholderia cenocepacia</i>	adult	IP (182)	N/A
	embryo	CV (183, 184)	Some recruitment and phagocytosis

			by neutrophils, most phagocytosis is by macrophages; both can serve as an intracellular niche for bacteria, (183)
<i>Citrobacter freundii</i>	adult	Immersion (185)	N/A
<i>Edwardsiella ictaluri</i>	adult	IM (186); Immersion (186)	Recruitment (186)
<i>Edwardsiella tarda</i>	adult	IM (187, 188); Immersion (189, 190); IP (191, 192)	Infection causes upregulation in genes involved in neutrophil recruitment (190)
	embryo	CV (193, 194); DC (195); Immersion (189, 193)	N/A
<i>Enterococcus faecalis</i>	embryo	DC (132)	Phagocytosis with most bacteria in macrophages; pu.1 morphants have increased mortality (132)
<i>Escherichia coli</i>	embryo	CV (14, 15, 196); DC/PC (61, 197, 198); mesenchyme between eye and OV (199); notochord (200)	Recruitment (14, 15, 61, 200) in neutrophils is mediated by Cxcl8 (199); phagocytosis (61); neutrophil degranulation and production of IL1 β (200); pu.1 morphants have increased mortality (61)

	larva	Immersion (175, 201); OV (15)	
<i>Flavobacterium columnare</i>	adult	IM, immersion after wounding ^a , IP (202)	N/A
	embryo	Immersion (203)	N/A
<i>Flavobacterium johnsoniae</i>	adult	IM, immersion after wounding ^a , IP (202)	N/A
<i>Francisella</i> spp.	adult	IP (204)	N/A
	embryo	DC, DM, OV (205)	Recruitment; more phagocytosis by macrophages; neutrophil phagocytosis is more efficient when microbe is attached to surface (205)
<i>Haemophilus influenzae</i>	embryo	DC (195)	N/A
<i>Lactococcus garvieae</i>	adult	IP (206)	Infiltration into optic lobes, lamina propria and gills (206); phagocytosis by macrophages (206)
<i>Leptospira interrogans</i>	embryo	CV, HBV (207)	Recruitment and phagocytosis (207)
<i>Listeria monocytogenes</i>	adult	IP (209)	N/A

	embryo	CV (210)	Phagocytosis by both, but limited phagocytosis by neutrophils; engulfed bacteria are always in vacuoles, usually degraded; neutrophils contact infected macrophages; macrophages form cellular aggregates with neutrophils and erythrocytes (210)
<i>Listonella anguillarum</i>	adult	IP (211)	Upregulation of neutrophil genes following infection (eg. <i>mpx</i> and <i>lyz</i>) (211)
	larva	Immersion (212)	N/A
<i>Mycobacterium abscessus</i>	embryo	CV (213)	Macrophage recruitment to bacteria, neutrophil recruitment to macrophage granulomas; phagocytosis (213)
<i>Mycobacterium marinum</i>	Adult	Immersion (215); oral intubation (215); IP (215, 216)	Infection induces upregulation of neutrophil and macrophage genes following infection (229)
	embryo	CV (44, 58, 109, 194, 217-219);	Macrophage recruitment and formation of granulomas (44, 58,

	larva	HBV (44, 58, 109, 220, 217, 218, (221- 225, 230); Yolk (219, 226, 227) Tail fin (228)	109, 148, 155, 217, 226, 230, 232); Rare recruitment and phagocytosis at infection site by neutrophils (44); Neutrophils are recruited and have a scavenger role at macrophage granuloma (44); pu.1 morphants have increased mortality (232); RNS production by neutrophils (66); Oxidative burst by neutrophils (44) Recruitment; macrophages contain some bacteria in autophagic vacuoles, or phagosomes or cytoplasm (228)
<i>Mycobacterium peregrinum</i>	adult	Immersion, IP, oral intubation (215)	N/A
<i>Pseudomonas aeruginosa</i>	embryo larva	CV (233, 234); DC (195, 235, 236); HBV (195) Immersion (174, 175, 201); OV (133, 237, 238); Yolk (237)	Recruitment by neutrophils (195); Phagocytosis (195, 233, 235); pu.1 morphants have increased mortality (233, 235) Recruitment of neutrophils; (133, 237, 238) phagocytosis by

			neutrophils (237); LAD model supports critical role of neutrophils for survival (133)
<i>Pseudomonas fluorescens</i>	larva	Immersion (177)	N/A
<i>Salmonella arizonae</i>	embryo	CV (58)	N/A
<i>Salmonella enterica</i> serovar Typhimurium	embryo larva	CV (194, 196, 239, 240); HBV (63, 65); OV (241); DM (241); Yolk (242) Immersion (243)	Recruitment (63, 65, 241); macrophages phagocytose (196, 241); infection increases neutrophil and macrophage production (65) N/A
<i>Shigella flexneri</i>	larva	CV (244)	Phagocytosis; scavenger role for neutrophils (244)
<i>Staphylococcus aureus</i>	embryo	CV (245); eye (245); HBV (245); DC (78, 246); PC (245 -247); Yolk (246, 247)	Recruitment (245); Phagocytosis (69, 245); possible intracellular niche for bacteria (69); Neutrophil or macrophage ablation increases susceptibility to infection (69); pu.1 and irf8 morphants have

			increased mortality (69)
<i>Staphylococcus epidermidis</i>	embryo	Yolk (227)	N/A
<i>Staphylococcus chromogenes</i>	adult	Immersion after wounding ^a (185)	N/A
<i>Stenotrophomonas maltophilia</i>	adult	IP (248, 249)	N/A
<i>Streptococcus agalactiae</i>	adult	IM (250); IP (251, 252)	N/A
<i>Streptococcus equi</i>	adult	IM, IP (253)	Leukocyte recruitment (253)
<i>Streptococcus iniae</i>	adult	IM, immersion after wounding ^a , IP (169, 170)	Leukocyte recruitment (169, 170)
	larva	OV (54)	Recruitment; phagocytosis; LAD model supports critical role of neutrophils in survival (54); irf8 morphants support role of macrophages in survival (Chapter 3)
<i>Streptococcus pneumoniae</i>	adult	IM, IP (254)	N/A
	embryo	DC (255)	Phagocytosis by Spi1 ⁺ cells; pu.1

			and WASp morphants have increased mortality (255)
<i>Streptococcus pyogenes</i>	adult	IP (170, 208, 210, 256, 257); IM (59, 170, 210, 256-258)	Lack of infiltrating leukocytes (170, 208, 210, 256, 257)
	embryo	Yolk (59)	N/A
	larva	DM (59)	Lack of neutrophil recruitment (59); neutrophil recruitment to SLS-mutant (59)
<i>Streptococcus suis</i>	adult	IP (259, 260)	N/A
<i>Vibrio alginolyticus</i>	adult	IM (261)	N/A
<i>Vibrio anguillarum</i>	larva	Immersion (262)	N/A
<i>Vibrio vulnificus</i>	adult	IP (263)	N/A
<i>Vibrio cholerae</i>	adult;	Oral gavage, immersion (214)	N/A
	larva	Immersion (214)	N/A
<i>Yersinia ruckeri</i>	embryo	CV (264)	N/A
Intestinal Microbiota	larva	Immersion (174, 177, 201, 224, 226, 265)	Presence of microbiota results in: establishment of neutrophil homeostasis in the gut (177, 224,

			265); enhanced neutrophil recruitment to wound (224, 226); neutrophil priming to produce H ₂ O ₂ upon PMA stimulation (226)
Human Intestinal Microbiota	larva	Injection into gut; immersion; (266)	N/A
Mouse Intestinal Microbiota	larva	Immersion (174)	N/A
Fungus	Age of Zebrafish	Route of Infection	Role of Neutrophils
<i>Aspergillus fumigatus</i>	embryo	HBV (153)	Macrophage recruitment to conidia and aggregation around hyphae; neutrophil recruitment to hyphae but not conidia; LAD model supports critical role of neutrophils for survival and irf8 morphants have increased invasive disease supporting critical role for macrophages (153)
<i>Candida albicans</i>	adult	IP (231, 267)	N/A
	embryo	HBV (146, 231, 268); Y	Recruitment (268, 269) mediated by

	larva	(268) Swimbladder (injection) (268); Swimbladder (immersion) (269)	NADPH oxidase (268); Phagocytosis by both but neutrophils may be more efficient at killing yeast cells (146); macrophages can inhibit germination of yeast into hyphae
<i>Penicillium marneffe</i> (spores)	larva	Somatic muscle (10)	Phagocytosis (10)

^a as described in (169)

Supplemental Video Legend

Video 1: Neutrophil distribution in a 3 dpf zebrafish larva. A 3 dpf *Tg(mpx:dendra2)* larva was used to visualize neutrophil random motility and distribution. Time is in minutes.

Video 2: Neutrophil recruitment and phagocytosis of *P. aeruginosa*. A confocal microscope was used to observe neutrophil recruitment and phagocytosis after otic vesicle injection of mCherry-labeled *P. aeruginosa* (depicted as magenta) in a 3 dpf *Tg(mpx:dendra2)* larva using a 20x objective. Time is in minutes.

Video 3: Neutrophil recruitment and phagocytosis of *S. iniae*. A confocal microscope was used to observe neutrophil recruitment and phagocytosis after otic vesicle injection of CellTrackerRed-labeled *S. iniae* (depicted as magenta) in a 3 dpf *Tg(mpx:dendra2)* larva using a 20x objective. Time is in minutes.

Chapter 2

Innate immune response to *Streptococcus iniae* infection in zebrafish larvae

This Chapter was published in the following journal article:

Harvie, E. A., Green, J. M., Neely, M. N., and Huttenlocher, A. (2013) Innate immune response to *Streptococcus iniae* infection in zebrafish larvae. *Infection and Immunity*. 81(1): 110-121.

Abstract

Streptococcus iniae causes systemic infection characterized by meningitis and sepsis. Here, we report a larval zebrafish model of *S. iniae* infection. Injection of wild type *S. iniae* into the otic vesicle induced a lethal infection by 24 hours post infection. In contrast, a *S. iniae* mutant deficient in polysaccharide capsule (*cpsA*) was not lethal, with greater than 90% survival at 24 hours post infection. Live imaging demonstrated that both neutrophils and macrophages were recruited to localized otic infection with mutant and wild type *S. iniae* and were able to phagocytose bacteria. Depletion of neutrophils and macrophages impaired host survival following infection with wild type *S. iniae* and the *cpsA* mutant, suggesting that leukocytes are critical for host survival in the presence of both the wild type and mutant bacteria. However, zebrafish larvae with impaired neutrophil function but normal macrophage function had increased susceptibility to wild type bacteria but not the *cpsA* mutant. Taken together, we have developed a larval zebrafish model of *S. iniae* infection and have found that although neutrophils are important for controlling infection with wild type *S. iniae*, neutrophils are not necessary for host defense against the *cpsA* mutant.

Introduction

Streptococcus iniae is a major aquatic pathogen and a potential zoonotic pathogen capable of causing systemic disease characterized by meningitis and sepsis in both fish and humans. It is both aerobic and facultatively anaerobic, gram-positive, β -hemolytic, and non-typeable by the Lancefield grouping system (1). First isolated from the subcutaneous abscesses of a captive Amazon freshwater dolphin (*Inia geoffrensis*) in the 1970s, *S. iniae* has a worldwide distribution and can infect over 27 species of freshwater and saltwater fish (1-3). Although it is able to colonize the surface of fish and cause skin infections, *S. iniae* disease usually presents as meningoencephalitis with major involvement of the central nervous system (CNS) but can also cause sepsis and invasive systemic infection involving multiple organs. Mortality rates are as high as 30-50% in infected fishponds resulting in over \$100 million in global losses annually (2, 4, 5).

More recently, there have been reported human cases of *S. iniae* infection. The first reported human case of *S. iniae* infection was in Texas in 1991 (6). Since then there have been at least 25 reported human cases of *S. iniae* infection, although this number is thought to be an underestimate (2). *S. iniae* is an opportunistic pathogen infecting mainly elderly or immunocompromised people with a recent history of fish handling and causes invasive infection with clinical pathologies similar to Group A and Group B streptococci. Disease in humans is usually characterized by cellulitis of the upper extremities, similar to infection with Group A streptococci, but there have been cases of more systemic infection including sepsis and meningitis, similar to infection with Group B streptococci (6-10).

A better understanding of *S. iniae* disease pathogenesis requires an appropriate model system. The embryonic zebrafish (*Danio rerio*) has a number of advantages as a model that makes it an increasingly attractive vertebrate host in which to study infectious disease (11 - 24). The zebrafish is genetically tractable with a sequenced genome (http://www.sanger.ac.uk/Projects/D_rerio/) and is amenable to forward and reverse genetic screens. Small size and high fecundity make the zebrafish amenable to high throughput chemical and drug screens and also allow for studies of disease progression and pathogenesis.

Zebrafish embryos and larvae are more experimentally tractable than adults. Although adaptive immunity is not functionally mature until at least 2-3 weeks post fertilization (25-27), zebrafish embryos have a highly conserved vertebrate innate immune system including complement, Toll-like receptors, and neutrophils and macrophages that are capable of phagocytic activity by 28-30 hours post fertilization (hpf) (18, 28-32). The translucency of the embryonic and larval stages makes zebrafish more optically accessible and amenable to live imaging. In addition, genetic studies either relying on the injection of synthetic mRNA for overexpression or the injection of antisense morpholino oligonucleotides (morpholinos) for gene knockdown (33) are available during the embryonic and larval periods.

An adult zebrafish model of *S. iniae* infection has previously been reported (34). Intramuscular injection of 10^3 CFU *S. iniae* wild type strain 9117 results in an influx of inflammatory cells at the injection site and rapid host mortality within 36 to 48 hour post infection (hpi) with evidence of systemic infection including bacterial dissemination to the

brain and other organs (34). The rapid time to death suggests that this period is too short to engage the adaptive immune system, but it is unclear how the immune system responds to *S. iniae* in the adult fish because the tools to study the host immune response in adult zebrafish are limited. The optical transparency and genetic tractability of the embryonic and early larval stages of the zebrafish make it an attractive model for studying the host immune response to *S. iniae* infection in real time in vivo.

S. iniae utilizes a number of identified virulence factors to evade host defense and establish disease (35-40). In particular, the polysaccharide capsule of *S. iniae* is important for virulence in adult zebrafish (41-43). A mutagenesis screen for *S. iniae* mutants with attenuated virulence and decreased systemic spread was done in adult zebrafish. It was found that many of the identified mutants had insertions in genes required for capsule biosynthesis, including the *cpsA* mutant which has a mutation in the first gene of the putative *S. iniae* capsule operon (42-43). The *cpsA* gene encodes a transcriptional regulator of the operon and a polar insertion in this gene results in decreased transcription of the capsule operon and reduced production of capsule as determined by buoyant density in a Percoll gradient (42). In addition, many *S. iniae* capsule mutants were efficiently phagocytosed in human whole blood (43) and by cultured fish macrophages as compared to wild type *S. iniae* (41).

Here, we have developed a zebrafish larval-*S. iniae* infection model to study host-pathogen interactions using real time imaging. We visualized the innate immune response to *S. iniae* infection in real time and investigated how the innate immune response controls infection with the wild type *S. iniae* and the *cpsA* mutant. Our findings suggest that although

both neutrophils and macrophage are important for surviving infection with wild type *S. iniae*, neutrophils are not necessary for host defense against the *cpsA* mutant.

Results

Wild type *S. iniae* but not a capsule mutant impaired survival of zebrafish larvae.

We tested the susceptibility of zebrafish larvae to infection with a wild type strain of *S. iniae*. Larvae at ~72 hours post fertilization (hpf) were microinjected in the left otic vesicle with wild type bacteria (**Fig. 1A**). The otic vesicle forms during development when the ear placodal ectoderm cavitates to form a hollow cavity of epithelium (44, 45). The otic vesicle is normally devoid of leukocytes, but in response to local bacterial infection, leukocytes are recruited to the otic cavity (19). The otic vesicle has previously been used to study localized infection (19, 29, 46-49). We chose otic vesicle infection to allow for the direct observation of host neutrophil and macrophage responses to localized *S. iniae* infection.

Similar to infection of adult zebrafish (34), larvae were susceptible to *S. iniae* infection. An inoculum of ~100 CFU resulted in the death of about 40% of larvae by 24 hpi whereas mock infection with PBS did not result in host mortality (**Fig. 1B**) ($P < 0.0001$). Injections with increasing doses of bacteria indicated that lethality following *S. iniae* infection was dose dependent (**Fig. 1B**) with ~1000 CFU killing about 80% of infected larvae within 24 hpi, and doses as low as ~10 CFU killing more than 40% of infected larvae by 48

hpi. However, lethality required viable bacteria, as injection of heat-killed *S. iniae* did not affect host survival (**Fig. 1B**).

The polysaccharide capsule is an important virulence factor for *S. iniae* in establishing systemic disease in fish (36, 41-43, 50). We next sought to determine whether the *S. iniae* 9117 capsule mutant, *cpsA*, was virulent in zebrafish larvae. The *cpsA* mutant has an insertional mutation in a transcriptional regulator of the *S. iniae* capsule operon that results in decreased production of capsule and attenuated virulence in adult zebrafish compared to the wild type strain (41). In contrast to infection with wild type bacteria, greater than 90% of larvae injected with comparable doses of the *cpsA* mutant survived for at least 72 hpi (**Fig. 1C**). The attenuated virulence of the *cpsA* mutant in larvae parallels what has been shown in the adult zebrafish infection model (41). These data validate the use of zebrafish larvae in modeling streptococcal disease.

As a measure of disease progression, we monitored bacterial load over time in whole animals infected with ~100 CFU bacteria. Larvae were infected with the wild type strain or the *cpsA* mutant and at 0, 18, 24, 48, and 60 hpi, three larvae per condition were sacrificed, homogenized, and plated on colistin nalidixic acid (CNA) agar plates to select for the growth of gram-positive bacteria. In larvae infected with wild type *S. iniae*, the amount of recoverable bacteria increased over time from 100 CFU at the time of inoculation to the greatest bacterial loads around 10^4 CFU at 60 hpi (**Fig. 1D**). We noted that bacterial load and host susceptibility to infection corresponded with the physical appearance of infected larvae. Larvae infected with the wild type strain developed a dark and opaque yolk sac and

deteriorating necrotic body (**Fig. 1E**). The ability of some larvae to survive infection suggests that some individuals may be naturally more resistant to *S. iniae* infection than others or could reflect slight variations in inoculum. However, it should be noted that the inoculum size as determined by enumerating bacterial loads in whole embryos sacrificed immediately following microinjection (~100 CFU) was similar to the inoculum size determined by plating the injection volume from the needle taken before and after infections (data not shown).

In contrast to larvae infected with wild type bacteria, the amount of viable bacteria recovered from larvae infected with the *cpsA* mutant remained approximately equivalent to the initial inoculum over the 60 h monitoring period (~100 CFU) (**Fig. 1D**). This suggests that the *cpsA* mutant is deficient in its ability to proliferate in the host and establish disease. To differentiate between an inability to proliferate in the host and an overall growth defect, in vitro growth assays were performed, and the *cpsA* mutant was found to exhibit wild type growth (data not shown). Larvae infected with the *cpsA* mutant had a slight change in opacity of the yolk sac but overall, looked similar to the appearance of mock (PBS)-infected animals (**Fig. 1E**).

Host neutrophil-*S. iniae* interactions during the early stages of infection.

One advantage of developing a zebrafish larval model of *S. iniae* infection is that the optical transparency at this developmental stage allows for real time visualization of the host immune response to infection in vivo. Although B and T lymphocytes are not fully

functional until 2-3 weeks post fertilization, innate immunity develops early during zebrafish development. By the age of the larvae used in this study, there are both neutrophil and macrophage populations with antimicrobial capabilities including phagocytosis and respiratory bursts (18, 29, 51). To determine the contribution of neutrophils and macrophages to the host immune response, we used transgenic lines expressing the fluorescent protein Dendra2 specifically in neutrophils (*Tg(mpx:dendra2)*) (52) or macrophages (*Tg(mpeg1:dendra2)*). To visualize bacteria, the wild type strain and the *cpsA* mutant were labeled with the CellTracker Red CMPTX dye.

Neutrophils are an important part of the innate immune system and are typically the first responders to a site of infection. To quantify the number of neutrophils recruited to the otic vesicle during early *S. iniae* infection, we fixed infected larvae at 2 hpi and stained with the neutrophil specific stain, Sudan Black (29). Neutrophils were robustly recruited to the site of infection with wild type bacteria by 2 hpi (**Fig. 2A** and **2B**). The median number of neutrophils recruited to the site of infection ranged from ~9 neutrophils following injection of ~10 CFU wild type bacteria to ~20 neutrophils following injection of 1000 CFU (**Fig. 2B**). Injection of increasing doses of the wild type strain demonstrated that neutrophil recruitment was dose dependent, and neutrophils were also recruited to heat-killed bacteria (**Fig. 2A** and **2B**). Moreover, neutrophils were recruited to the *cpsA* mutant, similar to wild type bacteria. Therefore, although the *cpsA* mutant produces a non-lethal infection in larvae, the initial host neutrophil response to pathogenic wild type *S. iniae* and non-pathogenic *cpsA* mutant appear to be similar.

To visualize neutrophil responses to infection with wild type bacteria, we microinjected CellTracker Red-labeled bacteria into the left otic vesicle of the transgenic fish *Tg(mpx:dendra2)* at 72 hpf. The infected embryos were placed in a glass-bottom dish and immediately imaged in the left otic vesicle using a laser scanning confocal microscope. Neutrophils were recruited rapidly to the site of infection, even by the start of the movie at ~10 min post infection (mpi) (see supplemental Video 1 and **Fig. 3A**). Several green-labeled neutrophils entered the otic cavity and appeared to engulf red-labeled wild type bacterial cells. A neutrophil could be observed extending a thin protrusion towards some bacteria (see panel inset at 59 min of **Fig. 3A** and supplemental Video 1). As neutrophils took up bacteria, they became less motile and developed a rounded morphology (see panel insets in **Fig. 3A**). After phagocytosis, the neutrophils recovered their polarized morphology and migrated to a new location.

Tg(mpx:dendra2) larvae injected with the *cpsA* mutant resulted in a similar response to localized infection (see supplemental Video 2 and **Fig. 3B**). Green-labeled neutrophils were recruited to the site of infection by ~10 mpi and rapidly engulfed red-labeled *cpsA* mutant. The motility of these bacteria-laden neutrophils seemed to decrease and the neutrophils developed a rounded appearance, similar to what was seen following infection with wild type bacteria. In contrast to wild type bacteria, the *cpsA* mutant was seen in several small vacuoles in some neutrophils (denoted by the arrowhead in **Fig. 3B** and supplemental Video 2) and was also in large vacuoles in other neutrophils (denoted by the arrow in **Fig. 3B** and supplemental Video 2).

Host macrophage-*S. iniae* interactions during the early stages of infection.

To characterize the macrophage response to *S. iniae* infection, ~100 CFU CellTracker Red-labeled wild type bacteria were microinjected into the left otic vesicle of *Tg(mpeg1:dendra2)* larvae at ~72 hpf. Macrophage recruitment to the site of infection was quantified by fixing infected *Tg(mpeg1:dendra2)* larvae at 2 hpi. Macrophages were recruited following infection with either wild type bacteria or the *cpsA* mutant (**Fig. 4A** and **4B**), and on average between 35 and 40 macrophages were recruited to the otic vesicle following infection.

Real time imaging demonstrated that macrophages, like neutrophils, were also rapidly recruited to the site of *S. iniae* infection (see supplemental Video 3 and **Fig. 5A**). Occasionally, it was possible to observe a macrophage taking up bacteria (see panel inset at 45 min of **Fig. 5A** and supplemental Video 3). The bacteria-carrying macrophages appeared to lose polarity, had reduced motility and developed a rounded morphology. Additionally, there also appeared to be uninfected macrophages with large unfilled vacuoles characteristic of an activated phenotype.

Upon infection of *Tg(mpeg1:dendra2)* with red-labeled *cpsA* mutant, macrophages were rapidly recruited to the otic vesicle at ~10 mpi. This was similar to what was seen following infection with the wild type strain. It was possible to observe a macrophage extend a protrusion and capture bacteria (see panel inset at 6 min of **Fig. 5B** and supplemental Video 4). The phagocytosing macrophage lost its spindle shape and acquired a rounded appearance. The engulfed bacteria seemed to fill multiple vacuoles within the macrophage, but eventually

the bacteria-filled vacuoles appeared to move together towards a central location (see panel inset at 48 min of **Fig. 5B** and supplemental Video 4). It is also of note that it was easier to find macrophages phagocytosing the *cpsA* mutant compared to wild type bacteria (data not shown). In addition by 24 hpi, we observed both wild type and mutant bacteria in macrophages outside of the otic vesicle (data not shown) suggesting that macrophages may play a role in the dissemination of *S. iniae*. However, since we were unable to stably label the bacteria using fluorescent reporters we could not observe macrophage-mediated bacterial phagocytosis and dissemination over time due to dye dilution from bacterial proliferation.

Myeloid cells are important for host survival following infection with wild type *S. iniae* and the *cpsA* mutant.

Since both neutrophils and macrophages are rapidly recruited to the site of infection, we sought to genetically determine the contribution of host myeloid cells to defense against infection with the wild type or the mutant strain by targeted gene knockdown using morpholinos (33). To do this, we used a translation-blocking morpholino targeting Pu.1, a transcription factor important for the differentiation of the myelo-erythroid progenitor cells into cells of the myeloid lineage, including neutrophils and macrophages (53). A Pu.1 or a mismatch control morpholino was injected into double transgenic (*Tg(mpx:mcherry)* x *Tg(mpeg1:dendra2)*) embryos at the single-cell stage, and at 2 dpf, these morphants were infected with wild type bacteria or the *cpsA* mutant or were mock-treated with PBS. The morphants were monitored for survival. Because control larvae are highly susceptible to

infection with wild type *S. iniae*, we used a small inoculum (~10 CFU) of wild type bacteria for these studies to test whether Pu.1 morphants had increased sensitivity to infection. We found that Pu.1 morphants were significantly more susceptible to a low dose infection with the wild type strain compared to control morphants, with over 35% mortality in infected Pu.1 morphants by 24 hpi (**Fig. 6Aii**) compared to less than 10% mortality in infected control morphants (**Fig. 6Ai**) ($P < 0.0001$). Thus, although wild type *S. iniae* is able to establish disease and proliferate in wild type zebrafish larvae, disease progression is more rapid in the absence of myeloid cells. This suggests a role for neutrophils and/or macrophages in controlling infection with the wild type strain. Interestingly, Pu.1 morphants were also significantly more susceptible to infection with a higher dose (~100 CFU) of the *cpsA* mutant, with almost 40% mortality in Pu.1 morphants at 24 hpi compared to less than 10% mortality in control morphants (**Fig. 6Ai** and **6Aii**) ($P < 0.0001$). To test the sensitivity of Pu.1 morphants to infection with the *cpsA* mutant, we also infected morphants with a lower dose (~10 CFU). When infected with only ~10 CFU *cpsA*, there was greater than 40% mortality at 48 hpi compared to less than 10% mortality of control morphants infected with a comparable dose of *cpsA* (**Fig. 6Ai** and **6Aii**) ($P < 0.0001$). To confirm depletion of myeloid lineage cells in Pu.1 morphants, embryos were imaged using a laser scanning confocal prior to infection (**Fig. 6B**). Taken together, our findings show that Pu.1 morphants are more sensitive to infection with both the *cpsA* mutant and wild type bacteria. Our findings also suggest that neutrophils and/or macrophages are necessary to control infection with the *cpsA* mutant.

To monitor disease progression in the Pu.1 morphants, the bacterial loads were measured at 24 hpi. We found that the bacterial burden at this time point appeared to predict host mortality whereas at later time points, it was difficult to measure bacterial load because the majority of the Pu.1 morphants had already succumbed to infection. The overall trend was that Pu.1 morphants had higher bacterial loads than control morphants following infection with either wild type bacteria or the *cpsA* mutant. By 24 hpi, bacterial loads in Pu.1 morphants increased to $\sim 10^3$ to 10^4 CFU following infection with ~ 10 CFU wild type bacteria compared to control morphants in which bacterial loads were about 10 fold lower (**Fig 6C**). The increased susceptibility to infection with the *cpsA* mutant was also reflected in relative bacterial burdens. Pu.1 embryos infected with ~ 10 CFU *cpsA* had bacterial loads of $\sim 10^{2.5}$ CFU by 24 hpi and when infected with ~ 100 CFU *cpsA* had bacterial loads of 10^3 to 10^4 CFU. In contrast, in control morphants, there was not much increase in *cpsA* levels above the initial inocula (**Fig 6C**). This suggests that the ability of the bacteria to survive and proliferate in a host corresponds with increased mortality, and in the absence of myeloid cells, zebrafish larvae are susceptible to both a pathogenic and non-pathogenic strain of *S. iniae*.

Neutrophils are important for controlling infection with wild type *S. iniae* but not the *cpsA* mutant.

To determine the role of neutrophils in controlling *S. iniae* infection, we monitored the infection process in larvae with impaired neutrophil function. We used a previously generated zebrafish model of Leukocyte Adhesion Deficiency in which the human dominant

inhibitory mutation in *Rac2*, D57N, is expressed specifically in neutrophils (46). Neutrophils expressing the inhibitory *Rac2*(D57N) mutation are unable to respond to inflammatory stimuli including otic infection with *Pseudomonas aeruginosa* (46). When larvae with the inhibitory *Rac2*(D57N) mutation expressed specifically in neutrophils were infected with the wild type strain or the *cpsA* mutant, we observed that neutrophils were not recruited to the otic vesicle even though they were recruited in larvae ectopically expressing the wild type *Rac2* gene (*Rac2*(WT)) as shown by Sudan Black staining (**Fig. 7A** and **7B**). This corresponds to what was previously shown regarding the inability of neutrophils expressing the mutated *Rac2*(D57N) to respond to local bacterial infection (46). However, the *Rac2*(D57N) dominant inhibitory mutation expressed in neutrophils did not affect macrophage recruitment to the otic vesicle following infection with either wild type bacteria or the *cpsA* mutant (**Fig. 7C** and **7D**). The *Rac2*(D57N) larvae were more susceptible to infection with a low dose inoculum (~10 CFU) of wild type bacteria compared to larvae with the wild type *Rac2* gene (*Rac2*(WT)) with over 70% mortality of *Rac2*(D57N) fish compared to only 40% mortality of *Rac2*(WT) fish by 48 hpi (**Fig. 7E**) ($P=0.0004$). This supports a role for neutrophils in controlling infection with wild type bacteria. These data, when considered in combination with the Pu.1 morphants, indicate that both neutrophils and macrophages contribute to host defense against wild type *S. iniae* infection. Interestingly, and in contrast to the response to wild type bacteria, the *Rac2*(D57N) fish were not susceptible to infection with even ~100 CFU of the *cpsA* mutant (**Fig. 7E**). These findings suggest that neutrophils are not important for host defense against the *cpsA* mutant, suggesting that

macrophages are likely to play a key role in controlling infection with the *cpsA* mutant.

Therefore, both neutrophils and macrophages are important for controlling infection with wild type *S. iniae*, but neutrophils are not necessary to control infection with the *cpsA* mutant.

Discussion

Here we report a new model for the real time observation of the innate immune response to *S. iniae* disease using zebrafish larvae. Injection of wild type *S. iniae* into the otic vesicle of zebrafish larvae resulted in a dose dependent host mortality accompanied by an increase in bacterial burden (**Fig. 1**). Zebrafish larvae were highly sensitive to wild type *S. iniae* infection with as few as ~10 CFU resulting in lethal infection (**Fig. 1B**) and increasing bacterial burdens during the first 60 hpi (**Fig. 1D**). This infection model provided a powerful tool to differentiate host response and outcome to a *S. iniae* capsule mutant with an insertion in the *cpsA* gene. The *S. iniae cpsA* mutant, which had attenuated virulence in adult zebrafish, was also attenuated in zebrafish larvae, further validating the use of this model (42) (**Fig. 1**). Unlike infection with wild type bacteria, infection of zebrafish larvae with the *cpsA* mutant at doses as large as 1000 CFU was not lethal (**Fig. 1C**), and there was no increase in relative bacterial burden in the first 60 hpi (**Fig. 1D**) indicating that the host was able to control infection.

Although the majority of larvae infected with wild type *S. iniae* did not survive infection, some larvae survived past 96 hpi. This variability may be due to individual variation in the ability of the host to control *S. iniae* disease because zebrafish lines cannot be

highly inbred. In support of this idea, some of the surviving embryos had non-lethal carriage of dye-labeled wild type and mutant *S. iniae* up to 72 hpi (data not shown). It is also possible that the variability in survival was due to differences in the dose of inoculum or the site of injection since we cannot exclude the possibility that when retracting the microinjection needle, some bacteria may be deposited outside the otic vesicle as was previously reported in a study by Colucci-Guyon et al. (48). An additional consideration is that our method of measuring bacterial burden was not a specific measure of *S. iniae* burden, but rather, was a measure of the number of culturable gram-positive organisms. Indeed, there were bacteria recovered from the PBS mock-infected larvae that are likely to be part of the normal zebrafish microbiota. According to a study done by Roeselers et al., some potential members of the zebrafish gut microbiota are gram-positive bacteria including members from the phyla *Actinobacteria* and *Firmicutes* (54). Despite these caveats, there was an overall trend where wild type-infected larvae had an increase in bacterial burden over time while *cpsA*-infected larvae had relatively constant bacterial burdens. However, we cannot rule out the possibility that the increase in bacterial burden in the wild type-infected larvae may have resulted from infection-associated changes in the host that altered the composition of the gram-positive members of the microbiota.

Although the wild type strain and the *cpsA* mutant differed in their ability to establish lethal infection and proliferate in the larval host, both strains were similar in their ability to attract neutrophils and macrophages to localized sites of infection (**Fig. 2-5**). The mechanism of neutrophil and macrophage recruitment into the otic vesicle is not clear, but it likely

involves transmigration from blood vessels and movement through interstitial spaces in response to chemoattractive signals. It is possible that only a subset of host phagocytes have the surface receptor expression required to sense the signals that recruit the cells into the otic vesicle. Neutrophils are among the first cells recruited to the site of infection and were able to phagocytose both wild type bacteria and the *cpsA* mutant (**Fig. 3** and supplemental Videos 1 and 2). Neutrophils that phagocytosed bacteria developed a rounded appearance that was accompanied by decreased motility. This motility was quickly recovered in the case of infection with the wild type strain (see supplemental Video 1), but neutrophils phagocytosing the *cpsA* mutant became laden with bacteria and did not quickly regain their motility (see supplemental Video 2). It is possible that neutrophils are more efficient at phagocytosing the *cpsA* mutant and that their apparent inability to immediately regain motility was due to larger amounts of internalized bacteria compared to infection with wild type bacteria.

Macrophages were also able to phagocytose both wild type bacteria and the *cpsA* mutant. In the case of wild type infection, it was possible to find many uninfected macrophages that had an activated morphology (**Fig. 5A** and supplemental Video 3) suggesting that even in the absence of phagocytosis, the macrophages still became activated by wild type *S. iniae*. It was more common to see macrophages that had phagocytosed *cpsA* mutant than wild type bacteria. In addition, the *cpsA* mutant was contained in multiple separate vacuoles in the macrophages, as well as in single phagosomes (**Fig. 5B** and supplemental Video 4). Although our findings suggested that macrophages were more efficient at phagocytosing the *cpsA* mutant than wild type bacteria, we were not able to

quantify the efficiency of phagocytosis by neutrophils and macrophages because of the inability to reliably track *S. iniae* using stable fluorescent bacteria.

Wild type *S. iniae* and the *cpsA* mutant differ in terms of polysaccharide capsule production. The capsule of *S. iniae* is closely related to the capsule of *S. agalactiae* (Group B *Streptococcus*), which is known to have antiphagocytic properties. The polysaccharide capsule of Group B *Streptococcus* interferes with the deposition of the complement molecule C3b preventing activation of the alternative complement pathway and also disrupting the opsonophagocytic abilities of host phagocytes (55). The capsule of *S. iniae* is thought to have similar antiphagocytic properties. In vitro studies have demonstrated that *S. iniae* mutants with decreased capsule production are more prone to whole blood killing in either human (43) or fish (41) blood and are more susceptible to phagocytosis by cultured fish macrophages (41). Accordingly, we found that the *cpsA* mutant seemed more susceptible to phagocytosis since we observed more host phagocytes with internalized *cpsA* mutant compared to infection with wild type bacteria. Although initial recruitment of host phagocytes to the site of infection is similar for both wild type bacteria and the *cpsA* mutant, subsequent bacterial-phagocyte interactions seem to be different and likely contribute to the wild type strain being pathogenic and the *cpsA* mutant non-pathogenic.

Phagocytosis of bacteria is important for controlling infection but may also play a role in bacterial dissemination. Intracellular residence in macrophages has been suggested to provide *S. iniae* with an intracellular niche for dissemination throughout the host (56). It has been shown that *S. iniae* can survive inside cultured mouse RAW 267.4 macrophages (57)

and salmon macrophages (56) for at least 24 hours. A challenge for future investigation will be to develop the tools to determine if host phagocytes contribute to bacterial dissemination with *S. iniae* infection in zebrafish larvae.

As a first step, we were interested in determining if host phagocytes control disease in *S. iniae* infection of zebrafish. To examine the importance of neutrophils and macrophages in host defense, we depleted myeloid cells using a Pu.1 morpholino. It has been previously shown that myeloid cells are important for controlling infection with *P. aeruginosa* (11, 14), *Mycobacterium marinum* (15), *S. pneumoniae* (22), and *Staphylococcus aureus* (21). However, clearance of bacterial pathogens is not always dependent on the presence of myeloid cells as Pu.1 morphants are able to clear infection with non-pathogenic *Escherichia coli* (15). Using the Pu.1 morphants, we show that myeloid cells are important for host defense in *S. iniae* infection, since the Pu.1 morphants had increased lethality following localized infection with both wild type bacteria and the *cpsA* mutant (**Fig. 6A**). In the case of the Pu.1 morphants, deposition of even a few bacteria outside the otic vesicle could explain why the morphants develop a lethal infection when there are no host phagocytes to disseminate bacteria. However, the lethality in the Pu.1 morphants may also occur because without host phagocytes, bacterial burden can rapidly reach lethal numbers.

Our findings also demonstrate that neutrophils are necessary for controlling infection with wild type *S. iniae* but not the *cpsA* mutant (**Fig. 7E**). *Rac2(D57N)* larvae were more susceptible than control larvae to a low dose inoculum of wild type bacteria, but not to the *cpsA* mutant (**Fig. 7E**). These results suggest that although neutrophils play a role in

controlling infection with wild type *S. iniae*, they are dispensable for controlling infection with the non-pathogenic *cpsA* mutant. These findings raise the intriguing idea that macrophages, but not neutrophils, are critical for controlling infection with the *cpsA* mutant. The development of transgenic zebrafish lines with conditional tissue-specific ablation will help further elucidate the individual contribution of macrophages to host defense (58, 59). A further challenge will be to determine if macrophages are able to serve as “Trojan horses” which facilitate systemic spread of wild type *S. iniae* under some conditions (56).

The ability of neutrophils and macrophages to respond and phagocytose bacteria has been shown to be pathogen-specific in various zebrafish models of microbial infection. Both primitive neutrophils and macrophages phagocytose *P. aeruginosa* (11, 14), but neutrophils, and not macrophages, are necessary to control *P. aeruginosa* infection (46). Although both zebrafish neutrophils and macrophages are recruited to sites of infection with *E. coli* (15, 18, 29, 60), *Staphylococcus aureus* (21), *Listeria monocytogenes* (61), *Burkholderia cenocepacia* (24), and *Salmonella enterica* serovar Typhimurium (60, 62), primitive macrophages play a more critical role in the phagocytosis of these microorganisms, with only minimal phagocytosis by neutrophils. Additionally, macrophages, but not neutrophils, are recruited and are important for the phagocytosis of *Mycobacterium marinum* (15). Host phagocytes are also important for defense against *S. pneumoniae* infection (22), since Pu.1 morphants are more susceptible to disease. Here, we have shown that both neutrophils and macrophages are crucial for the control of wild type *S. iniae* infection but that in the absence of functional neutrophils, other host leukocytes such as macrophages control infection with the non-

pathogenic *S. iniae cpsA* mutant. Interestingly, the observation that neutrophils phagocytose wild type *S. iniae* and the *cpsA* mutant following infection in the otic vesicle is in contrast with a recent report from Colucci-Guyon, et al. (48). This report showed that unlike macrophages, neutrophils were ineffective at phagocytosing *E. coli* injected into closed fluid-filled body cavities such as the otic vesicle and were only highly phagocytic when bacteria were attached to a surface (48). This suggests that the ability of neutrophils to efficiently phagocytose bacteria in fluid-filled body cavities may be dependent on the particular type of invading microbe.

In summary, we have developed a zebrafish larval infection model with the fish pathogen *S. iniae*. The optical accessibility of this model allowed for the real-time observation of host phagocyte-*S. iniae* interactions in vivo. The genetic tractability of the zebrafish allowed for components of the host immune system, such as neutrophils or macrophages, to be altered to investigate how defects in innate immunity affect *S. iniae* disease outcome. We found that while both neutrophils and macrophages provide protection against infection with wild type *S. iniae*, neutrophils are not necessary for host survival following infection with the *S. iniae cpsA* capsule mutant. Moreover, this model was able to differentiate between *S. iniae* strains with altered virulence allowing for the real time observation of host-pathogen interactions when both host and pathogen components are altered.

Materials and Methods

Zebrafish maintenance. Adult fish and embryos were maintained in accordance with the University of Wisconsin-Madison Research Animal Resources Center (Madison, WI, USA). A light cycle of 10 h darkness and 14 h light was used. Wild type fish, type AB, were used in these experiments and to generate all transgenic lines; this population of AB wild type fish was not inbred. Embryos were obtained by natural spawning and were raised at 28.5°C in E3 medium (63). For experiments performed using embryos aged 2 days post fertilization (dpf), embryos were dechorionated with pronase. For bacterial infection and live imaging, embryos were anesthetized in E3 medium containing 0.2 mg/ml tricaine (ethyl 3-aminobenzoate; Sigma-Aldrich, St. Louis, MO, USA). The previously published transgenic lines *Tg(mpx:dendra2)* (52), *Tg(mpx:mCherry-2A-rac2wt)* and *Tg(mpx:mCherry-2A-rac2-d57n)* (46) were used in these studies.

Generation of the transgenic *Tg(mpeg1:dendra2)* zebrafish line. The *mpeg1* promoter region was cloned from a BAC construct (clone DKEY-67k20, Imagene, Hanover, NH, USA) into a backbone vector containing minimal Tol2 elements (64) using previously reported primers (65) to amplify nucleotides 30437143–30438999 from chromosome 8. This generated a 1.86 kb sequence immediately proximal to the *mpeg1* 5'-untranslated region. The *mpeg1* region was PCR-amplified with primers (F: ACGTGGATCCTTTTGCTGTCTCCTGC and R: ACGTCTCGAGTGTTGGAGCACATCTG), then inserted into the *Tg(mpx:dendra2)* vector

(52). The *Tg(mpx:dendra2)* vector and PCR product were cut with *BamHI/XhoI*, then ligated to remove the *mpx* promoter and replace it with the *mpeg1* promoter. One-cell stage wild type AB embryos were injected with a 3 nl solution containing 25 ng/ μ l *Tg(mpeg1:dendra2)* DNA along with 35 ng/ μ l transposase mRNA and grown at 28.5°C.

Bacterial strains, media, and culture conditions. The *S. iniae* wild type strain 9117 and a *S. iniae* capsule mutant with a polar insertional mutation in the *cpsA* gene (*cpsA*) have been previously described (42, 66). The *cpsA* gene is the first gene of the *S. iniae* capsule operon and encodes a transcriptional regulator (42). Therefore, the mutation of this gene results in the decreased transcription of the capsule operon and thus, decreased production of capsule (42). Bacteria were cultured in Todd-Hewitt medium (Sigma-Aldrich, St. Louis, MO, USA) supplemented with 0.2% yeast extract (BD Biosciences, San Jose, CA, USA) and 2% proteose peptone (vegetable) (Sigma-Aldrich, St. Louis, MO, USA) (THY+P). Bacteria were cultured in sealed tubes without agitation at 37°C. Solid THY+P plates were made by supplementing liquid media with Bacto agar (BD Biosciences, San Jose, CA, USA) to a final concentration of 1.4%.

Preparation of streptococci. Bacterial cultures were grown overnight at 37°C in THY+P without agitation. Overnight cultures were diluted 1:100 in fresh THY+P media, incubated at 37°C, and harvested in mid-logarithmic phase of growth when the optical density at 600 nm reached 0.250 (corresponding to $\sim 10^8$ CFU/ml) as determined by a Nanodrop

spectrophotometer. Bacteria were pelleted by centrifugation at 1500 g for 5 min, washed in fresh PBS, repelleted and resuspended in PBS to achieve the desired optical density at 600 nm. Phenol red tracking dye was added to bacterial aliquots prior to injection at a final concentration of 0.1%. For infections with heat-killed bacteria, an equivalent of 1000 CFU wild type *S. iniae* was heated at 95°C for 30 minutes. Heat-killing reduced the number of viable bacteria to undetectable levels as confirmed by plating an injection volume on solid THY+P medium.

Microinjection of bacteria into zebrafish embryos. Bacterial cells were microinjected in a 1 nl volume into the otic vesicle as previously described (19). The inoculum size was determined by injecting an equal volume of bacteria into PBS before and after zebrafish injections with each needle and plating on THY+P agar to quantify CFU. The scoring of live or dead embryos was determined based on the presence of a heartbeat and response to gentle touching with a pipet tip. After injection, zebrafish were returned to E3 medium and incubated at 28.5°C and monitored for survival at the indicated time points or fixed for Sudan Black staining at 2 hpi.

Sudan Black staining. Embryos were fixed at 2 hpi in 4% paraformaldehyde in PBS, and neutrophils were stained with Sudan Black as previously described (29). Neutrophil recruitment was determined by obtaining visual counts of stained neutrophils in the otic vesicle using a Nikon SMZ 745 stereomicroscope (Melville, NY, USA).

Bacterial enumeration from infected embryos. At the indicated times, embryos were anesthetized, rinsed in E3 medium, and collected in 100 μ l of 0.2% Triton X-100 in PBS and homogenized by passing up and down 5 times through a 27 $\frac{1}{2}$ - gauge needle. Serial dilutions of the homogenates were made in PBS and plated onto Columbia CNA agar (dotScientific Inc., Burton, MI, USA) for selective isolation of gram-positive bacteria. CFU were enumerated after 48 h of incubation at 37°C. Log values of CFU counts were recorded.

Morpholino oligonucleotide (MO) injection. All MOs were purchased from Gene Tools, LLC (Philomath, OR), resuspended in distilled water and stored at room temperature at a stock concentration of 1 mM. Three nanoliters of MOs were injected into the yolk of 1-cell stage AB wild type embryos at the indicated concentrations (Pu.1 MO, 500 μ M; standard control MO, 500 μ M). The translation-blocking Pu.1 MO was previously described (53). Elimination of the myeloid lineage in Pu.1 morphants was confirmed by injection into the double transgenic *Tg(mpx:mcherry) x Tg(mpeg1:dendra2)*.

Microscope analysis/Live imaging. Anesthetized larvae were settled onto the bottom of a custom-made, glass-bottom dish. Time-lapse fluorescence images were acquired with a laser scanning confocal microscope (Fluoview FV1000, Olympus, Center Valley, PA, USA) using a numeric aperture 0.75/20x objective. For confocal imaging, each fluorescent channel (488 nm and 543 nm) and DIC images were acquired by sequential line scanning. Z-series were

acquired using a 250 μm pinhole and 2-6 μm step sizes. Z-stacked fluorescence images were overlaid with a single DIC plane. Where indicated, bacteria were labeled with 5 μM CellTracker Red CMPTX dye (catalog number C34552; Molecular Probes, Invitrogen, Grand Island, NY, USA) according to the manufacturer's instructions.

Statistical analyses. All statistical analyses were performed using GraphPad Prism, versions 4 and 6. For quantification of neutrophil and macrophage recruitment, the Kruskal-Wallis test followed by Dunn's multiple comparison posttest was used. To monitor survival, a Kaplan-Meier curve was calculated for each inoculum as well as for PBS mock-infected larvae. Differences in survival of bacteria-infected larvae compared to mock-infected larvae were calculated by the log-rank test.

Acknowledgements

The authors would like to thank P. Y. Lam and D. C. LeBert for critical reading of the manuscript and lab members for zebrafish maintenance.

This work was supported by the National Institutes of Health, National Research Service Award AI55397 to E. A. Harvie and a Burroughs Wellcome grant to A. Huttenlocher.

References

1. **Pier GB, Madin SH.** 1976. *Streptococcus iniae* sp. nov., a Beta-Hemolytic *Streptococcus* Isolated from an Amazon Freshwater Dolphin, *Inia geoffrensis*. *International Journal of Systematic Bacteriology* **26**:545–553.
2. **Agnew W, Barnes AC.** 2007. *Streptococcus iniae*: An aquatic pathogen of global veterinary significance and a challenging candidate for reliable vaccination. *Veterinary Microbiology* **122**:1–15.
3. **Pier GB, Madin SH, Al-Nakeeb S.** 1978. Isolation and Characterization of a Second Isolate of *Streptococcus iniae*. *International Journal of Systematic Bacteriology* **28**:311–314.
4. **Eldar A, Bejerano Y, Bercovier H.** 1995. Experimental streptococcal meningo-encephalitis in cultured fish. *Veterinary Microbiology* **43**:33–40.
5. **Shoemaker CA, Klesius PH, Evans JJ.** 2001. Prevalence of *Streptococcus iniae* in tilapia, hybrid striped bass, and channel catfish on commercial fish farms in the United States. *Am. J. Vet. Res.* **62**:174–177.
6. **Weinstein MR, Litt M, Kertesz DA, Wyper P, Rose D, Coulter M, McGeer A, Facklam R, Ostach C, Willey BM, Borczyk A, Low DE.** 1997. Invasive Infections Due to a Fish Pathogen, *Streptococcus iniae*. *New England Journal of Medicine* **337**:589–594.
7. **Facklam R, Elliott J, Shewmaker L, Reingold A.** 2005. Identification and Characterization of Sporadic Isolates of *Streptococcus iniae* Isolated from Humans. *J. Clin. Microbiol.* **43**:933–937.

8. **Koh TH, Kurop A, Chen J.** 2004. Streptococcus iniae Discitis in Singapore. Emerg. Infect. Dis. **10**:1694–31696.
9. **Lau SKP, Woo PCY, Luk W-K, Fung AMY, Hui W-T, Fong AHC, Chow C-W, Wong SSY, Yuen K-Y.** 2006. Clinical isolates of Streptococcus iniae from Asia are more mucoid and β -hemolytic than those from North America. Diagnostic Microbiology and Infectious Disease **54**:177–181.
10. **Lau SKP, Woo PCY, Tse H, Leung K-W, Wong SSY, Yuen K-Y.** 2003. Invasive Streptococcus iniae infections outside North America. J. Clin. Microbiol. **41**:1004–1009.
11. **Brannon MK, Davis JM, Mathias JR, Hall CJ, Emerson JC, Crosier PS, Huttenlocher A, Ramakrishnan L, Moskowitz SM.** 2009. Pseudomonas aeruginosa Type III secretion system interacts with phagocytes to modulate systemic infection of zebrafish embryos. Cell Microbiol **11**:755–768.
12. **Brothers KM, Newman ZR, Wheeler RT.** 2011. Live Imaging of Disseminated Candidiasis in Zebrafish Reveals Role of Phagocyte Oxidase in Limiting Filamentous Growth. Eukaryotic Cell **10**:932–944.
13. **Chao CC, Hsu PC, Jen CF, Chen IH, Wang CH, Chan HC, Tsai PW, Tung KC, Wang CH, Lan CY, Chuang YJ.** 2010. Zebrafish as a Model Host for Candida albicans Infection. Infection and Immunity **78**:2512–2521.
14. **Clatworthy AE, Lee JSW, Leibman M, Kostun Z, Davidson AJ, Hung DT.** 2009. Pseudomonas aeruginosa Infection of Zebrafish Involves both Host and Pathogen

- Determinants. *Infection and Immunity* **77**:1293–1303.
15. **Clay H, Davis JM, Beery D, Huttenlocher A, Lyons SE, Ramakrishnan L.** 2007. Dichotomous Role of the Macrophage in Early *Mycobacterium marinum* Infection of the Zebrafish. *Cell Host & Microbe* **2**:29–39.
 16. **Davis JM, Clay H, Lewis JL, Ghori N, Herbomel P, Ramakrishnan L.** 2002. Real-time visualization of mycobacterium-macrophage interactions leading to initiation of granuloma formation in zebrafish embryos. *Immunity* **17**:693–702.
 17. **Davis JM, Haake DA, Ramakrishnan L.** 2009. *Leptospira interrogans* Stably Infects Zebrafish Embryos, Altering Phagocyte Behavior and Homing to Specific Tissues. *PLoS Negl Trop Dis* **3**:e463.
 18. **Herbomel P, Thisse B, Thisse C.** 1999. Ontogeny and behaviour of early macrophages in the zebrafish embryo. *Development* **126**:3735–3745.
 19. **Levraud J-P, Colucci-Guyon E, Redd MJ, Lutfalla G, Herbomel P.** 2008. In vivo analysis of zebrafish innate immunity. *Methods Mol. Biol.* **415**:337–363.
 20. **Lin A, Loughman JA, Zinselmeyer BH, Miller MJ, Caparon MG.** 2009. Streptolysin S Inhibits Neutrophil Recruitment during the Early Stages of *Streptococcus pyogenes* Infection. *Infection and Immunity* **77**:5190–5201.
 21. **Prajsnar TK, Cunliffe VT, Foster SJ, Renshaw SA.** 2008. A novel vertebrate model of *Staphylococcus aureus* infection reveals phagocyte-dependent resistance of zebrafish to non-host specialized pathogens. *Cell Microbiol* **10**:2312–2325.
 22. **Rounioja S, Saralahti A, Rantala L, Parikka M, Henriques-Normark B,**

- Silvennoinen O, Rämets M.** 2012. Defense of zebrafish embryos against *Streptococcus pneumoniae* infection is dependent on the phagocytic activity of leukocytes. *Developmental & Comparative Immunology* **36**:342–348.
23. **van Soest JJ, Stockhammer OW, Ordas A, Bloemberg GV, Spalink HP, Meijer AH.** 2011. Comparison of static immersion and intravenous injection systems for exposure of zebrafish embryos to the natural pathogen *Edwardsiella tarda*. *BMC Immunology* **12**:58.
24. **Vergunst AC, Meijer AH, Renshaw SA, O'Callaghan D.** 2010. *Burkholderia cenocepacia* Creates an Intramacrophage Replication Niche in Zebrafish Embryos, Followed by Bacterial Dissemination and Establishment of Systemic Infection. *Infection and Immunity* **78**:1495–1508.
25. **Danilova N, Steiner LA.** 2002. B cells develop in the zebrafish pancreas. *PNAS* **99**:13711–13716.
26. **Lam SH, Chua HL, Gong Z, Lam TJ, Sin YM.** 2004. Development and maturation of the immune system in zebrafish, *Danio rerio*: a gene expression profiling, in situ hybridization and immunological study. *Developmental & Comparative Immunology* **28**:9–28.
27. **Willett CE, Cortes A, Zuasti A, Zapata A.** 1999. Early Hematopoiesis and Developing Lymphoid Organs in the Zebrafish. *Dev. Dyn.* **214**:323–336.
28. **Jault C, Pichon L, Chluba J.** 2004. Toll-like receptor gene family and TIR-domain adapters in *Danio rerio*. *Mol. Immunol.* **40**:759–771.

29. **Le Guyader D, Redd MJ, Colucci-Guyon E, Murayama E, Kissa K, Briolat V, Mordelet E, Zapata A, Shinomiya H, Herbomel P.** 2008. Origins and unconventional behavior of neutrophils in developing zebrafish. *Blood* **111**:132–141.
30. **Meijer AH, Gabby Krens SF, Medina Rodriguez IA, He S, Bitter W, Ewa Snaar-Jagalska B, Spaik HP.** 2004. Expression analysis of the Toll-like receptor and TIR domain adaptor families of zebrafish. *Mol. Immunol.* **40**:773–783.
31. **Seeger A, Mayer WE, Klein J.** 1996. A Complement Factor B-Like cDNA clone from the Zebrafish (*Brachydanio rerio*). *Mol. Immunol.*
32. **van der Sar AM, Stockhammer OW, van der Laan C, Spaik HP, Bitter W, Meijer AH.** 2006. MyD88 innate immune function in a zebrafish embryo infection model. *Infection and Immunity* **74**:2436–2441.
33. **Nasevicius A, Ekker SC.** 2000. Effective targeted gene “knockdown” in zebrafish. *Nature Genetics* **26**:216–220.
34. **Neely MN, Pfeifer JD, Caparon MG.** 2002. Streptococcus-Zebrafish Model of Bacterial Pathogenesis. *Infection and Immunity* **70**:3904–3914.
35. **Baiano JC, Tumbol RA, Umopathy A, Barnes AC.** 2008. Identification and molecular characterisation of a fibrinogen binding protein from *Streptococcus iniae*. *BMC Microbiology* **8**:67.
36. **Buchanan JT, Stannard JA, Lauth X, Ostland VE, Powell HC, Westerman ME, Nizet V.** 2005. *Streptococcus iniae* phosphoglucomutase is a virulence factor and a target for vaccine development. *Infection and Immunity* **73**:6935–6944.

37. **Eyngor M, Lublin A, Shapira R, Hurvitz A, Zlotkin A, Tekoah Y, Eldar A.** 2010. A pivotal role for the *Streptococcus iniae* extracellular polysaccharide in triggering proinflammatory cytokines transcription and inducing death in rainbow trout. *FEMS Microbiology Letters* **305**:109–120.
38. **Fuller J, Camus A, Duncan C, Nizet V, Bast D, Thune R, Low DE, de Azavedo JCS.** 2002. Identification of a Streptolysin S-Associated Gene Cluster and Its Role in the Pathogenesis of. *Infection and Immunity* **70**:5730–5739.
39. **Locke JB, Aziz RK, Vicknair MR, Nizet V, Buchanan JT.** 2008. *Streptococcus iniae* M-Like Protein Contributes to Virulence in Fish and Is a Target for Live Attenuated Vaccine Development. *PLoS ONE* **3**:e2824.
40. **Milani CJE, Aziz RK, Locke JB, Dahesh S, Nizet V, Buchanan JT.** 2010. The novel polysaccharide deacetylase homologue Pdi contributes to virulence of the aquatic pathogen *Streptococcus iniae*. *Microbiology* **156**:543–554.
41. **Locke JB, Colvin KM, Datta AK, Patel SK, Naidu NN, Neely MN, Nizet V, Buchanan JT.** 2007. *Streptococcus iniae* Capsule Impairs Phagocytic Clearance and Contributes to Virulence in Fish. *Journal of Bacteriology* **189**:1279–1287.
42. **Lowe BA, Miller JD, Neely MN.** 2007. Analysis of the Polysaccharide Capsule of the Systemic Pathogen *Streptococcus iniae* and Its Implications in Virulence. *Infection and Immunity* **75**:1255–1264.
43. **Miller JD, Neely MN.** 2005. Large-scale screen highlights the importance of capsule for virulence in the zoonotic pathogen *Streptococcus iniae*. *Infection and Immunity*

- 73:921–934.
44. **Haddon C, Lewis J.** 1996. Early Ear Development in the Embryo of the Zebrafish, *Danio rerio*. *the journal of comparative neurology* **365**:113–128.
 45. **Whitfield TT, Riley BB, Chiang M-Y, Phillips B.** 2002. Development of the zebrafish inner ear. *Dev. Dyn.* **223**:427–458.
 46. **Deng Q, Yoo SK, Cavnar PJ, Green JM, Huttenlocher A.** 2011. Dual Roles for Rac2 in Neutrophil Motility and Active Retention in Zebrafish Hematopoietic Tissue. *Developmental Cell* **21**:735–745.
 47. **Benard EL, van der Sar AM, Ellett F, Lieschke GJ, Spaink HP, Meijer AH.** 2012. Infection of zebrafish embryos with intracellular bacterial pathogens. *J Vis Exp.*
 48. **Colucci-Guyon E, Tinevez JY, Renshaw SA, Herbomel P.** 2011. Strategies of professional phagocytes in vivo: unlike macrophages, neutrophils engulf only surface-associated microbes. *Journal of Cell Science* **124**:3053–3059.
 49. **Deng Q, Harvie EA, Huttenlocher A.** 2012. Distinct signaling mechanisms mediate neutrophil attraction to bacterial infection and tissue injury. *Cell Microbiol.*
 50. **Bolotin S, Fuller JD, Bast DJ, Beveridge TJ, de Azavedo JCS.** 2007. Capsule expression regulated by a two-component signal transduction system in *Streptococcus iniae*. *FEMS Immunology & Medical Microbiology* **50**:366–374.
 51. **Hermann AC, Millard PJ, Blake SL, Kim CH.** 2004. Development of a respiratory burst assay using zebrafish kidneys and embryos. *Journal of Immunological Methods* **292**:119–129.

52. **Yoo SK, Huttenlocher A.** 2011. Spatiotemporal photolabeling of neutrophil trafficking during inflammation in live zebrafish. *Journal of Leukocyte Biology* **89**:661–667.
53. **Rhodes J, Hagen A, Hsu K, Deng M, Liu TX, Look AT, Kanki JP.** 2005. Interplay of pu.1 and gata1 determines myelo-erythroid progenitor cell fate in zebrafish. *Developmental Cell* **8**:97–108.
54. **Roeselers G, Mittge EK, Stephens WZ, Parichy DM, Cavanaugh CM, Guillemin K, Rawls JF.** 2011. Evidence for a core gut microbiota in the zebrafish. *The ISME Journal* 1–14.
55. **Marques MB, Kasper DL, Pangburn MK, Wessels MR.** 1992. Prevention of C3 deposition by capsular polysaccharide is a virulence mechanism of type III group B streptococci. *Infection and Immunity* **60**:3986–3993.
56. **Zlotkin A, Chilmonczyk S, Eynigor M, Hurvitz A, Ghittino C, Eldar A.** 2003. Trojan Horse Effect: Phagocyte-Mediated *Streptococcus iniae* Infection of Fish. *Infection and Immunity* **71**:2318–2325.
57. **Miller JD, Neely MN.** 2004. Zebrafish as a model host for streptococcal pathogenesis. *Acta Tropica* **91**:53–68.
58. **Curado S, Anderson RM, Jungblut B, Mumm J, Schroeter E, Stainier DYR.** 2007. Conditional targeted cell ablation in zebrafish: A new tool for regeneration studies. *Dev. Dyn.* **236**:1025–1035.
59. **Curado S, Stainier DYR, Anderson RM.** 2008. Nitroreductase-mediated cell/tissue

- ablation in zebrafish: a spatially and temporally controlled ablation method with applications in developmental and regeneration studies. *Nat Protoc* **3**:948–954.
60. **Meijer AH, van der Sar AM, Cunha C, Lamers GEM, Laplante MA, Kikuta H, Bitter W, Becker TS, Spaik HP.** 2008. Identification and real-time imaging of a myc-expressing neutrophil population involved in inflammation and mycobacterial granuloma formation in zebrafish. *Developmental & Comparative Immunology* **32**:36–49.
 61. **Levraud J-P, Disson O, Kissa K, Bonne I, Cossart P, Herbomel P, Lecuit M.** 2009. Real-time observation of *Listeria monocytogenes*-phagocyte interactions in living zebrafish larvae. *Infection and Immunity* **77**:3651–3660.
 62. **van der Sar AM, Musters RJP, van Eeden FJM, Appelmelk BJ, Vandenbroucke-Grauls CMJE, Bitter W.** 2003. Zebrafish embryos as a model host for the real time analysis of *Salmonella typhimurium* infections. *Cell Microbiol* **5**:601–611.
 63. **Nüsslein-Volhard C, Dahm R.** 2002. *Zebrafish: A Practical Approach*. Oxford University Press, New York, NY.
 64. **Urasaki A, Morvan G, Kawakami K.** 2006. Functional Dissection of the Tol2 Transposable Element Identified the Minimal cis-Sequence and a Highly Repetitive Sequence in the Subterminal Region Essential for Transposition. *Genetics* **174**:639–649.
 65. **Ellett F, Pase L, Hayman JW, Andrianopoulos A, Lieschke GJ.** 2011. mpeg1 promoter transgenes direct macrophage-lineage expression in zebrafish. *Blood*

117:e49–56.

66. **Fuller J, Bast D, Nizet V, Low D.** 2001. *Streptococcus iniae* virulence is associated with a distinct genetic profile. *Infection and Immunity*.

Figure Legends

Figure 2-1: Zebrafish larvae are susceptible to otic vesicle infection with wild type *S.*

***iniae* but not the *cpsA* mutant.** (A) Image of the head region of a zebrafish larva at 72 hpf.

The site of microinjection in the otic vesicle is indicated. Scale bar, 200 μm . (B) Survival of

72 hpf larvae microinjected with various doses of viable wild type *S. iniae* or an equivalent of

1000 CFU wild type bacteria heat-killed at 95°C for 1 h. (n= 24 per group). Compared to

mock-infected larvae, each dose showed a significant difference in survival as calculated by

the log-rank test ($P < 0.0001$). The data are from 3 independent experiments each with 24

larvae per condition. (C) Survival of 72 hpf larvae microinjected with various doses of wild

type bacteria or the *cpsA* mutant. (n = 24 per group). Compared to larvae infected with wild

type bacteria, larvae infected with comparable doses of the *cpsA* mutant showed a significant

difference in survival as determined by the log-rank test (100 CFU *cpsA* vs 100 CFU *S. iniae*,

$P < 0.0001$; 1000 CFU *cpsA* vs 1000 CFU *S. iniae*, $P < 0.0001$). The data are from 3

independent experiments each with 24 larvae per condition. (D) Enumeration of viable

bacteria from individual larvae at the indicated time points post infection. The larvae were

microinjected with PBS, ~100 CFU wild type or ~100 CFU *cpsA*, and individual larvae were

ethanized, homogenized and plated on CNA agar. Results are representative of at least 3

independent experiments. (E) Bright field images of larvae microinjected with PBS, ~100

CFU wild type or ~100 CFU *cpsA* taken at 24 hpi. Scale bar, 500 μm .

Figure 2-1:

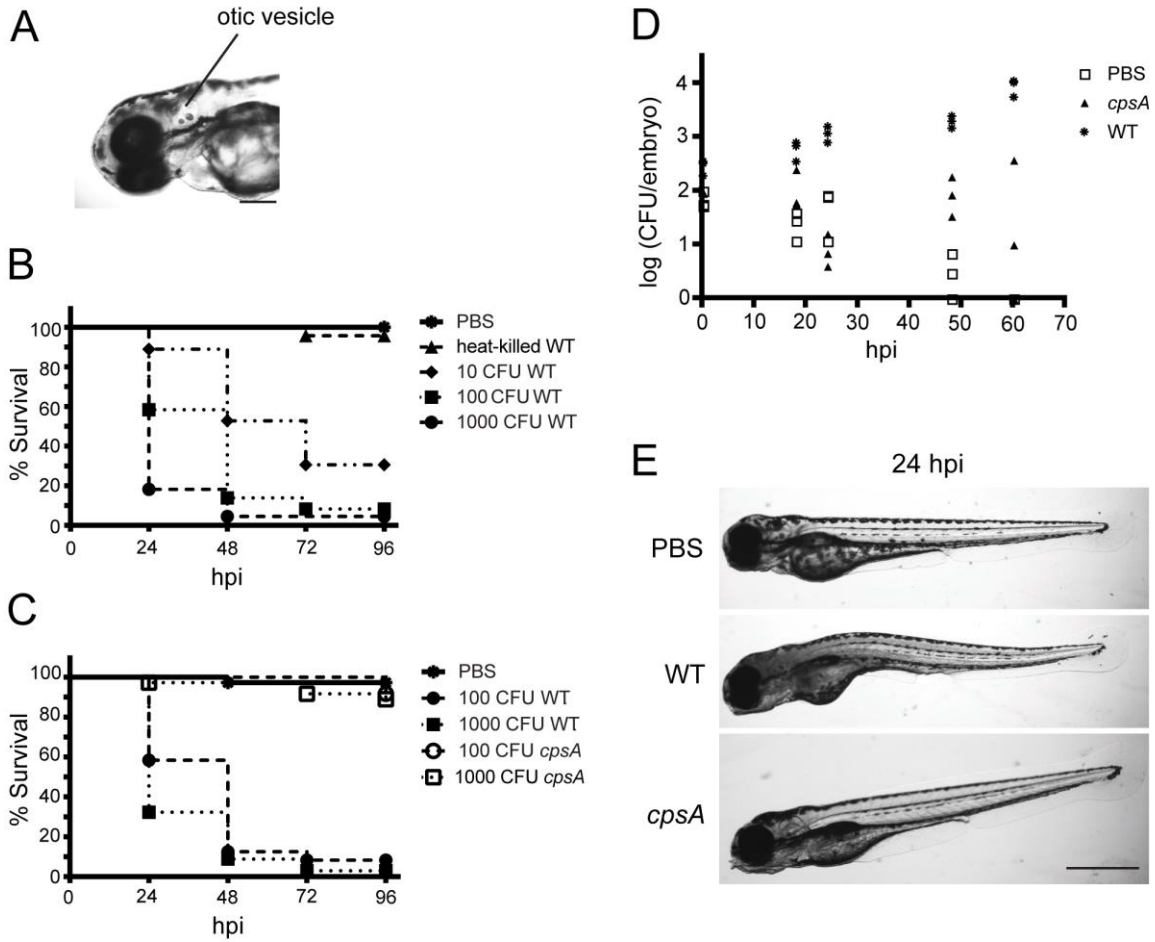


Figure 2-2: Neutrophils are recruited to sites of localized *S. iniae* infection. (A) Sudan Black staining of neutrophils recruited to the otic vesicle in larvae infected at 72 hpf with different doses of the wild type strain as indicated. Larvae were fixed at 2 hpi. Representative images are shown for larvae microinjected with PBS, ~1000 CFU wild type bacteria or an equivalent of 1000 CFU heat-killed bacteria. (n = 25-35 per group). Scale bar 200 μ m. (B) Quantification of the Sudan Black-stained larvae from (A). Each dot represents neutrophil counts in the otic vesicle for an individual larva. (C) Sudan Black staining of neutrophils recruited to the otic vesicle in larvae infected at 72 hpf with either PBS, ~100 CFU wild type or ~100 CFU *cpsA*. Larvae were fixed at 2 hpi. (n=11-16 per group). Scale bar, 300 μ m. (D) Quantification of Sudan Black stained larvae from (C). Each dot represents neutrophil counts for an individual larva. Results are representative of 3 independent experiments. *** P<0.001; ** P<0.01; ns, not significant, as determined by Kruskal-Wallis with Dunn's multiple comparison posttest.

Figure 2-2:

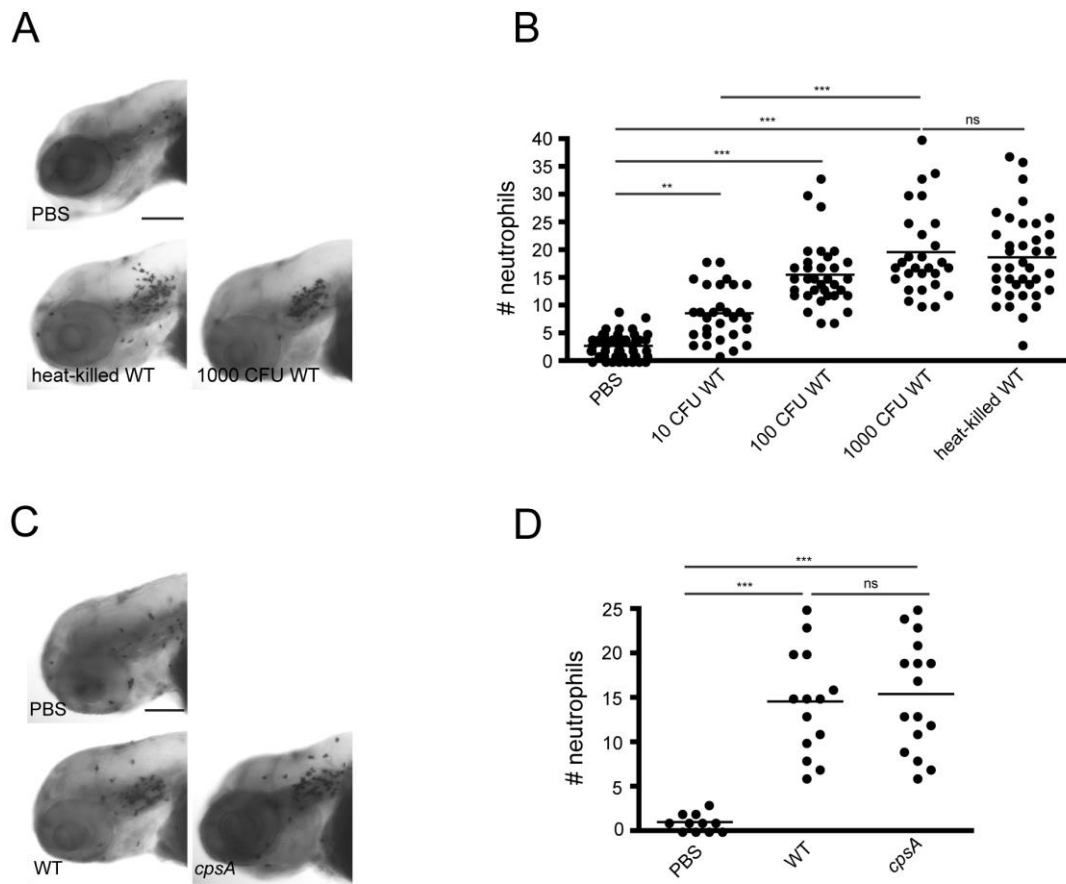
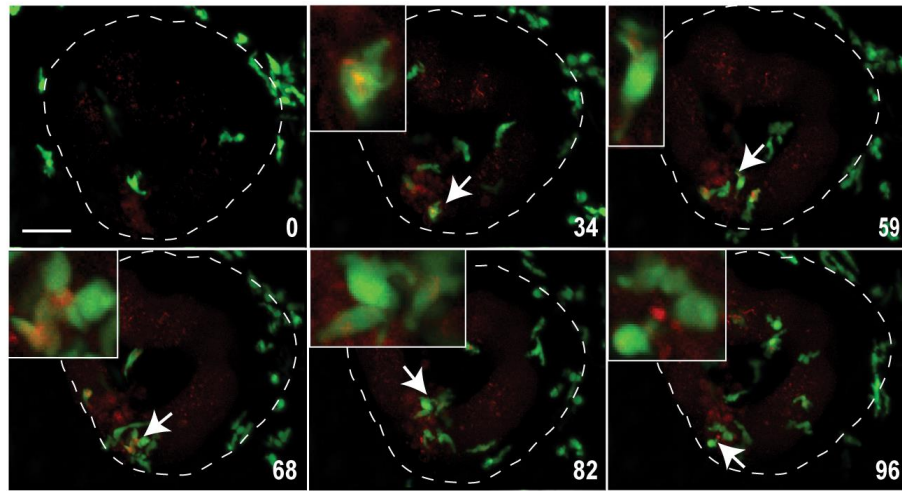


Figure 2-3: Real-time imaging of neutrophil responses to *S. iniae* infection. A confocal microscope was used to observe the neutrophil response to infection with the wild type strain or the *cpsA* mutant using a 20x objective. *Tg(mpx-dendra2)* larvae were infected at 72 hpf with ~100 CFU wild type (A) or ~100 CFU *cpsA* (B) labeled with 5 μ M CellTracker Red dye. Six frames were extracted from a 96 min or a 90 min movie, respectively. The number in the lower right corner of each frame represents the time in minutes. Time 0 is at ~10 mpi. The otic vesicle is outlined in white. The inset shows an enlarged picture of the cell indicated by the arrow or arrowhead colocalized with labeled bacteria. Scale bar, 40 μ m. Results are representative of 3 movies from 3 independent experiments. See also Movie S1 and S2.

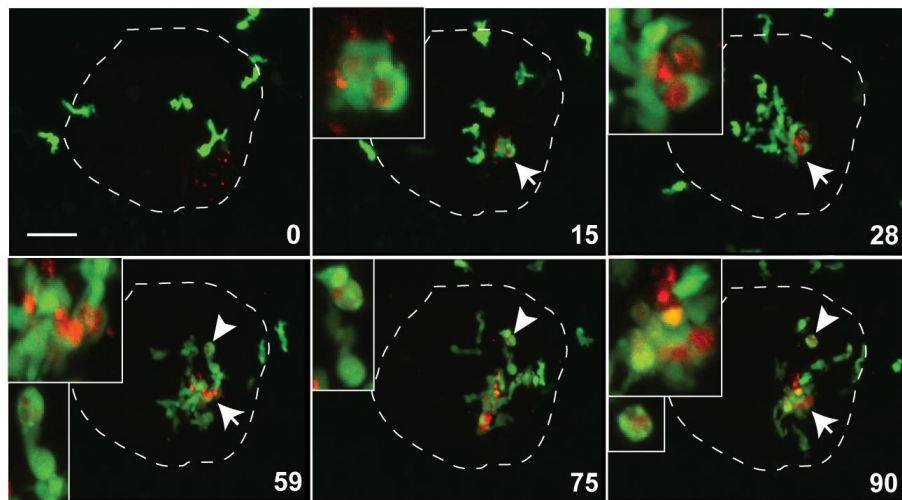
Figure 2-3:

A



Tg(mpx:dendra2) neutrophils CellTracker Red WT

B



Tg(mpx:dendra2) neutrophils CellTracker Red *cpsA*

Figure 2-4: Macrophages are recruited to sites of localized *S. iniae* infection. (A)

Fluorescence images of *Tg(mpeg1:dendra2)* larvae infected at 72 hpf with ~100 CFU wild type or ~100 CFU *cpsA*. Larvae were fixed at 2 hpi and imaged using a confocal laser scanning microscope 20x objective. Scale bar, 40 μ m. (B) Quantification of the number of macrophages recruited to the otic vesicle at 2 hpi in the larvae from (A). Each dot represents an individual larva. (n=15-20 per group). Results are representative of 3 independent experiments. *** $P < 0.001$; ns, not significant, as determined by Kruskal-Wallis test followed by Dunn's multiple comparison posttest.

Figure 2-4:

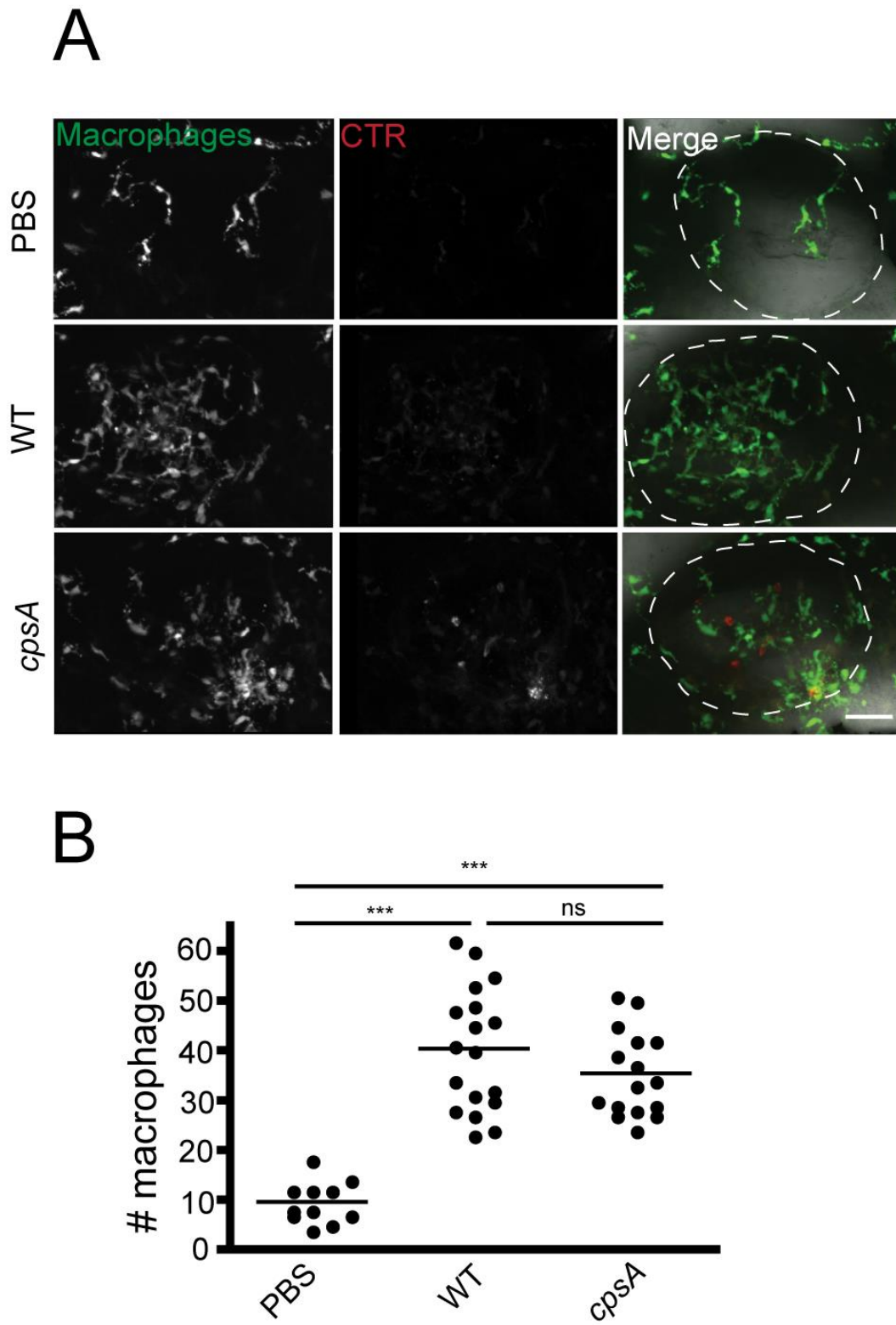
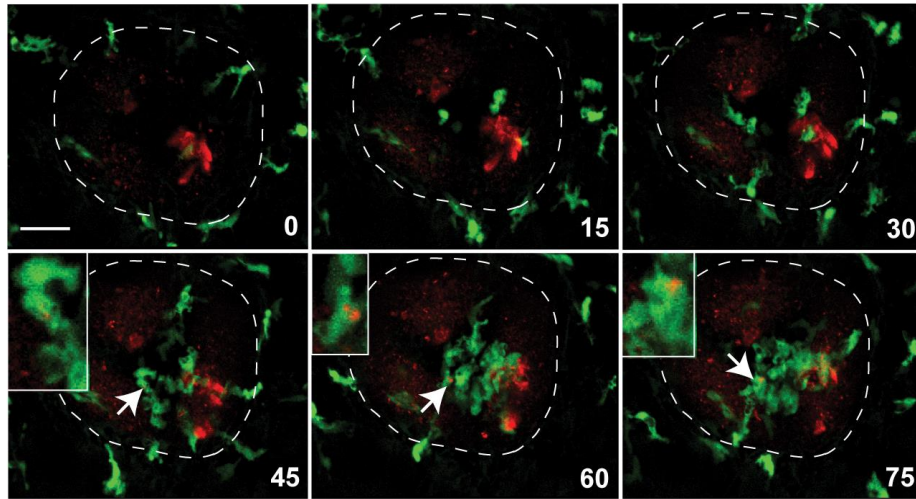


Figure 2-5: Real time imaging of macrophage responses to *S. iniae* infection. A confocal microscope was used to observe the macrophage response to infection with wild type bacteria or the *cpsA* mutant using a 20x objective. *Tg(mpeg1:dendra2)* larvae were infected at 72 hpf with ~100 CFU wild type (A) or ~100 CFU *cpsA* (B) labeled with 5 μ M CellTracker Red dye. Six frames were extracted from a 90 min or a 48 min movie, respectively. The number in the lower right corner of each frame represents the time in minutes. Time 0 is at ~10 mpi. The otic vesicle is outlined in white. The inset shows an enlarged picture of a cell indicated by the arrow colocalized with labeled bacteria. Scale bar, 50 μ m. Results are representative of 3 movies from 3 independent experiments. See also Movie S3 and S4.

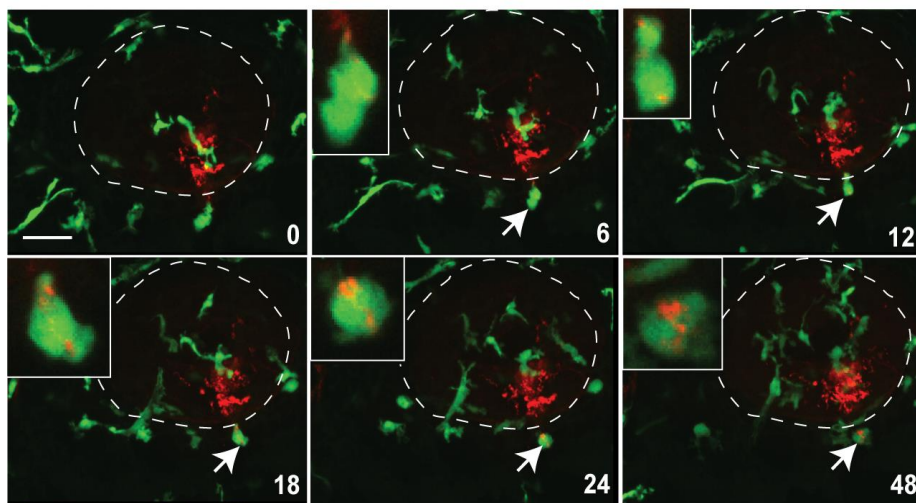
Figure 2-5:

A



Tg(mpeg1:dendra2) macrophages CellTracker Red WT

B



Tg(mpeg1:dendra2) macrophages CellTracker Red *cpsA*

Figure 2-6: Myeloid cells are important for host survival following wild type *S. iniae* and *cpsA* mutant infection. Double transgenic embryos (*Tg(mpx:mCherry)* x *Tg(mpeg1:dendra2)*) were injected at the single cell stage with either 500 μ M Pu.1 MO or 500 μ M control (Ctrl) MO. (A) Survival curves of Ctrl (Ai) and Pu.1 (Aii) morphants infected at 2 dpf with PBS, ~10 CFU wild type, ~10 CFU *cpsA* or ~100 CFU *cpsA*. (n=24 per group). Compared to infected control morphants, Pu.1 morphants had a significant decrease in survival when infected with ~10 CFU wild type ($P < 0.0001$) or with either ~10 CFU or ~100 CFU of the *cpsA* mutant ($P < 0.0001$, $P < 0.0001$) as determined by the log-rank test. The data are from 3 independent experiments each with 24 larvae per condition. (B) To monitor the efficiency of targeted knockdown, embryos were screened prior to infection on a laser scanning confocal microscope. Representative images are shown for Ctrl and Pu.1 morphants. Scale bar, 100 μ m. (C) Enumeration of viable bacteria from morphants infected at 48 hpf with PBS, ~10 CFU wild type, ~10CFU *cpsA* or ~100 CFU *cpsA*. Morphants were euthanized at 24 hpi, homogenized and plated on CNA agar. Results are representative of 3 independent experiments.

Figure 2-6:

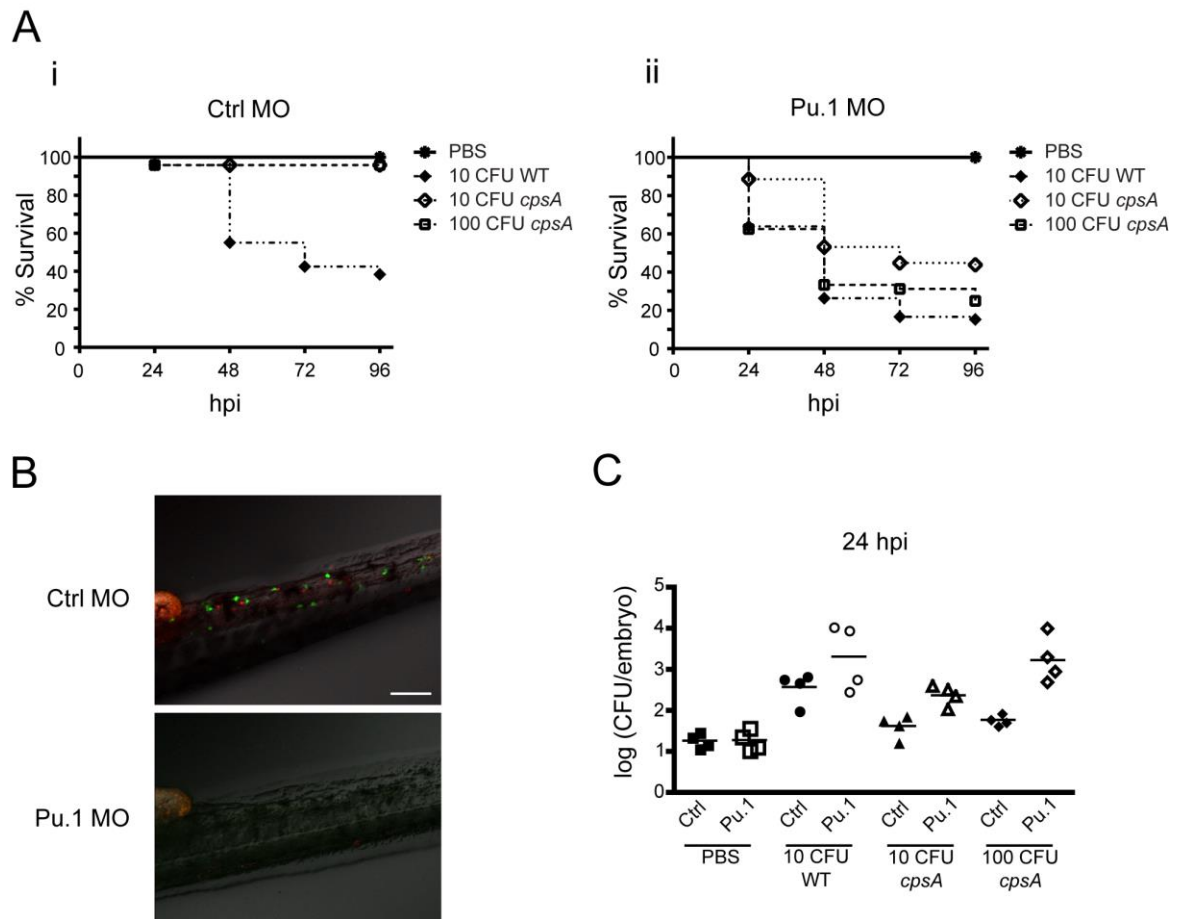
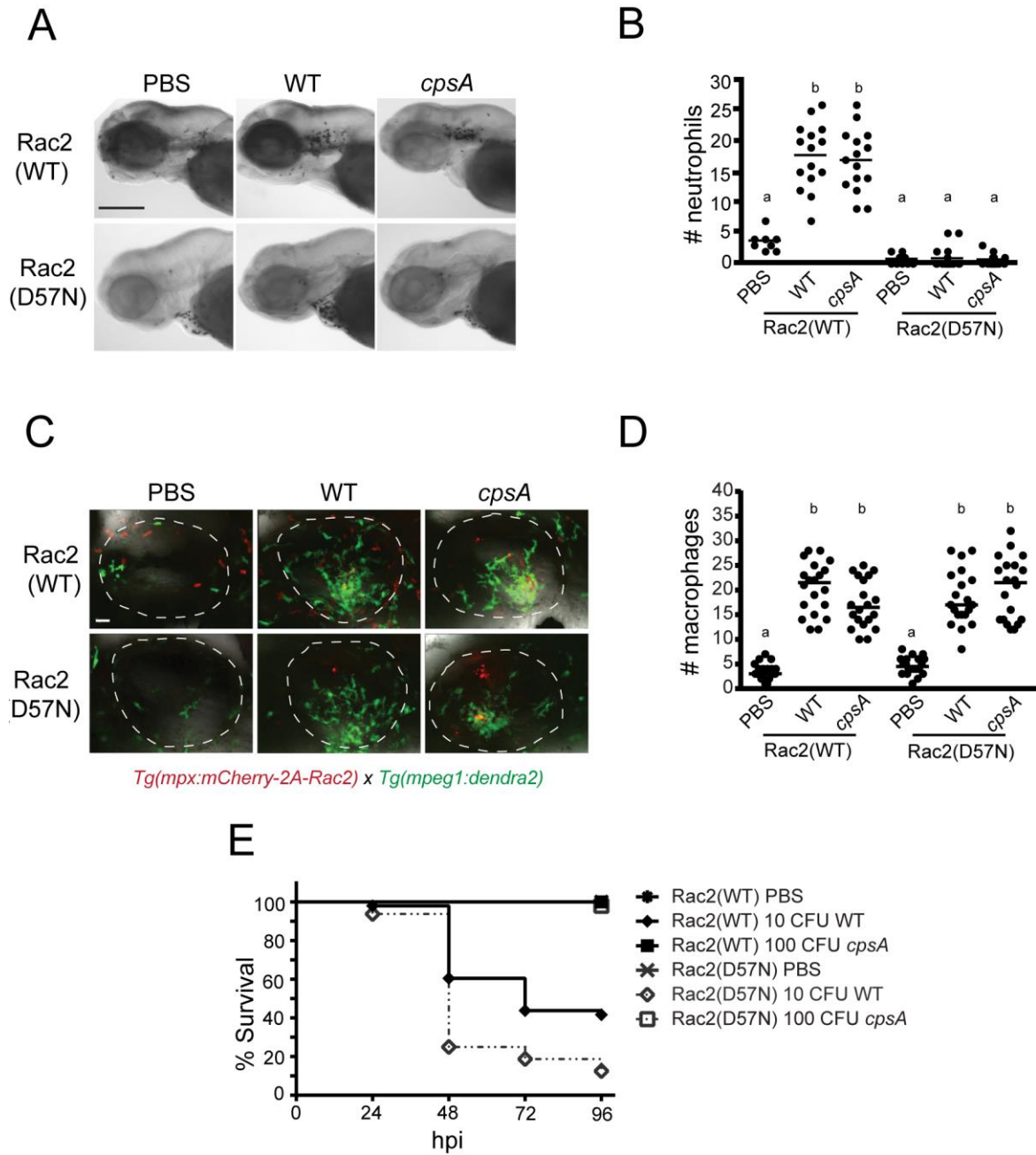


Figure 2-7: Neutrophils are important for controlling infection with wild type *S. iniae*

but not the *cpsA* mutant. *Tg(mpx:mCherry-2A-Rac2)* (Rac2(WT)) or *Tg(mpx:mCherry-2A-Rac2D57N)* (Rac2(D57N)) larvae were infected at 48 or 72 hpf with PBS, wild type *S. iniae* or the *cpsA* mutant. (A) Larvae infected at 72 hpf were fixed at 2 hpi and stained with Sudan Black. Representative images are shown for larvae microinjected with PBS, ~100 CFU wild type or ~100 CFU *cpsA*. Scale bar, 300 μ m. (B) Quantification of neutrophil recruitment to the otic vesicle in (A). (n= 8-15 per group). Medians with common letters indicate $P>0.05$ by Kruskal-Wallis with Dunn's multiple comparison posttest. Results are representative of 3 independent experiments. (C) Both the Rac2(WT) and Rac2(D57N) transgenic lines were crossed to *Tg(mpeg1:dendra2)* and the resulting double transgenics were infected at 72 hpf and fixed at 2 hpi. Representative images are shown for larvae microinjected with PBS, ~100 CFU wild type or ~100 CFU *cpsA*. Scale bar, 20 μ m. (D) Quantification of macrophage recruitment to the otic vesicle in (C). (n=20 per group). Medians with common letters indicate $P>0.05$ by Kruskal-Wallis with Dunn's multiple comparison posttest. Results are representative of 3 independent experiments. (E) Survival curves of larvae infected at 48 hpf with PBS, ~10 CFU wild type or ~100 CFU *cpsA*. (n=24 per group). Compared to infected Rac2(WT) larvae, Rac2(D57N) larvae had a significant difference in mortality when infected with wild type bacteria ($P=0.0004$) but no significant difference when infected with the *cpsA* mutant as determined by the log-rank test. The data are from 3 independent experiments each with 24 larvae per condition.

Figure 2-7:



Supplemental Video Legend

Video 1. Neutrophil recruitment and phagocytosis of wild type *S. iniae* at the otic vesicle.

Confocal microscopy, 20x objective. *Tg(mpx:dendra2)* larvae were microinjected in the otic vesicle at 72 hpf with ~100 CFU *S. iniae* 9117 labeled with 5 μ M CellTracker Red dye. The movie starts ~10 mpi. Green fluorescent neutrophils were initially recruited to the localized site of infection. Several neutrophils took up red-labeled wild type bacteria. Total movie duration was 1 h 36 min. This movie is representative of at least 3 movies taken from 3 separate experiments.

Video 2. Neutrophil recruitment and phagocytosis of the *cpsA* mutant at the otic vesicle.

Confocal microscopy, 20x objective. *Tg(mpx:dendra2)* larvae were microinjected in the otic vesicle at 72 hpf with ~100 CFU *cpsA* labeled with 5 μ M CellTracker Red dye. The movie starts ~10 mpi. Green fluorescent neutrophils were initially recruited to the localized site of infection. Several neutrophils phagocytosed large amounts of red-labeled *cpsA* mutant. The engulfed bacteria were concentrated into single, large vacuoles in the neutrophils. Total movie duration was 1 h 28m. This movie is representative of at least 3 movies taken from 3 separate experiments.

Video 3. Macrophage recruitment and phagocytosis of wild type *S. iniae* at the otic vesicle.

Confocal microscopy, 20x objective. *Tg(mpeg1:dendra2)* larvae were microinjected in the otic vesicle at 72 hpf with ~100 CFU *S. iniae* 9117 labeled with 5 μ M CellTracker Red

dye. The movie starts ~10 mpi. Green fluorescent macrophages were initially recruited to the localized site of infection. One macrophage could be seen taking up red-labeled wild type bacteria. Total movie duration was 1 h 31m. This movie is representative of at least 4 movies taken from 4 separate experiments.

Video 4. Macrophage recruitment and phagocytosis of the *cpsA* mutant at the otic vesicle. Confocal microscopy, 20x objective. *Tg(mpeg1:dendra2)* larvae were microinjected in the otic vesicle at 72 hpf with ~100 CFU *cpsA* labeled with 5 μ M CellTracker Red dye. The movie starts ~10 mpi. Green fluorescent macrophages were initially recruited to the localized site of infection. At least one macrophage can be seen taking up red-labeled *cpsA* mutant. The bacteria were initially taken up into multiple vacuoles. Total movie duration was 50 min. This movie is representative of at least 3 movies taken from 3 separate experiments.

Chapter 3

Regulation of macrophage inflammation in a larval zebrafish model of *Streptococcus iniae* infection

Abstract

Understanding how immune cells communicate during infection will reveal insights into how the immune system can be manipulated to provide enhanced defense against a broad spectrum of infections while minimizing damage from infection-induced inflammation. The larval zebrafish allows the real-time *in vivo* analysis of innate immune cell interactions during infection, and we have previously shown that both neutrophils and macrophages are important for controlling *Streptococcus iniae* infection. Here, we report the formation of organized macrophage aggregates as part of the host inflammatory response to infection, a process mediated, at least in part, by leukotriene A4 hydrolase (Lta4h) signaling. Depletion of Lta4h, which catalyzes the last step in leukotriene B4 (LTB4) synthesis, resulted in enhanced susceptibility to infection and abrogation of macrophage aggregation. Neutrophil immunodeficient fish also have worse survival and defects in macrophage aggregation following *S. iniae* infection. Neutrophil-specific expression of *lta4h* was sufficient to rescue the macrophage aggregation and survival defects in Lta4h-deficient larvae. Taken together, we have found that neutrophil expression of Lta4h modulates the macrophage inflammatory response to *S. iniae* infection in zebrafish larvae.

Introduction

The innate immune system is an important first line of defense against invading microbes, and neutrophils are typically the first type of leukocyte recruited to sites of bacterial infection (1). Once activated, neutrophils exhibit a wide range of antimicrobial effector functions including: phagocytosis, secretion of granule proteins and other antimicrobial peptides, production of reactive oxygen species (ROS) and release of neutrophil extracellular traps (NETs) (2, 3). In addition to their directly antimicrobial activities, activated neutrophils serve as modulators of the immune response by releasing pro-inflammatory molecules and cytokines/chemokines to recruit other immune cells to the infection site. Currently, little is known about how neutrophils regulate macrophage behavior and coordinate the innate immune response to infection.

Activated leukocytes, particularly neutrophils, release a variety of pro-inflammatory mediators, including the eicosanoid, leukotriene B₄ (LTB₄) (4, 5). LTB₄ is synthesized from leukotriene A₄, a downstream metabolite of arachidonic acid, by leukotriene A₄ hydrolase (LTA₄H). The first *in vivo* study to suggest an antimicrobial role for leukotrienes reported that exogenous LTB₄ enhances clearance of *Salmonella enterica* serovar Typhimurium infection in mice (6). Since this initial study, the generation of leukotriene-deficient mice (7, 8) has revealed that leukotrienes play important roles in infection with bacteria (9-11), fungi (12), and parasites (13). In addition to functioning as a leukocyte chemoattractant (14, 15), LTB₄ boosts the antimicrobial activity of leukocytes by enhancing phagocytosis (6, 16, 17), increasing lysosomal enzyme (18) and granule protein release (19), activating NADPH

oxidase to produce reactive oxygen species (ROS) (20), increasing production of antimicrobials (21, 22) and nitric oxide (23). LTB₄ also stimulates the production of cytokines such as TNF α (24), IL-8 (25) and IL-6 (26) to further augment the pro-inflammatory response to infection. These properties make LTB₄ an effective means of communication between immune cells in the host response to infection.

In order to investigate neutrophil-macrophage interactions *in vivo*, it is necessary to use a model that is amenable to non-invasive live imaging. Although adaptive immunity is not functional until at least 2-3 weeks post fertilization (27-29), larvae have a highly conserved innate immune system with complement (30), Toll-like receptors (31-32), neutrophils (33-34) and macrophages. Larval zebrafish phagocytes are capable of a variety of antimicrobial functions including phagocytosis by 28-30 hpf (34-35) and a respiratory burst by 72 hpf (36). Additionally, zebrafish larvae are both genetically tractable and optically transparent, allowing for the generation of transgenic lines with fluorescently labeled leukocytes to study leukocyte behavior during infection in real time.

A number of bacterial infection models have been established in zebrafish to study the neutrophil and macrophage responses to infection (reviewed in (37) and (38), respectively), but how neutrophils and macrophages interact with one another during bacterial infection is currently not well understood. Localized injection of *Streptococcus iniae* into the otic vesicle of zebrafish larvae results in the rapid and robust recruitment of neutrophils and macrophages (39). Although neutrophils are important in the host response to infection with a wild-type strain of *S. iniae* (39), the individual contribution of macrophages to host defense and how

neutrophils and macrophages interact during the immune response to this pathogen have not yet been investigated.

Here, we use the zebrafish larval model of *S. iniae* infection (39) to show that macrophages are important in the response to infection, and infection-induced macrophage inflammation is characterized by cell aggregation in the tail/trunk of infected fish. Interestingly, both neutrophils and *Lta4h* signaling are important for the development of macrophage aggregation and are critical for host survival following *S. iniae* infection, indicating these macrophage structures may provide some protective role in host defense. Lastly, neutrophil-specific expression of *lta4h* is sufficient to induce this inflammatory macrophage phenotype in *Lta4h*-deficient larvae following *S. iniae* infection. Thus, this study demonstrates how neutrophils can influence macrophage behavior through *Lta4h* signaling and modulate the immune response to bacterial infection.

Results

Macrophages are important for host defense against *S. iniae* infection and infection with wild type *S. iniae* induces organized macrophage aggregation

Previous work has shown that both neutrophils and macrophages are recruited to otic vesicle infection with either a wild-type strain of *S. iniae* or a capsule-deficient *S. iniae cpsA* mutant (40), and depletion of both neutrophils and macrophages results in increased susceptibility to infection (39). Using a zebrafish model of leukocyte adhesion deficiency (LAD) where neutrophil function is impaired (41), LAD larvae were increasingly susceptible

to infection with the wild-type strain, but the *cpsA* mutant remained avirulent (39), suggesting that a cell type other than neutrophils is important for the control of this non-pathogenic mutant. Since macrophages are the other major type of white blood cell present at this developmental stage in zebrafish, we sought to determine the specific contribution of macrophages to host defense against *S. iniae* infection.

To determine the individual contribution of macrophages in defense against *S. iniae* infection, we depleted macrophages with a morpholino targeting *irf8*, a transcription factor important in cell fate choice during primitive myelopoiesis. Expression of Irf8 promotes the formation of macrophages while suppressing neutrophil formation, and suppression of Irf8 function results in depletion of macrophages (42). Irf8 morphants had increased susceptibility to infection with 50 CFU wild-type bacteria, with ~10% survival of Irf8 morphants compared to ~50% survival of control morphants (**Fig. 1A**) ($p = 0.0002$). Irf8 morphants also had enhanced susceptibility to infection with the *cpsA* mutant with ~40% survival of Irf8 morphants compared to ~80% survival of control morphants (**Fig. 1A**) ($p = 0.0004$). This suggests an important role for macrophages in host defense against infection with *S. iniae* but also shows that while neutrophils are not necessary (39), macrophages are critical for control of infection with the *cpsA* mutant. Interestingly, we observed that although macrophages are necessary for control of infection with both wild-type and mutant strains, only infection with wild-type *S. iniae* induced a macrophage inflammatory response characterized by aggregation of infected and uninfected macrophages by 24 hours post infection (hpi) (**Fig. 1B, 1C, 1E**). The proportion of infected larvae that developed these macrophage inflammatory structures

increased in a dose-dependent manner. Injection of 10 CFU of wild-type *S. iniae* did not induce this macrophage inflammation, even by 96 hpi (data not shown), but by 24 hpi, ~20% of larvae injected with 50 CFU and ~50% of larvae injected with 100 CFU had formed macrophage aggregates. The average size and number of aggregates per larva varied greatly from fish to fish; the average area of an aggregate in larvae infected with 50-100 CFU wild-type *S. iniae* was 1500 μm^2 (**Fig. 1D**), and larvae had 3-4 aggregates on average (data not shown). In larvae that formed macrophage aggregates, these structures formed in the trunk, including around the region of the caudal hematopoietic tissue (CHT), and also extended to the tip of the tail. Injection of similar doses of *S. iniae* into the hindbrain ventricle or duct of Cuvier also resulted in the formation of these macrophage structures in the same location (**Supplemental Fig. 1A**). Interestingly, co-injection of heat-killed or formalin-killed wild-type bacteria with viable *cpsA* mutant induced a similar macrophage inflammatory response compared to infection with viable wild-type bacteria (**Supplemental Fig. 1B** and **1C**). This suggested that this particular macrophage inflammation may be in response to a combination of *S. iniae* capsule as well as infection-induced pro-inflammatory signals.

Disruption of Lta4h signaling abrogates macrophage aggregation

To determine the mechanisms that regulate *S. iniae*-induced macrophage aggregation, we first targeted zebrafish Lta4h signaling. Lta4h is responsible for the synthesis of pro-inflammatory LTB₄, an important molecule that mediates leukocyte recruitment and antimicrobial functions. Additionally, Lta4h signaling has been found to regulate

Mycobacterium-induced granuloma formation in zebrafish (10, 43). In the zebrafish model of *M. marinum* infection, both Lta4h deficiency and excess result in hypersusceptibility, increased bacterial burdens and larger granuloma formation (10, 43). In *S. iniae* infection, morpholino-mediated depletion of Lta4h resulted in failure of larvae to form macrophage aggregates (**Fig. 2B** and **2C**), suggesting that the macrophage inflammatory response to *S. iniae* infection is regulated in a different manner than *M. marinum* –induced granulomas. Whereas approximately 20% of control morphants infected with 50 CFU wild-type *S. iniae* developed macrophage aggregates, none of the Lta4h morphants developed aggregates (**Fig. 2B** and **2C**). Susceptibility to infection was also increased in Lta4h morphants with ~60% of Lta4h-deficient larvae succumbing to infection compared to only 40% of control larvae when infected with a low dose of 10 CFU (**Fig. 2A**) ($p = 0.0458$). Since Lta4h morphants are increasingly susceptible to infection and do not form macrophage aggregates, this supports a host-protective role for macrophage aggregates. Treatment of infected larvae with a pharmacological inhibitor of Lta4h (Bestatin) or infection of an Lta4h-deficient mutant (10) also resulted in defects in macrophage aggregation (**Supplemental Fig. 2C, 2D, 2F, 2G**), but a minimal effect on host survival (**Supplemental Fig. 2B** and **2D**).

Since Lta4h produces LTB₄, we next tested whether exogenous LTB₄ added to the water of infected larvae was sufficient to rescue the macrophage aggregation defect in Lta4h-deficient larvae. Although LTB₄ treatment did not significantly affect host survival even in the Lta4h morphants (**Fig. 2D**), exogenous LTB₄ was sufficient to rescue the macrophage aggregation defect in Lta4h morphants. About 30% of Lta4h morphants treated with LTB₄

formed aggregates compared to ~25% of control morphants treated with LTB₄ and 0% of ethanol-treated Lta_{4h} morphants (**Fig. 2E** and **2F**). Thus, Lta_{4h} signaling through production of LTB₄ regulates the formation of *S. iniae*-induced macrophage aggregates.

Neutrophils drive macrophage inflammation and aggregation in response to *S. iniae* infection

Since LTA_{4H} signaling affects host survival and the macrophage inflammatory phenotype seen during the host response to *S. iniae* (**Fig. 2**), and neutrophils are also important for host survival during *S. iniae* infection (39) and can also express Lta_{4h}, we wanted to determine if neutrophil Lta_{4h} signaling was necessary for the observed macrophage aggregation. To address this, we used the zebrafish model of LAD in which neutrophils expressing the dominant inhibitory Rac2D57N mutation (LAD larvae) had impaired neutrophil recruitment to localized infection (39, 41). LAD larvae infected with 50 CFU wild-type *S. iniae* did not form macrophage aggregates even though larvae expressing Rac2WT (control larvae) did (**Fig. 3A** and **3B**), indicating that neutrophils are critical in driving the macrophage inflammatory response characterized by aggregation. Additionally, since neutrophils are important in host defense against infection with wild-type *S. iniae* (39), and neutrophil immunodeficient larvae do not form macrophage aggregates, this also supports a protective role for the aggregates in *S. iniae* infection. The dominant inhibitory Rac2D57N mutation responsible for the LAD phenotype has been found to not only affect neutrophil migration but also reactive oxygen species (ROS) production in human patients

(44, 45). To determine if the defect in macrophage aggregation in LAD larvae was due to a defect in neutrophil ROS signaling, we used a morpholino targeting the membrane-bound p22^{phox} subunit of the NADPH oxidase complex. Macrophages formed aggregates in response to infection with 50 CFU wild-type *S. iniae* in the p22^{phox} morphants, in a similar manner to what was seen in control morphants (**Fig. 3C, 3D, 3E**) with no survival defect (**Fig. 3F**). Taken together, these data suggest that neutrophils modulate macrophage aggregation independently of ROS signaling.

Although neutrophils are in the vicinity of macrophage aggregates but do not aggregate, we hypothesized that neutrophils are producing a signal critical in driving this macrophage behavior. Both neutrophils and Lta4h signaling are important in the formation of macrophage aggregates, leading to the hypothesis that neutrophil-specific Lta4h signaling influences *S. iniae*-induced macrophage aggregation. Exogenous LTB4 added to the water of *S. iniae*-infected LAD larvae resulted in a rescue in the macrophage aggregation defect with ~20-25% of LTB4-treated LAD and control larvae forming macrophage aggregates, similar to the ~25% of ethanol-treated control larvae (**Fig. 4B and 4C**).

Neutrophil-specific expression of Lta4h modulates macrophage behavior

To test if neutrophil-specific expression of *lta4h* was sufficient to rescue the macrophage aggregation defect seen in Lta4h-deficient fish, we generated a transgenic line in which *lta4h* was expressed downstream of the neutrophil-specific promoter, *lyz* (46, 47). Neutrophil-specific expression of *lta4h* in Lta4h-deficient larvae was sufficient to rescue both

the macrophage aggregation defect (**Fig. 5A** and **5B**) and survival defect (**Fig. 5C**). Lta4h morphants with neutrophil-specific expression of *lta4h* (OE Lta4h morphants) have significantly better survival than Lta4h morphants without overexpression of *lta4h* (WT Lta4h morphants) ($p = 0.0335$). Also, OE Lta4h morphants and OE control morphants do not have a significant difference in survival. These findings suggest that neutrophil production of Lta4h drives macrophage inflammation and protective host defense against infection with *S. iniae*.

Discussion

Despite the importance of neutrophils in the innate immune response to infection, little is known about how these cells regulate macrophages to coordinate host defense. Here, we show that neutrophil Lta4h signaling modulates macrophage inflammation in the host response to *S. iniae* infection. Both neutrophils (39) and macrophages (**Fig. 1A**) contribute to host defense against infection with wild-type *S. iniae*, but only macrophages are necessary for controlling infection with the capsule-deficient *cpsA* mutant (**Fig. 1A**). Although early macrophage responses towards the wild-type and *cpsA* mutant strains are similar in terms of recruitment and phagocytosis (39), subsequent bacterium-phagocyte interactions are different. In response to infection with wild-type *S. iniae*, aggregates of infected and uninfected macrophages form in the trunk/tail of a proportion of infected larvae (**Fig. 1E**). This variability in the macrophage inflammatory response from larva-to-larva may be due to individual variation in the response to infection since zebrafish lines are not highly inbred.

Alternatively, variations in the infectious dose, due to bacteria settling in the needle, may also result in this variable macrophage inflammatory response since we show here that larger infectious doses result in a larger proportion of infected larvae developing macrophage aggregates early in infection (**Fig. 1B** and **1C**). To control for potential differences in injected doses, needles are changed periodically throughout the experiment and injection volumes at the beginning and end of each needle are plated on media to record colony counts and ensure that larvae are injected with approximately the same number of bacteria throughout a given experiment. Additionally, these macrophage aggregates appear to develop in the same location in larvae regardless of the infection route (**Supplemental Fig. 1A**). A future challenge will be to determine the signaling mechanisms important for recruiting aggregating macrophages to this region. It is also of interest to determine why some macrophages are recruited to the aggregate structures while others are not.

Disruption of Lta4h signaling abrogates macrophage aggregation revealing an important role for Lta4h signaling in regulating the macrophage response to *S. iniae* infection (**Fig. 2B** and **2C**). This is in contrast to what has been shown in a zebrafish larval model of *M. marinum* infection in which Lta4h-deficient larvae formed larger aggregates compared to controls (10). Thus, *S. iniae*-induced macrophage aggregates are regulated differently than *Mycobacterium*-induced granulomas. Additionally, disruption to Lta4h signaling enhances susceptibility to infection (**Fig. 2A**), indicating a protective role for these macrophage structures in host defense against *S. iniae* infection. Interestingly, exogenous LTB4 was able to rescue the macrophage aggregation defect in Lta4h-deficient larvae (**Fig. 2E** and **2F**)

suggesting that LTB₄-induced pro-inflammatory functions are critical to the formation of these macrophage structures in response to *S. iniae* infection.

Neutrophils are important for the immune response to wild-type *S. iniae* infection but not to the *cpsA* mutant (39), and since wild-type *S. iniae*, but not the *cpsA* mutant, induces the formation of macrophage aggregates (**Fig. 1B-1E**), the role of neutrophils in influencing macrophage aggregation was investigated. LAD larvae expressing the dominant inhibitory Rac2D57N mutation in neutrophils have defects in neutrophil emigration and chemotaxis to sites of infection (39, 41). These immunodeficient larvae did not develop macrophage aggregates in response to *S. iniae* infection (**Fig. 3A and 3B**) revealing an important role for neutrophils in macrophage aggregation. A similar requirement for neutrophils in modulating the macrophage response to bacterial infection was demonstrated in a study by Seiler et al., where neutrophils are required for early granuloma formation in a mouse model of *M. tuberculosis* infection (48). Although the underlying Rac2D57N mutation of the LAD phenotype in humans results in decreased NADPH oxidase activity (44, 45), defects in ROS production were not the cause of the macrophage aggregation defect seen in LAD larvae. Disruption to ROS signaling, achieved with a p22^{phox} morpholino (49), had no effect on macrophage aggregate formation (**Fig. 3C and 3D**). This suggests that defects in macrophage aggregation in LAD larvae were not due to defective neutrophil ROS signaling but were due to some other neutrophil-mediated response.

Neutrophils can produce LTB₄, and since both *Lta4h* and neutrophils are both necessary for macrophage aggregation in response to *S. iniae* infection, we sought to

determine if neutrophil Lta4h signaling was responsible for regulating the development of macrophage aggregates. Exogenous LTB₄ was enough to rescue the macrophage aggregation defect in LAD larvae (**Fig. 4B** and **4C**), but to determine if neutrophil-specific expression of *lta4h* was sufficient to induce macrophage aggregation, we generated a transgenic line expressing *lta4h* downstream of a neutrophil-specific promoter. Neutrophil-specific expression of Lta4h was sufficient to rescue the macrophage aggregation defect in Lta4h-deficient larvae (**Fig. 5A** and **5B**) as well as the survival defect (**Fig. 5C**). Taken together, we have shown here that neutrophils are able to modulate the macrophage inflammatory response to *S. iniae* infection through Lta4h signaling.

There is growing evidence to suggest that neutrophils are more than just efficient microbe-killing phagocytes; they also have immunomodulatory behavior and have been shown to influence macrophage antimicrobial activities. Following engagement of their pattern recognition receptors, neutrophils can become activated to secrete cytokines, chemokines and other immunomodulatory molecules to regulate the immune response to infection. Several studies have found that the anti-mycobacterial activity of macrophages is enhanced after acquisition of neutrophil-produced granule peptides both *in vitro* (50) and in a mouse model (51). Here, we show that neutrophils modulate the macrophage inflammatory response to *S. iniae* infection in zebrafish larvae. Understanding how immune cells interact is essential for the development of anti-infective therapies aimed at modulating the host immune response. For example, in a study by Scott et al., it was reported that innate defense regulatory peptide 1 (IDR-1), a peptide synthesized to be similar in function to neutrophil

antimicrobial peptides, was not directly antimicrobial but offered host protection in multiple mouse models of bacterial infection by stimulating monocyte/macrophage recruitment to infection while controlling the infection-induced pro-inflammatory response (52). Since such host-directed anti-infective therapies do not act directly on the microbe, they may provide treatment for a wide variety of infections while also reducing concerns of contributing to the rise in antibiotic resistance.

In summary, we have shown that neutrophil-specific expression of *lta4h* modulates the macrophage inflammatory response to infection with *S. iniae* in zebrafish larvae. Our results indicate that beyond their phagocytic and antimicrobial roles, neutrophils also are important regulators of the early innate immune response. By furthering our understanding of immune cell crosstalk, we can develop anti-infective therapies aimed at modulating infection-induced inflammation to target a broader range of infections while also controlling infection-induced inflammation.

Materials and Methods

Zebrafish maintenance and drug treatment. Embryos, larvae and adults were maintained in accordance with the University of Wisconsin-Madison Research Animal Resources Center (Madison, WI). A light cycle of 10h darkness and 14h light was used. Wild-type AB fish were used to generate all transgenic lines and the following transgenic lines were used in these studies: *Tg(mpx:mCherry)*, *Tg(mpeg1:dendra2)* (39), *Tg(mpx:mCherry-2A-rac2wt)* and *Tg(mpx:mCherry-2a-rac2d57n)* (41). Additionally, a previously described *lta4h*-deficient

mutant with a retroviral insertion in the seventh exon of *lta4h* (10) was generously provided by Lalita Ramakrishnan. Embryos were obtained by natural spawning and were raised at 28.5°C in E3 medium as previously described (53). To prevent pigment formation, some larvae were maintained in E3 containing 0.2 mM *N*-phenylthiourea (Sigma-Aldrich, St. Louis, MO). For infections and live imaging, larvae were anesthetized in E3 medium containing 0.2 mg/ml tricaine (ethyl 3-amino-benzoate; Sigma-Aldrich). Where indicated, E3 was supplemented with the following drugs immediately following infection and drug solutions were changed daily: 100 µM Bestatin (Cayman Chemical, Ann Arbor, MI), 0.1% DMSO, 30 nM LTB4 (Cayman Chemical) 0.1% ethanol.

Bacterial strains and microinjection of bacteria. *S. iniae* wild-type strain 9117 and a capsule-deficient *S. iniae* mutant with a polar insertional mutation in the *cpsA* gene (*cpsA* mutant) have been previously described (40,54). *S. iniae* was prepared and microinjected into the otic vesicle of zebrafish aged 2-3 dpf as described (39). Hindbrain ventricle and duct of Cuvier injections were performed as previously described (55). Where indicated, heat-killing was achieved by placing bacteria at 95°C for 30 min and formalin-killing was achieved by resuspending bacteria in 1 ml of 4% paraformaldehyde and incubating at 37°C for 30 min. Also where indicated, bacteria were labeled with 5 µM CellTracker Red CMPTX dye (catalog number C34552; Molecular Probes, Invitrogen, Grand Island, NY) according to the manufacturer's instructions.

MO injection. All morpholino oligonucleotides were purchased from Gene Tools, LLC (Philomath, OR), resuspended in distilled water and stored at room temperature at a stock concentration of 1 mM. One-cell stage wild-type AB embryos were injected with 3 nl of morpholinos at the following concentrations: Irf8 MO, 400 μ M; Lta4h (I7E8) MO, 150 μ M; p22^{phox} MO, 500 μ M. Comparable doses of the standard control MO were used in each experiment. The Irf8 (42) and p22^{phox} (49) morpholinos were previously described. MO oligo sequences are as follows:

Lta4h: 5'- CAGTCTGATCAAGAGAAAGACTCGA-3'

p22^{phox}: 5'-ATCATAGCATGTAAGGATACATCCC-3'

Irf8: 5'- AATGTTTCGCTTACTTTGAAAATGG-3'

Elimination of macrophages in Irf8 morphants was confirmed by injecting into *Tg(mpeg1:dendra2)* line with fluorescent green macrophages. Confirmation of Lta4h morpholino was achieved by RT-PCR of mRNA extracted from 2-4 dpf larvae (**Supplemental Fig. 2A**).

Lta4h Primers for RT-PCR:

lta4hF: 5'-TCTGAGAAGGAATATGTGGATGAA-3'

lta4hR: 5'-CAGCAAGAGATCTGTCTCCA-3'

Generation of the transgenic *Tg(lyz:lta4h-2a-mCherry)* zebrafish line. DNA encoding *lta4h-2a-mCh* (zebrafish *lta4h* (Open Biosystems Clone ID 6961761, Accession CD760387, BC068394) was PCR amplified and inserted into a backbone vector containing minimal Tol2

elements for efficient integration, the *lyz* promoter for neutrophil-specific expression (46) and an SV40 polyadenylation sequence (Clontech Laboratories, Inc.). A viral 2A peptide linker sequence was used to facilitate production of multiple protein products from a single transgene (56). One-cell stage wild-type AB embryos were injected with a 3 nl solution containing 25 ng/ μ l DNA and 35 ng/ μ l transposase mRNA and were grown at 28.5°C.

Antibody staining. Zebrafish were fixed in formaldehyde overnight at 4°C and immunolabeled as previously described (57) using rabbit antibodies to zebrafish L-plastin (58). L-plastin is expressed in both neutrophils and macrophages (46).

Microscope analysis and live imaging. Anesthetized larvae were settled onto the bottom of a custom-made, glass-bottom dish. Time-lapse fluorescence images were acquired with a laser scanning confocal microscope (Fluoview FV1000; Olympus, Center Valley, PA) using a numerical aperture 0.75/20X objective. Each fluorescent channel (488 nm and 543 nm) and differential interference contrast (DIC) images were acquired by sequential line scanning. Z-series were acquired using a 200-300 μ m pinhole and 6-10 μ m step sizes.

Statistical analyses. All statistical analyses were performed using GraphPad Prism, version 6. Resulting p values are included in the figure legends for each experiment. Area of macrophage aggregates was calculated using ImageJ software.

Acknowledgements

We would like to thank lab members for zebrafish maintenance.

References

1. **Amulic B, Cazalet C, Hayes GL, Metzler KD, Zychlinsky A.** 2012. Neutrophil Function: From Mechanisms to Disease. *Annu. Rev. Immunol.* **30**:459–489.
2. **Borregaard N.** 2010. Neutrophils, from Marrow to Microbes. *Immunity* **33**:657–670.
3. **Nathan C.** 2006. Neutrophils and immunity: challenges and opportunities. *Nature Reviews Immunology* **6**:173–182.
4. **Peters-Golden M, Canetti C, Mancuso P, Coffey MJ.** 2005. Leukotrienes: Underappreciated Mediators of Innate Immune Responses. *Journal of Immunology* (Baltimore, Md. : 1950) **174**:589–594.
5. **Flamand N, Mancuso P, Serezani CHC, Brock TG.** 2007. Leukotrienes: Mediators that have been typecast as villains. *Cell. Mol. Life Sci.* **64**:2657–2670.
6. **Demitsu T, Katayama H, Saito-Taki T, Yaoita H, Nakano M.** 1989. Phagocytosis and bactericidal action of mouse peritoneal macrophages treated with leukotriene B4. *Int. J. Immunopharmacol.* **11**:801–808.
7. **Chen X-S, Sheller JR, Johnson EN, Funk CD.** 1994. Role of leukotrienes revealed by targeted disruption of the 5-lipoxygenase gene. *Nature.*
8. **Goulet JL, Snouwaert JN, Latour AM, Coffman TN, Koller BH.** 1994. Altered inflammatory responses in leukotriene-deficient mice. *PNAS* **91**:12852–12856.

9. **Mancuso P, Lewis C, Serezani CH, Goel D, Peters-Golden M.** 2010. Intrapulmonary Administration of Leukotriene B4 Enhances Pulmonary Host Defense against Pneumococcal Pneumonia. *Infection and Immunity* **78**:2264–2271.
10. **Tobin DM, Vary JC Jr, Ray JP, Walsh GS, Dunstan SJ, Bang ND, Hagge DA, Khadge S, King M-C, Hawn TR, Moens CB, Ramakrishnan L.** 2010. The *Ita4h* Locus Modulates Susceptibility to Mycobacterial Infection in Zebrafish and Humans. *Cell* **140**:717–730.
11. **Peres CM, de Paula L, Medeiros AI, Sorgi CA, Soares EG, Carlos D, Peters-Golden M, Silva CL, Faccioli LH.** 2007. Inhibition of leukotriene biosynthesis abrogates the host control of *Mycobacterium tuberculosis*. *Microbes Infect.* **9**:483–489.
12. **Medeiros AI, Sá-Nunes A, Turato WM, Secatto A, Frantz FG, Sorgi CA, Serezani CH, Deepe GS, Faccioli LH.** 2008. Leukotrienes are potent adjuvant during fungal infection: effects on memory T cells. *The Journal of Immunology* **181**:8544–8551.
13. **Serezani CH, Perrela JH, Russo M, Peters-Golden M, Jancar S.** 2006. Leukotrienes Are Essential for the Control of *Leishmania amazonensis* Infection and Contribute to Strain Variation in Susceptibility. *Journal of Immunology (Baltimore, Md. : 1950)* **177**:3201–3208.
14. **Ford-Hutchinson AW, Bray MA, Doig MV, Shipley ME, Smith MJH.** 1980. Leukotriene B, a potent chemokinetic and aggregating substance released from polymorphonuclear leukocytes. *Nature*.
15. **Matsukawa A, Hogaboam CM, Lukacs NW, Lincoln PM, Strieter RM, Kunkel**

- SL.** 1999. Endogenous Monocyte Chemoattractant Protein-1 (MCP-1) Protects Mice in a Model of Acute Septic Peritonitis: Cross-Talk Between MCP-1 and Leukotriene B₄. *Journal of Immunology* (Baltimore, Md. : 1950) **163**:6148–6154.
16. **Bailia MB, Standiford TJ, Laichalk LL, Coffey MJ, Strieter R, Peters-Golden M.** 1996. Leukotriene-Deficient Mice Manifest Enhanced Lethality from Klebsiella Pneumonia in Association with Decreased Alveolar Macrophage Phagocytic and Bactericidal Activities. *Journal of Immunology* (Baltimore, Md. : 1950).
17. **Mancuso P, Standiford TJ, Marshall T, Peters-Golden M.** 1998. 5-Lipoxygenase reaction products modulate alveolar macrophage phagocytosis of Klebsiella pneumoniae. *Infection and Immunity* **66**:5140–5146.
18. **Serhan CN, Radin A, Smolen JE, Korchak H, Samuelsson B, Weissmann G.** 1982. Leukotriene B₄ is a complete secretagogue in human neutrophils: A kinetic analysis. *Biochem. Biophys. Res. Commun.*
19. **Borgeat P, Naccache PH.** 1990. Biosynthesis and biological activity of leukotriene B₄. *Clin. Biochem.* **23**:459–468.
20. **Dewald B, Baggiolini M.** 1985. Activation of NADPH Oxidase in Human Neutrophils. Synergism Between fMLP and the Neutrophil Products PAF and LTB₄. *Biochem. Biophys. Res. Commun.*
21. **Flamand L, Borgeat P, Lalonde R, Gosselin J.** 2004. Release of Anti-HIV Mediators after Administration of Leukotriene B₄ to Humans. *The Journal of Infectious Diseases* **189**:2001–2009.

22. **Wan M, Sabirsh A, Wetterholm A, Agerberth B, Haeggstrom JZ.** 2007. Leukotriene B4 triggers release of the cathelicidin LL-37 from human neutrophils: novel lipid-peptide interactions in innate immune responses. *The FASEB Journal* **21**:2897–2905.
23. **Talvani A, Machado FS, Santana GC, Klein A, Barcelos L, Silva JS, Teixeira MM.** 2002. Leukotriene B4 Induces Nitric Oxide Synthesis in *Trypanosoma cruzi*-Infected Murine Macrophages and Mediates Resistance to Infection. *Infection and Immunity* **70**:4247–4253.
24. **Goldman G, Welbourn R, Kobzik L, Valeri CR, Shepro D, Hechtman HB.** 1993. Lavage with leukotriene B4 induces lung generation of tumor necrosis factor-alpha that in turn mediates neutrophil diapedesis. *Surgery* **113**:297–303.
25. **Kuhns DB, Nelson EL, Alvord WG, Gallin JI.** 2001. Fibrinogen induces IL-8 synthesis in human neutrophils stimulated with formyl-methionyl-leucyl-phenylalanine or leukotriene B(4). *Journal of Immunology (Baltimore, Md. : 1950)* **167**:2869–2878.
26. **Brach MA, de Vos S, Arnold C, Gruss HJ, Mertelsmann R, Herrmann F.** 1992. Leukotriene B4 transcriptionally activates interleukin-6 expression involving NK-chi B and NF-IL6. *Eur. J. Immunol.* **22**:2705–2711.
27. **Danilova N, Steiner LA.** 2002. B cells develop in the zebrafish pancreas. *PNAS* **99**:13711–13716.
28. **Lam SH, Chua HL, Gong Z, Lam TJ, Sin YM.** 2004. Development and maturation of the immune system in zebrafish, *Danio rerio*: a gene expression profiling, in situ

- hybridization and immunological study. *Developmental & Comparative Immunology* **28**:9–28.
29. **Willett CE, Cortes A, Zuasti A, Zapata A.** 1999. Early Hematopoiesis and Developing Lymphoid Organs in the Zebrafish. *Dev. Dyn.* **214**:323–336.
 30. **Seeger A, Mayer WE, Klein J.** 1996. A Complement Factor B-Like cDNA clone from the Zebrafish (*Brachydanio rerio*). *Mol. Immunol.*
 31. **Jault C, Pichon L, Chluba J.** 2004. Toll-like receptor gene family and TIR-domain adaptors in *Danio rerio*. *Mol. Immunol.* **40**:759–771.
 32. **Meijer AH, Gabby Krens SF, Medina Rodriguez IA, He S, Bitter W, Ewa Snaar-Jagalska B, Spaink HP.** 2004. Expression analysis of the Toll-like receptor and TIR domain adaptor families of zebrafish. *Mol. Immunol.* **40**:773–783.
 33. **Lieschke GJ.** 2001. Morphologic and functional characterization of granulocytes and macrophages in embryonic and adult zebrafish. *Blood* **98**:3087–3096.
 34. **Le Guyader D, Redd MJ, Colucci-Guyon E, Murayama E, Kissa K, Briolat V, Mordelet E, Zapata A, Shinomiya H, Herbomel P.** 2008. Origins and unconventional behavior of neutrophils in developing zebrafish. *Blood* **111**:132–141.
 35. **Herbomel P, Thisse B, Thisse C.** 1999. Ontogeny and behaviour of early macrophages in the zebrafish embryo. *Development* **126**:3735–3745.
 36. **Hermann AC, Millard PJ, Blake SL, Kim CH.** 2004. Development of a respiratory burst assay using zebrafish kidneys and embryos. *Journal of Immunological Methods* **292**:119–129.

37. **Harvie EA, Huttenlocher A.** 2015. Neutrophils in host defense: new insights from zebrafish. *Journal of Leukocyte Biology.*
38. **Torraca V, Masud S, Spaink HP, Meijer AH.** 2014. Macrophage-pathogen interactions in infectious diseases: new therapeutic insights from the zebrafish host model. *Disease Models & Mechanisms* **7**:785–797.
39. **Harvie EA, Green JM, Neely MN, Huttenlocher A.** 2013. Innate Immune Response to *Streptococcus iniae* Infection in Zebrafish Larvae. *Infection and Immunity* **81**:110–121.
40. **Lowe BA, Miller JD, Neely MN.** 2007. Analysis of the Polysaccharide Capsule of the Systemic Pathogen *Streptococcus iniae* and Its Implications in Virulence. *Infection and Immunity* **75**:1255–1264.
41. **Deng Q, Yoo SK, Cavnar PJ, Green JM, Huttenlocher A.** 2011. Dual Roles for Rac2 in Neutrophil Motility and Active Retention in Zebrafish Hematopoietic Tissue. *Developmental Cell* **21**:735–745.
42. **Li L, Jin H, Xu J, Shi Y, Wen Z.** 2011. Irf8 regulates macrophage versus neutrophil fate during zebrafish primitive myelopoiesis. *Blood* **117**:1359–1369.
43. **Tobin DM, Roca FJ, Oh SF, McFarland R, Vickery TW, Ray JP, Ko DC, Zou Y, Bang ND, Chau TTH, Vary JC, Hawn TR, Dunstan SJ, Farrar JJ, Thwaites GE, King M-C, Serhan CN, Ramakrishnan L.** 2012. Host Genotype-Specific Therapies Can Optimize the Inflammatory Response to Mycobacterial Infections. *Cell* **148**:434–446.

44. **Williams DA, Tao W, Yang F, Kim C, Gu Y, Mansfield P, Levine JE, Petryniak B, Derrow CW, Harris C, Jia B, Zheng Y, Ambruso DR, Lowe JB, Atkinson SJ, Dinauer MC, Boxer L.** 2000. Dominant negative mutation of the hematopoietic-specific Rho GTPase, Rac2, is associated with a human phagocyte immunodeficiency. *Blood* **96**:1646–1654.
45. **Accetta D, Syverson G, Bonacci B, Reddy S, Bengston C, Surfus J, Harbeck R, Huttenlocher A, Grossman W, Routes J, Verbsky J.** 2011. Human phagocyte defect caused by a Rac2 mutation detected by means of neonatal screening for T-cell lymphopenia. *Journal of Allergy and Clinical Immunology* **127**:535–538.
46. **Meijer AH, van der Sar AM, Cunha C, Lamers GEM, Laplante MA, Kikuta H, Bitter W, Becker TS, Spaink HP.** 2008. Identification and real-time imaging of a myc-expressing neutrophil population involved in inflammation and mycobacterial granuloma formation in zebrafish. *Developmental & Comparative Immunology* **32**:36–49.
47. **Yang C-T, Cambier CJ, Davis JM, Hall CJ, Crosier PS, Ramakrishnan L.** 2012. Neutrophils exert protection in the early tuberculous granuloma by oxidative killing of mycobacteria phagocytosed from infected macrophages. *Cell Host & Microbe* **12**:301–312.
48. **Seiler P, Aichele P, Bandermann S, Hauser AE, Lu B, Gerard NP, Gerard C, Ehlers S, Mollenkopf HJ, Kaufmann SHE.** 2003. Early granuloma formation after aerosol *Mycobacterium tuberculosis* infection is regulated by neutrophils via CXCR3-

- signaling chemokines. *Eur. J. Immunol.* **33**:2676–2686.
49. **Tauzin S, Starnes TW, Becker FB, Lam PY, Huttenlocher A.** 2014. Redox and Src family kinase signaling control leukocyte wound attraction and neutrophil reverse migration. *The Journal of Cell Biology* **207**:589–598.
 50. **Silva MT, Silva MNT, Appelberg R.** 1989. Neutrophil-macrophage cooperation in the host defense against mycobacterial infections. *Microb. Pathog.* 369–380.
 51. **Tan BH, Meinken C, Bastian M, Bruns H, Legaspi A, Ochoa MT, Krutzik SR, Bloom BR, Ganz T, Modlin RL, Stenger S.** 2006. Macrophages Acquire Neutrophil Granules for Antimicrobial Activity against Intracellular Pathogens. *The Journal of Immunology* **177**:1864–1871.
 52. **Scott MG, Dullaghan E, Mookherjee N, Glavas N, Waldbrook M, Thompson A, Wang A, Lee K, Doria S, Hamill P, Yu JJ, Li Y, Donini O, Guarna MM, Finlay BB, North JR, Hancock REW.** 2007. An anti-infective peptide that selectively modulates the innate immune response. *Nat Biotechnol* **25**:465–472.
 53. **Nüsslein-Volhard C, Dahm R.** 2002. *Zebrafish: A Practical Approach.* Oxford University Press, New York, NY.
 54. **Fuller J, Bast D, Nizet V, Low D.** 2001. *Streptococcus iniae* virulence is associated with a distinct genetic profile. *Infection and Immunity.*
 55. **Benard EL, van der Sar AM, Ellett F, Lieschke GJ, Spaink HP, Meijer AH.** 2012. Infection of zebrafish embryos with intracellular bacterial pathogens. *J Vis Exp.*
 56. **Provost E, Rhee J, Leach SD.** 2007. Viral 2A peptides allow expression of multiple

proteins from a single ORF in transgenic zebrafish embryos. *genesis* **45**:625–629.

57. **Mathias JR, Perrin BJ, Liu TX, Kanki J, Look AT, Huttenlocher A.** 2006.

Resolution of inflammation by retrograde chemotaxis of neutrophils in transgenic zebrafish. *Journal of Leukocyte Biology* **80**:1281–1288.

58. **Mathias JR, Dodd ME, Walters KB, Rhodes J, Kanki JP, Look AT, Huttenlocher**

A. 2007. Live imaging of chronic inflammation caused by mutation of zebrafish Hai1. *Journal of Cell Science* **2012**:3372–3383.

Figure Legends

Fig. 3-1: Macrophages are important for host defense against *S. iniae* infection. (A)

Tg(mpeg1:dendra2) embryos were injected at the single-cell stage with either the Irf8 or standard control MO and were mock-infected with PBS or infected with 50 CFU wild-type *S. iniae* (WT) or 100 CFU *cpsA* mutant at 2 dpf and monitored for survival. Compared to control morphants, Irf8 morphants have significantly worse survival (wild-type *S. iniae* (WT), $p = 0.0002$; *cpsA* mutant, $p=0.0004$). (B and C) Infection of *Tg(mpeg1:dendra2)* larvae at 3 dpf with 50 or 100 CFU WT, but not heat-killed (HK) WT (50 CFU equivalent) or 100 CFU *cpsA* mutant, results in development of macrophage aggregates in the trunk/tail of a proportion of infected fish by 24 hpi. Representative pictures shown in (B). Scale bar, 80 μ m. (D) Average area of macrophage aggregates at 24 hpi following infection with 50 or 100 CFU WT. (E) A macrophage aggregate in *Tg(mpeg1:dendra2)* larva 24 hpi with 50 CFU WT. Aggregates contain both uninfected and infected (indicated by white arrows) macrophages. *S. iniae* was labeled with CellTracker Red dye. Scale bar, 20 μ m. The data are from at least 3 independent experiments, each with 24 larvae per condition.

Fig. 3-1:

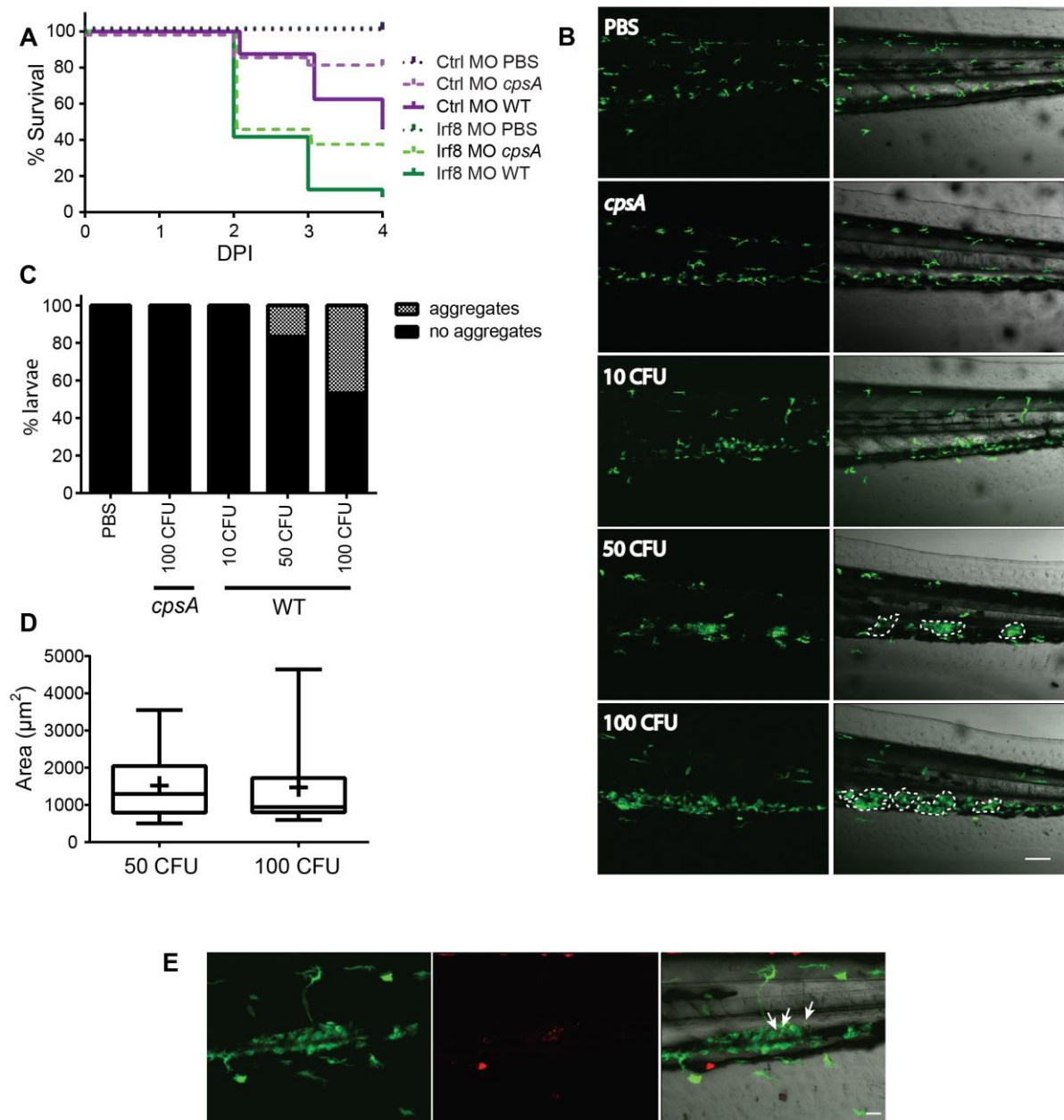


Fig. 3-2: Disruption of Lta4h signaling abrogates macrophage aggregation. (A)

Tg(mpeg1:dendra2) embryos were injected at the single-cell stage with either the Lta4h MO or standard control MO and were mock-infected with PBS or infected with 10 CFU wild-type *S. iniae* (WT) at 2 dpf and monitored for survival. Compared to control morphants, Lta4h morphants infected with WT have significantly worse survival ($p = 0.0458$). (B and C) Lta4h or control morphants were infected at 2 dpf with 50 CFU WT or mock-infected with PBS. By 24 hpi, macrophage aggregates form in a proportion of WT-infected control morphants. Representative pictures are shown in (C). Scale bar, 40 μ m. (D) Survival of 2 dpf Lta4h or control morphants microinjected with 50 CFU wild-type *S. iniae* (WT) or mock-infected with PBS and treated with 30 nM LTB4 or 0.1% ethanol. Lta4h morphants have significantly worse survival than control morphants, regardless of LTB4 treatment (ethanol treated, $p=0.0001$; LTB4 treated, $p=0.0072$). (E and F) Immediately following infection with 50 CFU WT, Lta4h and control morphants were treated with 0.1% ethanol or 30 nM LTB4. Control morphants with ethanol or LTB4 treatment can form macrophage aggregates, whereas only LTB4-treated Lta4h morphants, not ethanol-treated Lta4h morphants, can develop macrophage aggregates by 24 hpi. Representative pictures are shown in (F). Scale bar, 40 μ m. The data are from at least 3 independent experiments, each with 24 larvae per condition.

Fig. 3-2:

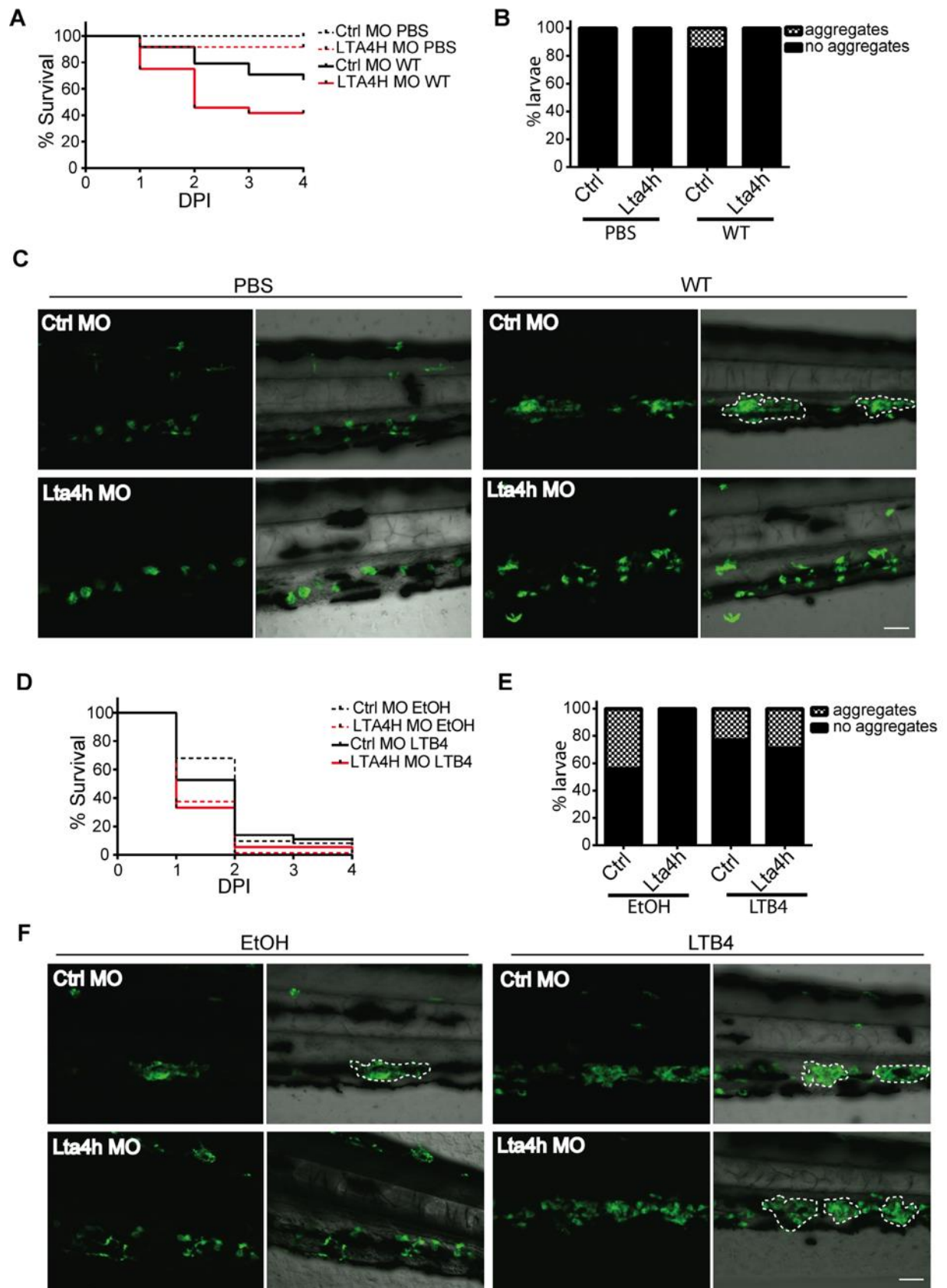


Fig. 3-3: Neutrophils drive macrophage inflammation and aggregation in response to *S.*

***iniae* infection in a ROS-independent manner.** (A and B) *Tg(mpx:mCherry-2a-rac2wt)*

(Rac2WT) or *Tg(mpx:mCherry-2a-rac2d57n)* (Rac2D57N; LAD larvae) (red neutrophils)

was crossed to *Tg(mpeg1:dendra2)* (green macrophages) and resulting double transgenic

larvae were infected with 50 CFU WT or mock-infected with PBS. Only infected Rac2WT

larvae develop macrophage aggregates by 24 hpi. Representative pictures are shown in (A).

Scale bar, 80 μ m. (C-F) *Tg(mpeg1:dendra2)* embryos were injected at the single-cell stage

with either a p22^{phox} or control MO and infected at 2 dpf with 50 CFU WT or mock-infected

with PBS. Both control and p22^{phox} morphants developed macrophage aggregates by 24 hpi

(C and D). Representative pictures are shown in (D). Scale bar, 80 μ m. There was no

significant difference in average aggregate size between control and p22^{phox} morphants (E) or

in survival (F). The data are from at least 3 independent experiments, each with 24 larvae per

condition.

Fig. 3-3:

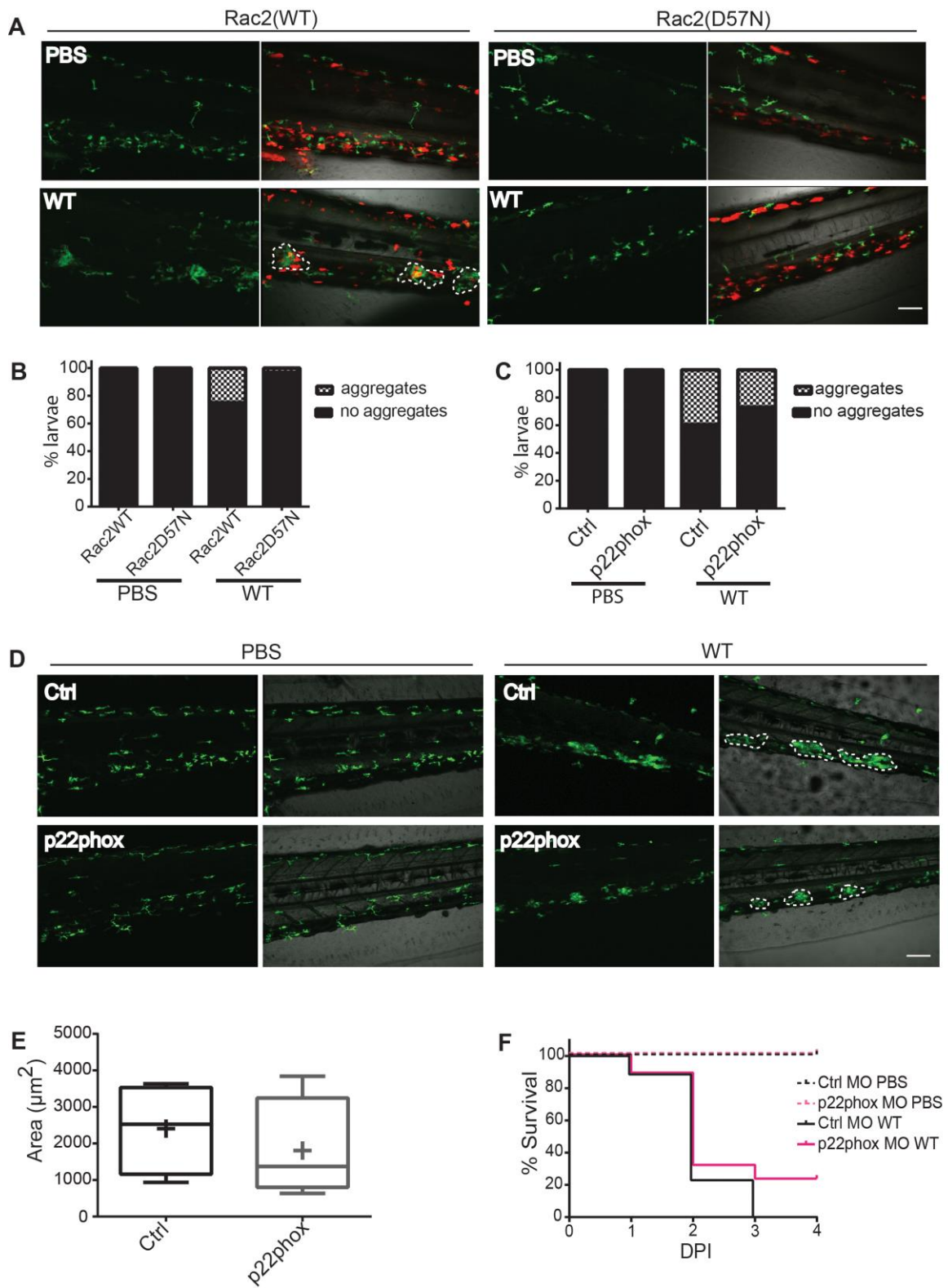


Fig. 3-4: Exogenous LTB4 treatment of LAD larvae results in a rescue of the macrophage aggregation defect. *Tg(mpx:mCherry-2a-rac2wt)* (Rac2WT) or *Tg(mpx:mCherry-2a-rac2d57n)* (Rac2D57N; LAD larvae) (red neutrophils) was crossed to *Tg(mpeg1:dendra2)* (green macrophages) and resulting double transgenic larvae were infected with 50 CFU WT and immediately treated with 30 nM LTB4 or 0.1% ethanol. There is no significant difference in survival between ethanol-treated and LTB4-treated larvae (A). (B and C) Rac2WT larvae treated with ethanol or LTB4 treatment developed macrophage aggregates, whereas only LTB4-treated Rac2D57N, not ethanol-treated, larvae developed macrophage aggregates by 24 hpi. Representative pictures are shown in (C) Scale bar, 80µm. The data are from at least 3 independent experiments, each with 24 larvae per condition.

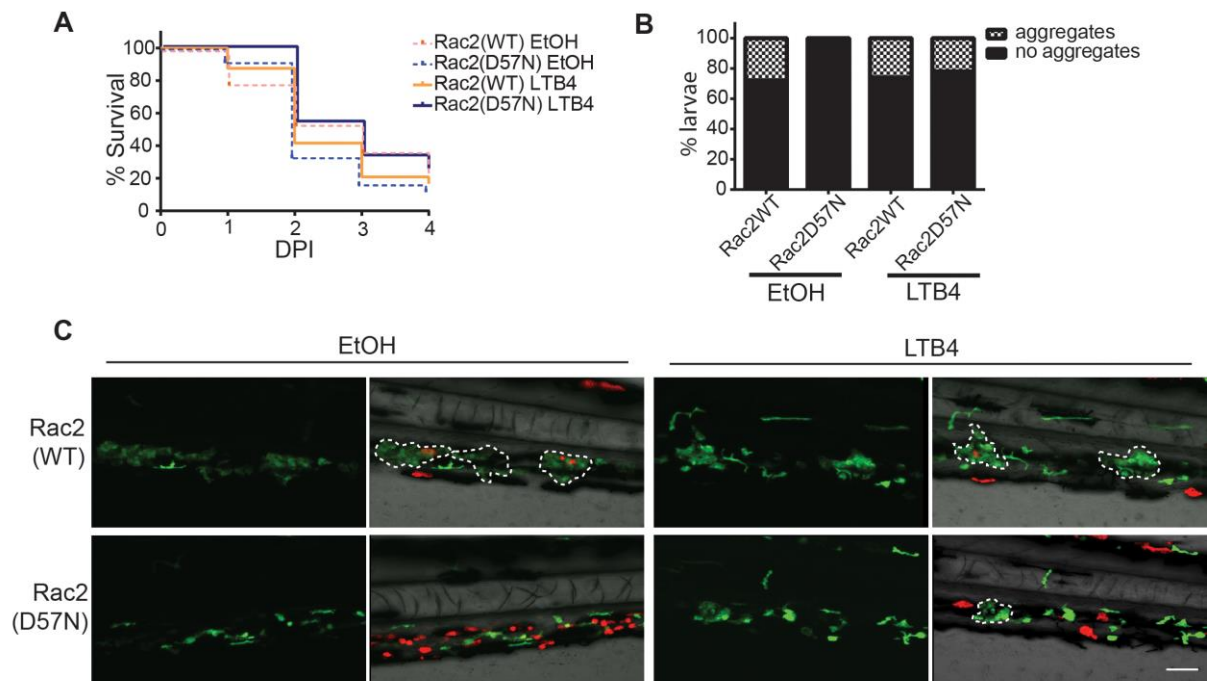
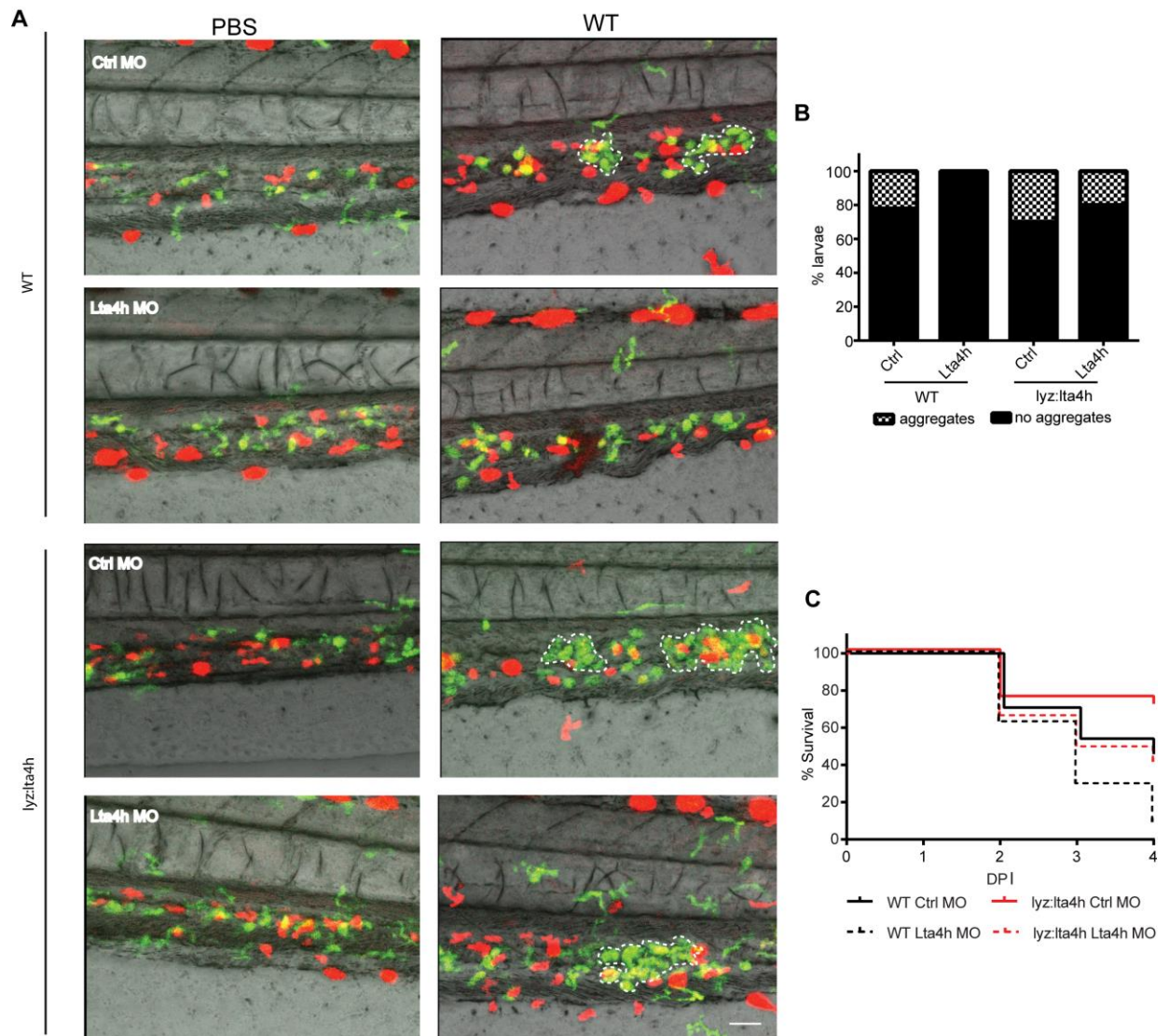
Fig. 3-4:

Fig. 3-5: Neutrophil-specific expression of *Lta4h* modulates macrophage behavior. (A and B) *Tg(lyz:lta4h-2a-mCherry)* (OE) or *Tg(mpx:mCherry)* (WT) (red neutrophils) was crossed to *Tg(mpeg1:dendra2)* (green macrophages) and injected with either a standard control MO or *Lta4h* MO. Double transgenic morphants were infected at 2 dpf with 50 CFU WT or mock-infected with PBS and monitored for macrophage aggregation at 24 hpi. Infected WT control morphants but not WT *Lta4h* morphants develop macrophage aggregates. However, OE control morphants and OE *Lta4h* morphants both develop macrophage aggregates indicating that overexpression of *lta4h* specifically in neutrophils is sufficient to induce macrophage aggregation. Representative pictures are shown in (A). Scale bar, 80 μ m. (C) Survival of double transgenic control and *Lta4h* morphants infected at 2 dpf with 50 CFU WT. Compared to WT control morphants, WT *Lta4h* morphants have worse survival ($p = 0.0134$). Compared to OE control morphants, OE *lta4h* morphants do not have significantly worse survival. Additionally, OE *Lta4h* morphants have significantly better survival than WT *Lta4h* morphants ($p=0.0335$) indicating that neutrophil-specific overexpression of *lta4h* rescues the survival defect of *lta4h*-deficient larvae. The data are from at least 3 independent experiments, each with 24 larvae per condition.

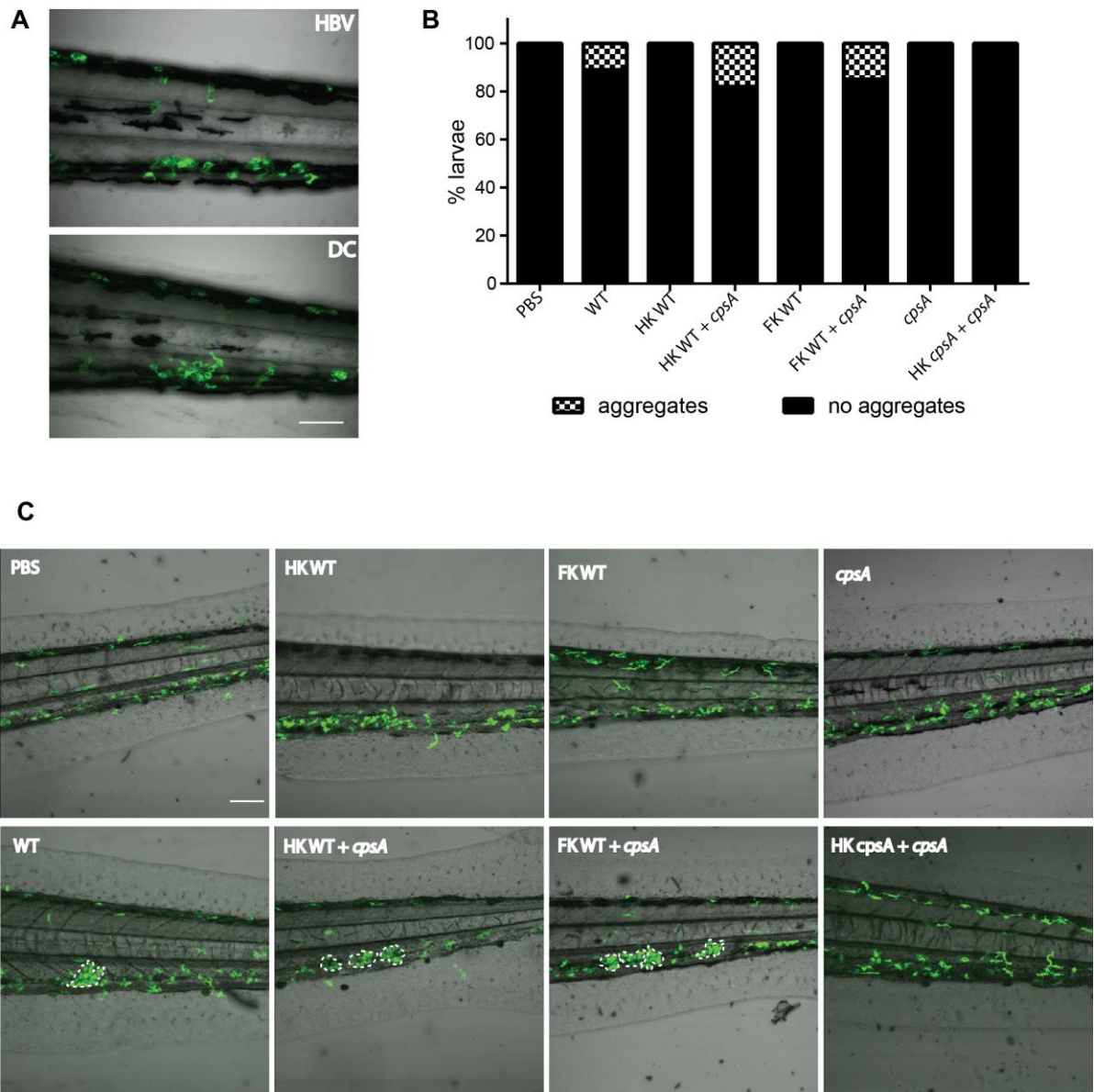
Fig. 3-5:



Supplemental Figures:

Supplemental Fig. 3-1: (A) Macrophages form aggregates in *Tg(mpeg1:dendra2)* larvae by 24 hpi with 50 CFU WT injected into the hind brain (i) or duct of Cuvier (ii). Scale bar, 80µm. (B and C) Coinjection of a 50 CFU equivalent of heat-killed (HK WT) or formalin-killed (FK WT) wild-type bacteria and 100 CFU *cpsA* mutant resulted in the formation of macrophage aggregates by 24 hpi, similar to injection of 50 CFU WT. Coinjection of heat-killed *cpsA* (HK *cpsA*) and *cpsA* did not induce aggregation. Scale bar, 80µm. The data are from at least 3 independent experiments, each with 24 larvae per condition.

Supplemental Fig. 3-1:



Supplemental Fig. 3-2: (A) RT-PCR of *lta4h* from mRNA extracted from 2-4 dpf zebrafish.

The arrow denotes the presence of an alternative transcript in larvae injected with a splice-

blocking *Lta4h* morpholino. 1 = control MO, 2 = 100 μ M *Lta4h* MO, 3 = 200 μ M *Lta4h* MO,

4 = 500 μ M *Lta4h* MO. (B-D) 3 dpf *Tg(mpeg1:dendra2)* larvae were infected with 50 CFU

WT or PBS and immediately treated with 0.1% DMSO or 100 μ M of the *Lta4h* inhibitor,

Bestatin. Bestatin treatment had no significant effect on survival (B) but resulted in an

abrogation in macrophage aggregation at 24 hpi (C and D). Scale bar, 40 μ m. (E-G) 3 dpf

lta4h-deficient mutants or AB-WT larvae were infected with 50 CFU WT, fixed at 24 hpi and

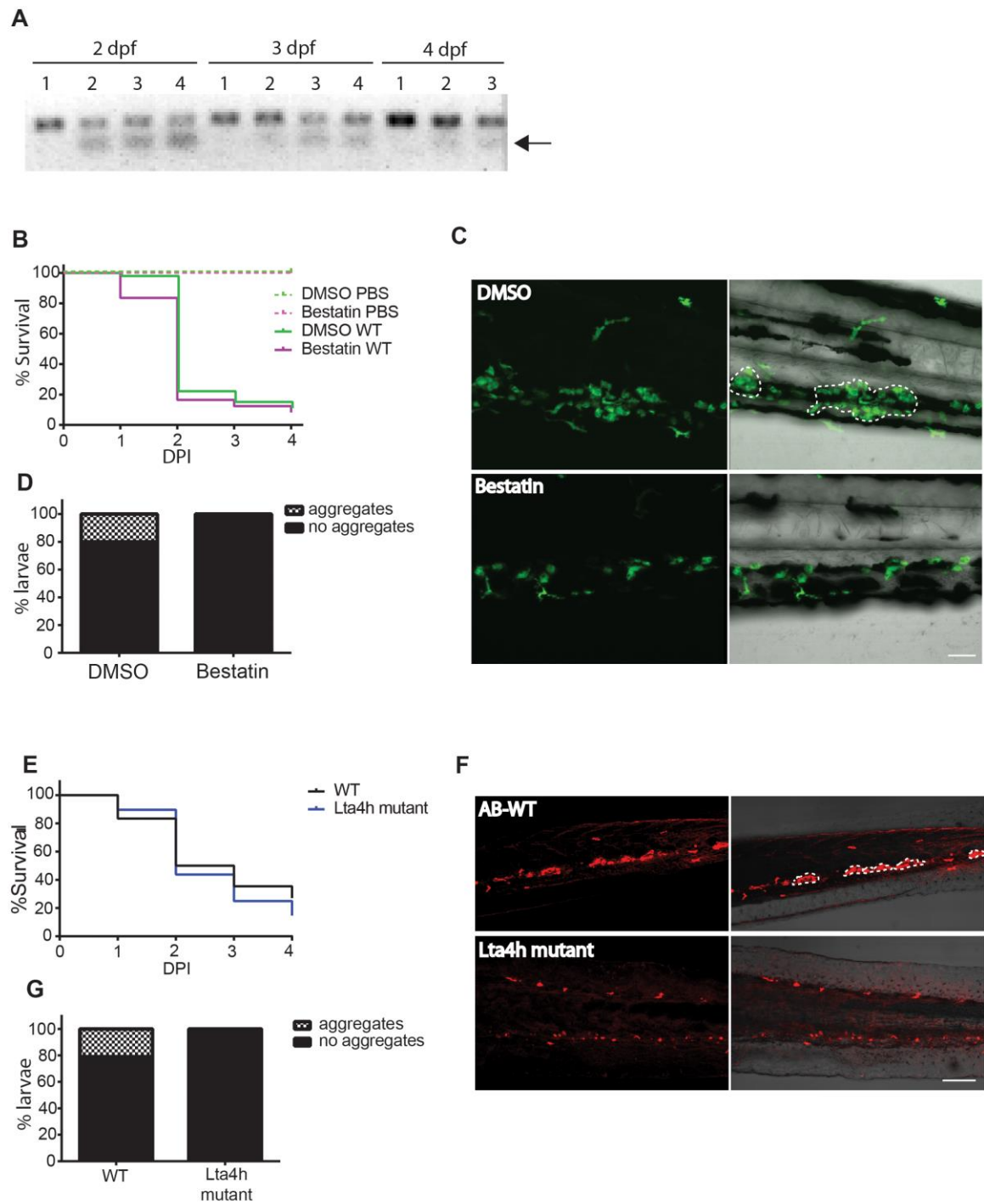
immunolabeled with an antibody to L-plastin to label all leukocytes. Although there was no

significant difference in survival (E) *Lta4h* mutants did not develop macrophage aggregates

(F and G). Scale bar, 80 μ m. The data are from at least 3 independent experiments, each with

24 larvae per condition.

Supplemental Fig. 3-2:



Chapter 4

Conclusions and Future Directions

The outcome of infectious disease is determined by interplay between host defense mechanisms and pathogen virulence factors. Neutrophils and macrophages are important early responders to infection and have a large arsenal of antimicrobial activities by which to control infection. However, some pathogens have evolved ways in which to evade the host immune response or hijack host immune cells to facilitate dissemination. Thus, the immune response must be intricately coordinated to both contain the infection and limit non-specific inflammation, and this coordination requires crosstalk between host cells. The focus of this dissertation has been on how host immune cells interact with a bacterial pathogen in addition to how immune cells modulate each other's behavior to direct the host response to infection. Gaining insights into signaling mechanisms involved in cell-cell communication will drive the development of host-directed immunotherapies that could protect against a broad range of infections while also controlling excessive infection-induced hyperinflammation.

In **Chapter 2**, I presented the first larval zebrafish model of *Streptococcus iniae* infection. The development of such a model is important not only to understanding host-pathogen interactions *in vivo*, but is also important for the study *S. iniae* disease pathogenesis. *S. iniae* is an important fish pathogen, causing hundreds of millions of dollars in annual losses for the aquaculture industry, and also causes disease in humans with clinical pathologies similar to diseases caused by Group A and Group B streptococci. Therefore, investigating *S. iniae* disease in the context of a natural host will reveal insight into how related streptococci cause disease in human hosts. Localized otic vesicle infection with *S. iniae* results in neutrophil and macrophage recruitment and phagocytosis. Neutrophils, in

particular, exhibit a type of behavior known as “swarming” in which there is initial chemotaxis of neutrophils close to the infection site followed by a second phase of amplified recruitment and clustering of neutrophils at the infection site. This behavior has also been described in mice where it requires LTB₄ (1). Since I have shown in **Chapter 3** that LTB₄ is important in mediating the host inflammatory response to *S. iniae* infection in zebrafish, it is possible that LTB₄ may also be responsible for this swarming behavior seen in response to localized *S. iniae* infection. Such similarities in immune cell behavior in zebrafish and mammalian models further validate the use of zebrafish to study immune responses to infection. In addition, identifying the signals important for immune cell recruitment to sites of infection can provide targets for future therapeutics aimed at dampening harmful and excessive infection-induced inflammation.

There are an increasing number of infection models established in zebrafish embryos and larvae, and there is growing evidence, including the data presented in this dissertation, that neutrophil and macrophage responses are pathogen-specific. Although neutrophils and macrophages are recruited to sites of infection with a broad range of bacteria, neutrophils, but not macrophages, are necessary to control infection with *Pseudomonas aeruginosa* (2). On the other hand, macrophages are more important in the phagocytosis of *Escherichia coli* (3-6), *Bacillus subtilis* (6), *Burkholderia cenocepacia* (7), *Enterococcus faecalis* (8), *Francisella* sp. (9), *Listeria monocytogenes* (10), *Salmonella enterica* (5, 11) and *Shigella flexneri* (12) in zebrafish. In these studies, a number of different infection sites have been used. A study by Colucci-Guyon, et al. reported that the relative contribution of neutrophils

and macrophages during the initial response to infection was dependent on the site of infection, regardless of the pathogen (6). The study showed that neutrophils, unlike macrophages, were unable to efficiently phagocytose *E. coli* or *B. subtilis* injected into closed fluid-filled body cavities (eg. otic vesicle) and only were efficient at phagocytosis when bacteria were attached to a surface (eg. dorsal muscle) (6). In a study of *Francisella* infection, similar observations were made where neutrophils only phagocytosed bacteria following injection into the dorsal muscle, not following blood infection (9). In contrast to these mentioned studies, I have shown in this dissertation that neutrophils and macrophages are both able to efficiently phagocytose *S. iniae* and *P. aeruginosa* following injection into the fluid-filled otic vesicle (**Chapter 1, Chapter 2, Appendix I, Appendix III**). Therefore, my dissertation work has shown that in contrast to the previous belief that phagocyte response to infection in zebrafish is context-dependent, the ability of neutrophils to efficiently phagocytose bacteria is actually dependent on the specific pathogen, not the anatomical location of infection.

Using a combination of morpholinos and a transgenic zebrafish model of primary immunodeficiency (LAD larvae), I have shown that both neutrophils and macrophages are critical in the host response to *S. iniae* infection (**Chapter 2, Chapter 3**); macrophages form protective, bacteria-containing aggregate structures, and neutrophils regulate this inflammation through leukotriene A4 hydrolase (Lta4h) signaling (**Chapter 3**). Although initially a localized infection, *S. iniae* infection becomes systemic and aggregates of both infected and uninfected macrophages form in the trunk and tail of infected fish. These

structures seem to provide some protection to the host since disruption of macrophage aggregation, such as when neutrophils are not functional or when Lta4h signaling is disrupted, impairs host survival in response to infection. It is possible that these structures help contain the infection and prevent further dissemination of bacteria. If these structures are, in fact, host protective, then it would be interesting to see if induction of macrophage aggregation through co-injection of heat-killed wild-type bacteria and viable *cpsA* mutant, a combination which can induce macrophage aggregation but does not induce host death, protects a subsequent infection with wild-type *S. iniae*. Additionally, the activation state of macrophages in aggregates is currently unknown, but there are several reporter lines available that will allow for characterization of the activation profiles of these macrophages; there are currently reporters of TNF (13) and NF κ B (14) expression. The activation state of macrophages under neutrophil- or Lta4h-deficient conditions should also be examined. Understanding the activation state of macrophages in these bacteria-containing structures, and how macrophage activation is different under various conditions, can guide future therapeutic strategies aimed at manipulating macrophage behavior during infection.

Although best known for their antimicrobial functions, there is growing evidence, including the work presented here in **Chapter 3**, that neutrophils are also important regulators of the immune response and can influence macrophage behavior. Following engagement of their pattern recognition receptors, neutrophils become activated and can secrete antimicrobial peptides or pro-inflammatory molecules such as LTB₄ and cytokines/chemokines to coordinate the macrophage response to infection. Macrophages that

ingest neutrophil granules have enhanced anti-mycobacterial behavior both *in vitro* (15, 16) and in a mouse model (16). Similar neutrophil-macrophage cooperation can enhance phagocytosis of *Trypanosoma cruzi* (17) and has also been demonstrated in *Legionella pneumophila* infection (18). Additionally, macrophages can be activated following phagocytosis of bacterially-infected neutrophils (19). In **Chapter 3**, I showed that neutrophils modulate the macrophage inflammatory response to *S. iniae* infection in zebrafish larvae through Lta4h signaling. Understanding how immune cells interact during infection will lead to the development of new anti-infective therapies aimed at modulating the immune response. For example, one study found that Innate Defense Regulatory Peptide 1 (IDR-1), a peptide synthesized to be similar to a neutrophil granule peptide, was not directly antimicrobial, but rather, increased host protection in multiple mouse models of bacterial infection by stimulating macrophage recruitment while also reducing infection-mediated inflammation (20). Since host-based therapies do not directly target bacteria, they are more likely to be useful in a broad range of infections while also reducing the risk of contributing to antibiotic resistance. Additionally, such therapies would have the benefit of increasing antimicrobial activity while also minimizing the damaging effects of excessive infection-induced inflammation.

The balance between protective and excessive inflammation is critical for effective host defense against infection to control pathogen growth while limiting non-specific, damaging inflammation. A better understanding of how immune cells influence one another will enable us to manipulate their interactions to alter the balance of inflammation during

infection. Eicosanoids, such as pro-inflammatory leukotrienes and anti-inflammatory lipoxins, are important molecules released by leukocytes in response to infection that can alter this balance. Here, we show that pro-inflammatory LTB₄ is important for macrophage inflammation and host survival during *S. iniae* infection (**Chapter 3**). We targeted LTB₄ signaling by depleting larvae of *Lta4h*, but another method of decreasing LTB₄ activity is through overexpression of the LTB₄ dehydrogenase (LTB₄DH), the enzyme that inactivates LTB₄ (21). Is neutrophil-specific expression of LTB₄DH sufficient to disrupt macrophage aggregation? An additional challenge will be to investigate how lipoxins might also regulate the response to *S. iniae* infection in zebrafish. Will increased production of anti-inflammatory lipoxins provide a survival benefit to the host in the wake of a highly pro-inflammatory response or will lipoxins disrupt macrophage inflammation and result in enhanced susceptibility to infection? The role of leukotrienes and lipoxins has been investigated in the zebrafish model of *Mycobacterium marinum* infection, and many different drug treatments are available to alter the production levels of these molecules (21).

In conclusion, neutrophils and macrophages both play critical roles in the host response to *S. iniae* infection in zebrafish larvae. Besides their role as efficient phagocytes, neutrophils also have immunomodulatory functions, and neutrophil expression of *Lta4h* helps coordinate the macrophage response to infection. Uncovering the mechanisms by which immune cells interact and regulate one another will allow us to develop host-directed therapies to a wide range of infections while also controlling potentially damaging infection-induced inflammation.

References

1. **Lämmermann T, Afonso PV, Angermann BR, Wang JM, Kastenmüller W, Parent CA, Germain RN.** 2013. Neutrophil swarms require LTB4 and integrins at sites of cell death in vivo. *Nature* **498**:371–375.
2. **Deng Q, Yoo SK, Cavnar PJ, Green JM, Huttenlocher A.** 2011. Dual Roles for Rac2 in Neutrophil Motility and Active Retention in Zebrafish Hematopoietic Tissue. *Developmental Cell* **21**:735–745.
3. **Herbomel P, Thisse B, Thisse C.** 1999. Ontogeny and behaviour of early macrophages in the zebrafish embryo. *Development* **126**:3735–3745.
4. **Le Guyader D, Redd MJ, Colucci-Guyon E, Murayama E, Kissa K, Briolat V, Mordelet E, Zapata A, Shinomiya H, Herbomel P.** 2008. Origins and unconventional behavior of neutrophils in developing zebrafish. *Blood* **111**:132–141.
5. **Meijer AH, van der Sar AM, Cunha C, Lamers GEM, Laplante MA, Kikuta H, Bitter W, Becker TS, Spaink HP.** 2008. Identification and real-time imaging of a myc-expressing neutrophil population involved in inflammation and mycobacterial granuloma formation in zebrafish. *Developmental & Comparative Immunology* **32**:36–49.
6. **Colucci-Guyon E, Tinevez JY, Renshaw SA, Herbomel P.** 2011. Strategies of professional phagocytes in vivo: unlike macrophages, neutrophils engulf only surface-associated microbes. *Journal of Cell Science* **124**:3053–3059.

7. **Vergunst AC, Meijer AH, Renshaw SA, O'Callaghan D.** 2010. Burkholderia cenocepacia Creates an Intramacrophage Replication Niche in Zebrafish Embryos, Followed by Bacterial Dissemination and Establishment of Systemic Infection. *Infection and Immunity* **78**:1495–1508.
8. **Prajsnar TK, Renshaw SA, Ogryzko NV, Foster SJ, Serror P, Mesnage S.** 2013. Zebrafish as a Novel Vertebrate Model To Dissect Enterococcal Pathogenesis. *Infection and Immunity* **81**:4271–4279.
9. **Brudal E, Ulanova LS, O Lampe E, Rishovd AL, Griffiths G, Winther-Larsen HC.** 2014. Establishment of Three Francisella Infections in Zebrafish Embryos at Different Temperatures. *Infection and Immunity* **82**:2180–2194.
10. **Levraud J-P, Disson O, Kissa K, Bonne I, Cossart P, Herbomel P, Lecuit M.** 2009. Real-time observation of *Listeria monocytogenes*-phagocyte interactions in living zebrafish larvae. *Infection and Immunity* **77**:3651–3660.
11. **van der Sar AM, Musters RJP, van Eeden FJM, Appelmelk BJ, Vandenbroucke-Grauls CMJE, Bitter W.** 2003. Zebrafish embryos as a model host for the real time analysis of *Salmonella typhimurium* infections. *Cell Microbiol* **5**:601–611.
12. **Mostowy S, Boucontet L, Mazon Moya MJ, Sirianni A, Boudinot P, Hollinshead M, Cossart P, Herbomel P, Levraud J-P, Colucci-Guyon E.** 2013. The zebrafish as a new model for the in vivo study of *Shigella flexneri* interaction with phagocytes and bacterial autophagy. *PLoS Pathog* **9**:e1003588.
13. **Marjoram L, Alvers A, Deerhake ME, Bagwell J, Mankiewicz J, Cocchiaro JL,**

- Beerman RW, Willer J, Sumigray KD, Katsanis N, Tobin DM, Rawls JF, Goll MG, Bagnat M.** 2015. Epigenetic control of intestinal barrier function and inflammation in zebrafish. *PNAS* **112**:2770–2775.
14. **Kanther M, Sun X, Mühlbauer M, Mackey LC, Flynn EJ, Bagnat M, Jobin C, Rawls JF.** 2011. Microbial Colonization Induces Dynamic Temporal and Spatial Patterns of NF- κ B Activation in the Zebrafish Digestive Tract. *YGAST* **141**:197–207.
15. **Silva MT, Silva MNT, Appelberg R.** 1989. Neutrophil-macrophage cooperation in the host defense against mycobacterial infections. *Microb. Pathog.* 369–380.
16. **Tan BH, Meinken C, Bastian M, Bruns H, Legaspi A, Ochoa MT, Krutzik SR, Bloom BR, Ganz T, Modlin RL, Stenger S.** 2006. Macrophages Acquire Neutrophil Granules for Antimicrobial Activity against Intracellular Pathogens. *The Journal of Immunology* **177**:1864–1871.
17. **Lima MF, Kierszenbaum F.** 1985. Lactoferrin effects on phagocytic cell function. *The Journal of Immunology* **134**:4176–4183.
18. **Byrd TF, Horwitz MA.** 1991. Lactoferrin inhibits or promotes *Legionella pneumophila* intracellular multiplication in nonactivated and interferon gamma-activated human monocytes depending upon its degree of iron saturation. *J. Clin. Invest.* 1103–1112.
19. **Persson YAZ, Blomgran-Julinder R, Rahman S, Zheng L, Stendahl O.** 2008. *Mycobacterium tuberculosis*-induced apoptotic neutrophils trigger a pro-inflammatory response in macrophages through release of heat shock protein 72, acting in synergy

- with the bacteria. *Microbes and Infection* **10**:233–240.
20. **Scott MG, Dullaghan E, Mookherjee N, Glavas N, Waldbrook M, Thompson A, Wang A, Lee K, Doria S, Hamill P, Yu JJ, Li Y, Donini O, Guarna MM, Finlay BB, North JR, Hancock REW.** 2007. An anti-infective peptide that selectively modulates the innate immune response. *Nat Biotechnol* **25**:465–472.
21. **Tobin DM, Roca FJ, Oh SF, McFarland R, Vickery TW, Ray JP, Ko DC, Zou Y, Bang ND, Chau TTH, Vary JC, Hawn TR, Dunstan SJ, Farrar JJ, Thwaites GE, King M-C, Serhan CN, Ramakrishnan L.** 2012. Host Genotype-Specific Therapies Can Optimize the Inflammatory Response to Mycobacterial Infections. *Cell* **148**:434–446.

Appendix I

Non-invasive imaging of the innate immune response in a zebrafish larval model of *Streptococcus iniae* infection

This Chapter was published in the following journal article:

Harvie, E. A. and Huttenlocher, A. (2015) Non-invasive imaging of the innate immune response in a zebrafish larval model of *Streptococcus iniae* infection. *Journal of Visualized Experiments*.

Short Abstract:

Here, we present a protocol for the generation and imaging of a localized bacterial infection in the zebrafish otic vesicle.

Long Abstract:

The aquatic pathogen, *Streptococcus iniae*, is responsible for over 100 million dollars in annual losses for the aquaculture industry and is capable of causing systemic disease in both fish and humans (1). A better understanding of *S. iniae* disease pathogenesis requires an appropriate model system. The genetic tractability and the optical transparency of the early developmental stages of zebrafish allow for the generation and non-invasive imaging of transgenic lines with fluorescently tagged immune cells. The adaptive immune system is not fully functional until several weeks post fertilization, but zebrafish larvae have a conserved vertebrate innate immune system with both neutrophils and macrophages (2-6). Thus, the generation of a larval infection model allows the study of the specific contribution of innate immunity in controlling *S. iniae* infection.

The site of microinjection will determine whether an infection is systemic or initially localized. Here, we present our protocols for otic vesicle injection of zebrafish aged 2-3 days post fertilization as well as our techniques for fluorescent confocal imaging of infection. A localized infection site allows observation of initial microbe invasion, recruitment of host cells and dissemination of infection. Our findings using the zebrafish larval model of *S. iniae* infection indicate that zebrafish can be used to examine the differing contributions of host

neutrophils and macrophages in localized bacterial infections. In addition, we describe how photolabeling of immune cells can be used to track individual host cell fate during the course of infection.

Introduction:

Streptococcus iniae is a major aquatic pathogen that is capable of causing systemic disease in both fish and humans. While *S. iniae* is responsible for large losses for the aquaculture industry, it is also a potential zoonotic pathogen, capable of causing disease in immunocompromised human hosts with clinical pathologies similar to those caused by other streptococcal human pathogens. Given its similarities with human pathogens, it is important to study *S. iniae* disease pathogenesis in the context of a natural host. An adult zebrafish model of *S. iniae* infection revealed robust infiltration of host leukocytes to the localized site of infection as well as a rapid time to host death, a time too short to involve the adaptive immune system (7). In order to gain an in-depth look into the innate immune response to *S. iniae* infection *in vivo*, it is necessary to use a model that is more amenable to non-invasive live imaging.

The larval zebrafish has a number of advantages that make it an increasingly attractive vertebrate model for studying host-pathogen interactions. Zebrafish are relatively inexpensive and easy to use and maintain compared to mammalian models. Adaptive immunity is not functionally mature until 4-6 weeks post fertilization, but larvae have a highly conserved vertebrate innate immune system with complement, Toll-like receptors,

cytokines, and neutrophils and macrophages with antimicrobial capabilities including phagocytosis and respiratory burst (2-6, 8-11). In addition, the genetic tractability and optical transparency of the embryonic and larval stages of development allow for the generation of stable transgenic lines with fluorescently labeled immune cells making it possible to examine host-pathogen interactions in real time *in vivo*. The generation of these transgenic lines using a photoconvertible protein such as Dendra2 allows for the tracking of individual host cell origin and fate over the course of infection (12).

When developing a zebrafish larval infection model, the chosen site of microinjection will determine whether an infection is initially localized or systemic. Systemic blood infections into the caudal vein or Duct of Cuvier are most commonly used to study microbial pathogens in zebrafish and are useful for studying interactions between host and microbial cells, cytokine responses, and differences in virulence between pathogen strains. For slower growing microorganisms, early injection into the yolk sac of an embryo at the 16-1000 cell stage can be used to generate a systemic infection (13, 14), with the optimal developmental stage for microinjection of a slow-growing microorganism found to be between the 16 to 128 cell stage (15). However, yolk sac injections of many microbes at later stages of host development tend to be lethal to the host due to the nutrient-rich environment for the microbe and lack of infiltrating leukocytes (16 -18).

A localized infection usually results in directed migration of leukocytes towards the site of infection that can be easily quantified with non-invasive imaging. This type of infection can allow for dissection of the mechanisms that mediate leukocyte migration as well

as investigation of different migratory and phagocytic capabilities of various leukocyte populations. Localized infections are also useful when examining differences in virulence between bacterial strains as well as studying microbe invasion mechanisms since physical host barriers must be crossed for a localized infection to become systemic. Zebrafish are typically raised at temperatures of 25-31 °C (19), but they can also be maintained at temperatures as high as 34-35 °C for studies of the invasiveness of certain human pathogens with strict temperature requirements for virulence (20, 21).

Many different sites have been used to generate an initially localized bacterial infection including the hindbrain ventricle (22), dorsal tail muscle (18), pericardial cavity (23), and otic vesicle (ear) (5, 16, 24). However, it has been found that injection of bacteria into tail muscle can cause tissue damage and inflammation independent of the bacteria, which may skew results when investigating leukocyte response (13). Although less damage is associated with injection into the hindbrain and although it is initially devoid of leukocytes in young embryos, the hindbrain ventricle steadily gains more immune cells over time as microglia take up residence. The hindbrain ventricle is also a more difficult location to image. The otic vesicle is a closed hollow cavity with no direct access to the vasculature (25, 26). It is normally devoid of leukocytes, but leukocytes can be recruited to the otic vesicle in response to inflammatory stimuli such as infection. It is also a preferred site of microinjection of bacteria in zebrafish aged 2-3 days post fertilization (dpf) because of the ease of imaging and the visualization of the injection. Therefore, we chose the otic vesicle as our site of localized bacterial infection.

Protocol:

Adult and embryonic zebrafish were maintained in accordance with the University of Wisconsin-Madison Research Animal Resources Center.

1. Preparing Microinjection Needles

1.1) Prepare thin wall glass capillary injection needles (1.0 OD/.75 ID) using a micropipette puller device with the following settings: air pressure 200, heat 502, pull 90, velocity 80, time 70, air time at start of pull 5, air time at end of pull 5.

1.2) Using fine tweezers, break off the tip of the pulled needle so that the tip opening has a diameter of approximately 10 μm .

2. Preparing Larval Injection Dishes

2.1) Rinse a gel comb with lane width of approximately 4-5 mm in sterile water and allow to dry.

2.2) Prepare a 1.5-2% high melt agarose solution in E3 medium(19) and microwave until the solution is clear. Once cooled, pour some of the agarose into a Petri dish (100 mm x 15 mm) and swirl, adding just enough agarose to completely cover the bottom of the dish.

- 2.3) Once the agarose layer has solidified, place the rinsed and dried gel comb on top so that the non-combed end is just resting on the top of the Petri dish and the combed end is touching the agarose. Ensure that the comb is as horizontal as possible, creating about a 30° angle with respect to the bottom agarose layer.
- 2.4) Pour an additional small amount of agarose at the interface between the comb and bottom agar layer so that the fresh agarose layer covers the wells of the comb. Allow to cool completely before removing the comb. Using a pipet tip, remove any overhanging pieces of agarose from the wells.
- 2.5) Pour E3 medium on top of the injection mold and store at 4 °C.
- 2.6) Before each use, replace with fresh medium and warm injection ramps at 28.5 °C for at least an hour before injection.
- 2.7) Immediately prior to injections, replace the E3 on the injection ramp with E3 medium containing 200 µg/ml ethyl 3-aminobenzoate (tricaine).

3. Preparing *S. iniae* Inoculum

- 3.1) Prepare and autoclave Todd Hewitt broth medium supplemented with 0.2% yeast extract and 2% proteose peptone (THY+P): 30 g/L Todd Hewitt, 2 g/L yeast extract, 20 g/L proteose peptone. For agar plates, add 14 g/L agar.

- 3.2) Prepare bacterial cultures the night before infections by pipetting a 100 µl aliquot of frozen bacterial stock into 10 ml of THY+P broth in a sealed 15 ml tube. Incubate overnight without agitation at 37 °C. After 14-16 hours of growth, use the overnight culture either to make freezer stocks or prepare for use in injections.

- 3.3) Make freezer stocks by placing 1 ml of the overnight culture in 500 µl of 80% glycerol in a 1.7 ml centrifuge tube. To avoid freeze-thaw cycles, make 100 µl one-use aliquots from this mix and store at -80 °C.

- 3.4) For *S. iniae* used in infections, dilute the overnight culture 1:100 for a total volume of 10 ml culture by adding 0.1 ml of overnight culture to 9.9 ml of THY+P broth. Grow at 37 °C without agitation for approximately 4-5 hours. Monitor the optical density (OD) at 600 nm using a Nanodrop spectrophotometer and harvest the bacteria in mid-logarithmic phase when the OD_{600 nm} reaches 0.250-0.500. An OD_{600 nm} of 0.250 corresponds to approximately 10⁸ colony forming units (CFU)/ml.

3.5) Pellet 1 ml of the bacterial culture in a 1.7 ml centrifuge tube at 1500 x *g* for 5 min.

Resuspend in 1 ml of fresh PBS and repeat. Measure the OD₆₀₀ nm of the bacteria in PBS, pellet, and resuspend in PBS to achieve the desired concentration.

3.6) To aid in the visualization of microinjection, add phenol red to the bacterial suspensions prior to injection for a final concentration of 0.1%.

3.7) For experiments involving the injection of heat-killed bacteria, heat the bacteria in PBS at 95 °C for 30 minutes. Confirm that the heat-killing process reduced the number of viable bacteria to undetectable levels by plating an injection volume (approximately 1 nl) on solid THY+P agar plates and incubating overnight at 37 °C.

4. Labeling *S. iniae* with a CellTracker Red Fluorescent Dye:

4.1) To label living bacterial cells, prepare a stock solution of a CellTracker fluorescent dye or equivalent. As the CellTracker Red CPTX dye used comes in 20 x 50 µg aliquots of powder and needs to be resuspended in DMSO, add 7.3 µl DMSO to the tube to obtain a 10 mM stock concentration.

4.2) Test a range of dye concentrations (e.g. 0.5-25 µM) on the bacteria to determine the lowest optimal concentration that stains the cells. Rapidly dividing cells and longer experiments may require a higher concentration of dye.

4.2.1) Pellet 1.0 ml of bacterial culture in a 1.7 ml tube by centrifugation as described above (section 3). Resuspend the pellet in 1 ml fresh PBS and add the appropriate volume of dye to the bacterial culture.

4.2.2) Incubate without agitation at 37 °C for 30 min. Spin down the bacteria and resuspend in 1 ml of pre-warmed THY+P broth and incubate without agitation for an additional 30 min at 37 °C.

4.2.3) Spin down the bacteria and wash two times in PBS before measuring the OD600 nm and diluting the bacteria for microinjection as detailed above (section 3). We typically inject approximately 100 CFU in 1 nl injection volume for our studies of leukocyte recruitment and phagocytosis.

5. Preparation of Zebrafish Larvae for Infections:

5.1) Set up breeding pairs the night before and collect embryos as described by Rosen *et al.* (27). Incubate embryos in E3 medium at 28.5 °C until ready to infect.

5.2) For zebrafish that will be imaged, prevent the development of pigment (melanization) by adding *N*-Phenylthiourea (PTU) to the E3 medium at 24 hours post fertilization (hpf) for a final concentration of 0.2 nM.

5.3) For infections involving embryos aged 2 dpf, dechorionate embryos manually with a pair of fine tweezers. Alternatively, embryos can be dechorionated by removing E3 and replacing with pronase (2 mg/ml) for about 5 min or until gentle pipetting breaks embryos out of their chorion. Most larvae should have hatched naturally by 3 dpf.

5.4) Anesthetize zebrafish several minutes prior to infection by placing dechorionated larvae into E3 medium containing 200 µg/ml tricaine.

6. Otic Vesicle Injection of *S. iniae* into Three Day Old Larvae:

6.1) Turn on the Picospritzer III microinjector and set the time range to “millisecond”.

Open the valve on the carbon dioxide tank to let gas into the line. The pressure of the microinjector should read approximately 20 PSI. Adjust the pressure in the microinjector unit by clockwise turning of the black knurled knob for increased pressure or counterclockwise turning for decreased pressure.

6.2) Vortex the prepared *S. iniae* culture in phenol red and PBS and use a microloader tip to load 2-3 µl of the culture into a pulled capillary injection needle.

6.3) Mount the loaded needle on a micromanipulator connected to a magnetic stand and position it under a stereomicroscope so that the needle is at approximately a 45-65° angle with respect to the base of the microscope.

6.4) Press on the foot pedal of the microinjector to dispense a drop of the inoculum onto the tip of the needle. Measure the diameter of the drop using the scale bar in the ocular lens of the microscope.

6.4.1) Alternatively, estimate the diameter of the drop by injecting a volume into a drop of mineral oil on a glass microscope slide with a scale bar. The diameter of the drop should be approximately 0.10 mm, which is about a 1 nl volume.

6.4.2) Adjust the drop size by adjusting the duration setting on the microinjector or by clipping off more of the needle tip with fine tweezers. Note that the injection time should be between 20-35 milliseconds to avoid causing too much tissue damage.

6.5) Using a plastic transfer pipet, transfer 12 anesthetized larvae into each well of the injection mold.

6.6) Use a glass rod, hair loop, or plastic tip to gently position the larvae so that the heads are pointed towards the back of the microscope and the yolk sacs are against the left side of the well. The left ear of the larva should be pointed up towards the ceiling.

6.7) Looking through the ocular lens of the stereomicroscope, use the knobs on the micromanipulator to line up the loaded needle with the otic vesicle so that both are in the same field of view. Pierce the outer epithelial layer of the otic vesicle with the needle tip so that the needle tip is just inside the vesicle.

6.8) Press on the foot pedal to inject 1 nl of the desired dose of *S. iniae*. Be sure to use a low enough pressure so as not to rupture the cavity. If the injection is successful, the otic vesicle, but not the surrounding tissue, should fill with the phenol red inoculum (**Fig. 1Ai**). Immediately remove any mis-injected fish from the injection plate.

6.9) Carefully retract the needle out of the larva and move the injection plate by hand so that the next larva is in view. Do this under 5x magnification.

Note: Retraction of the needle may result in the deposition of some bacteria outside of the otic vesicle, which may skew survival and leukocyte recruitment results. To avoid this, it is recommended to inject fluorescent dye-labeled bacteria and visually scan

injected larvae under a fluorescent microscope to remove any larvae where this has occurred. A correctly injected larva is shown in (**Fig. 1Bi**).

6.10) To ensure the injection volume/inoculum remains the same over the course of the experiment, inject a drop of the bacterial suspension into a 1.7 ml centrifuge tube containing 100 μ l sterile PBS after every 48th embryo. Plate the 100 μ l on THY+P agar plates at 37 °C overnight to determine the CFU in the injection volume.

6.11) When the entire group of 12 larvae on the injection ramp has been injected, carefully use a plastic transfer pipette to remove the larvae from the wells and place them into a new Petri dish (35 mm x 10 mm). Remove the tricaine solution and replace with approximately 2 ml fresh E3 medium to allow the larvae to recover.

6.12) Pipet injected larvae into single wells of a 96 well plate and incubate at 28.5 °C. Larvae can be monitored over time for survival in these plates or can later be removed for imaging or CFU counts.

7. Sudan Black Staining of Neutrophils

Note: The following steps can be done at room temperature in a small Petri dish (35 mm x 10 mm) on an orbital shaker unless otherwise stated. For each step, the amount

of reagent used is approximately 2 ml per dish, using just enough liquid to completely cover the larvae.

7.1) For fixation of infected larvae, use a glass Pasteur pipette to remove E3 medium and replace with an ice-cold 4% paraformaldehyde in PBS solution. Immediately place the fish at 4 °C to euthanize. Fix overnight at 4 °C.

7.2) Wash three times in PBS for 5 minutes each.

7.3) Stain with Sudan Black (0.18% stock diluted 1:5 in 70% ethanol, 0.1% phenol) for 30 min to 5 hours. Use a stereomicroscope to check if neutrophil granules have taken up the stain.

7.4) Perform a series of 5 minute washes starting with a single wash in 70% ethanol followed by a single wash of a 1:1 ratio of 70% ethanol and PBS, followed by a final wash in PBS.

7.5) Rehydrate into PBS plus 0.1% tween (PBT).

7.6) To clear pigment from the larvae, wash in 1% potassium hydroxide/1% hydrogen peroxide for about 6-10 min. Monitor the sample closely and after about 5 min, check the

larvae under a stereomicroscope to see how much of the pigment has cleared. If the solution is left on too long, the yolk sacs will swell and burst.

7.7) Wash three times for 5 min each in PBS.

7.8) Store the samples in either PBS or PBT at 4 °C for up to one week until ready to image and count.

7.9) To image Sudan Black-stained larvae, transfer the fish into PBT and then into 80% glycerol and place onto a single cavity depression slide. Position fixed larvae under a stereomicroscope using a pipette tip. Image using a color digital camera on a stereomicroscope (**Fig. 1Aii-iv**).

8. Enumeration of Viable Bacteria from Infected Larvae:

8.1) Euthanize larvae at the desired times post infection in an ice-cold 200-300 mg/L solution of tricaine in E3 medium.

8.2) Pipet euthanized larvae into 1.7 ml centrifuge tubes. Remove the tricaine solution and replace with 100 µl of 0.2% Triton X-100 in PBS (PBSTx).

8.3) Homogenize larvae by passing up and down 10 times through a 27-gauge needle.

8.4) Prepare serial dilutions of homogenates in sterile PBS. For example, if the infectious dose is 100 CFU, pipet 100 μ l of the homogenate into 900 μ l sterile PBS. Using a new pipet tip, transfer 100 μ l of the diluted homogenate into 900 μ l sterile PBS.

8.5) Plate 100 μ l of the dilutions on Columbia CNA agar for selective isolation of gram-positive bacteria, and incubate at 37 °C for 48 hr. This medium will provide greater selection than the THY+P agar plates, which will support growth of both gram-negative and gram-positive bacteria.

8.6) On plates with fewer than 500 individual colonies, count the number of colonies and multiply by the dilution factor to determine the number of CFU.

9. Fixation of Larvae for Imaging:

9.1) Fix larvae in an ice-cold 4% paraformaldehyde in PBS solution as described in section 7.

9.2) At room temperature, wash three times for 5 min each in PBS before imaging.

10. Preparation of Larvae for Live Imaging:

10.1) Prepare a 1.5% low-melting-point agarose solution in E3 by heating in the microwave until the solution is clear.

10.2) Place agarose solution in a 55 °C water bath to let it cool but not harden.

10.3) Add tricaine to the agarose to a final concentration of 0.016%.

10.4) Using a plastic transfer pipette, place 4-5 anesthetized larvae in a glass bottom dish on the stage of a stereomicroscope.

10.5) Remove the tricaine and agarose solution from the 55 °C water bath and let it cool at room temperature for 1-2 minutes. While the agarose is cooling, remove as much liquid from the anesthetized larvae as possible.

10.6) Pour the cooled agarose into the dish until about half of the surface is covered. Swirl the dish to spread the agarose. Note that if the agarose is too hot, it will kill the larvae. Also, if too much agarose is added to the dish, the objective lens of the microscope may hit the bottom of the dish when focusing through the agarose.

10.7) Using a transfer pipette, pick up the larvae that have floated to the sides of the dish and pipet them back into the center.

10.8) Under the stereomicroscope, gently position the larvae as desired with a hair loop, a long pipette tip or a glass rod. For imaging of the otic vesicle, position the larvae so that the left otic vesicle is flat against the bottom of the dish.

10.9) Let the agarose cool for about 10 minutes before moving the dish. The larvae may shift positions if the agarose is not solid. Gently pipet some tricaine and E3 solution to the top of the agarose layer to keep it moist.

11. Confocal Imaging of Infection:

11.1) Place the glass bottom dish with larvae onto the stage of an inverted microscope with an FV-1000 laser scanning confocal system.

11.2) Set the pinhole to 200-300 μm and using a numeric aperture 0.75/20x objective lens, set z-stacks with 3-6 μm slices.

11.3) Use continuous line scanning to adjust the laser power and detector gain for each channel.

11.4) Using sequential line scanning for each fluorescence channel (e.g. 488 and 543 nm) and differential interference contrast (DIC), conduct a time lapse movie of the left otic vesicle every 3 min for 2-6 hr to observe initial recruitment and phagocytosis by neutrophils and

macrophages. For longer time courses, place a lid on the Petri dish to prevent evaporation and drying out of the agarose.

11.5) Acquire still images of fixed (**Fig. 1B**) or live (**Fig. 2**) larvae at 20x or 40x magnification.

12. Photoconversion of Dendra2-labeled Leukocytes at the Otic Vesicle:

Dendra2 can be photoconverted from green to red fluorescence by focusing a 405 nm laser (50-70% laser power should be sufficient) on the region of interest (ROI) for 1 min. Below is the step-by-step protocol used for the FV-1000 laser scanning confocal system:

12.1) Visualize the sample using a z-stack scan with the 488 nm and 543 nm lasers. Use continuous line scanning to adjust the laser power and detector gain. Check to make sure there is no accidentally photoconverted red fluorescence.

12.2) On the “Image Acquisition Control” window, under “Stimulus Setting” select the “Use Scanner” tool and choose “main”. Select the 405 nm laser and set it at 70% power. Using the circle option, define the ROI in the otic vesicle.

12.3) Under “Stimulus Start Setting” select “Activation in series” with a preactivation of 1 frame and an activation time of 60,000 msec. On the “Acquisition Setting” window under the “Time Scan heading”, choose 2 intervals of 00:01:00 (one for pre- and one for post-photoconversion).

Note: After the time lapse series scan is complete, the Dendra2 should have been photoconverted to its red fluorescent state.

12.4) Scan the sample by a z-stack using the 488 nm and 543 nm lasers to visualize the photoconverted red fluorescence as well as any remaining green fluorescence (**Fig. 3**).

Representative Results:

Microinjection of *S. iniae* into the otic vesicle (**Fig. 1** and **Fig. 2**) results in an initially localized host response. When injected correctly, the bacteria should only be seen in the otic vesicle and not in the surrounding tissue or blood. This can be visualized during microinjection using phenol red dye (**Fig. 1A**). Alternatively, if labeled bacteria are injected, a quick scan of infected larvae immediately post injection can confirm the bacteria are only in the otic vesicle and not the surrounding tissue (**Fig. 1B**). Although a dose as little as 10 CFU wild type *S. iniae* is able to establish a lethal infection within 24-48 hours post infection (hpi), injection of 1000 CFU of an avirulent strain, *cpsA*, does not result in lethal infection and that

strain seems unable to proliferate in the host (24). Thus, this localized infection model is able to differentiate between bacterial strains of altered virulence.

Microinjection sites of initially localized infection are useful for studying leukocyte chemotaxis. Leukocyte recruitment can be quantified by either Sudan Black staining of neutrophil granules (**Fig. 1A**) or formaldehyde fixation of fluorescent transgenic lines (**Fig. 1B**). To visualize the recruitment and phagocytic capabilities of immune cells, we used transgenic lines expressing the green fluorescent protein Dendra2 specifically in macrophages *Tg(mpeg1:dendra2)* (24) or neutrophils *Tg(mpx:dendra2)* (12). When *S. iniae* is injected into the otic vesicle of 3 dpf larvae, both neutrophils and macrophages are rapidly recruited within the first 2 hpi (**Fig. 1**). However, when performed correctly, microinjection of PBS into the otic vesicle does not result in the same robust recruitment of host leukocytes (**Fig. 1**). In addition to recruitment, live confocal time lapse imaging of fluorescent transgenic lines injected with fluorescently-labeled bacteria reveals the phagocytic capabilities of both neutrophils and macrophages. Red dye-labeled *S. iniae* can be found inside both neutrophils and macrophages (**Fig. 2**). Using the photoconvertible protein Dendra2 to label neutrophils or macrophages allows for non-invasive photolabeling for tracking individual cell fate over the course of the infection. Macrophages that were recruited to the otic vesicle at 5 hpi were photoconverted and then tracked over the following 24 hours. Although some photoconverted cells remain in the otic vesicle or head region, some can also be found disseminated throughout the body of the larvae (**Fig. 3**).

Discussion:

The infection method used here is useful for the study of the host immune response to an initially localized infection in 2-3 dpf embryos and larvae. The focus of an inflammatory stimulus, such as infection, in a closed cavity such as the otic vesicle allows for the study of neutrophil and macrophage chemotaxis and phagocytosis. One caveat of injecting bacteria into the otic vesicle is that the ability of neutrophils to efficiently phagocytose bacteria in fluid-filled cavities may be dependent on the particular microbe. Although *Escherichia coli* and *Bacillus subtilis* are not easily phagocytosed by neutrophils in the otic vesicle (28), we have found that neutrophils are able to phagocytose both *Pseudomonas aeruginosa* and *S. iniae* in this location (16, 24). Localized infection is also useful when studying the invasiveness of various pathogens. In order to cause a systemic infection following injection into a closed cavity such as the otic vesicle, the microbe must be able to traverse physical host barriers. Alternatively, different pathogens may rely on host cells for transportation and dissemination from the initial site of infection. This makes localized injections useful for comparing strains of altered virulence. During microinjection, to avoid bacteria settling and clogging the needle, change needles either after each condition or after about 50 larvae. This will help ensure the suspension in the needle is more uniform. If settling of bacteria in the needle seems to be a problem, a mix of PBS, 2% PVP40, and 10% glycerol may help keep a homogenous suspension. To ensure that each larva is being injected with approximately the same number of bacteria, check CFU counts by homogenizing a larva immediately following injection and plating the homogenate on CNA agar. CNA agar will select for the growth of

culturable gram-positive bacteria, not only *S. iniae*, but it will provide an idea of how consistent the injection doses are between each individual larva. With a target inoculum of 100 CFU per larva, there are typically between 75-150 colonies on a CNA plate. The number of non-*S. iniae* gram-positive colonies growing on a CNA plate is probably very low, since most PBS injected fish usually result in between 0-20 colonies. At later time points during the infection, it is not uncommon for there to be variation of up to half a log in colony counts between larvae infected with the same infectious dose. This could represent slight differences between individual larva in their ability to control the infection or could reflect differences in the amount of culturable gram-positive bacteria in the larvae or E3 medium.

While injecting into the otic vesicle, it is important not to inject too large a volume or with too high a pressure as this may cause the cavity to rupture. Injection volumes should be kept to approximately 1 nl. If the needle is too large, microinjection can cause damage to the surrounding tissue, which may affect the recruitment of host leukocytes to the site of infection or may allow bacteria to leak out of the otic vesicle. It is also important to confirm injection into the correct space. If the needle is inserted too deep, it may poke through the otic vesicle or it may hit blood vessels flowing around the otic vesicle. This may lead to the deposition of bacteria into the blood stream or outside the vesicle, which may alter host responses.

It is also possible that when the needle is extracted, some bacteria may be accidentally deposited outside the otic vesicle as shown by Colucci-Guyon *et al.* (28), but we find this to only be the case in less than 5% of the injections. Trying to inject into the center of the otic

vesicle may help avoid this situation. In a successful infection, the otic vesicle should fill up with the phenol red dye, but the dye should not leak out into the surrounding tissues. Any mis-injected larvae should be immediately discarded. Injecting labeled bacteria is a useful way to confirm a successful injection (**Fig. 1B**). One of the disadvantages of using a CellTracker dye is that this dye will become diluted as the bacteria divide, eventually preventing the bacteria from being visualized under fluorescence. We chose a red dye because we used green-labeled neutrophil and macrophage transgenic lines for the majority of our studies.

Dendra2 is a photoconvertible protein derived from octocoral *Dendronephthya sp.* which can be photoconverted from a green to a red fluorescent state with a 405 nm laser (29). This photoconversion is a noninvasive way to mark cells and track their fate over the course of infection. Leukocytes recruited to the site of infection can be photoconverted and followed over time to monitor their dissemination throughout host tissues (**Fig. 3**). Alternatively, leukocytes could be photoconverted prior to infection and then monitored post-microinjection to determine the origin of cells recruited to the site of infection. Labeling bacteria and immune cells allows for the study of leukocyte-pathogen interactions *in vivo* including recruitment and phagocytosis (**Fig. 1B and Fig. 2**). Distinguishing the red-labeled *S. iniae* from the red fluorescence of a photoconverted leukocyte is difficult, so a different fluorescent CellTracker dye could be used. This would be particularly useful to determine which of the photoconverted immune cells that leave the otic vesicle contain *S. iniae*.

Future applications of the otic vesicle infection method could include measuring the speed and directionality by which neutrophils and macrophages move in response to various infections. The infection kinetics can also be studied to see which cell types are the first to arrive to a site of infection and which cell types are most robustly recruited in addition to where the cells originate or where they disseminate (30). In addition to studying the recruitment to an initially localized infection, this infection model can be used to study the function of host immune system components during initial infection. Antisense morpholino oligonucleotides that target specific RNAs can be used to knock down expression of host immune components including Toll-like receptors, cytokine receptors and leukocytes, and CRISPR-Cas or TALEN technology can be used to create genetic mutants. Gene expression using RNAseq or qPCR can also be used to characterize the expression of certain host genes in response to infection.

Acknowledgements:

The authors would like to thank lab members for zebrafish care and maintenance. This work was supported by National Institutes of Health, National Research Service Award A155397 to E. A. Harvie and NIH R01GM074827 to Anna Huttenlocher.

Disclosures:

The authors declare that they have no competing financial interests.

References

1. **Agnew W, Barnes AC.** 2007. *Streptococcus iniae*: An aquatic pathogen of global veterinary significance and a challenging candidate for reliable vaccination. *Veterinary Microbiology* **122**:1–15.
2. **Danilova N, Steiner LA.** 2002. B cells develop in the zebrafish pancreas. *PNAS* **99**:13711–13716.
3. **Lam SH, Chua HL, Gong Z, Lam TJ, Sin YM.** 2004. Development and maturation of the immune system in zebrafish, *Danio rerio*: a gene expression profiling, in situ hybridization and immunological study. *Developmental & Comparative Immunology* **28**:9–28.
4. **Willett CE, Cortes A, Zuasti A, Zapata A.** 1999. Early Hematopoiesis and Developing Lymphoid Organs in the Zebrafish. *Dev. Dyn.* **214**:323–336.
5. **Le Guyader D, Redd MJ, Colucci-Guyon E, Murayama E, Kissa K, Briolat V, Mordelet E, Zapata A, Shinomiya H, Herbomel P.** 2008. Origins and unconventional behavior of neutrophils in developing zebrafish. *Blood* **111**:132–141.
6. **Herbomel P, Thisse B, Thisse C.** 1999. Ontogeny and behaviour of early macrophages in the zebrafish embryo. *Development* **126**:3735–3745.
7. **Neely MN, Pfeifer JD, Caparon MG.** 2002. *Streptococcus-Zebrafish* Model of Bacterial Pathogenesis. *Infection and Immunity* **70**:3904–3914.
8. **Jault C, Pichon L, Chluba J.** 2004. Toll-like receptor gene family and TIR-domain

- adapters in *Danio rerio*. *Mol. Immunol.* **40**:759–771.
9. **Meijer AH, Gabby Krens SF, Medina Rodriguez IA, He S, Bitter W, Ewa Snaar-Jagalska B, Spaink HP.** 2004. Expression analysis of the Toll-like receptor and TIR domain adaptor families of zebrafish. *Mol. Immunol.* **40**:773–783.
 10. **Hermann AC, Millard PJ, Blake SL, Kim CH.** 2004. Development of a respiratory burst assay using zebrafish kidneys and embryos. *Journal of Immunological Methods* **292**:119–129.
 11. **Seeger A, Mayer WE, Klein J.** 1996. A Complement Factor B-Like cDNA clone from the Zebrafish (*Brachydanio rerio*). *Mol. Immunol.*
 12. **Yoo SK, Huttenlocher A.** 2011. Spatiotemporal photolabeling of neutrophil trafficking during inflammation in live zebrafish. *Journal of Leukocyte Biology* **89**:661–667.
 13. **Benard EL, van der Sar AM, Ellett F, Lieschke GJ, Spaink HP, Meijer AH.** 2012. Infection of Zebrafish Embryos with Intracellular Bacterial Pathogens. *J Vis Exp* 1–9.
 14. **Carvalho R, de Sonnevile J, Stockhammer OW, Savage ND, Veneman WJ, Ottenhoff THM, Dirks RP, Meijer AH, Spaink HP.** 2011. A High-Throughput Screen for Tuberculosis Progression. *PLoS ONE* **6**:e16779.
 15. **Veneman WJ, Marín-Juez R, de Sonnevile J, Ordas A, Jong-Raadsen S, Meijer AH, Spaink HP.** 2014. Establishment and Optimization of a High Throughput Setup to Study *Staphylococcus epidermidis* and *Mycobacterium marinum* Infection as a Model for Drug Discovery. *J Vis Exp.*

16. **Deng Q, Harvie EA, Huttenlocher A.** 2012. Distinct signaling mechanisms mediate neutrophil attraction to bacterial infection and tissue injury. *Cell Microbiol.*
17. **van der Sar AM, Musters RJP, van Eeden FJM, Appelmelk BJ, Vandenbroucke-Grauls CMJE, Bitter W.** 2003. Zebrafish embryos as a model host for the real time analysis of *Salmonella typhimurium* infections. *Cell Microbiol* **5**:601–611.
18. **Lin A, Loughman JA, Zinselmeyer BH, Miller MJ, Caparon MG.** 2009. Streptolysin S Inhibits Neutrophil Recruitment during the Early Stages of *Streptococcus pyogenes* Infection. *Infection and Immunity* **77**:5190–5201.
19. **Nüsslein-Volhard C, Dahm R.** 2002. *Zebrafish: A Practical Approach.* Oxford University Press, New York, NY.
20. **He S, Lamers GE, Beenakker J-WM, Cui C, Ghotra VP, Danen EH, Meijer AH, Spaik HP, Snaar-Jagalska BE.** 2012. Neutrophil-mediated experimental metastasis is enhanced by VEGFR inhibition in a zebrafish xenograft model. *J. Pathol.* **227**:431–445.
21. **Haldi M, Ton C, Seng WL, McGrath P.** 2006. Human melanoma cells transplanted into zebrafish proliferate, migrate, produce melanin, form masses and stimulate angiogenesis in zebrafish. *Angiogenesis.*
22. **Davis JM, Clay H, Lewis JL, Ghori N, Herbomel P, Ramakrishnan L.** 2002. Real-time visualization of mycobacterium-macrophage interactions leading to initiation of granuloma formation in zebrafish embryos. *Immunity* **17**:693–702.
23. **Wiles TJ, Bower JM, Redd MJ, Mulvey MA.** 2009. Use of Zebrafish to Probe the

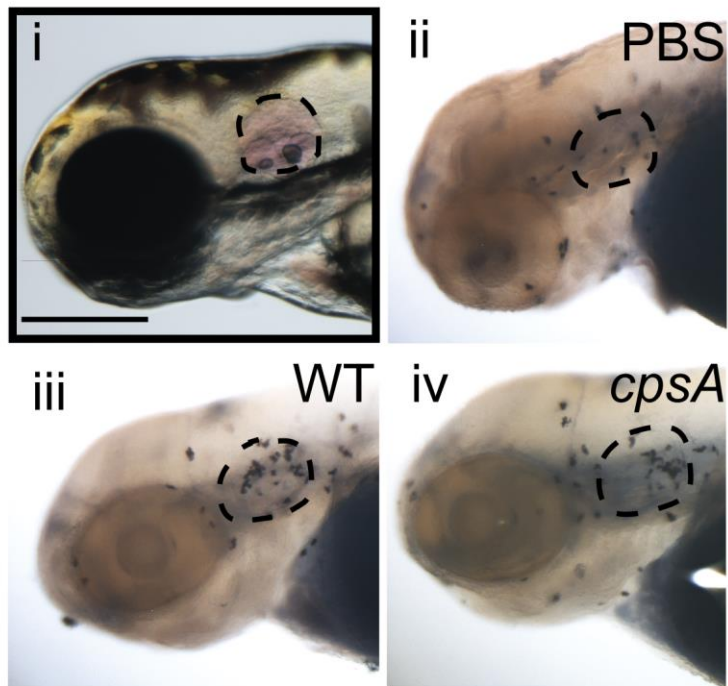
- Divergent Virulence Potentials and Toxin Requirements of Extraintestinal Pathogenic *Escherichia coli*. *PLoS Pathog* **5**:e1000697.
24. **Harvie EA, Green JM, Neely MN, Huttenlocher A.** 2013. Innate Immune Response to *Streptococcus iniae* Infection in Zebrafish Larvae. *Infection and Immunity* **81**:110–121.
 25. **Haddon C, Lewis J.** 1996. Early Ear Development in the Embryo of the Zebrafish, *Danio rerio*. *the journal of comparative neurology* **365**:113–128.
 26. **Whitfield TT, Riley BB, Chiang M-Y, Phillips B.** 2002. Development of the zebrafish inner ear. *Dev. Dyn.* **223**:427–458.
 27. **Rosen JN, Sweeney MF, Mably JD.** 2009. Microinjection of zebrafish embryos to analyze gene function. *J Vis Exp*.
 28. **Colucci-Guyon E, Tinevez JY, Renshaw SA, Herbomel P.** 2011. Strategies of professional phagocytes in vivo: unlike macrophages, neutrophils engulf only surface-associated microbes. *Journal of Cell Science* **124**:3053–3059.
 29. **Gurskaya NG, Verkhusha VV, Shcheglov AS, Staroverov DB, Chepurnykh TV, Fradkov AF, Lukyanov S, Lukyanov KA.** 2006. Engineering of a monomeric green-to-red photoactivatable fluorescent protein induced by blue light. *Nat Biotechnol* **24**:461–465.
 30. **Deng Q, Sarris M, Bennin DA, Green JM, Herbomel P, Huttenlocher A.** 2013. Localized bacterial infection induces systemic activation of neutrophils through *Cxcr2* signaling in zebrafish. *Journal of Leukocyte Biology* **93**:761–769.

Figure Legends

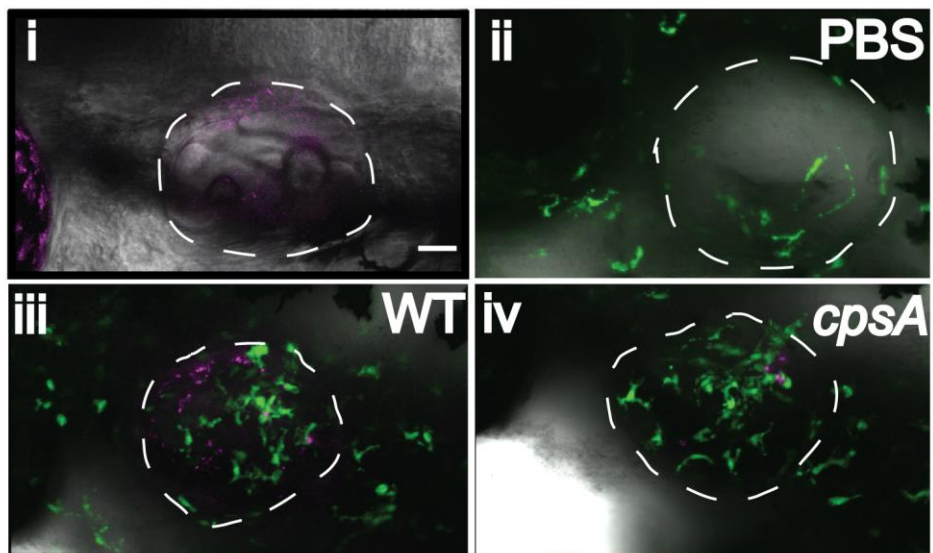
Figure I-1: Leukocyte recruitment to otic vesicle infection with *S. iniae*. (A) Neutrophil recruitment to *S. iniae* infection. (i) Successful injection of a phenol red-labeled inoculum into the otic vesicle. (ii-iv) Sudan Black staining of larvae for investigation of neutrophil recruitment at 2 hpi. PBS mock-infected larvae show little recruitment of neutrophils to the otic vesicle (ii) whereas infection with either wild type *S. iniae* or the *cpsA* mutant results in robust neutrophil recruitment (iii, iv). Scale bar, 300 μm . (B) Macrophage recruitment to *S. iniae* infection. (i) Successful microinjection of red-labeled *S. iniae* (depicted in magenta) into the otic vesicle. (ii-iv) Fluorescent confocal images of microinjected transgenic *mpeg1:dendra2* larvae fixed at 2 hpi. PBS mock-infected larvae show little macrophage recruitment (ii), but larvae infected with CellTracker Red-labeled (depicted in magenta) wild type *S. iniae* or the *cpsA* mutant show robust macrophage recruitment to the otic vesicle at 2 hpi (iii, iv). Scale bar, 30 μm .

Figure I-1:

A



B



Macrophages *S. iniae*

Figure I-2: Phagocytosis of *S. iniae* by phagocytes in the otic vesicle. Transgenic *mpx:dendra2* (A) or *mpeg1:dendra2* (B) larva infected with red-labeled *S. iniae* (depicted in magenta) and imaged at 60 min post infection using a laser scanning confocal microscope.

Scale bar, 30 μm .

Figure I-2:

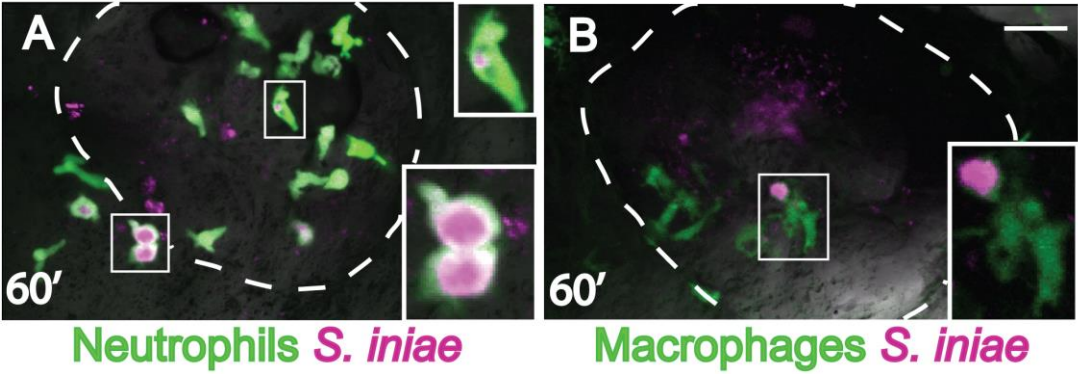
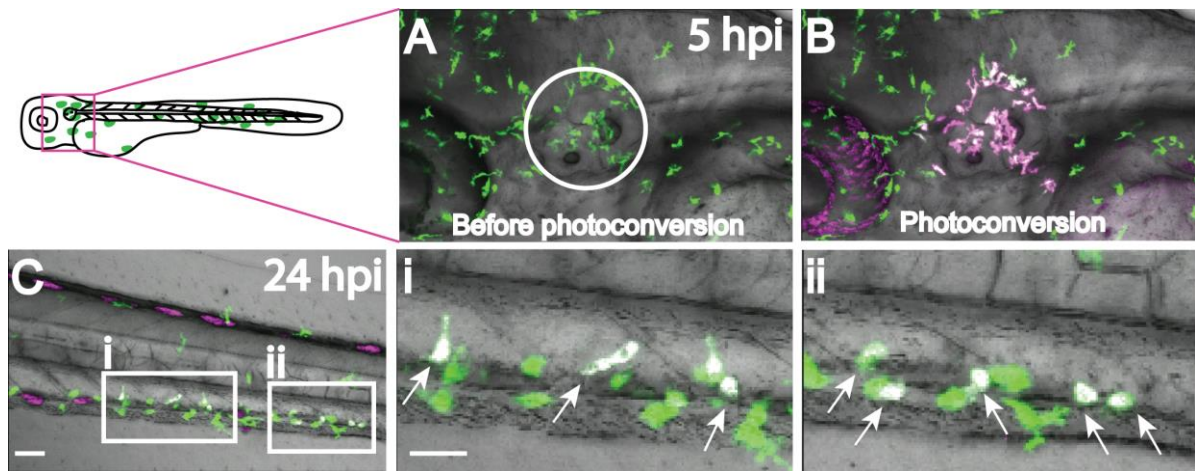


Figure I-3: Photoconversion of macrophages at the otic vesicle 5 hpi with *S. iniae*.

Macrophages (depicted in green) at the otic vesicle, designated by the circle (A), were photoconverted (B) using a 405 nm laser on a confocal microscope and tracked over time. By 24 hpi, photoconverted macrophages (depicted in magenta) have migrated as far as the trunk/caudal hematopoietic tissue (C); scale bar, 50 μm . Higher magnifications of the boxed regions in C are shown in (i) and (ii), scale bar 30 μm ; arrows point to photoconverted macrophages. Photoconverted cells appear white because of the merged 543 nm red fluorescence and any remaining 488 nm green fluorescence.

Figure I-3:



Appendix II

Heat shock modulates neutrophil motility in zebrafish

This Chapter was published in the following journal article:

Lam P.Y., Harvie E.A., and Huttenlocher A. (2013) Heat shock modulates neutrophil motility in zebrafish. *PLoS One*, Dec 19;8(12):e84436.

I helped design and perform all infection experiments (as shown in Fig. II-1 and II-5) and helped edit the manuscript.

Abstract

Heat shock is a routine method used for inducible gene expression in animal models including zebrafish. Environmental temperature plays an important role in the immune system and infection progression of ectotherms. In this study, we analyzed the impact of short-term heat shock on neutrophil function using zebrafish (*Danio rerio*) as an animal model. Short-term heat shock decreased neutrophil recruitment to localized *Streptococcus iniae* infection and tail fin wounding. Heat shock also increased random neutrophil motility transiently and increased the number of circulating neutrophils. With the use of the translating ribosome affinity purification (TRAP) method for RNA isolation from specific cell types such as neutrophils, macrophages and epithelial cells, we found that heat shock induced the immediate expression of heat shock protein 70 (*hsp70*) and a prolonged expression of heat shock protein 27 (*hsp27*). Heat shock also induced cell stress as detected by the splicing of X-box binding protein 1 (*xbp1*) mRNA, a marker for endoplasmic reticulum (ER) stress. Exogenous expression of Hsp70, Hsp27 and spliced Xbp1 in neutrophils or epithelial cells did not reproduce the heat shock induced effects on neutrophil recruitment. The effect of heat shock on neutrophils is likely due to a combination of complex changes, including, but not limited to changes in gene expression. Our results indicate that routine heat shock can alter neutrophil function in zebrafish. The findings suggest that caution should be taken when employing a heat shock-dependent inducible system to study the innate immune response.

Introduction

Fever is an evolutionarily conserved response during infection. In ectotherms such as fish, where regulation of body temperature depends on external sources, behavioral fever is often displayed as a result of infection, manifested as an acute change in thermal preference. Examples of this can be found in largemouth blackbass and bluegill sunfish which prefer elevated water temperatures after injection with killed *Aeromonas hydrophila* (*A.h*) (1). Goldfish maintained at a febrile temperature had a higher survival rate after injection with live *A.h* (2). Rainbow trout show an increased preferred temperature and enhanced expression of inflammatory cytokine interleukin-1 β after bacterial lipopolysaccharide (LPS) injection (3). Zebrafish also exhibit behavioral fever following viral infection, accompanied by upregulation of anti-viral genes (4). Knowledge of what effect an elevated temperature has on immune cell function is limited. Several studies suggest that heat can affect neutrophil activation under some conditions. For example, heat exposure down-regulates TNF α signaling in suspended neutrophils but not in neutrophils interacting with fibronectin *in vitro* (5). Heat inhibits LPS-induced neutrophil NF- κ B activation in mice (6). The physiological and molecular consequences of elevated body temperature on immune cell function *in vivo* are not clear.

In addition to environmental temperature changes, short-term heat shock is a routine method for inducible gene expression with the use of heat shock protein promoters in various model organisms including mouse (7), zebrafish (8), *Drosophila* (9) and *Caenorhabditis elegans* (10, 11). Elevated temperature increases the expression of heat shock proteins

(HSPs), which play important roles in innate and adaptive immunity (reviewed in (12, 13).

Heat stress can also induce the unfolded protein response (UPR) and immune systems rely on intact UPR functions (reviewed in (14, 15). This study will address potential implications of the short-term heat shock procedure on neutrophil function.

In this paper, we focused on the effect of short-term temperature elevation on innate immune function using zebrafish (*Danio rerio*) as an animal model. The immune system of the zebrafish is highly conserved and has emerged as a powerful vertebrate disease model of both innate and adaptive immunity (reviewed in (16, 17). Our data suggest that short-term heat shock affects innate immune function *in vivo* including a decrease in neutrophil recruitment to sites of infection and wound, and an increase in the mobilization of neutrophils into the circulation. This short-term heat shock, however, had no effect on larval survival with infection. Short-term heat shock increased neutrophil motility in a transient manner while the effect of heat shock on neutrophil wound response was long lasting. We showed that heat shock induced the expression of heat shock proteins such as Hsp70 and Hsp27 as well as the splicing of X-box binding protein 1 (*xbp1*) as part of the unfolded protein response. We adapted the translating ribosome affinity purification (TRAP) method for RNA isolation from specific cell types (18, 19) in zebrafish and found that heat shock induced specific changes in gene expression in neutrophils, macrophages and epithelial cells. Neutrophil specific over-expression of Hsp70, Hsp27 and spliced Xbp1 did not recapitulate the observed heat shock phenotypes. These findings suggest against a cell autonomous role for these specific heat shock-induced genes on neutrophil function. Our findings suggest that

caution should be taken when using the heat shock procedure to study innate immune responses since heat shock alone can induce changes in neutrophil function.

Results and Discussion

Heat shock induces changes in the innate immune response

Zebrafish are normally maintained at 28.5°C. Heat shock (HS) was performed at 38-39°C for 1 hour in a water bath. To assess the effect of heat shock on immune cells, we performed the previously established methods of *Streptococcus iniae* (*S.i*) otic vesicle infections (**Fig. 1A**) (20) and tail fin wound assays (**Fig. 1B**) (21) on zebrafish larvae at 3 days post fertilization (dpf). At this stage of development, adaptive immunity has not sufficiently matured (22, 23), allowing for the direct study of innate immunity in isolation. Neutrophils, as the first responders to sites of infection or wounds (reviewed in (24)), are an important part of the innate immune response. Larvae were infected with *S.i* or injected with a PBS control in the otic vesicle and fixed at 2 hours post infection (hpi) for Sudan Black staining and quantification of neutrophil recruitment. There was a decrease in neutrophil recruitment to the site of *S.i* otic infection in HS larvae compared to controls (**Fig. 1C**). Since it has been shown that tilapia are more susceptible to *S.i* infection at higher temperatures (25), we then tested if short-term HS can affect the survival of zebrafish larvae after *S.i* infection. In our system, short-term HS for 1 hour did not alter survival 4 days post infection (**Fig. 1D**). HS also decreased neutrophil recruitment to the tail fin wound at 4 hours post wounding (hpw) when compared to controls (**Fig. 1E**). Since HS did not significantly change the total

number of neutrophils (**Fig. 1F**), the effect was likely due to a change in neutrophil behavior after HS. Taken together, our results suggest that HS impairs neutrophil recruitment to sites of infection and tissue damage.

Heat shock affects neutrophil motility

It has previously been reported that isolated human neutrophils display an increase in motility at higher temperatures (26). To further characterize the effects of heat shock, we analyzed the speed of neutrophils undergoing random motility in the head region of zebrafish larvae. We observed an increase in neutrophil speed immediately after HS followed by a return to baseline motility at 3 hours post heat shock (hpHS) (**Fig. 2A**). By contrast, the effect of HS on neutrophil wound recruitment was long lasting. When larvae were wounded at 3 hpHS and then assayed four hours later, there was a significant decrease in the number of neutrophils at the tail wound site at 4 hpw (**Fig. 2B**).

Heat shock increases neutrophil mobilization

Since HS impaired neutrophil wound recruitment without affecting global numbers of neutrophils (**Fig. 1F**), we next tested if we could detect a change in neutrophil distribution induced by HS. Previous work has established that neutrophils in zebrafish larvae reside outside the vasculature, in a region known as the caudal hematopoietic tissue (CHT) and only mobilize into the circulation upon infection (27), wounding (28) or with leukocyte adhesion deficiency (29). Using the zebrafish transgenic lines (*Tg(mpx:dendra2)*) or

Tg(mpx:mCherry)), expressing fluorescent proteins specifically in neutrophils, we were able to perform live imaging of circulating neutrophils *in vivo*. We observed an increase in circulating neutrophils, particularly at 3 hpHS (**Fig. 3A** and **3B**). This may indicate that HS leads to either activation of the neutrophils or impaired retention of neutrophils within the CHT.

Heat shock induces changes in gene expression

We were interested in exploring the idea that heat shock-induced changes in gene expression might be responsible for the modification in neutrophil behavior. We looked at changes in gene expression immediately after HS and at 3 hpHS to assess the immediate-early and longer-term changes in gene expression. We focused on three candidate genes, *hsp70*, *hsp27* and the splicing of *xbp1*, due to their roles in immune function. Cell stress such as heat shock, infection, fever, inflammation, malignancy or autoimmunity can induce heat shock protein (HSP) synthesis (reviewed in (30)). HSP70 is involved in both innate and adaptive immunity and has been extensively reviewed (13, 33-36)). The role of HSP70 in inflammation is controversial. Recent studies suggest that it has pro-inflammatory functions (31) as well as anti-inflammatory functions (32). HSP27 has been shown to function in different cellular processes such as protein folding, actin remodeling and in the reduction of oxidative stress (reviewed in (33)). HSP27 binds to the barbed end of actin filaments and inhibits actin polymerization (34-36). HSP27 has also been shown to be important for cell motility in human cancer cells (37). It has previously been reported that HSP27 regulates

neutrophil chemotaxis, however, this role is independent of its role in regulating actin reorganization (38). Although research on zebrafish Hsp27 is limited, it has been shown to have similar functions and to be regulated like mammalian HSP27 (39, 40).

Upon ER stress induced unfolded protein response, the mRNA encoding the X-box-binding protein-1 (XBP1) is spliced by IRE1 to generate a more potent transcription factor XBP1S (41). XBP1 protects *Caenorhabditis elegans* during the activation of its innate immune response upon infection with pathogenic bacteria (42). It has been shown that toll-like receptor activation leads to the production of spliced XBP1 in mouse macrophages, which is required for optimal production of proinflammatory cytokines (43). XBP1 has also been linked to intestinal inflammation (44). The splicing of *xbp1* in response to ER stress is conserved in zebrafish (45).

We found that heat shock induced a global increase in *hsp70* and *hsp27* expression as well as the splicing of *xbp1* (**Fig. 4A**). These specific heat shock proteins are normally expressed during development in certain tissue but not others. *hsp70*, for example, is normally expressed during lens development in zebrafish (46), while *hsp27* is normally expressed in skeletal and cardiac muscle tissues (47). To assess changes in gene expression in specific cell types and to identify translationally active mRNAs from steady-state total mRNAs (48), we adapted the translating ribosome affinity purification (TRAP) method that was previously developed for murine models (18, 19). This method involves the expression of EGFP-tagged mouse ribosomal protein L10a in defined cell populations, allowing characterization of actively translating genes in specific cell types. Since zebrafish L10a

shares considerable homology with its mouse counterpart, we predicted the same construct could be employed for zebrafish TRAP. We generated three transgenic fish lines where EGFP-L10a is specifically expressed in neutrophils (*lyz:TRAP*), macrophages (*mpeg1:TRAP*) or epithelial cells (*krt4:TRAP*). The enriched mRNAs isolated from these transgenic lines were then analyzed. As expected, the *lyz:TRAP* and *mpeg1:TRAP* lines showed the expression of either the neutrophil marker (*mpx*) or macrophage marker (*mpeg1*), respectively (**Fig 4B**). In the *krt4:TRAP* line, we detected the expression of the epithelial marker *krt4* but not the muscle marker *myoD* (**Fig. 4C**). We then used these transgenic lines to assess whether or not HS induced the expression of *hsp70*, *hsp27* and the splicing of *xbp1* specifically in these subsets of cells. Using the TRAP method, we observed that HS did indeed induce the expression of *hsp70* and *hsp27* in neutrophils, macrophages and epithelial cells (**Fig. 4D**). At 3 hpHS, expression of *hsp27* persisted while the expression of *hsp70* returned to baseline levels. Heat shock induced splicing of *xbp1* occurred in all three cell populations tested, but appears to be short lived since there was no *xbp1* splicing detectable at 3 hpHS (**Fig. 4D**).

The role of Hsp70, Hsp27 and spliced Xbp1 in neutrophil motility

In an attempt to determine if elevated levels of Hsp70, Hsp27 and spliced Xbp1 directly affect innate immune functions, we specifically expressed these proteins in neutrophils and/or epithelial cells. Expression of Hsp70 or spliced Xbp1 in neutrophils and epithelial cells did not affect the neutrophil response to *S.i.* otic infection (**Fig. 5A and 5C**).

Similar results were observed when Hsp27 was specifically expressed in neutrophils (**Fig. 5B**). We next asked if over-expression of Hsp70, Hsp27 or spliced Xbp1 individually in neutrophils or epithelial cells could reproduce the HS phenotypes. As seen in **Fig. 5D-5H**, this approach did not reproduce the HS phenotype of altering neutrophil recruitment. However, we cannot rule out the involvement of these genes and must consider that constitutive expression of HSPs and spliced Xbp1 may not faithfully recapitulate the short-term HS condition. Furthermore, the HS effects on neutrophil function may not be neutrophil cell autonomous. For example, it has been shown that elevated body temperatures can enhance LPS-induced proinflammatory cytokine TNF α production in macrophages (49). Similarly, the effect of heat shock on neutrophil function is likely due to a combination of differential gene expression within neutrophils as well as in other cell types that act to guide or influence the behavior of neutrophils.

Our results show that the effect of heat shock on the innate immune response should be taken into consideration when using heat shock as a tool for inducible gene expression. This is particularly important in the zebrafish field since heat shock is routinely used for temporal control of gene expression (8, 56-58) and the Hsp70 promoter is commonly used in the zebrafish community. As the expression of *hsp27* persisted long after the initial heat shock, researchers may want to explore the use of the Hsp27 promoter for inducible gene expression in zebrafish, keeping in mind its endogenous tissue expression (50).

Conclusion

Our data suggest that short-term HS results in changes in neutrophil behavior including increased motility and mobilization but decreased response to infection and wounding. HS induces changes in gene expression including *hsp70* and *hsp27* and in the splicing of *xbp1*. These findings suggest that caution should be taken when employing a HS-dependent inducible system to study the innate immune system. The effect of long-term temperature increase on innate immunity will require further investigation.

Materials and Methods

Ethics Statement

All animal studies were approved by the University of Wisconsin – Madison Animal Care and Use Committee and performed in accordance with the guidelines.

Heat shock, tail fin wounding, otic vesicle injection and Sudan Black staining

Heat shock was performed in a water bath at 38-39°C for 1 hour. For tail fin wounding, larvae at 3 dpf were anesthetized using 0.2 mg/mL tricaine and wounded with a 33 gauge needle. Preparation of *Streptococcus iniae* and microinjection of bacteria into zebrafish larvae has been previously described (20). 1 nl volume of 100 CFU of *S. iniae* wild-type strain 9117 (or a PBS control) was microinjected into the otic vesicle of larvae at 3 dpf.

Larvae were then fixed at the time points indicated with 4% formaldehyde overnight at room temperature and stained with Sudan Black as described previously (51).

Purification of mRNA from TRAP zebrafish larvae and RT-PCR

A protocol previously used for TRAP mRNA purification from mouse tissue (19) was adapted for zebrafish larvae with slight modifications. Briefly, a glass dounce homogenizer was used to homogenize the larvae. Purified rabbit anti-GFP antibody (Invitrogen A11122) was used for immunoprecipitation. After immunoprecipitation and high-salt polysome buffer washing steps, RNA was purified using an RNeasy Mini Kit (Qiagen) with in-column DNase digestion. RT-PCR was performed using the OneStep RT-PCR Kit (Qiagen) according to the manufacturer's instruction. Primers used to amplify *ef1 α* , *mpx* (52) and *xbp1* (45) have been described previously. The other primer sequences used in this study were as follow:

hsp27-F 5'-CGGATCCATGGCCGAGAGACGCATC-3'

hsp27-R 5'-TTATTTTGTGGTGCTGACGG-3'

hsp70-F 5'-CACCCAGCTATGTTGCCTTCAC-3'

hsp70-R 5'-CACCATGCGGTTGTCAAAGTCC-3'

krt4-F 5'-CTATGGAAGTGGTCTTGGTGGAGG-3'

krt4-R 5'-CCTGAAGAGCATCAACCTTGGC-3'

mpeg1-F 5'-CTTTAATTCAGAGCCACGGAGGAGC-3'

mpeg1 R 5'-GTAGACAACCCTAAGAAACCACAGG-3'

myoD-F 5'-CCTTGCTTCAACACCAACGACATG-3'

myoD-R 5'-GTCATAGCTGTTCCGTCCTTCTCGTC-3'

PCR products were analyzed using 1% agarose electrophoresis with the exception of *xbp1* RT-PCR in which 8% polyacrylamide gel made in TAE buffer was used.

DNA injection

All DNA expression vectors contained the zebrafish lysozyme C (*lyz*) promoter for neutrophil expression (24, 62), *mpeg1* promoter for macrophage expression (20), or *krt4* promoter for epithelial cell expression (63, 64). To facilitate the production of multiple protein products from a single transgene, a viral 2A peptide linker sequence was used (53). All expression vectors contain minimal Tol2 elements for efficient integration (54) and an SV40 polyadenylation sequence (Clontech Laboratories, Inc). The following constructs were generated: *lyz-EGFP-L10a*, *mpeg1-EGFP-L10a*, *krt4-EGFP-L10a*, *lyz-hsp27-2A-mCherry* (Zebrafish *hsp27* (ATCC 10809422, accession BC097148)), *lyz-hsp70-2A-EGFP* (Zebrafish *hsp70* (Open Biosystems Clone Id:6789418, accession BC056709)), *krt4-hsp70-2A-mCherry*, *lyz-xbp1-2A-EGFP* (Zebrafish spliced *xbp1* (Open Biosystems Clone Id:3816043, accession BC044134)) and *krt4-xbp1-2A-mCherry*. Expression of constructs was obtained by injecting 3 nL of solution containing 12.5 ng/ μ L of DNA plasmid and 17.5 ng/ μ L *in vitro* transcribed (Ambion) Tol2 transposase mRNA into the cytoplasm of one-cell stage embryo.

Live imaging and image quantification

Larvae at 3 dpf were anesthetized using 0.2 mg/mL tricaine and mounted on a glass-bottom dish with 1% low melt agarose for live imaging. Time-lapse fluorescence images were acquired using a confocal microscope (FluoView FV1000, Olympus) using a NA 0.75/20x objective. Z-stack images were collected for 30 minutes with 1 minute intervals. 3-dimensional tracking of neutrophils has been previously described (21). Quantification of circulating neutrophils has been previously described (27). Briefly, *Tg(mpx:mCherry)* or *Tg(mpx:dendra2)* were used and neutrophils that circulate through the posterior cardinal vein were scored in individual 3 minute movies with 3 second intervals using a Nikon SMZ-1500 zoom microscope equipped with epifluorescence and a CoolSnap ES camera (Roper Scientific, Duluth, GA).

Statistics

Experimental results were analyzed with Prism version 4 (GraphPad Software) statistical software. The resulting *P* values are included in the figure legends for each experiment.

Acknowledgments

We thank Julie M. Green for her support in the generation and maintenance of zebrafish lines.

Funding

Funding provided by National Institutes of Health [grant numbers GM074827 to
A.H.].

References

1. **Reynolds WW, Casterlin ME, Covert JB.** 1976. Behavioural fever in teleost fishes. *Nature* **259**:41–42.
2. **Covert JB, Reynolds WW.** 1977. Survival value of fever in fish. *Nature* **267**:43–45.
3. **Gräns A, Rosengren M, Niklasson L, Axelsson M.** 2012. Behavioural fever boosts the inflammatory response in rainbow trout *Oncorhynchus mykiss*. *J. Fish Biol.* **81**:1111–1117.
4. **Boltaña S, Rey S, Roher N, Vargas R, Huerta M, Huntingford FA, Goetz FW, Moore J, Garcia-Valtanen P, Estepa A, Mackenzie S.** 2013. Behavioural fever is a synergic signal amplifying the innate immune response. *Proc. Biol. Sci.* **280**:20131381.
5. **Salanova B, Choi M, Rolle S, Wellner M, Scheidereit C, Luft FC, Kettritz R.** 2005. The effect of fever-like temperatures on neutrophil signaling. *The FASEB Journal* **19**:816–818.
6. **Kettritz R, Choi M, Salanova B, Wellner M, Rolle S, Luft FC.** 2006. Fever-like temperatures affect neutrophil NF-kappaB signaling, apoptosis, and ANCA-antigen expression. *J. Am. Soc. Nephrol.* **17**:1345–1353.
7. **Dietrich P, Dragatsis I, Xuan S, Zeitlin S, Efstratiadis A.** 2000. Conditional mutagenesis in mice with heat shock promoter-driven cre transgenes. *Mamm. Genome* **11**:196–205.
8. **Shoji W, Sato-Maeda M.** 2008. Application of heat shock promoter in transgenic

- zebrafish. *Dev. Growth Differ.* **50**:401–406.
9. **Phelps CB, Brand AH.** 1998. Ectopic gene expression in *Drosophila* using GAL4 system. *Methods* **14**:367–379.
 10. **Bacaj T, Shaham S.** 2007. Temporal control of cell-specific transgene expression in *Caenorhabditis elegans*. *Genetics* **176**:2651–2655.
 11. **Davis MW, Morton JJ, Carroll D, Jorgensen EM.** 2008. Gene activation using FLP recombinase in *C. elegans*. *PLoS Genet.* **4**:e1000028.
 12. **Colaco CA, Bailey CR, Walker KB, Keeble J.** 2013. Heat shock proteins: stimulators of innate and acquired immunity. *Biomed Res Int* **2013**:461230.
 13. **Wallin RPA, Lundqvist A, Moré SH, Bonin von A, Kiessling R, Ljunggren H-G.** 2002. Heat-shock proteins as activators of the innate immune system. *Trends in Immunology* **23**:130–135.
 14. **Costa CZF, da Rosa SEA, de Camargo MM.** 2011. The unfolded protein response: how protein folding became a restrictive aspect for innate immunity and B lymphocytes. *Scand. J. Immunol.* **73**:436–448.
 15. **Todd DJ, Lee A-H, Glimcher LH.** 2008. The endoplasmic reticulum stress response in immunity and autoimmunity. *Nature Reviews Immunology* **8**:663–674.
 16. **Deng Q, Huttenlocher A.** 2012. Leukocyte migration from a fish eye's view. *Journal of Cell Science* **125**:3949–3956.
 17. **Meeker ND, Trede NS.** 2008. Immunology and zebrafish: Spawning new models of human disease. *Developmental & Comparative Immunology* **32**:745–757.

18. **Doyle JP, Dougherty JD, Heiman M, Schmidt EF, Stevens TR, Ma G, Bupp S, Shrestha P, Shah RD, Doughty ML, Gong S, Greengard P, Heintz N.** 2008. Application of a Translational Profiling Approach for the Comparative Analysis of CNS Cell Types. *Cell* **135**:749–762.
19. **Heiman M, Schaefer A, Gong S, Peterson JD, Day M, Ramsey KE, Suárez-Fariñas M, Schwarz C, Stephan DA, Surmeier DJ, Greengard P, Heintz N.** 2008. A Translational Profiling Approach for the Molecular Characterization of CNS Cell Types. *Cell* **135**:738–748.
20. **Harvie EA, Green JM, Neely MN, Huttenlocher A.** 2013. Innate Immune Response to *Streptococcus iniae* Infection in Zebrafish Larvae. *Infection and Immunity* **81**:110–121.
21. **Lam P-Y, Yoo SK, Green JM, Huttenlocher A.** 2012. The SH2-domain-containing inositol 5-phosphatase (SHIP) limits the motility of neutrophils and their recruitment to wounds in zebrafish. *Journal of Cell Science* **125**:4973–4978.
22. **Lam SH, Chua HL, Gong Z, Lam TJ, Sin YM.** 2004. Development and maturation of the immune system in zebrafish, *Danio rerio*: a gene expression profiling, in situ hybridization and immunological study. *Developmental & Comparative Immunology* **28**:9–28.
23. **Willett CE, Cortes A, Zuasti A, Zapata A.** 1999. Early Hematopoiesis and Developing Lymphoid Organs in the Zebrafish. *Dev. Dyn.* **214**:323–336.
24. **Lam P-Y, Huttenlocher A.** 2013. Interstitial leukocyte migration in vivo. *Curr. Opin.*

- Cell Biol. **25**:650–658.
25. **Ndong D, Chen Y-Y, Lin Y-H, Vaseeharan B, Chen J-C.** 2007. The immune response of tilapia *Oreochromis mossambicus* and its susceptibility to *Streptococcus iniae* under stress in low and high temperatures. *Fish & Shellfish Immunology* **22**:686–694.
 26. **Nahas GG, Tannieres ML, Lennon JF.** 1971. Direct measurement of leukocyte motility: effects of pH and temperature. *Proc. Soc. Exp. Biol. Med.* **138**:350–352.
 27. **Deng Q, Sarris M, Bennin DA, Green JM, Herbomel P, Huttenlocher A.** 2013. Localized bacterial infection induces systemic activation of neutrophils through Cxcr2 signaling in zebrafish. *Journal of Leukocyte Biology* **93**:761–769.
 28. **Yoo SK, Huttenlocher A.** 2011. Spatiotemporal photolabeling of neutrophil trafficking during inflammation in live zebrafish. *Journal of Leukocyte Biology* **89**:661–667.
 29. **Deng Q, Yoo SK, Cavnar PJ, Green JM, Huttenlocher A.** 2011. Dual Roles for Rac2 in Neutrophil Motility and Active Retention in Zebrafish Hematopoietic Tissue. *Developmental Cell* **21**:735–745.
 30. **Wu T, Tanguay RM.** 2006. Antibodies against heat shock proteins in environmental stresses and diseases: friend or foe? *Cell Stress Chaperones* **11**:1–12.
 31. **Senf SM, Howard TM, Ahn B, Ferreira LF, Judge AR.** 2013. Loss of the inducible Hsp70 delays the inflammatory response to skeletal muscle injury and severely impairs muscle regeneration. *PLoS ONE* **8**:e62687.

32. **Vinokurov M, Ostrov V, Yurinskaya M, Garbuz D, Murashev A, Antonova O, Evgen'ev M.** 2012. Recombinant human Hsp70 protects against lipoteichoic acid-induced inflammation manifestations at the cellular and organismal levels. *Cell Stress Chaperones* **17**:89–101.
33. **Vidyasagar A, Wilson NA, Djamali A.** 2012. Heat shock protein 27 (HSP27): biomarker of disease and therapeutic target. *Fibrogenesis Tissue Repair* **5**:7.
34. **Benndorf R, Hayess K, Ryazantsev S, Wieske M, Behlke J, Lutsch G.** 1994. Phosphorylation and supramolecular organization of murine small heat shock protein HSP25 abolish its actin polymerization-inhibiting activity. *The Journal of Biological Chemistry* **269**:20780–20784.
35. **Miron T, Vancompernelle K, Vandekerckhove J, Wilchek M, Geiger B.** 1991. A 25-kD inhibitor of actin polymerization is a low molecular mass heat shock protein. *The Journal of Cell Biology* **114**:255–261.
36. **Schneider GB, Hamano H, Cooper LF.** 1998. In vivo evaluation of hsp27 as an inhibitor of actin polymerization: hsp27 limits actin stress fiber and focal adhesion formation after heat shock. *J. Cell. Physiol.* **177**:575–584.
37. **Doshi BM, Hightower LE, Lee J.** 2009. The role of Hsp27 and actin in the regulation of movement in human cancer cells responding to heat shock. *Cell Stress Chaperones* **14**:445–457.
38. **Jog NR, Jala VR, Ward RA, Rane MJ, Haribabu B, McLeish KR.** 2007. Heat shock protein 27 regulates neutrophil chemotaxis and exocytosis through two

- independent mechanisms. *Journal of Immunology* (Baltimore, Md. : 1950) **178**:2421–2428.
39. **Mao L, Bryantsev AL, Chechenova MB, Shelden EA.** 2005. Cloning, characterization, and heat stress-induced redistribution of a protein homologous to human hsp27 in the zebrafish *Danio rerio*. *Exp. Cell Res.* **306**:230–241.
40. **Tucker NR, Shelden EA.** 2009. Hsp27 associates with the titin filament system in heat-shocked zebrafish cardiomyocytes. *Exp. Cell Res.* **315**:3176–3186.
41. **Yoshida H, Matsui T, Yamamoto A, Okada T, Mori K.** 2001. XBP1 mRNA is induced by ATF6 and spliced by IRE1 in response to ER stress to produce a highly active transcription factor. *Cell* **107**:881–891.
42. **Richardson CE, Kooistra T, Kim DH.** 2010. An essential role for XBP-1 in host protection against immune activation in *C. elegans*. *Nature* **463**:1092–1095.
43. **Martinon F, Chen X, Lee A-H, Glimcher LH.** 2010. TLR activation of the transcription factor XBP1 regulates innate immune responses in macrophages. *Nature Immunology* **11**:411–418.
44. **Kaser A, Lee A-H, Franke A, Glickman JN, Zeissig S, Tilg H, Nieuwenhuis EES, Higgins DE, Schreiber S, Glimcher LH, Blumberg RS.** 2008. XBP1 links ER stress to intestinal inflammation and confers genetic risk for human inflammatory bowel disease. *Cell* **134**:743–756.
45. **Hu M-C, Gong H-Y, Lin G-H, Hu S-Y, Chen MH-C, Huang S-J, Liao C-F, Wu J-L.** 2007. XBP-1, a key regulator of unfolded protein response, activates transcription

- of IGF1 and Akt phosphorylation in zebrafish embryonic cell line. *Biochem. Biophys. Res. Commun.* **359**:778–783.
46. **Blechinger SR, Evans TG, Tang PT, Kuwada JY, Warren JT, Krone PH.** 2002. The heat-inducible zebrafish hsp70 gene is expressed during normal lens development under non-stress conditions. *Mech. Dev.* **112**:213–215.
47. **Tucker NR, Ustyugov A, Bryantsev AL, Konkell ME, Shelden EA.** 2009. Hsp27 is persistently expressed in zebrafish skeletal and cardiac muscle tissues but dispensable for their morphogenesis. *Cell Stress Chaperones* **14**:521–533.
48. **Kudo K, Xi Y, Wang Y, Song B, Chu E, Ju J, Russo JJ, Ju J.** 2010. Translational control analysis by translationally active RNA capture/microarray analysis (TriP-Chip). *Nucleic Acids Research* **38**:e104.
49. **Lee C-T, Zhong L, Mace TA, Repasky EA.** 2012. Elevation in body temperature to fever range enhances and prolongs subsequent responsiveness of macrophages to endotoxin challenge. *PLoS ONE* **7**:e30077.
50. **Wu Z, Zhang W, Lu C.** 2008. Immunoproteomic assay of surface proteins of *Streptococcus suis* serotype 9. *FEMS Immunology & Medical Microbiology* **53**:52–59.
51. **Le Guyader D, Redd MJ, Colucci-Guyon E, Murayama E, Kissa K, Briolat V, Mordelet E, Zapata A, Shinomiya H, Herbomel P.** 2008. Origins and unconventional behavior of neutrophils in developing zebrafish. *Blood* **111**:132–141.
52. **Mathias JR, Dodd ME, Walters KB, Yoo SK, Ranheim EA, Huttenlocher A.** 2009. Characterization of zebrafish larval inflammatory macrophages. *Developmental*

- & Comparative Immunology **33**:1212–1217.
53. **Provost E, Rhee J, Leach SD.** 2007. Viral 2A peptides allow expression of multiple proteins from a single ORF in transgenic zebrafish embryos. *genesis* **45**:625–629.
54. **Urasaki A, Morvan G, Kawakami K.** 2006. Functional Dissection of the Tol2 Transposable Element Identified the Minimal cis-Sequence and a Highly Repetitive Sequence in the Subterminal Region Essential for Transposition. *Genetics* **174**:639–649.

Figure Legends

Fig. II-1. Heat shock effects on neutrophil recruitment. (A) Schematic illustration of the experimental setup for otic vesicle infection shown in C. (B) Schematic illustration of the experimental setup for tail fin wounding shown in E. The red rectangle indicates heat shock at 38-39°C for 1 hour. Grey circles indicate the time point for neutrophil counting. (C) Quantification of neutrophils at the otic vesicle (yellow dotted line) in control (cntl) and heat shocked (HS) larvae at 2 hours post infection (2 hpi). Larvae were injected with 100 CFU of *Streptococcus iniae* (*S.i*) into the otic vesicle (ear) at 3 days post fertilization (dpf). HS larvae showed decreased neutrophil recruitment compared with controls. $**P < 0.01$ (two-tailed, unpaired t-test). (Right panel) Representative images of Sudan Black-stained larvae. Lateral view of the head of larvae at 2 hpi. (D) Survival of control (cntl) and heat shocked (HS) larvae infected with *S.i* in the ear over time. Control and HS larvae showed a similar survival rate. dpi; days post infection. (E) Quantification of neutrophils at wounds in control (cntl) and heat shocked (HS) larvae at 1 and 4 hour post wounding (hpw). HS larvae showed fewer neutrophils at wounds at 4 hpw compared with controls. $****P < 0.0001$; ns, not significant (two-tailed, unpaired t-test). (Right panel) Representative images of Sudan Black-stained larvae. Lateral view of the tail fin of larvae at 3 dpf. (F) Quantification of neutrophils in whole larvae for control (cntl), heat shocked (HS) and 3 hours post heat shocked (3 hpHS) larvae. (Right panel) Representative images of Sudan Black-stained larvae. Data are representative of at least three experiments.

Fig. II-1

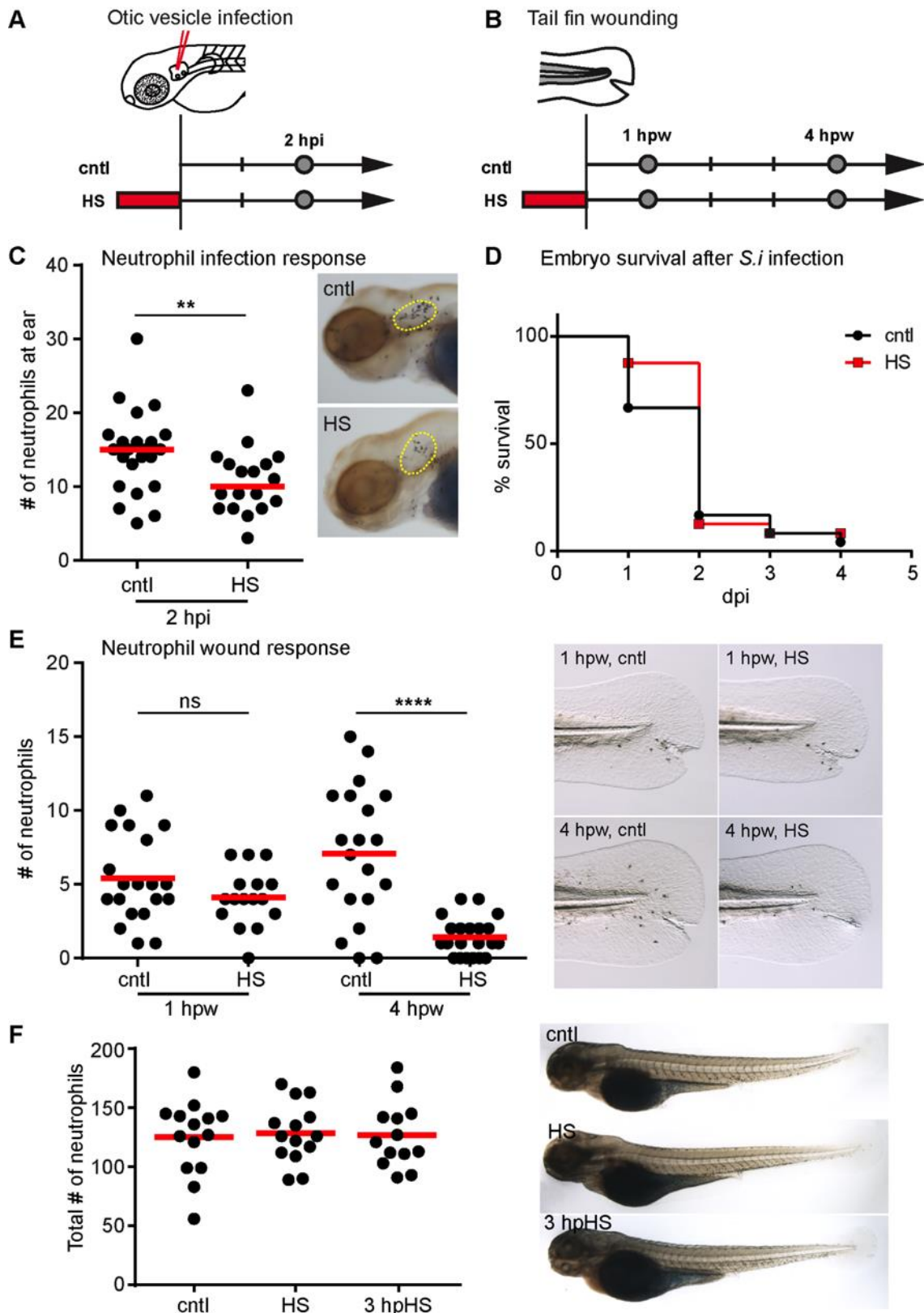


Fig. II-2. Heat shock induces transient changes in neutrophil random motility and

sustained effects on recruitment to wounds. (A) (Top) Schematic illustration of the experimental setup for quantification of neutrophil speed. The red rectangles indicate heat shock at 38-39°C for 1 hour. Arrows indicate the time point for neutrophil live imaging in the same larva before heat shock (cntl), right after heat shock (HS) and at 3 hours post heat shock (3 hpHS). (Bottom) Scatter plot showing the mean speed of *Tg(mpx:dendra2)* neutrophils at time points indicated. Neutrophils were tracked in 3 dimensions (3D) using Image J software and the MTrackJ plugin. HS larvae showed increased neutrophil speed compared with controls. At 3 hpHS, the speed of neutrophils went back to control levels. ** $P < 0.01$; ns, not significant (one way ANOVA with Dunn's multiple comparison test). (B) (Top) Schematic illustration of the experimental setup for tail fin wounding. Larvae were wounded without heat shock (cntl), right after heat shock (HS) or at 3 hours post heat shock (3 hpHS). Larvae were then fixed at 4 hours post wounding (hpw) for quantification of neutrophils (grey circles). (Bottom) Quantification of neutrophils at tail fin wounds at 4 hpw. The effect of HS on neutrophil wound response persisted even when the wound was induced at 3 hpHS. **** $P < 0.0001$ (one way ANOVA with Dunn's multiple comparison test). Data are representative of at least three experiments.

Fig. II-2

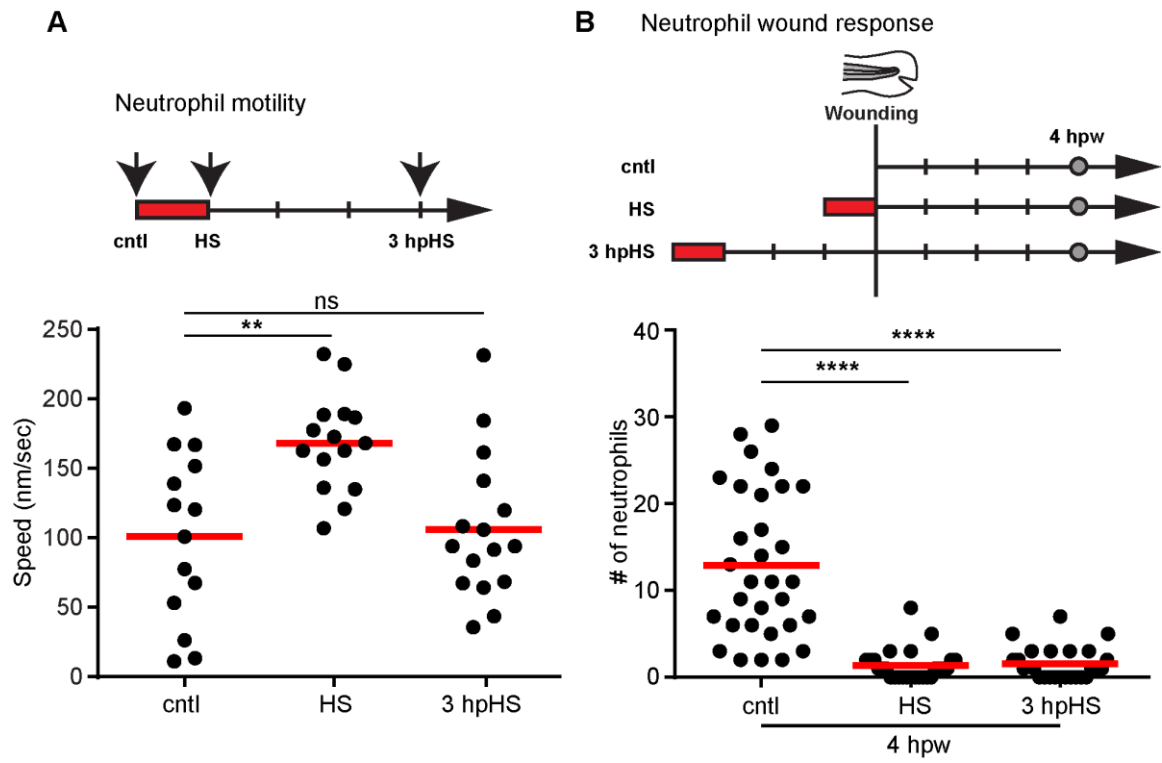


Fig. II-3. Heat shock induces neutrophil mobilization. (A) Quantification of circulating neutrophils in larvae at 3 dpf. There was an increase in circulating neutrophils at 3 hpHS. $**P < 0.01$; ns, not significant (one way ANOVA with Dunn's multiple comparison test). (B) (Left panel) Yellow box indicates area where kymograph was generated. Fluorescent signal in boxed region was stacked vertically into a one-dimensional line at each time point. Scale bar = 100 μm . (Right panel) Kymograph of 3 minute movies with a 3 second interval indicating the presence or absence of circulating neutrophils is shown. Data are representative of at least three experiments.

Fig. II-4. Heat shock induces changes in gene expression. (A) RT-PCR analysis of *hsp70*, *hsp27* and splicing of *xbp1* (p, pre-sliced; s, spliced) in control (cntl) or heat shock (HS) larvae. (B-C) RT-PCR analysis of the enrichment of RNA from neutrophils (*lyz:TRAP*), macrophages (*mpeg1:TRAP*) or epithelial cells (*krt4:TRAP*) from *Tg(lyz:EGFP-L10a)*, *Tg(mpeg1:EGFP-L10a)* or *Tg(krt4:EGFP-L10a)* larvae, respectively. Whole larvae RNA (WT) or translating ribosome affinity purification (TRAP) RNA was used and specific markers for neutrophils (*mpx*), macrophages (*mpeg1*), epithelial cells (*krt4*) and muscle cells (*myoD*) were tested. (D) Heat shock (HS) induced expression of *hsp70*, *hsp27* and splicing of *xbp1* (p, pre-sliced; s, spliced) in neutrophils (*lyz:TRAP*), macrophages (*mpeg1:TRAP*) and epithelial cells (*krt4:TRAP*). Expression of *hsp27* persisted at 3 hours post heat shock (3 hpHS) while expression of *hsp70* and splicing of *xbp1* returned to control levels at 3 hpHS. Data are representative of at least two experiments.

Fig. II-4

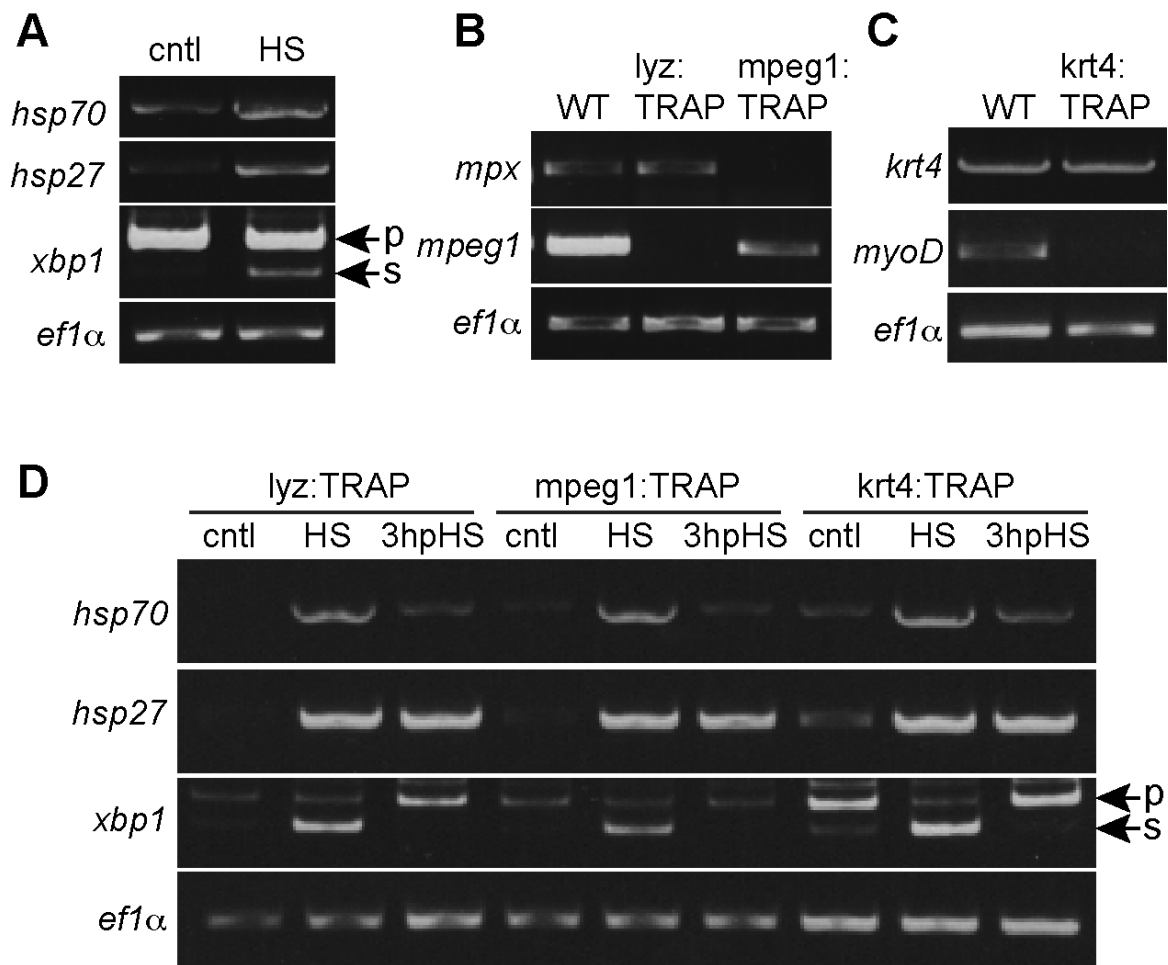
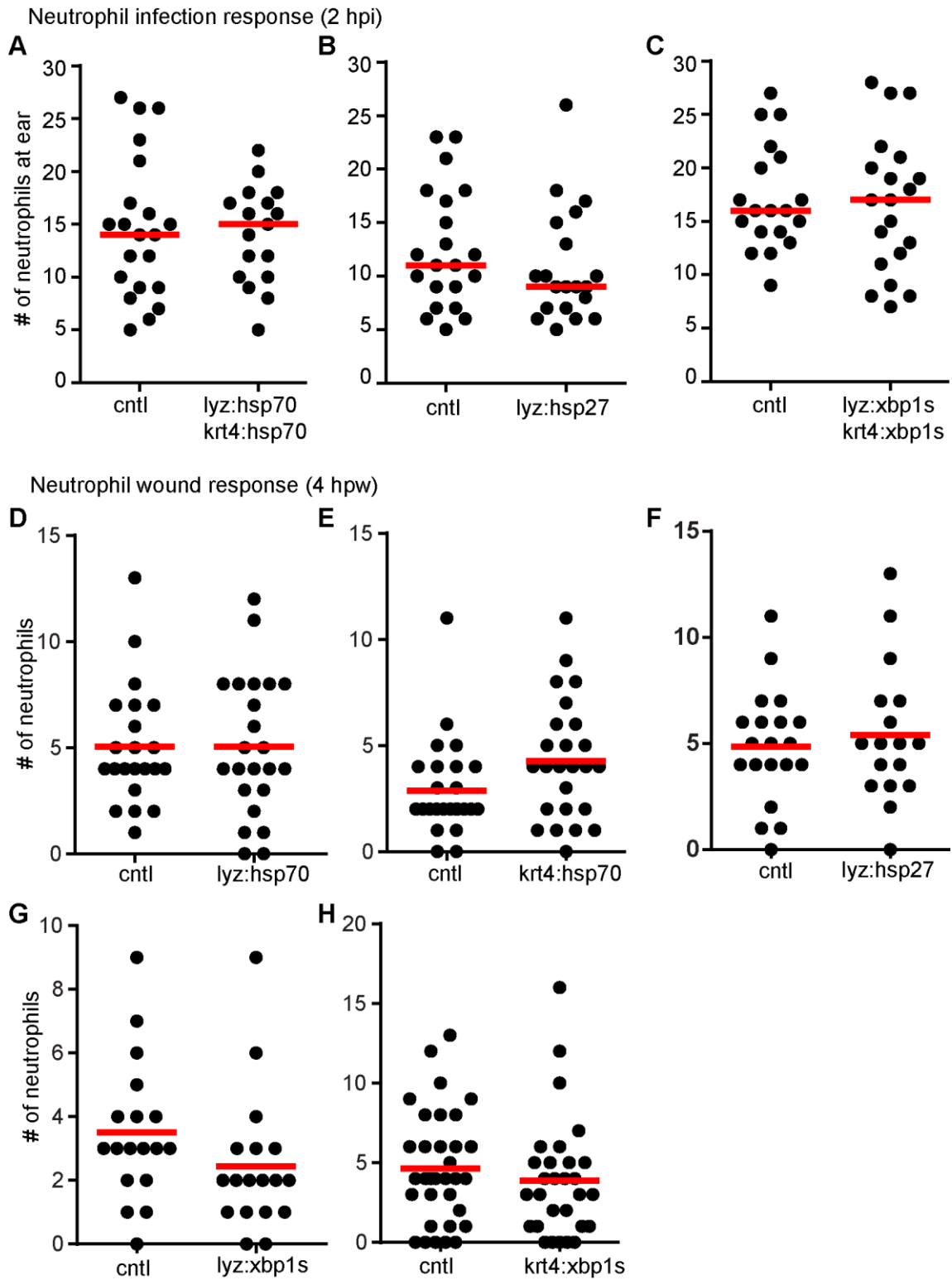


Fig. II-5. Expression of Hsp27, Hsp70 or spliced Xbp1 in neutrophils or epithelial cells

does not alter neutrophil recruitment. (A-C) Quantification of neutrophils at the otic vesicle (ear) of larvae at 2 hours post infection (hpi) with 100 CFU *S.i.* ear infection.

Experiments were performed on the larvae of transgenic lines *Tg(lyz:hsp70-2A-EGFP)* x *Tg(krt4:hsp70-2A-mCherry)* (A), *Tg(lyz:hsp27-2A-mCherry)* (B) or *Tg(lyz:xbp1s-2A-EGFP)* x *Tg(krt4:xbp1s-2A-mCherry)* (C) at 3 dpf. Controls (cntl) were siblings with no transgene expression. Expression of Hsp27, Hsp70 and spliced Xbp1 (Xbp1s) did not have a significant effect on neutrophil recruitment to ear infection. (D-H) Quantification of neutrophils at tail fin wounds at 4 hpw. Experiments were performed on *Tg(lyz:hsp70-2A-EGFP)* (D), *Tg(krt4:hsp70-2A-mCherry)* (E), *Tg(lyz:hsp27-2A-mCherry)* (F), *Tg(lyz:xbp1s-2A-EGFP)* (G) or *Tg(krt4:xbp1s-2A-mCherry)* (H) larvae at 3 dpf. Controls (cntl) were siblings with no transgene expression. Expression of Hsp27, Hsp70 and spliced Xbp1 (Xbp1s) did not have a significant effect on neutrophil numbers at the wound at 4 hpw. Data are representative of at least two experiments.

Fig. II-5



Appendix III

Distinct signaling mechanisms mediate neutrophil attraction to bacterial infection and tissue injury

This Chapter was published in the following journal article:

Deng, Q., Harvie, E. A., and Huttenlocher, A. 2012. Distinct signaling mechanisms mediate neutrophil attraction to bacterial infection and tissue injury. *Cellular Microbiology*. 14(4): 517-528.

I designed and performed the experiment in Fig. III-7 and edited the manuscript.

Abstract

The signals that differentially guide neutrophils to sites of tissue injury or infection remain elusive. H_2O_2 has been implicated in neutrophil sensing of tissue injury, however its role in neutrophil recruitment to infection has not been explored. Here, using a pharmacological inhibitor of NADPH oxidases, DPI, and genetic depletion of an epithelial specific NADPH oxidase, we show that H_2O_2 is not required for neutrophil detection of localized infection with the Gram-negative bacterium *Pseudomonas aeruginosa*. In contrast, PI(3)K signaling is required for neutrophil responses to both wounding and infection. In vivo imaging using a H_2O_2 probe demonstrates a robust gradient of H_2O_2 generated at wound sites but not at infection sites. Moreover, DPI did not inhibit neutrophil wound attraction when *Pseudomonas aeruginosa* is present in the media. Finally, DPI also fails to inhibit neutrophil recruitment to localized infection with the Gram-positive bacterium, *Streptococcus iniae*. Our findings demonstrate that differential signals are involved in sensitizing neutrophils to pathogen versus non-pathogen induced tissue damage, providing a potential target to preferentially suppress non-specific immune damage without affecting the response to infection.

Introduction

Neutrophils are a key component of the innate immune system and the first responders to infection or tissue injury. Upon acute injury or infection, neutrophils transmigrate across the endothelium barrier, undergo interstitial migration to reach the inflamed site, where they engulf microorganisms, secrete granule contents, generate reactive oxygen species and/or release nuclear extracellular traps to control infection and promote wound healing (1). Defects in neutrophil function can result in immunodeficiency, characterized by recurrent infections and poor wound healing. The inability of neutrophils to enter the circulation is seen in neutropenic patients with Warts, Hypogammaglobulinemia, Infections, and Myelokathexis (WHIM) syndrome (2). Moreover, the trapping of neutrophils within the blood stream is a hallmark of leukocyte adhesion deficiency (3) and the failure of neutrophils to undergo oxidative burst is associated with chronic granulomatous disease (4). On the other hand, neutrophilic inflammation must be controlled to prevent non-specific damage to host tissues. Improper neutrophil infiltration is a hallmark of chronic inflammatory airway diseases (5), inflammatory bowel disease (6), autoimmunity (7) and other chronic inflammatory disorders. Attenuation of neutrophilic infiltration remains an attractive target to alleviate clinical symptoms or slow disease progression. Therefore, understanding the mechanisms that regulate neutrophil trafficking to sites of infection or inflammation in vivo is fundamental to human health.

Although numerous *in vitro* studies using isolated neutrophils have identified mechanisms of neutrophil directed migration, the physiological signaling events that differentially guide neutrophil infiltration to sites of tissue injury or infection are still elusive. Recently, a stepwise dissection of the signaling events that guide neutrophil recruitment to a site of sterile inflammation was reported (8). However, the signaling events that guide neutrophil recruitment to bacterial infection are still largely unknown.

The zebrafish, *Danio rerio*, is gaining popularity as a model system to study innate immunity and leukocyte function. The innate immune system in the zebrafish larvae is highly conserved (9). Transparent larvae have made zebrafish an attractive model to observe leukocyte behavior in live animals. Ease of pharmacological and genetic manipulation has led to the discovery of novel signals that regulate rapid neutrophil recruitment *in vivo*. A gradient of hydrogen peroxide (H_2O_2) generated at injured epithelial cells are shown to mediate rapid detection of wounds by neutrophils (10). Pharmacological inhibition of nicotinamide adenine dinucleotide phosphate (NADPH) oxidase enzymes or depletion of a key oxidase in epithelial cells, dual oxidase (Duox), attenuated neutrophilic infiltration in the first 20 min post tissue injury. Although it is not clear how H_2O_2 is sensed by neutrophils, this breakthrough in wound biology highlighted the power of zebrafish for studying neutrophil function. In addition, similar H_2O_2 signaling is generated by oncogene-transformed melanoblasts and goblet cells in zebrafish, which mediates attraction of both neutrophils and macrophages (11). A balanced role for reactive oxygen species in host defense against infection is implicated in *Drosophila* gut immunity. Depletion of dDuox from the intestine results in a marked increase

in mortality rate after natural gut infection (12). Moreover, depletion of extracellular immune-regulated catalase, an enzyme that converts H_2O_2 to H_2O , also shows a high mortality rate after similar gut infection (13). It is speculated that H_2O_2 burst is a general primary response to various stressors that induce inflammatory feedback of leukocytes (11-14). However, whether the H_2O_2 signaling is involved in neutrophil detection of bacterial infection has not been determined.

Although a collection of bacterial infection models have been established in zebrafish, the majority of studies focused on models of systemic infection have observed direct pathogen-leukocyte interactions inside the vasculature (15-20). A limited number of studies have investigated neutrophil recruitment to localized infection (18, 21-23). Here we adapted a localized *Pseudomonas* infection model that is optimal for monitoring leukocyte-pathogen interactions. We found that H_2O_2 is dispensable for neutrophil attraction to localized bacterial infection. Our results provide evidence that neutrophils detect tissue injury and infection by distinct signaling pathways and positions tissue-generated hydrogen peroxide as an attractive target to differentially modulate neutrophil reaction to infection versus tissue damage.

Results

Generation of a localized infection model to monitor neutrophil recruitment

Many locations in zebrafish have been explored as sites for localized infections, including the pericardial cavity (24), hindbrain ventricle (18, 21), the yolk sac (23-25), the left inner ear (22) and the dorsal muscle (23). To select an infection model best suited to monitor neutrophil recruitment to a contained infection, we first tested *Pseudomonas aeruginosa* infection into the left inner ear or the yolk sac. Bacteria constitutively expressing the red fluorescent protein mCherry (15), in combination with the transgenic fish expressing green fluorescent protein Dendra2 specifically in neutrophils (26), allows direct visualization of infection and neutrophil responses in real-time (**Fig. 1A** and **Fig. 2B**). Four hours post infection, Dendra2 labeled neutrophils are recruited to the infected ear, demonstrated by their co-localization with mCherry-labeled PAK in the otic vesicle (**Fig. 1**). A mock injection with sterile PBS did not induce neutrophil infiltration, indicating that neutrophils respond to bacterial infection specifically. In contrast, neutrophils are not recruited to infection localized in the yolk sac (**Fig. 1B**). Neutrophils, however, can sense the presence of bacteria, revealed by increased neutrophil presence on top of the yolk sac. These neutrophils are highly motile, constantly patrolling the yolk sac (data not shown), but fail to infiltrate into the infection site. Zebrafish larvae are highly resistant to localized ear infection (**Fig. 1C**). Injection of ~63,000 cfu of PAK results in ~30% mortality of 3 dpf larvae. In contrast, when injected into the yolk sac, 2,100 cfu of PAK cause 100% mortality of 3 dpf larvae, which is probably due to the lack of neutrophil recruitment (**Fig. 1D**). Taken together, the otic vesicle is a preferred site that allows direct observation of neutrophil recruitment to localized infection.

Phagocytosis of PAK by neutrophils and resolution of inflammation

To better observe neutrophil behavior at the infected ear, a confocal movie was taken right after bacterial inoculation into the otic vesicle (**Fig. 2**). Neutrophils infiltrate into the ear immediately after infection and their number in the ear peaks ~ 6 h post infection. After that, neutrophilic inflammation slowly resolves and by 12 h post infection, neutrophil number at the infected ear significantly decreases. Bacteria taken up by neutrophils are readily observed throughout the infection process. At 12 hpi, several neutrophils containing phagocytosed bacteria are visible outside the ear, indicating that neutrophils migrate away from the site of infection, contributing to the resolution of inflammation.

Neutrophil recruitment to bacterial infection is not dependent on tissue generated H₂O₂

The signals that mediate rapid neutrophil detection of bacterial infection are still obscure. H₂O₂ is generated by wounded epithelium (10) or oncogene-transformed cells (11) to mediate neutrophil recruitment to tissue injury or transformed cells, respectively. We next investigated the role of H₂O₂ in mediating neutrophil recruitment to PAK infection. DPI, an inhibitor for the NADPH complex that generates reactive oxygen species (ROS), results in a significant inhibition of neutrophil recruitment to tissue injury compared with vehicle control (**Fig. 3A**). Injecting PAK into the left ear leads to significant neutrophil recruitment compared with injecting sterile PBS alone. However, DPI does not inhibit PAK-induced neutrophil recruitment (**Fig. 3B**). LY294002, a pan-phosphatidylinositol 3-kinase (PI3K)

inhibitor previously shown to reduce neutrophil motility in vivo (27), inhibits neutrophil responses to both tissue injury and PAK infection.

To complement the DPI results with genetic approaches, a key component of the tissue-specific NADPH complex, Duox, was depleted from zebrafish larvae using MO (10). At 3 dpf, RT-PCR shows a partial inhibition of *duox* pre-mRNA splicing, indicated by a smaller band corresponding to exclusion of the target exon (**Fig. 4C**). Neutrophil recruitment to wounding is abolished in the *duox* morphant, suggesting functional inhibition of Duox (**Fig. 4A**). Reduced numbers of neutrophils are present in the rostral mesenchymal tissues in *duox* morphants (**Fig. 4B**). When the number of neutrophils that are attracted to the infected ear is normalized to the total number of neutrophils within the head, there is no significant difference in the percentage of head resident neutrophils that are recruited to ear infection between *duox* morphants and control (**Fig. 4D**), indicating that Duox knockdown does not specifically inhibit neutrophil responses to localized PAK infection. The smaller fin and reduced neutrophil numbers in the *duox* morphants may be due to non-specific toxicity of the *duox* MO. Taken together, our data suggest that H₂O₂ is dispensable for neutrophil recruitment to PAK infection.

Absence of H₂O₂ generation at localized PAK infection

A tissue gradient of H₂O₂ is generated by injured tissue (10) and transformed cells (11) to attract neutrophils. Although the H₂O₂ signal is not required for neutrophil recruitment

to localized PAK infection (Fig. 3), we next determined whether this is due to an absence of H_2O_2 at a PAK infected ear, or a dispensable role for H_2O_2 (if generated) to attract neutrophils. Using a genetically-encoded H_2O_2 probe, HyPer (10), we find robust signal of H_2O_2 generated at wound sites but not from the infected ear (**Fig. 5** and supplemental Video 1). At infected tissue, a weak signal of H_2O_2 is observed within the ear that does not propagate into the surrounding tissue. The slight increase in H_2O_2 signal in the ear could be due to the injection process which causes a very small wound or imaging artifact from fluid inside the ear, since mock infection with sterile PBS shows a similar H_2O_2 signal (data not shown). To confirm the function of the HyPer probe, the other ear of the same fish was wounded mechanically and H_2O_2 generation was imaged under the same acquisition parameters. Consistent with previous findings (10), the wounded ear bursts a H_2O_2 wave which accompanies rapid neutrophil infiltration (**Fig. 5** and supplemental Video 1). Taken together, localized PAK infection does not result in a robust H_2O_2 gradient, consistent with the dispensable role of H_2O_2 in neutrophil attraction to infection.

DPI selectively impairs neutrophil attraction to wounds in the presence of infection

A signal hierarchy has been described in isolated human neutrophils where neutrophils preferentially migrate to target chemoattractants (e.g., fMLP and C5a) emanating from the site of infection over intermediary endogenous chemoattractants (e.g., IL-8 and LTB₄) (28). To determine whether signals generated at the infection sites compete with

wound signals, we performed infection and wounding in the same larvae. Efficient neutrophil recruitment to both wound and infection is observed, indicating that neutrophils can sense different signals generated at tissue injury or bacterial infection without competition (**Fig. 6** and supplemental Video 2). The result is not affected regardless of whether wounding or PAK infection is performed first (data not shown). Therefore, no obvious competition between infection and wound generated signals is observed in this whole fish setting. However, it is possible that individual neutrophils are not exposed to competing signals due to the physical distance between the ear and the tail. Nevertheless, DPI treatment attenuates neutrophil attraction to tail transection, but not to PAK infection in the same larvae. The PI3K inhibitor LY294002 reduces neutrophil motility and impairs neutrophil infiltration both to sites of tissue injury and PAK infection (**Fig. 6** and supplemental Video 2). These findings again confirm a differential role for H₂O₂ in mediating neutrophil recruitment to tissue injury or bacterial infection.

DPI does not inhibit neutrophil attraction to PAK wound-infection

To complement our results with localized infection, we next determined the requirement of H₂O₂ in neutrophil recruitment in a wound-infection model with the addition of PAK to the embryo medium during the wound response (29). A typical neutrophilic inflammation induced by a wound is characterized by initial recruitment of neutrophils during the first hours post wounding, followed by a resolution phase. The presence of PAK in

embryo medium does not affect neutrophil recruitment to the tissue injury, but delays the resolution of inflammation, as indicated by increased numbers of neutrophils at the tail wound 6 hours post wounding (**Fig. 7A**), suggesting that the presence of PAK alters the neutrophil response. DPI attenuates neutrophil attraction (during the first two hour post wounding) to tissue injury. However, in the presence of PAK in the media, neutrophil recruitment is not significantly affected by DPI treatment (**Fig. 7B**), indicating that PAK induces neutrophil recruitment that is independent of the H₂O₂ generated at the wound. Taken together, our results indicate that PAK detection by zebrafish neutrophils is independent of H₂O₂.

DPI does not inhibit neutrophil attraction to localized infection by *S. iniae*

Since most of the experiments were performed with Gram-negative bacterium, we next tested the effect of DPI on neutrophil recruitment to *Streptococcus iniae*, a Gram-positive bacterium and a natural zebrafish pathogen (30). Similarly, under conditions that attenuate neutrophil attraction to tissue injury, neutrophil recruitment to localized *S. iniae* infection is not significantly affected by DPI treatment (**Fig. 8**), indicating that detection of Gram-positive bacteria by zebrafish is also independent of H₂O₂.

Discussion

Here we report that zebrafish localized otic infection is suited for real-time observation of neutrophil infiltration and identification of host signaling pathways that sensitize neutrophils to bacterial infection. Neutrophils are recruited immediately to the site of infection (supplemental Video 2) and pathogen-leukocyte interactions are readily observed at the onset of the infection (**Fig. 2**). In contrast, neutrophils respond 90 min post infection with another strain of *Pseudomonas*, PA14, injected into the hindbrain ventricle (HBV) in 2 dpf larvae (18). The potential difference in the dynamics of neutrophil infiltration into the ear or HBV may be due to the developmental stage of the larvae, dose and type of bacterial strains used, or the immune-privileged nature of the brain, which is well known in humans and other higher vertebrates. Although direct comparison of neutrophil recruitment in the ear and HBV infection is technically difficult (31), our study indicates that neutrophil responses to infection can be readily observed with the ear infection model in larvae 3 dpf. The yolk sac, on the other hand, is not a good site to investigate leukocyte-pathogen interactions since neutrophils fail to infiltrate into the yolk sac, making the larvae more susceptible to infection, consistent with a previous report (25). Nonetheless, neutrophils are able to sense the presence of bacteria inside the yolk, indicated by the increased numbers and motility of neutrophils patrolling on top of the yolk in response to infection (**Fig. 1** and data not shown). Taken together, our findings identify localized otic infection as a powerful model system to characterize mechanisms that mediate leukocyte recruitment to sites of localized bacterial infection using real-time imaging.

Since the identification of the requirement of H_2O_2 in mediating leukocyte wound detection and recruitment to transformed cells, the enhanced production of H_2O_2 is speculated to be a universal mechanism used by the host to sense the destruction of tissue homeostasis by various insults and to activate the appropriate innate immune response (11-14). In animal cells, H_2O_2 is known to serve as a second messenger that regulates transcription, proliferation or enzyme activity (32). Surprisingly, we visualize minimal H_2O_2 generation upon localized *Pseudomonas aeruginosa* infection (**Fig. 5**). Accordingly, neutrophil recruitment to localized infection with both Gram-negative and Gram-positive bacteria are independent of tissue generated H_2O_2 (**Fig. 3,4,6,7,8**), suggesting a context dependent requirement of H_2O_2 signaling in sensitizing professional phagocytes. However, whether tissue generated H_2O_2 is required for efficient clearance of bacterial infection in zebrafish has not been determined (due to the limitation of current tools).

Although H_2O_2 is considered to be an antiseptic and routinely used for treating minor wounds, it remains questionable whether physiologically generated H_2O_2 could directly kill microbes since H_2O_2 is only microbicidal at high concentrations (33). Secondary oxidant that has higher destructive capacity, such as HOCl generated by neutrophil-derived myeloperoxidase, is more likely to conduct direct microbicidal activities (34-35). Therefore, tissue generated H_2O_2 may primarily modulate the local environment, which can mediate leukocyte infiltration and inflammation. Leukocytes, on the other hand, are the major effectors that clear microbes by phagocytosis, releasing ROS and neutrophil extracellular traps.

The identities of the signals that mediate neutrophil recognition of bacterial infection and recruitment *in vivo* still remain elusive. The neutrophil chemoattractant could be bacterially-derived peptides with formylated N-terminal methionine groups, which is recognized by host N-formyl peptide receptor (FPR) and mediate neutrophil chemotaxis (36). However, fMLP, a synthetic peptide that mimics the activity of bacterially-derived peptides, fail to attract neutrophils when injected into the ear (data not shown). In addition, treatment with cyclosporin H, an FPR inhibitor, does not affect neutrophil recruitment to either infection or wounding (data not shown). Collectively, these results suggest that N-formyl peptides are not likely to be involved in rapid neutrophil detection of infection in zebrafish. Other candidate signaling molecules include those in the complement system, such as C5a. The complement system is being extensively studied in zebrafish (37) and multiple *mannose binding lectin* loci have been identified (38). However, it remains to be determined whether the complement system mediates rapid neutrophil detection of pathogens.

The responses of neutrophils can also be driven by a diverse array of pattern recognition receptors (PRRs) that bind pathogen-associated molecular patterns (PAMPs). The toll-like receptor (TLR) family of cell surface receptors recognizes different foreign biomolecules including those exposed on the cell surface of both Gram-negative and Gram-positive bacteria, such as lipopeptides, lipopolysaccharide (LPS) and flagellin. TLRs signal through several intracellular adaptor molecules, among which, MyD88 plays a pivotal role. TLRs and MyD88 are well conserved in the zebrafish (39). However, depleting endogenous MyD88 with two separate morpholino oligonucleotides indicates a dispensable role for

MyD88 in mediating neutrophil recruitment to PAK infection (data not shown). It is possible that MyD88 plays roles in later sustained neutrophil recruitment or activation, but not in the initial rapid neutrophil response. It is also possible that another adaptor protein, such as TRAM can function in place of MyD88 and mediate functional PRR signaling (40). In contrast, we find that MyD88 is involved in neutrophil wound detection, which is not entirely surprising since TLRs are implicated in recognition of endogenous ligands that are derived from necrotic cells, such as HMGB1 (41-42) or extracellular matrix components that are generated as a result of tissue injury (43). A challenge for future investigation will be to identify the specific signaling mechanisms that mediate leukocyte attraction to infected tissues in live animals.

In summary, we have identified a differential requirement for tissue generated H₂O₂ in mediating neutrophil recruitment to tissue injury and bacterial infection. Our results indicate that signals mediating leukocyte response to infection or acute injury are indeed unique and suggest the potential of identifying novel signaling events that are differentially involved in sensitizing immune cells to non-pathogen driven versus pathogen driven inflammation.

Experimental Procedures

Zebrafish maintenance and drug treatment

Adult fish were maintained in accordance with the University of Wisconsin-Madison Research Animal Resources Center (Madison, WI, USA). For live imaging or wounding assays, larvae were anesthetized in E3 containing 0.2 mg/ml Tricaine (ethyl 3-aminobenzoate; Sigma-Aldrich, St. Louis, MO, USA). To prevent pigment formation, some larvae were maintained in E3 containing 0.2 mM N-phenylthiourea (Sigma-Aldrich). Where indicated, larvae were pretreated with 32.5 μ M LY294002 (Calbiochem) (27) or 100 μ M DPI (Sigma) (10) in 1% DMSO in embryo medium (E3) to facilitate drug delivery for 1 hour. Following experiments were performed in E3 supplemented with indicated drug for indicated time.

Bacterial strains and culture methods

Pseudomonas aeruginosa strain, PAK carrying a constitutive plasmid-encoded red fluorescent protein mCherry (pMKB1::mCherry) was kindly provided by S. Moskowitz, University of Washington, Seattle, WA, USA (15). The *S. iniae* strain was kindly provided by M. Caparon, Washington University, St Louis, MO, USA (30). *S. iniae* for infection was prepared as described (30). Frozen stock obtained with single colony of PAK (pMKB1::mCherry) was streaked freshly on Vogel-Bonner minimal (VBM) plate supplemented with 200 μ g/mL carbenicillin the night before infection. Bacteria were resuspended in phosphate-buffered saline (PBS) and the optical density at 600 nm was measured with a Nanodrop spectrometer. To prepare the final inoculum, bacteria suspension was diluted or

pelleted by centrifugation at 1500 g for 5 min followed by resuspension to achieve the desired bacterial density. Phenol red tracking dye was added to bacterial aliquots prior to injection at a final concentration of 0.1%. After infection, the inoculum was injected into PBS, diluted when necessary and plated to quantify colony forming units.

Bacterial infection, tailfin wounding and Sudan Black staining

Bacterial infection in the otic vesicle was performed as described (31). For yolk infection, larvae were prepared as for otic infection with slight modifications: dorsal side (instead of ventral side for otic infection) was positioned against the injection groove. The tail fins of larvae at 3 dpf were either wounded with a needle or transected with a sterile razor blade. For wound-infection, PAK(pMKB1::mCherry) was added to E3 at a final OD₆₀₀ of 0.005 (29). Larvae were fixed at indicated time post wounding, and neutrophils were stained with Sudan Black as previously described (22).

Morpholino oligonucleotides (MO) microinjection and RT-PCR

All MOs were purchased from GeneTools, LLC, resuspended in distilled water and stored at RT at a stock concentration of 1 mM. 1 nl of MOs were injected into the yolk of 1 cell-stage embryos at concentrations indicated below. 100 μ M Duox MO (10) was injected in combination with 300 μ M p53 MO (10) to minimize non-specific MO toxicity. Efficient MO

mediated knockdown was confirmed with RT-PCR using mRNA extract from 3 dpf morphants. Primers to amplify *duox* (10) and *efl α* as a house keeping gene (44) were previously described. Primers for the neutrophil specific marker *mpx* were as follows: *mpx* forward: 5'-ACCAGTGA GCCTGAGACACGCA-3'; *mpx* reverse: 5'-TGCAGAC ACCGCTGGCAGTT-3'.

Live imaging and Hyper imaging

Larvae at 3 dpf were settled on a custom-made, glass-bottom dish. Time lapse fluorescence images were acquired with a confocal microscope (FluoView FV1000, Olympus, Center Valley, PA, USA) using a numeric aperture 0.75/20x objective or Nikon SMZ-1500 zoom microscope (Nikon, Melville, NY, USA). For confocal imaging, each fluorescence channel (488 nm and 543 nm) and DIC images were acquired by sequential line-scanning. Z-series was acquired using a 200- to 300- μ m pinhole and 2–10 μ m step sizes. Z-stacked fluorescence images were overlaid with a single DIC plane. For imaging of H₂O₂, 1-cell stage zebrafish embryos from Tg(*mpx:mCherry*) were injected with HyPer mRNA. At 3 dpf, larvae were infected with PAK (pMKB1::mCherry) in the left ear. The HyPer fluorescence was excited with 405 and 488 laser and corresponding YFP emission was acquired every 2 min after infection. Emission 510-525 nm was collected for YFP488 emission and 505-510 nm was collected for YFP405 emission. The right ear of the same fish was wounded right after the acquisition of the movie at infected side and the same conditions were used to

acquire the movie after wounding. For calculating HyPer ratio images, stacked, smoothed YFP488 and YFP405 images were divided.

Acknowledgements

The authors would like to thank Sa Kan Yoo for critical reading of the manuscript, lab members for zebrafish maintenance. This work is supported by grant from the National Institute of Health to A.H. (GM074827).

References

1. **Springer TA.** 1994. Traffic signals for lymphocyte recirculation and leukocyte emigration: the multistep paradigm. *Cell* **76**:301–314.
2. **ZUELZER WW.** 1964. “MYELOKATHEXIS--”A NEW FORM OF CHRONIC GRANULOCYTOPENIA. REPORT OF A CASE. *N. Engl. J. Med.* **270**:699–704.
3. **Etzioni A, Alon R.** 2004. Leukocyte adhesion deficiency III: a group of integrin activation defects in hematopoietic lineage cells. *Current Opinion in Allergy and Clinical Immunology* **4**:485–490.
4. **Baehner RL, Nathan DG.** 1967. Leukocyte oxidase: defective activity in chronic granulomatous disease. *Science* **155**:835–836.
5. **Gernez Y, Tirouvanziam R, Chanez P.** 2010. Neutrophils in chronic inflammatory airway diseases: can we target them and how? *European Respiratory Journal* **35**:467–469.
6. **Seibold F, Weber P, Klein R, Berg PA, Wiedmann KH.** 1992. Clinical significance of antibodies against neutrophils in patients with inflammatory bowel disease and primary sclerosing cholangitis. *Gut* **33**:657–662.
7. **Peng SL.** 2005. Neutrophil apoptosis in autoimmunity. *J Mol Med* **84**:122–125.
8. **McDonald B, Pittman K, Menezes GB, Hirota SA, Slaba I, Waterhouse CCM, Beck PL, Muruve DA, Kubes P.** 2010. Intravascular danger signals guide neutrophils to sites of sterile inflammation. *Science* **330**:362–366.

9. **Lieschke GJ, Trede NS.** 2009. Fish immunology. *Current Biology* **19**:R678–R682.
10. **Niethammer P, Grabher C, Look AT, Mitchison TJ.** 2009. A tissue-scale gradient of hydrogen peroxide mediates rapid wound detection in zebrafish. *Nature* **459**:996–999.
11. **Feng Y, Santoriello C, Mione M, Hurlstone A, Martin P.** 2010. Live imaging of innate immune cell sensing of transformed cells in zebrafish larvae: parallels between tumor initiation and wound inflammation. *PLoS Biol.* **8**:e1000562.
12. **Ha E-M, Oh C-T, Bae YS, Lee W-J.** 2005. A direct role for dual oxidase in *Drosophila* gut immunity. *Science* **310**:847–850.
13. **Ha E-M, Oh C-T, Ryu J-H, Bae YS, Kang S-W, Jang I-H, Brey PT, Lee W-J.** 2005. An antioxidant system required for host protection against gut infection in *Drosophila*. *Developmental Cell* **8**:125–132.
14. **Yoo SK, Huttenlocher A.** 2009. Innate immunity: wounds burst H₂O₂ signals to leukocytes. *Curr. Biol.* **19**:R553–5.
15. **Brannon MK, Davis JM, Mathias JR, Hall CJ, Emerson JC, Crosier PS, Huttenlocher A, Ramakrishnan L, Moskowitz SM.** 2009. *Pseudomonas aeruginosa* Type III secretion system interacts with phagocytes to modulate systemic infection of zebrafish embryos. *Cell Microbiol* **11**:755–768.
16. **Davis JM, Clay H, Lewis JL, Ghorri N, Herbomel P, Ramakrishnan L.** 2002. Real-time visualization of mycobacterium-macrophage interactions leading to initiation of granuloma formation in zebrafish embryos. *Immunity* **17**:693–702.

17. **Levraud J-P, Disson O, Kissa K, Bonne I, Cossart P, Herbomel P, Lecuit M.** 2009. Real-time observation of *Listeria monocytogenes*-phagocyte interactions in living zebrafish larvae. *Infection and Immunity* **77**:3651–3660.
18. **Phennicie RT, Sullivan MJ, Singer JT, Yoder JA, Kim CH.** 2010. Specific Resistance to *Pseudomonas aeruginosa* Infection in Zebrafish Is Mediated by the Cystic Fibrosis Transmembrane Conductance Regulator. *Infection and Immunity* **78**:4542–4550.
19. **Stoop EJM, Schipper T, Rosendahl Huber SK, Nezhinsky AE, Verbeek FJ, Gurcha SS, Besra GS, Vandenbroucke-Grauls CMJE, Bitter W, van der Sar AM.** 2011. Zebrafish embryo screen for mycobacterial genes involved in the initiation of granuloma formation reveals a newly identified ESX-1 component. *Disease Models & Mechanisms* **4**:526–536.
20. **Sullivan C, Kim CH.** 2008. Zebrafish as a model for infectious disease and immune function. *Fish & Shellfish Immunology* **25**:341–350.
21. **Brothers KM, Newman ZR, Wheeler RT.** 2011. Live Imaging of Disseminated Candidiasis in Zebrafish Reveals Role of Phagocyte Oxidase in Limiting Filamentous Growth. *Eukaryotic Cell* **10**:932–944.
22. **Le Guyader D, Redd MJ, Colucci-Guyon E, Murayama E, Kissa K, Briolat V, Mordelet E, Zapata A, Shinomiya H, Herbomel P.** 2008. Origins and unconventional behavior of neutrophils in developing zebrafish. *Blood* **111**:132–141.

23. **Lin A, Loughman JA, Zinselmeyer BH, Miller MJ, Caparon MG.** 2009. Streptolysin S Inhibits Neutrophil Recruitment during the Early Stages of Streptococcus pyogenes Infection. *Infection and Immunity* **77**:5190–5201.
24. **Wiles TJ, Bower JM, Redd MJ, Mulvey MA.** 2009. Use of Zebrafish to Probe the Divergent Virulence Potentials and Toxin Requirements of Extraintestinal Pathogenic Escherichia coli. *PLoS Pathog* **5**:e1000697.
25. **van der Sar AM, Musters RJP, van Eeden FJM, Appelmelk BJ, Vandenbroucke-Grauls CMJE, Bitter W.** 2003. Zebrafish embryos as a model host for the real time analysis of Salmonella typhimurium infections. *Cell Microbiol* **5**:601–611.
26. **Yoo SK, Huttenlocher A.** 2011. Spatiotemporal photolabeling of neutrophil trafficking during inflammation in live zebrafish. *Journal of Leukocyte Biology* **89**:661–667.
27. **Yoo SK, Deng Q, Cavnar PJ, Wu YI, Hahn KM, Huttenlocher A.** 2010. Differential Regulation of Protrusion and Polarity by PI(3)K during Neutrophil Motility in Live Zebrafish. *Developmental Cell* **18**:226–236.
28. **Heit B.** 2002. An intracellular signaling hierarchy determines direction of migration in opposing chemotactic gradients. *The Journal of Cell Biology* **159**:91–102.
29. **Brown SB, Tucker CS, Ford C, Lee Y, Dunbar DR, Mullins JJ.** 2007. Class III antiarrhythmic methanesulfonanilides inhibit leukocyte recruitment in zebrafish. *Journal of Leukocyte Biology* **82**:79–84.

30. **Neely MN, Pfeifer JD, Caparon MG.** 2002. Streptococcus-Zebrafish Model of Bacterial Pathogenesis. *Infection and Immunity* **70**:3904–3914.
31. **Levraud J-P, Colucci-Guyon E, Redd MJ, Lutfalla G, Herbomel P.** 2008. In vivo analysis of zebrafish innate immunity. *Methods Mol. Biol.* **415**:337–363.
32. **Bedard K, Krause K-H.** 2007. The NOX family of ROS-generating NADPH oxidases: physiology and pathophysiology. *Physiol. Rev.* **87**:245–313.
33. **Hampton MB, Kettle AJ, Winterbourn CC.** 1998. Inside the neutrophil phagosome: oxidants, myeloperoxidase, and bacterial killing. *Blood* **92**:3007–3017.
34. **Klebanoff SJ.** 1974. Role of the superoxide anion in the myeloperoxidase-mediated antimicrobial system. *The Journal of Biological Chemistry* **249**:3724–3728.
35. **Rosen H, Crowley JR, Heinecke JW.** 2002. Human Neutrophils Use the Myeloperoxidase-Hydrogen Peroxide-Chloride System to Chlorinate but Not Nitrate Bacterial Proteins during Phagocytosis. *Journal of Biological Chemistry* **277**:30463–30468.
36. **Migeotte I, Communi D, Parmentier M.** 2006. Formyl peptide receptors: a promiscuous subfamily of G protein-coupled receptors controlling immune responses. *Cytokine Growth Factor Rev.* **17**:501–519.
37. **Sun G, Li H, Wang Y, Zhang B, Zhang S.** 2010. Zebrafish complement factor H and its related genes: identification, evolution, and expression. *Funct. Integr. Genomics* **10**:577–587.

38. **Jackson AN, McLure CA, Dawkins RL, Keating PJ.** 2007. Mannose binding lectin (MBL) copy number polymorphism in Zebrafish (*D. rerio*) and identification of haplotypes resistant to *L. anguillarum*. *Immunogenetics* **59**:861–872.
39. **van der Sar AM, Stockhammer OW, van der Laan C, Spaik HP, Bitter W, Meijer AH.** 2006. MyD88 innate immune function in a zebrafish embryo infection model. *Infection and Immunity* **74**:2436–2441.
40. **Yamamoto M, Sato S, Hemmi H, Uematsu S, Hoshino K, Kaisho T, Takeuchi O, Takeda K, Akira S.** 2003. TRAM is specifically involved in the Toll-like receptor 4-mediated MyD88-independent signaling pathway. *Nature Immunology* **4**:1144–1150.
41. **Apetoh L, Ghiringhelli F, Tesniere A, Obeid M, Ortiz C, Criollo A, Mignot G, Maiuri MC, Ullrich E, Saulnier P, Yang H, Amigorena S, Ryffel B, Barrat FJ, Saftig P, Levi F, Lidereau R, Nogues C, Mira J-P, Chompret A, Joulin V, Clavel-Chapelon F, Bourhis J, André F, Delalogue S, Tursz T, Kroemer G, Zitvogel L.** 2007. Toll-like receptor 4-dependent contribution of the immune system to anticancer chemotherapy and radiotherapy. *Nat Med* **13**:1050–1059.
42. **Scaffidi P, Misteli T, Bianchi ME.** 2002. Release of chromatin protein HMGB1 by necrotic cells triggers inflammation. *Nature* **418**:191–195.
43. **Jiang D, Liang J, Li Y, Noble PW.** 2006. The role of Toll-like receptors in non-infectious lung injury. *Cell Res* **16**:693–701.

44. **Walters KB, Green JM, Surfus JC, Yoo SK, Huttenlocher A.** 2010. Live imaging of neutrophil motility in a zebrafish model of WHIM syndrome. *Blood* **116**:2803–2811.

Figure Legends

Fig. III-1. Localized *Pseudomonas* infection model. (A) PBS or PAK (pMKB1::mCherry) was injected into the otic vesicle of *Tg(mpx:dendra2)* at 3 day post fertilization (dpf). Images were taken 4 hours post infection (hpi). (B) Survival of wild type AB zebrafish larvae infected at 3 dpf in the otic vesicle with PBS or PAK at indicated colony forming units (cfu). (C) PBS or PAK (pMKB1::mCherry) was injected into the yolk of *Tg(mpx:dendra2)* at 3 dpf. Images were taken 4 hpi. (D) Survival of wild type AB zebrafish larvae infected at 3 dpf in the yolk with PBS or PAK at indicated cfu. Results are representative from 3 independent experiments. Scale bar: 100 μ m.

Fig. III-1:

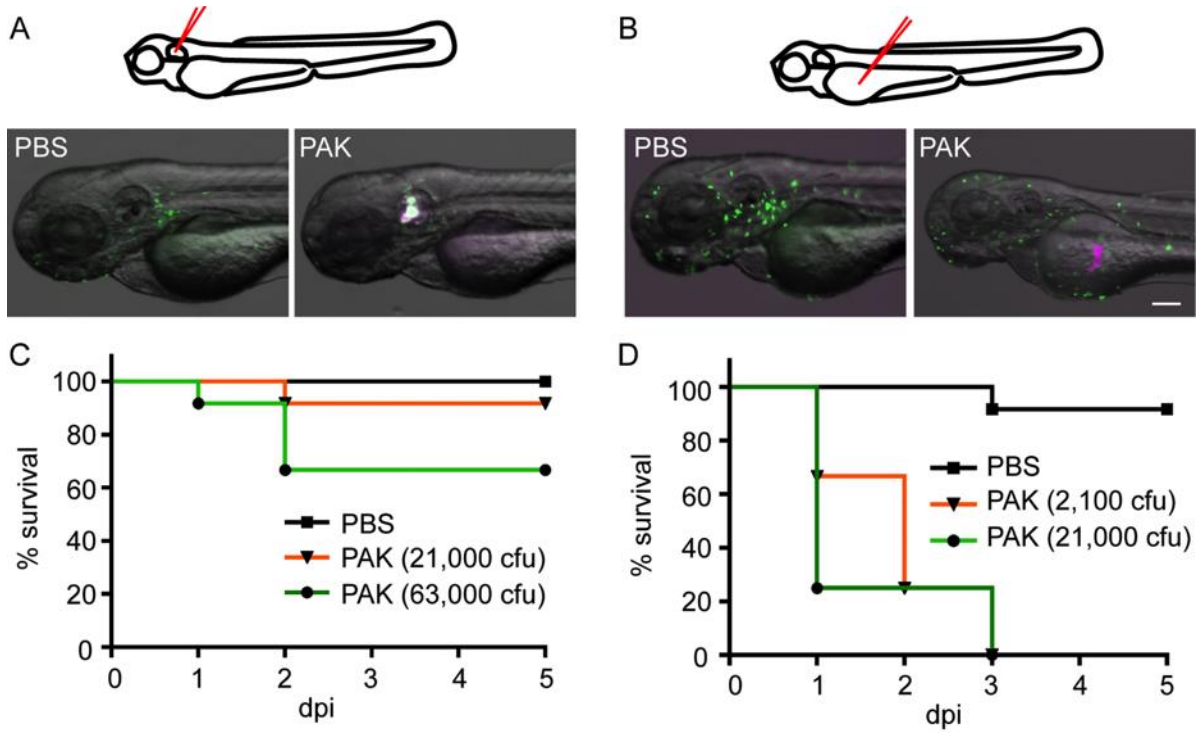


Fig. III-2. Phagocytosis of PAK by neutrophils. PAK (pMKB1::mCherry) ~12,000 cfu was injected into the otic vesicle of *Tg(mpx:dendra2)*. Still images at indicated time points from a representative confocal movie started right after infection are shown. Boxed regions are enlarged to show bacteria inside neutrophils. Scale bar: 50 μm .

Fig. III-2:

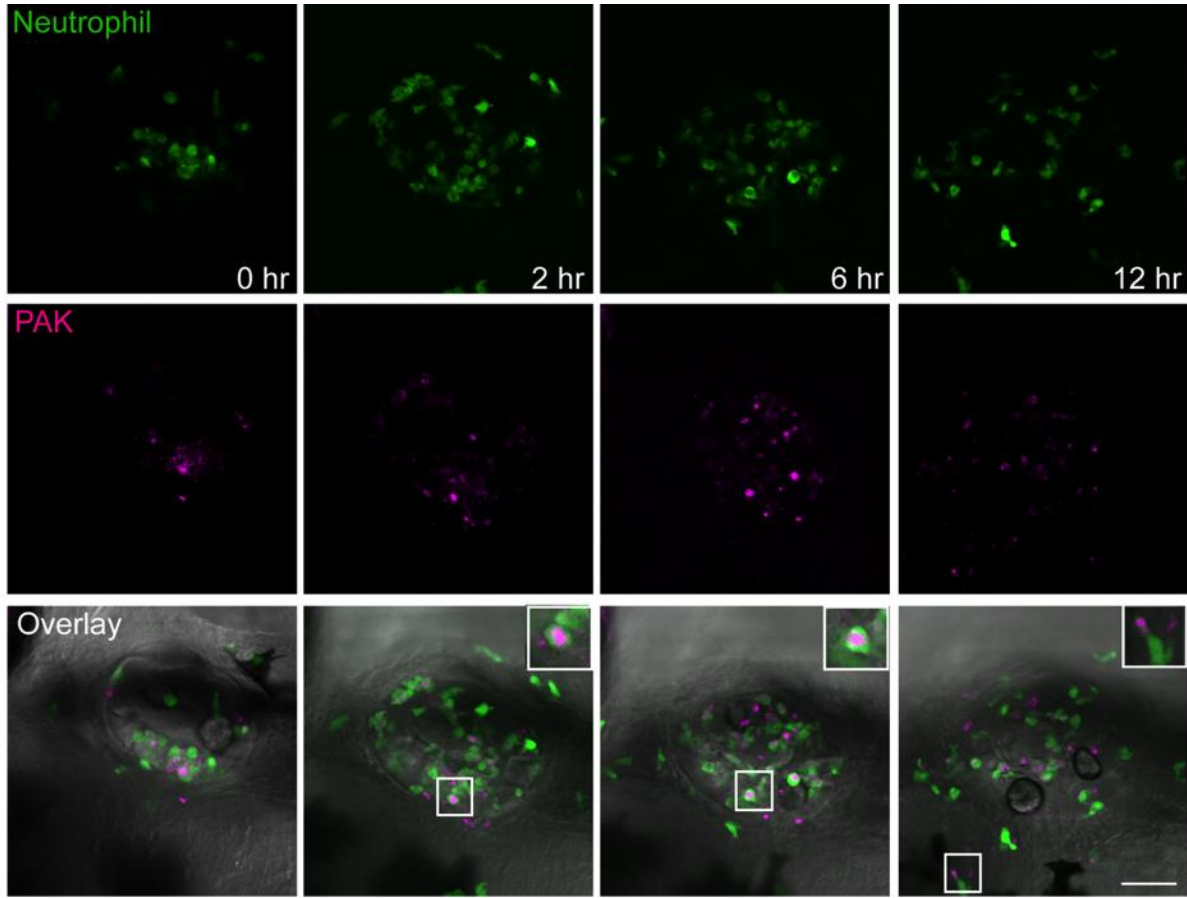


Fig. III-3. Neutrophil recruitment to wound, but not PAK infection is blocked by DPI. (A)

Wild-type AB zebrafish larvae at 3 dpf were pretreated with DMSO, DPI or LY for 1 h followed by needle wounding at the tail fin. Larvae were fixed 1 hour post wounding (hpw) and neutrophils were visualized by Sudan Black staining. Neutrophils recruited to the tail fin were quantified and representative images are shown. (B) Wild-type AB zebrafish larvae at 3 dpf were pretreated with DMSO, DPI or LY294002 (LY) for 1 h followed by ear infection with ~ 1, 200 cfu of PAK (pMKB1::mCherry). Larvae were fixed 1 hpi and neutrophils were visualized by Sudan Black staining. Neutrophils recruited to infected ear were quantified and representative images are shown. PBS was also injected into DMSO treated larvae as a control. Results are pooled from 3 independent experiments. ***, $p < 0.001$, Kruskal-Wallis test followed by Dunn's Multiple Comparison test. Scale bar: 50 μm .

Fig. III-3:

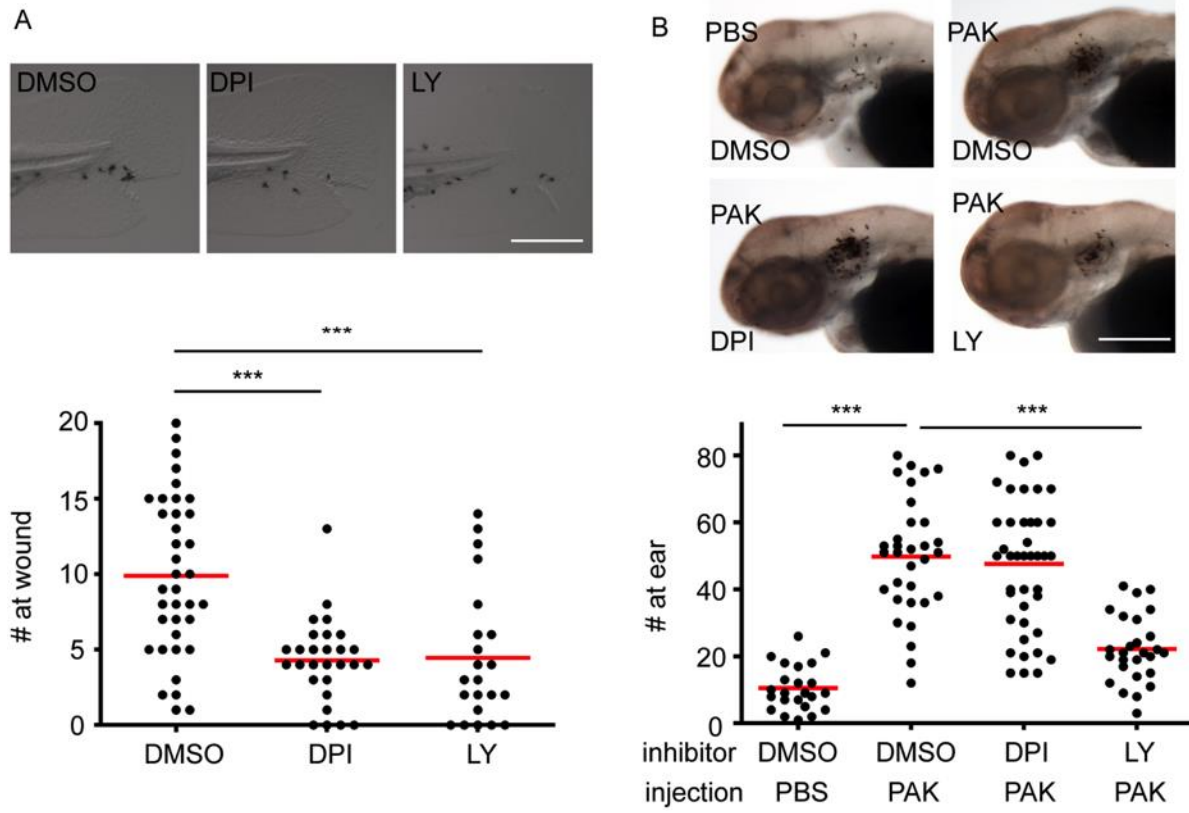


Fig. III-4. Neutrophil recruitment to wound, but not PAK infection is blocked in Duox morphants. Wild-type AB zebrafish larvae were injected with p53 together with or without Duox morpholino oligonucleotide at 1 cell stage. (A) 3 dpf p53 or duox morphants were fixed 1 hpw. Representative images and quantification of neutrophils recruited to wounds are shown. (B) 3 dpf p53 or duox morphants were fixed 1 hpi with ~ 1,200 cfu of PAK (pMKB1::mCherry). Representative images and quantification of neutrophils recruited to ear and total number of neutrophils present in the head are shown. (C) RT-PCR of duox and mpx from mRNA extracted from p53 or duox morphants at 3 dpf. (D) Percentage of neutrophils at head that were recruited to PAK ear infection in 3 dpf p53 or duox morphants. Results are representative from 3 independent experiments. ***, $P < 0.001$, two-tailed Mann-Whitney test. Scale bar: 30 μm .

Fig. III-4:

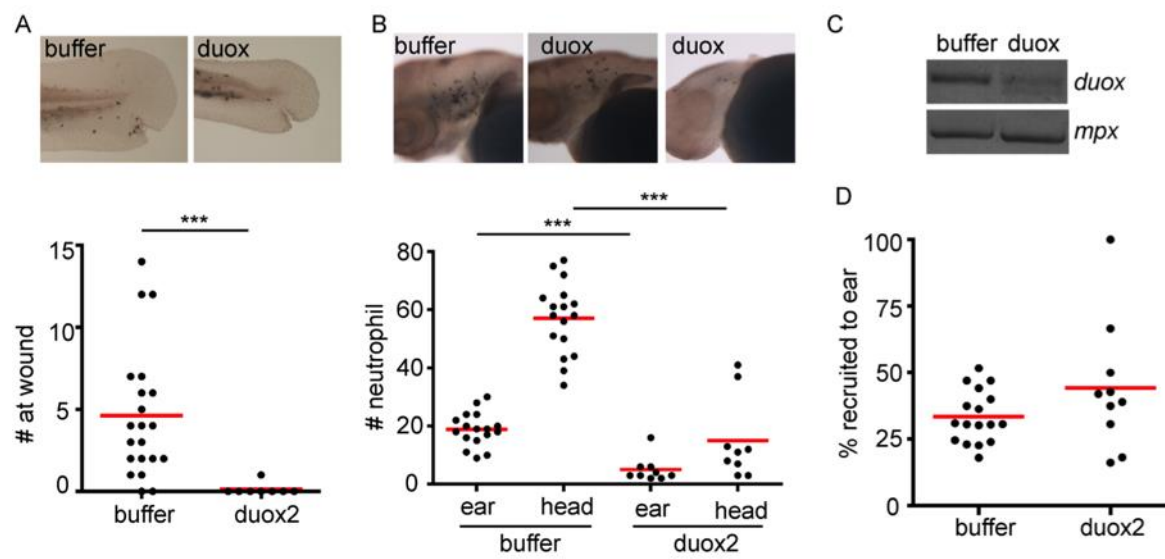


Fig. III-5. Absence of H₂O₂ burst with localized PAK infection. Wild-type AB zebrafish larvae were injected with Hyper mRNA at 1 cell stage. Larvae at 3 dpf were infected with ~1,400 cfu of PAK (pMKB1::mCherry) at the left ear and real-time ratiometric imaging was performed to measure relative amount of H₂O₂ generated in tissue. The right ear of the same fish was then wounded and generation of H₂O₂ was monitored by ratiometric imaging under the same conditions. Still images at indicted time after handling from a representative movie are shown. Images are representative for 10 movies from 4 separate experiments. * indicates wound site. Scale bar: 50 μ m.

Fig. III-5:

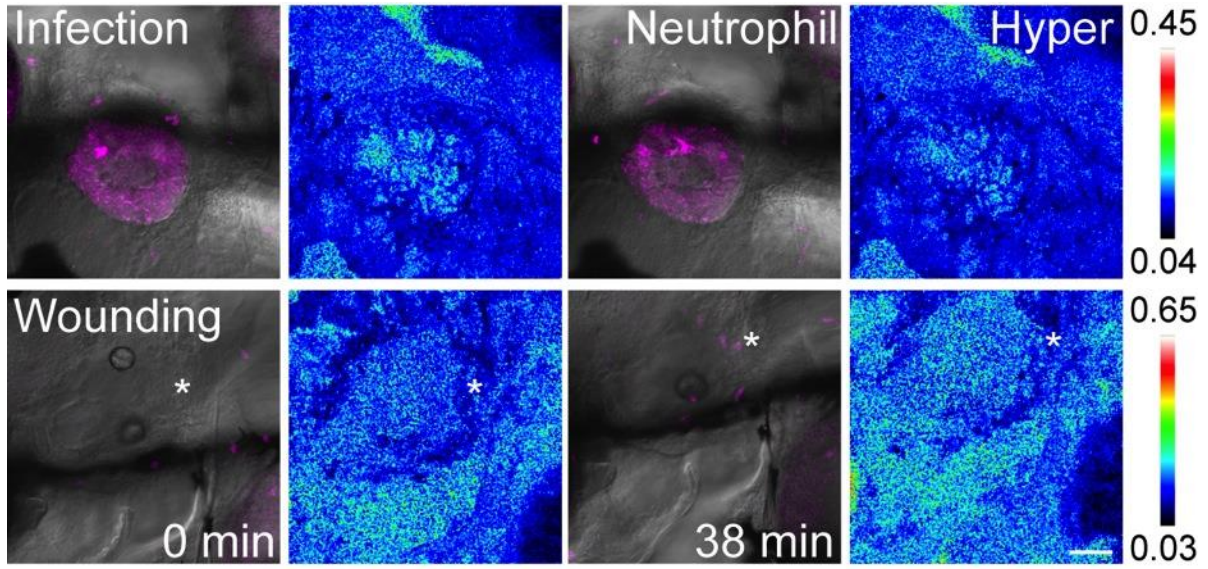


Fig. III-6. Differential sensitivity to DPI in response to simultaneous wounding and infection. Wild-type AB zebrafish larvae at 3 dpf were treated with DMSO, DPI or LY for 1 h, then infected with ~ 1,200 cfu of PAK (pMKB1::mCherry) right followed by tail transaction. Neutrophils recruited to either ear infection or close proximity to tail transaction were quantified and representative images are shown. Results are representative for 3 independent experiments. ***, $P < 0.001$, Kruskal-Wallis test followed by Dunn's Multiple Comparison test. Scale bar: 100 μm .

Fig. III-6:

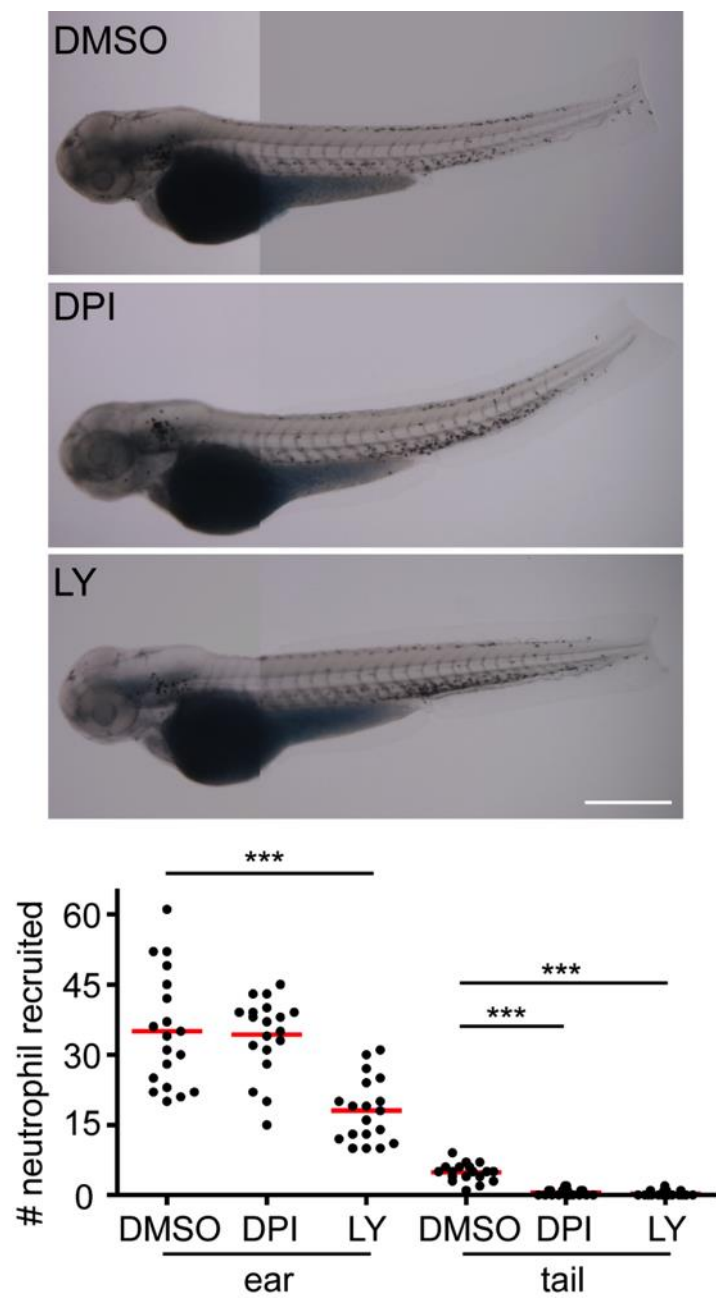


Fig. III-7. DPI does not inhibit neutrophil recruitment to wound in the presence of PAK.

(A) Time course of neutrophil recruitment to wound-infection. Wild-type AB zebrafish larvae at 3 dpf were treated with DMSO for 1 h, followed by tail transaction. Larvae were incubated in the presence or absence of PAK in the water (pMKB1::mCherry) and fixed after indicated times. Neutrophils recruited to within close proximity of tail transaction were quantified and representative images are shown. (B) DPI does not affect neutrophil recruitment to wounds in the presence of PAK. Wild-type AB zebrafish larvae at 3 dpf were treated with DMSO or DPI for 1 h, followed by tail transaction. Larvae were incubated in the presence or absence of PAK (pMKB1::mCherry) at final OD of 0.005 and fixed after indicated time. Neutrophils recruited within close proximity to tail transaction were quantified and representative images are shown. Results are representative from 3 independent experiments. ***, $p < 0.001$; *, $p < 0.05$, Kruskal-Wallis test followed by Dunn's Multiple Comparison test. Scale bar: 30 μm .

Fig. III-7:

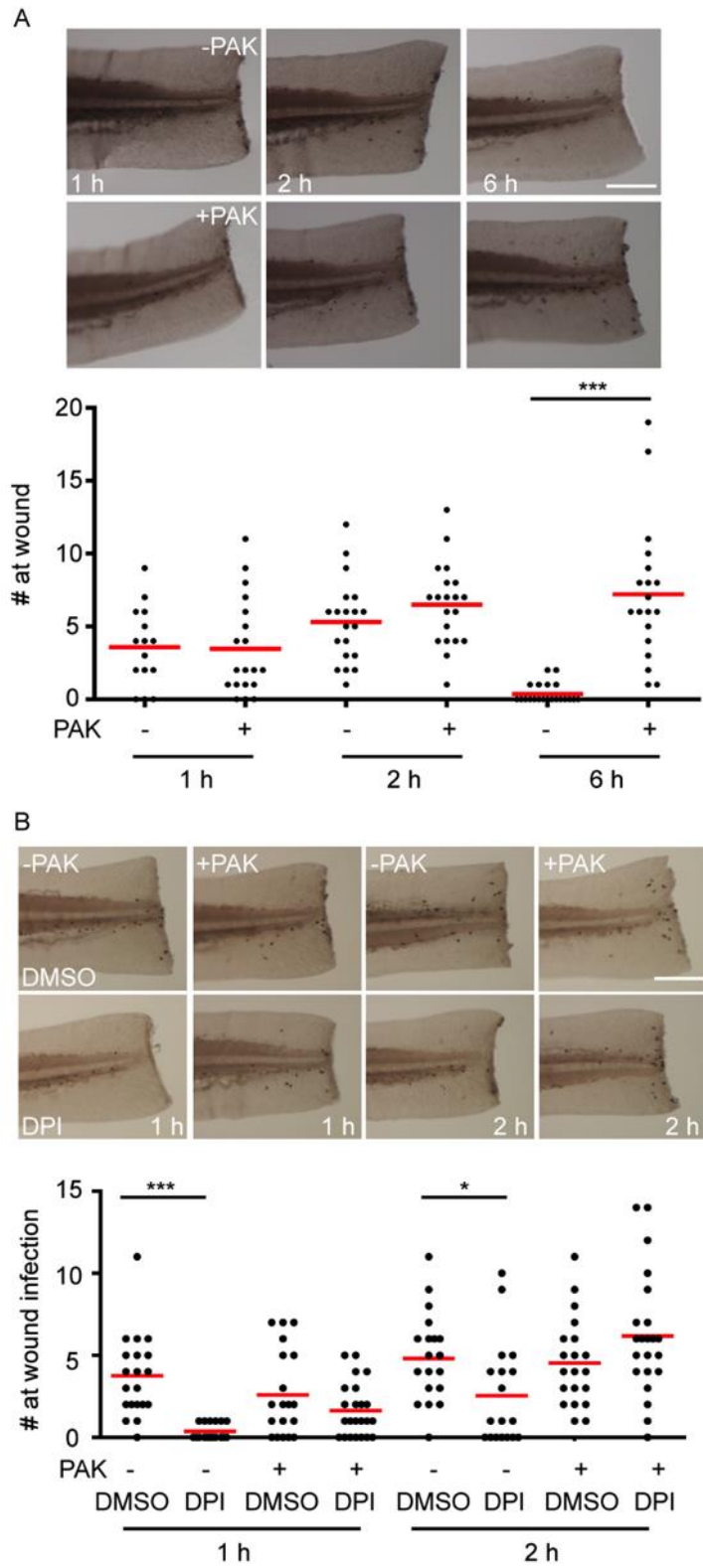


Fig. III-8. Neutrophil recruitment to *S.iniae* infection is not blocked by DPI. (A) Wild-type AB zebrafish larvae at 3 dpf were pretreated with DMSO, DPI or LY for 1 h followed by needle wounding at the tail fin. Larvae were fixed 1 hour post wounding (hpw) and neutrophils were visualized by Sudan Black staining. Neutrophils recruited to the tail fin were quantified and representative images are shown. (B) Wild-type AB zebrafish larvae at 3 dpf were pretreated with DMSO, DPI or LY294002 (LY) for 1 h followed by ear infection with ~100 cfu of *S. iniae*. Larvae were fixed 1 hpi and neutrophils were visualized by Sudan Black staining. Neutrophils recruited to infected ear were quantified and representative images are shown. Results are representative of 3 independent experiments. ***, $p < 0.001$, Kruskal-Wallis test followed by Dunn's Multiple Comparison test. Scale bar: 50 μm .

Supplemental Video Legend

Supplemental Video 1. Absence of H₂O₂ burst at localized PAK infection.

Wild-type AB zebrafish embryo were injected with HyPer mRNA at 1 cell stage. Embryos at 3 dpf were infected with ~ 1,400 cfu of PAK (pMKB1::mCherry) at the left ear and real-time ratiometric imaging was performed to measure relative amount of H₂O₂ generated in tissue. The right ear of the same fish was then wounded and generation of H₂O₂ was monitored under the same conditions. Movies are representative for 10 movies from 4 separate experiments. * indicates wound site. Scale bar: 50 μm.

Supplemental Video 2. Differential sensitivity to DPI during neutrophil response to simultaneous wounding and infection.

Tg(mpx:Dendra2) at 3 dpf were treated with DMSO, DPI or LY for 1 h, then infected with ~ 1,200 cfu of PAK (pMKB1::mCherry) immediately followed by tail transection. Movies are representative for 8 movies for each condition from 4 separate experiments.